Composition, distribution, and life history strategies of mesopelagic fauna in a changing Arctic Ocean

By

© Pierre Priou

A thesis submitted to the

School of Graduate Studies

in partial fulfillment of the requirements

for the degree of

Doctorate of Philosophy – Fisheries Science

Memorial University of Newfoundland

September, 2023

St. John’s, Newfoundland, Canada

i. General abstract

Micronekton and zooplankton inhabit the mesopelagic zone (200-1,000 m depth) which represents a unique environment in the global ocean where low-light levels structure predator-prey interactions. Because of the central position of mesopelagic organisms in food webs and the strong vertical gradient in light intensity, these animals conduct light-mediated diel vertical migrations (DVM) to maximize feeding while limiting mortality through visual predation. DVM contribute to the biological carbon pump by actively transporting carbon from the upper ocean to greater depths. The extreme light climate prevailing at high latitudes is hypothesized to prevent DVM during the midnight sun and polar night periods and hence prevent the establishment of viable mesopelagic populations in the Arctic Ocean. Yet, recent observations of mesopelagic layers in the European Arctic and the Central Arctic Ocean challenge this paradigm. There remain uncertainties regarding the spatial extent, species composition, life history strategies, and environmental drivers of the occurrence of mesopelagic organisms in the Arctic Ocean. Here, I used acoustic data collected at different spatial and temporal scales from multiple regions of the Arctic Ocean to investigate the distribution, structure, and dynamics of Arctic mesopelagic organisms. I demonstrate that mesopelagic organisms are commonly found in the Arctic Ocean and identified two distinct species assemblages that may be representative of larger biogeographic provinces. The seasonal vertical distribution of mesopelagic organisms generally followed a light comfort zone – a narrow range of light intensities. The seasonal cycle was characterized by two phases of active feeding on *Calanus* copepods in spring and autumn interspersed by oversummering and overwintering periods of vertical segregation with *Calanus* during the polar night and midnight sun. While the light comfort

zone hypothesis provides a comprehensive framework for understanding the structure and dynamics of the mesopelagic zone, not all size classes and taxa adhere to this hypothesis. In the Arctic, mesopelagic organisms exhibit complex and flexible behaviours to accommodate a broad range of changing environmental conditions. I conclude that the mesopelagic ecological niche is widespread in the Arctic Ocean. Future studies of the biological carbon pump and of trophic interactions in the Arctic should consider and include the mesopelagic niche.

ii. General summary

Below the sunlit and productive waters of the upper ocean lies the mesopelagic zone ranging between 200 to 1000 m depth. There, only a small fraction of the incoming surface light reaches those depths, and ambient light levels are low. The small fish and large zooplankton (> 20 mm) inhabiting the mesopelagic zone have developed specific physiological adaptations (e.g., extremely sensitive vision) and behaviours to take full advantage of the low light levels prevailing at mesopelagic depths. Because mesopelagic animals generally feed on small zooplankton found near the ocean's surface, they conduct diel vertical migrations aligning with the day-night light cycle. They ascend to surface waters at night to feed on small zooplankton and descend to deeper depths during daytime to avoid visual predators near the surface. Above the polar circle the annual light cycle is characterized by an extended period of complete darkness – the polar night – and daylight – the midnight sun – which could prevent diel vertical migrations of mesopelagic animals. Thus, mesopelagic fish and zooplankton are thought to be scarce in the Arctic Ocean. However, recent scientific surveys challenge this idea and have observed mesopelagic animals in some areas of the Arctic Ocean. In this thesis, I demonstrate that mesopelagic fish and zooplankton are, in fact, commonly found in the Arctic Ocean. I identified two distinct communities – one in the western Arctic dominated by the Arctic endemic species Arctic cod, and another one in the eastern Arctic that was more diverse with a combination of Arctic cod and species from the subarctic. Mesopelagic animals generally remained in a similar light environment throughout the day – a light comfort zone – which restricted their diel vertical migrations to spring and autumn when the day-night cycle occurs. Hence, I suggest that their annual life cycle is characterized by two phases of active feeding in spring and autumn separated by an overwintering and an oversummering period during the polar

night and midnight sun with possibly reduced feeding. I conclude that the mesopelagic zone represents a widespread habitat in the Arctic.

iii. Acknowledgments

This thesis work would not have been possible without the technical, financial, and scientific support of many people and organizations.

First, I sincerely thank my supervisor, Maxime Geoffroy, for supporting me during this project. His supervision, which leaves room for a great deal of autonomy and exploration, has allowed me to learn so much about various facets of scientific research and develop a project that matched my interests. Our discussions, whether they were in his office or during a skiing, climbing, or biking trip, were always insightful and helped me stay on track. Despite cruise cancellations due to weather or ship failures, a global pandemic, and a malfunctioning pressure switch, we have always managed to tackle those challenges and come up with new plans. There is no doubt that the knowledge and experience I gained from Maxime helped me grow as a scientist and as a person. Furthermore, I also want to thank my supervisory committee, Jørgen Berge and Jonathan Fisher, for their precious advice, patience, and support throughout this thesis.

I also want to thank my colleagues and friends from Geoffroy's laboratory: Julek Chawarski, Gérald Darnis, Muriel Dunn, Jenny Herbig, Eugenie Jacobsen, Jessica Randall, Einat Sandbank, Tiffany Small, and Jordan Sutton. The friendly atmosphere and the stimulating and creative working environment in this group were fantastic. I will never forget that fishing trip outside Petty Harbour and our genuine encounter with a sunfish. I want to especially thank Jenny Herbig and Muriel Dunn for the numerous discussions on acoustics, coding, and statistics.

Many collaborators contributed to the data collection in this thesis. I thank Andrew Majewski from Fisheries and Oceans Canada, Hauke Flores from the Alfred Wegener Institute, Jørgen Berge from the Arctic University of Norway, and Amundsen Science for the fruitful collaboration and providing acoustic and trawl data from the F/V *Frosti*, R/V *Polarstern*, R/V *Helmer Hanssen,* and CCGS *Amundsen*. I thank the officers and crew of the F/V *Frosti*, R/V *Polarstern*, R/V *Helmer Hanssen*, and CCGS *Amundsen* and the numerous colleagues who helped with data collection over the years. I also acknowledge the very dedicated work of Laure Vilgrain for the deployment and analyses of UVP6 data and Lisa Matthes, Guislain Bécu, and Edouard Leymarie for the light measurements during the DarkEdge campaign. A special thanks to Cyril Aubry for maintaining and constantly improving the precious trawl and net database of the CCGS *Amundsen*. I also thank my colleagues and friends from the Centre for Fisheries Ecosystems Research, particularly Wade Hiscock, for the acoustic data processing of some of the F/V *Frosti* data, Adam Templeton for the technical support and help during echosounder calibrations, and Arnault Le Bris for statistical advices.

The five years I spent in Newfoundland would not have been the same without the extraordinary people I met there. Marilena Geng, Caroline Gini, and Milo have made the infamous 15 Cabot St. the best home I could ever imagine. To all my friends, Tanya Prystay, Matt Robertson, Coline Tisserand, Dustin Porta, Cole Deal, Dom Smith, and so many others, you have seen me through the ups and downs of this PhD journey. Thank you for the laughs, dinners, Saturday night curling socials, house crawls, and great adventures in the constant breeze of Newfoundland. To MOSAiC School friends, we have been through intense moments on the R/V *Akademik Fedorov* and I look forward to working together in the future. I want to thank my colleagues at Akvaplan-niva and the midnight

sun in Tromsø for keeping my energy and vitamin D levels high during the final push to finish this manuscript.

Finalement, je tiens à chaleureusement remercier ma famille qui m'a toujours supporté et nourri mes rêves et ambitions. Merci à mes parents Anne et Dominique, mes frères François et Guillaume, Marie, et mon neveu et ma nièce Martin et Agathe de votre soutien inconditionnel malgré le fait que la recherche me porte si loin de vous.

This research was supported by the Ocean Frontier Institute through an award from the Canada First Research Excellence Fund, the Department of Fisheries and Oceans Canada, ArcticNet – a Network of Centres of Excellence Canada, by the ArcticABC project from the Norwegian Research Council, and the DarkEdge project from Takuvik.

Publication permission Chapter four

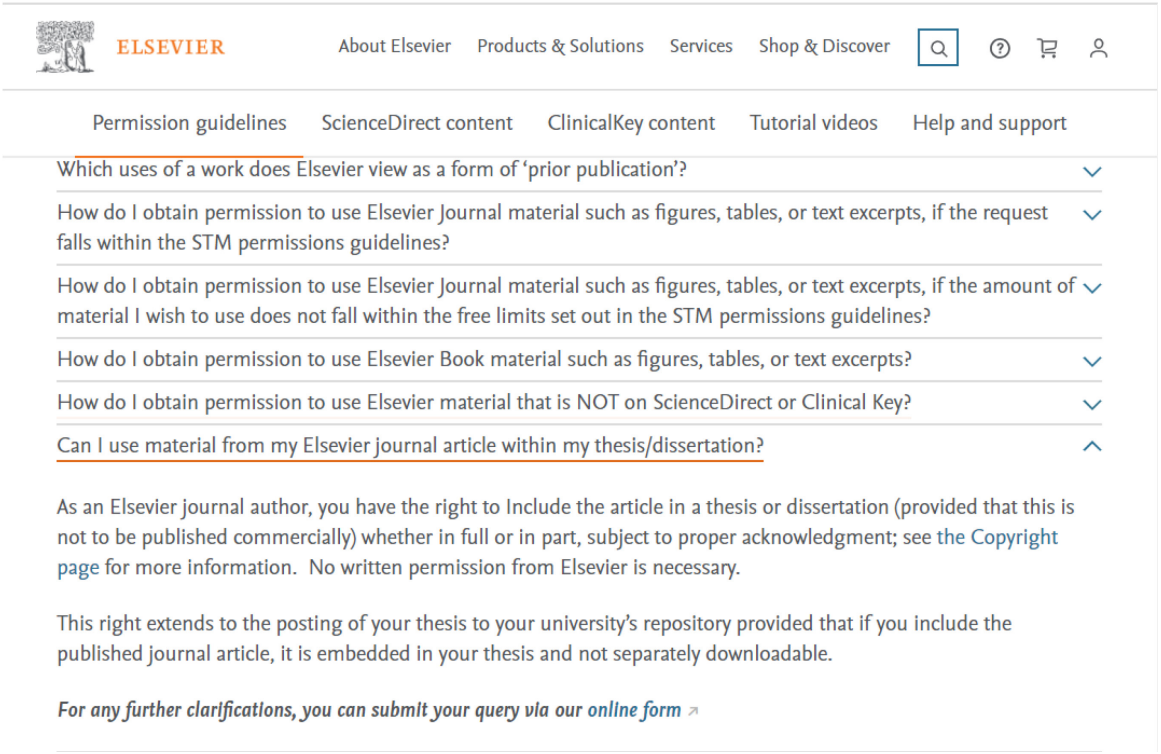

iv. Authorship statement

The following section presents the co-authorship statement using the CRediT Authorship Contribution Statement format.

Chapter 1 and 5

Pierre Priou: Writing – original draft, Writing – review & editing, Visualization. **Maxime Geoffroy**: Writing – review & editing, Supervision. **Jørgen Berge**: Writing – review & editing, Supervision. **Jonathan Fisher**: Writing – review & editing, Supervision.

Chapter 2

Pierre Priou: Conceptualization, Methodology, Validation, Formal analysis, Data curation, Writing – original draft, Writing – review & editing, Visualization. **Jørgen Berge**: Investigation, Writing – review & editing, Supervision, Funding acquisition. **Hauke Flores**: Investigation, Writing – review & editing. **Stéphane Gauthier**: Investigation, Writing – review & editing. **Andrew Majewski**: Investigation, Writing – review & editing. **Maxime Geoffroy**: Conceptualization, Methodology, Validation, Investigation, Resources, Writing – review & editing, Supervision, Project administration, Funding acquisition.

Chapter 3

Pierre Priou: Conceptualization, Methodology, Validation, Formal analysis, Data curation, Writing – original draft, Writing – review & editing, Visualization. **Anna Nikolopoulos**: Formal analysis, Investigation, Writing – review & editing. **Hauke Flores**: Investigation, Formal analysis, Writing – review & editing. **Rolf Gradinger**: Investigation, Writing – review & editing. **Erin Kunisch**: Investigation, Writing – review & editing. **Christian Katlein**: Investigation, Formal analysis, Writing – review & editing. **Giulia Castellani**: Investigation, Writing – review & editing. **Torsten Linders**: Investigation, Writing – review & editing. **Jørgen Berge**: Investigation, Writing – review & editing, Supervision, Funding acquisition. **Jonathan Fisher**: Writing – review & editing, Supervision. **Maxime Geoffroy**: Conceptualization, Methodology, Validation, Resources, Writing – review & editing, Supervision, Project administration, Funding acquisition.

Pierre Priou: Conceptualization, Methodology, Validation, Formal analysis, Investigation, Data curation, Writing – original draft, Writing – review & editing, Visualization. **Laure Vilgrain**: Formal analysis, Investigation, Writing – review & editing. **Lisa Matthes**: Investigation, Formal analysis. **Edouard Leymarie**: Investigation, Formal analysis. **Marcel Babin**: Investigation, Funding acquisition. **Maxime Geoffroy**: Conceptualization, Methodology, Validation, Investigation, Resources, Writing – review & editing, Supervision, Project administration, Funding acquisition.

Publications Arising

The following publications were produced as part of this dissertation:

Chapter 2:

Priou P, Majewski A, Berge J, Flores H, Gauthier S, Geoffroy M. (2021) Consistent occurrence of mesopelagic fish and macrozooplankton in high Arctic seas. *In prep*.

Chapter 3:

Priou P, Nikolopoulos A, Flores H, Gradinger R, Kunisch E, Katlein C, Castellani G, Linders T, Berge J, Fisher JA, Geoffroy M. (2021) Dense mesopelagic sound scattering layer and vertical segregation of pelagic organisms at the Arctic-Atlantic gateway during the midnight sun. *Progress in Oceanography* 196(102611) https://doi.org/10.1016/j.pocean.2021.102611

Chapter 4:

Priou P, Vilgrain L, Matthes L, Leymarie E, Babin M, Geoffroy M. Regular and inverse autumnal DVM by mesopelagic fish and zooplankton in Baffin Bay. *In prep*.

The work from this thesis has been presented in multiple international conferences and workshops:

Priou P, Berge J, Flores H, Majewski A, Gauthier S, Geoffroy M, (2022). Oral presentation. Ubiquitous occurrence of mesopelagic fish in high Arctic Seas. *Fourth ICES PICES Early Career Scientists Conference* in St John's, Canada.

Priou P, Berge J, Flores H, Majewski A, Gauthier S, Reist J, Geoffroy M, (2020). Oral presentation. Spatial variation of mesopelagic density within the Arctic Ocean. *ArcticNet Arctic Change*, online.

Priou P, Nikolopoulos A, Flores H, Linders T, Nicolaus M, Katlein C, Gradinger R, Kunisch E, Berge J, Fisher J, Geoffroy M, (2019). Oral presentation. Under-ice vertical distribution of pelagic organisms in the Arctic Ocean during the midnight sun. *ArcticNet Annual Science Meeting* in Halifax, Canada.

Priou P, Chawarski J, Berge J, Falk-Petersen S, Geoffroy M, (2018). Oral presentation. Arctic cod (*Boreogadus saida*) versus boreal fish species in the Barents Sea.

Ecosystem Studies of Subarctic and Arctic Seas (ESSAS) Annual Meeting in Fairbanks, USA.

Priou P, Nikolopoulos A, Flores H, Linders T, Nicolaus M, Katlein C, Gradinger R, Kunisch E, Berge J, Geoffroy M, (2018). Oral presentation. Linking vertical zooplankton and fish migrations to environmental cues under the Arctic pack ice during the midnight sun. *Synergy of physical, biological, and biogeochemical Arctic observations (SynArc)* in Delmenhorst, Germany.

Priou P, Kunisch E, Katlein C, Berge J, Gradinger R, Flores H, Geoffroy M, (2017). Poster. Vertical distribution of pelagic fish and zooplankton under the European Arctic pack ice. *Arctic Change* in Québec, Canada.

In addition to my thesis chapters, I have contributed to three peer-reviewed publications, one book chapter, two technical reports, and obtained two research project grants:

Flores H, Veyssiere G, Castellani G, Wilkinson J L, Hoppmann M, Karcher M, Valcic L, Cornils A, Geoffroy M, Nicolaus M, Niehoff B, **Priou P**, Schmidt K, Stroeve J. (*2023*) Sea-ice decline could keep zooplankton deeper for longer. *Nature Climate Change* 1–9. https://doi.org/10.1038/s41558-023-01779-1

Sandbank E, Dahl M, **Priou P**, Geoffroy M, (2023). Biomass estimates of Arctic cod (*Boreogadus saida*) in the Beaufort Sea in August 2022. *Centre for Fisheries and Ecosystems Research – Memorial University of Newfoundland*, commissioned by the Department of Fisheries and Oceans Canada. 18 pages.

Priou P, Hiscock W, Geoffroy M, (2022). Biomass estimations of Arctic cod (*Boreogadus saida*) in the Beaufort Sea in 2021. *Centre for Fisheries and Ecosystems Research – Memorial University of Newfoundland*, commissioned by the Department of Fisheries and Oceans Canada. 19 pages.

Geoffroy M, Langbehn T, **Priou P**, Varpe Ø, Johnsen G, Le Bris A, Fisher J, Daase M, McKee D, Cohen J., Berge J, (2021). Pelagic organisms avoid white, blue, and red artificial light from scientific instruments. *Scientific reports* 11(14941) https://doi.org/10.1038/s41598-021-94355-6

Geoffroy M, **Priou P**, (2020). Fish ecology in the polar night. *In Berge J, Johnsen G, Cohen J (eds), Polar Night Marine Ecology - Life and Light in the Dead of Night*. Springer, Cham. https://doi.org/10.1007/978-3-030-33208-2_7

Berge J, Geoffroy M, Daase M, Cottier F, **Priou P**, Cohen J, Johnsen G, McKee D, Kostakis I, Renaud P, Vogedes D, Anderson P, Last K, Gauthier S, (2020). Artificial light

during the polar night disrupts Arctic fish and zooplankton behavior down to 200 m depth. Communications biology 3 (1). https://doi.org/10.1038/s42003-020-0807-6

Priou P, Fisher J, Le Bris A, Geoffroy M. (2019) Baited Remote Underwater Video (BRUV) Avoidance. Research project on the avoidance of artificial light from baited remote underwater video by fish and zooplankton, funded by the Fisheries and Marine Institute through the Department of Fisheries and Oceans Canada ($18,026 CAD).

Priou P, Fisher J, Le Bris A, Geoffroy M. (2018) Abundance estimation of Bonne Bay Acadian redfish population. Research project on the abundance estimation of redfish (*Sebastes fasciatus*) in Bonne Bay (NL, Canada) combining hydroacoustics and baited remote underwater video, funded by the Fisheries and Marine Institute through the Department of Fisheries and Oceans Canada ($14,920 CAD).

v. Table of contents

vi. List of figures

vii. List of tables

viii. List of abbreviations

ADCP: Acoustic Doppler Current Profiler

ADW: Arctic Deep Waters

AIW: Arctic Intermediate Waters

ASW: Arctic Surface Waters

AW: Atlantic Waters

AZFP: Acoustic Zooplankton and Fish Profiler

CAO: Central Arctic Ocean

CTD: Conductivity Temperature Depth

dB: Decibel

DSL: Deep Sound Scattering Layer

DVM: Diel Vertical Migration

IKMT: Isaacs-Kidd Midwater Trawl

MAW: Modified Atlantic Water

MVBS: Mean Volume Backscattering Strength (decibels; logarithmic)

PH: Pacific Halocline

PSW: Polar Surface Waters

ROV: Remotely Operated Vehicle

s_A: Nautical Area Scattering Coefficient (linear)

S_A: Nautical Area Scattering strength (decibels; logarithmic)

SNR: Signal-to-Noise Ratio

SSL: Surface Sound Scattering Layer

S_V: Volume Backscattering Strength (decibels; logarithmic)

SVM: Seasonal Vertical Migration

TS: Target Strength (decibels; logarithmic)

UVP: Underwater Vision Profiler

WBAT: Wideband Autonomous Transceiver

WMD: Weighted Mean Depth

1 Chapter one: General introduction

1.1 The Arctic Ocean

1.1.1 Geography and physical oceanography

The Arctic Ocean is the northernmost and smallest of the world's five main oceans. It covers an area of 14 060 000 km^2 and forms a mediterranean sea surrounded by the European, Asian, North American land masses and the large island of Greenland (Figure 1-1). The Arctic Ocean is an integral part of the world's Ocean and links the Pacific and Atlantic. It is split between deep abyssal plains and shallow continental seas, each of them covering about half of the total area of the Arctic Ocean (Jakobsson et al., 2020). The Central Arctic Ocean (CAO) is composed of two main deep basins with bottom depths ranging between 3000 to 5000 m – the Amerasian (composed of the Canada Basin and Makarov Basin) and Eurasian Basin (composed of the Amundsen Basin and Nansen Basin) separated by the Lomonosov Ridge cutting through the North Pole. Numerous shallow shelf seas (ca. 200-300 m depths) are found around the CAO. The large shelf to basin area ratio is unique to the Arctic Ocean, in that abyssal plains dominate the other oceans. In this thesis, I define the Arctic Ocean as the CAO and its surrounding shelf seas (Bluhm et al., 2015).

The Arctic Ocean receives inflow from the Atlantic and Pacific Oceans and from North American and Siberian rivers (Figure 1-2a). The complex bathymetry of the Arctic Ocean is categorized into essential hydro-morphological domains (Carmack and Wassmann, 2006). These domains include inflow shelves, interior shelves, outflow shelves, riverine coastal domain (narrow zone of major influence of freshwater discharge near land masses; Carmack et al., 2015), the deep basins of the CAO, and ridges and land features (Figure 1-2b).

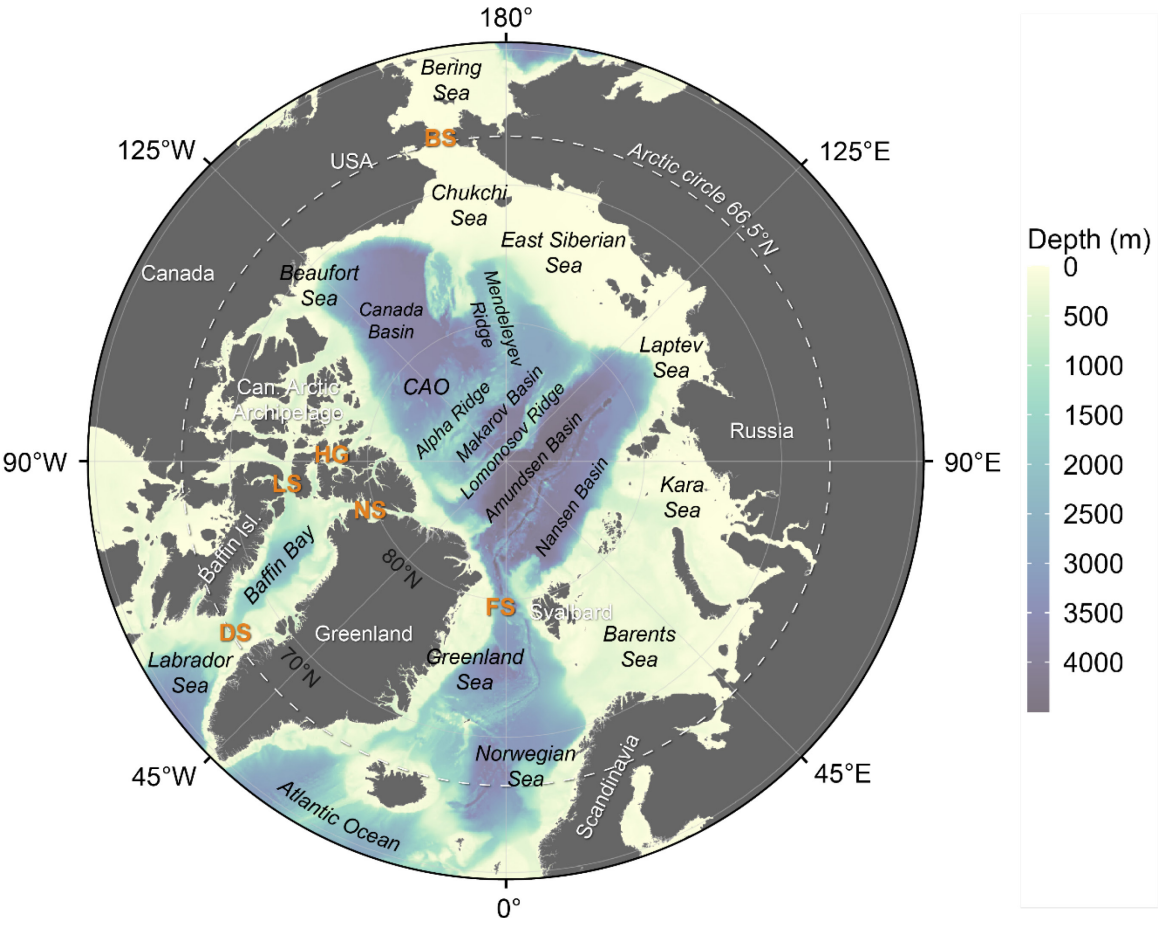

Figure 1-1. Bathymetry of the Arctic Ocean composed of the deep basins in the Central Arctic Ocean (CAO) and surrounding shelf seas. The main straits are indicated in orange – *BS*: Bering Strait; *DS*: Davis Strait; *FS*: Fram Strait; *HG*: Hell's Gate; *LS*: Lancaster Sound; *NS*: Nares Strait.

There are two main inflow shelves, one on the Atlantic side and one on the Pacific side, as well as two main outflow shelves on either side of Greenland-Baffin Bay and western Fram Strait. The largest inflow of Atlantic water into the Arctic Ocean is via eastern Fram Strait near Svalbard, estimated at ca. 7 Sverdrup[1], followed by the Barents Sea Opening at ca. 2 Sverdrup (Beszczynska-Möller et al., 2012; Schauer et al., 2004, 2002). Because the Fram Strait is the only deep-water connection to the CAO, its large inflow supplies most of the Atlantic water into the deep basins (Figure 1-2b; Rudels, 2015; Timmermans and Marshall, 2020). Some Atlantic water also penetrates into Baffin Bay through Davis Strait along

[1] One Sverdrup is equal to a flow rate of one million cubic metre per second (1 Sverdrup = 1 $hm^3\ s^{-1}$)

western Greenland via the West Greenland Current, but at a much lower magnitude compared to the Fram Strait (ca. 1 Sverdrup), and this inflow does not reach the CAO (Cuny et al., 2005; Curry et al., 2014; Münchow et al., 2006). Once in the Arctic, Atlantic water circulates in the subsurface (below ca. 200 m depth) cyclonically along the continental slope and ridge features (Rudels, 2015). During its journey, Atlantic water loses some of its heat to the atmosphere, particularly in the European Arctic around Svalbard and the Barents provoking sea ice melt (Årthun et al., 2012). Modified Atlantic water eventually exits through the western Fram Strait and the Canadian Arctic Archipelago via Nares Strait, Lancaster Sound and Hell's Gate (Rudels, 2015; Timmermans and Marshall, 2020; Wekerle et al., 2013).

The shallow Bering Strait connects the Pacific and Arctic Oceans (ca. 90 m depth; Woodgate and Peralta-Ferriz, 2021). The low salinity Pacific water entering the Arctic Ocean near the surface combined with the large freshwater river runoffs, and sea ice melt, form a vast reserve of relatively fresh water laying on top of Atlantic water which influences global climate and oceanic circulation (Figure 1-2c; Carmack et al., 2016; Rabe et al., 2014). These low salinity surface waters form the Pacific Halocline and lay on top of the more saline Atlantic water mass (Carmack, 2007). This halocline forms a strong physical barrier between sea ice and the warm Atlantic layer, limiting sea ice melt. The stratification also decreases mixing processes between surface and deep-waters, preventing nutrient renewal of surface waters and constraining primary production (Carmack and Wassmann, 2006; Tremblay et al., 2008). The Pacific Halocline is characteristic of the western part of the Arctic Ocean (Amerasian basin, Chukchi Sea and Beaufort Sea) and is less pronounced in the eastern part, with the Atlantic/Pacific Halocline front located above the Mendeleyev ridge (Figure 1-2c; McLaughlin et al., 1996). The main outflow areas of

Pacific-origin waters are Baffin Bay, through the Canadian Arctic Archipelago, and the western Fram Strait (Haine et al., 2015; Münchow et al., 2006).

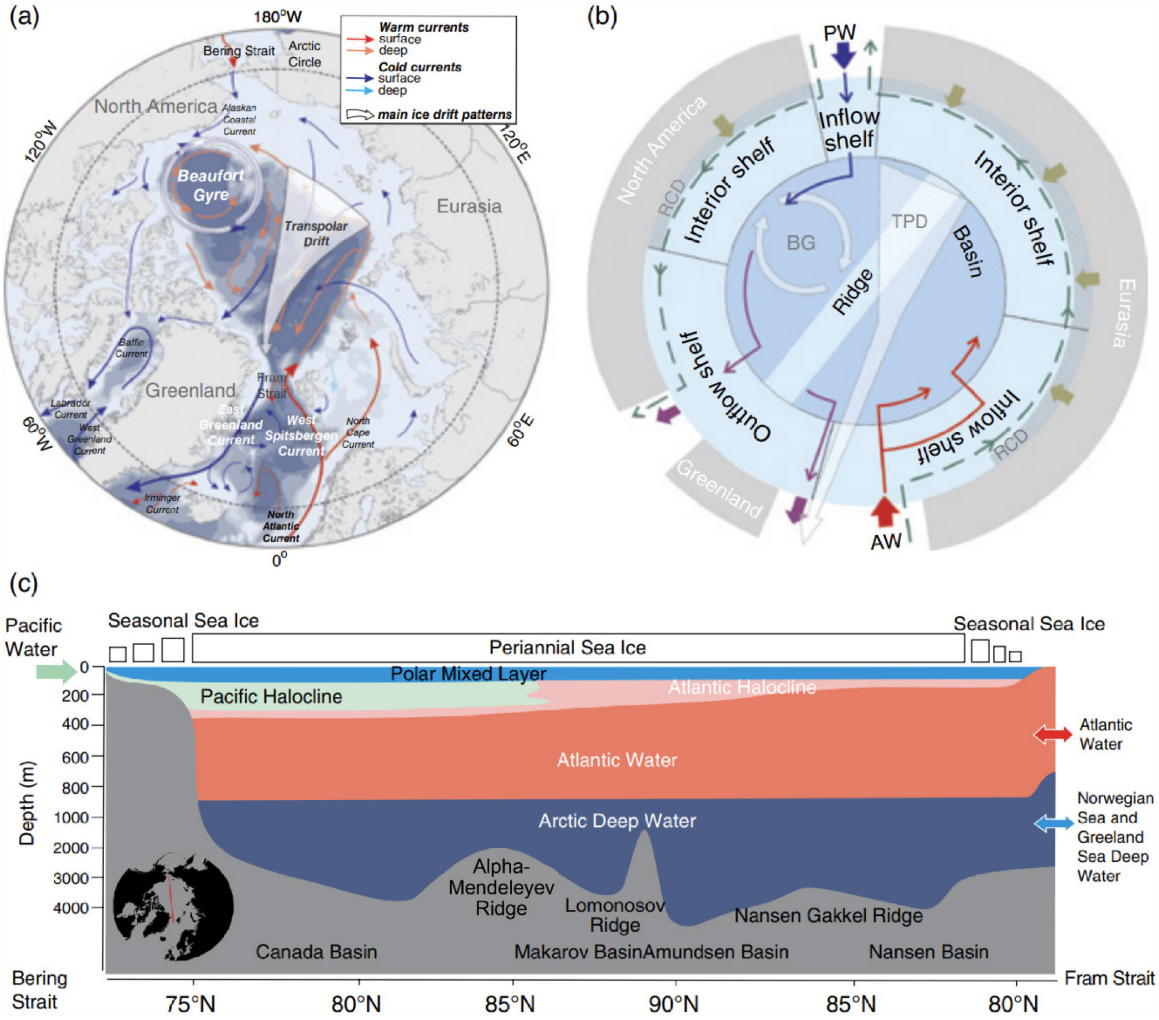

Figure 1-2. (a) Major surface and deep current systems of the Arctic Ocean, and (b) conceptual understanding of the hydrological regimes of the Arctic Ocean based on the nomenclature from Carmack and Wassmann (2006). *AW*: Atlantic Water; *BG*, Beaufort Gyre; *PW*, Pacific Water; *RCD*: River coastal domain; *TPD*: Transpolar Drift. Arrows denote component flow directions; large white arrows show major ice drift patterns. (c) Cross-section of the Arctic-Ocean from Bering Strait (left) to Fram Strait (right) showing the vertical distribution of water masses within the CAO. (modified from Daase et al., 2021).

Four main water masses can be defined according to their origin within the Arctic Ocean in order of increasing density (Figure 1-2c): Arctic surface waters – also referred to as Polar Surface Waters or Arctic Waters in the literature (ASW; temperature range: -1.7-4.0 °C, salinity range: 28.0-34.8 psu), the Pacific Halocline (PH; difference in salinity across the

halocline ranging from 2 to 10 psu), Atlantic-origin water (AW; temperature range: 0.6-3.0 °C, salinity range: 34.8-34.9 psu), and Arctic deep water (ADW; temperature range: -0.9 - -0.5 °C, salinity range: 34.92-34.95 psu; Bluhm et al., 2015). Their presence and characteristics vary spatially, for example, Atlantic waters are warmer in the Amundsen Basin than in the Canada Basin of the CAO (Carmack et al., 2016).

1.1.2 A highly seasonal environment

1.1.2.1 Sea ice cover

One of the most emblematic features of the Arctic Ocean is the presence of a sea ice cover. Sea ice primarily exists in polar regions, and since the late 1970s, when satellite-based estimates of sea ice extent became available, about 5 % of the world's oceans have been covered by sea ice at any one time (Stroeve and Notz, 2018). The low-salinity waters found at the surface of the Arctic Ocean, combined with the cold atmospheric temperatures prevailing in polar environments, create favourable conditions for sea ice formation. Arctic sea ice exhibits a yearly growth-melt cycle generally aligned with the solar cycle. The minimum sea ice extent is reached in September around the autumnal equinox when sea ice covers ca. 15.1 million km^2 (1991-2020 median extent; OSI SAF Global Sea Ice Concentration CDR 3.0 data retrieved from Copernicus on 09/05/2023). When the solar heat flux decreases in autumn, sea ice grows and eventually reaches a maximum extent of ca. 6.0 million km^2 (1991-2020 median extent) around the vernal equinox in March.

Sea ice is not static on top of the Arctic Ocean – it floats – and is thus influenced by wind and oceanic circulation. The main sea ice current is the Transpolar Drift Current, where sea ice is transported from the Siberian Arctic toward Svalbard and Greenland and exported

through the Fram Strait. In the Amerasian basin, the Beaufort Gyre retains sea ice within the Canada basin, which circulates anticyclonically (Bluhm et al., 2015).

Sea ice and snow shield surface waters of the Arctic Ocean from the atmosphere and considerably influence energy fluxes and global climate (Nicolaus et al., 2012; Vihma, 2014). Because not all the sea ice melts during the melt season, newly formed sea ice builds on top of old ice (multiyear ice) forming the perennial sea ice cover which can be over several metres thick (Kwok, 2018). Multiyear ice is primarily found in the Arctic (Serreze and Meier, 2019) and is nowadays primarily located in the Lincoln Sea north of Greenland (Lange et al., 2019).

The Arctic Ocean is under strong environmental pressure due to climate change. The sea ice and snow cover have a high albedo – index of reflectivity of a surface, e.g., an albedo of one reflects all the incoming radiation – reflecting most of the solar radiation. Because of rising atmospheric and oceanic temperatures, multiyear ice is gradually disappearing and is being replaced by a thinner seasonal sea ice cover (Serreze and Meier, 2019). For example, over the 1999-2017 period, the Arctic has lost about half of its multiyear ice (Kwok, 2018). Newly formed sea ice is more vulnerable to melting than multiyear ice because it is thinner. When sea ice melts, it is replaced by open waters with low albedo that absorbs more solar radiation than ice-covered areas, which increases oceanic temperatures and further enhances sea ice melt. This phenomenon is called the Arctic amplification and it contributes to making the Arctic one of the global regions with the fastest temperature increase, on average twice as fast as the global average (Hoegh-Guldberg and Bruno, 2010; Serreze and Barry, 2011). The increased inflow of warm water of Atlantic and Pacific origin also enhances sea ice melt (Polyakov et al., 2017; Woodgate and Peralta-Ferriz, 2021).

Climate models predict ice-free summers in the Arctic Ocean as early as the 2030s (Kim et al., 2023).

The thinning, decrease in spatial extent, and duration of sea ice is not homogeneous within the Arctic Ocean (Kwok, 2018; Polyakov et al., 2017). Areas such as the Lincoln Sea located north of Greenland, is one of the last areas in the Arctic with multiyear ice, and is expected to retain it the longest compared to other regions (Lange et al., 2019). In contrast, in the Barents Sea, the doubling of the volume of Atlantic water paired with a decrease by a factor of two of Arctic water volume has led to substantial decrease in sea ice coverage (Onarheim and Årthun, 2017; Oziel et al., 2016). Similarly, in the Chukchi Sea, sea ice duration has decreased due to the increased inflow and warming of Pacific water (Woodgate and Peralta-Ferriz, 2021). These inflow shelves can be seen as *"canaries in the coal mine"* – early indicators of climate change in the Arctic Ocean.

1.1.2.2 An extreme light regime

Another key characteristic of the Arctic Ocean is the presence of a strong seasonal light cycle. Above the Arctic Circle (66.5 °N), the photoperiod, (i.e., the duration of daylight over a 24-h cycle) alternates between periods of constant darkness, the polar night, and constant daylight, the polar day or midnight sun. The duration of polar night or polar day is not constant within the Arctic Circle but increases poleward (Figure 1-3). For example, at 75 °N, the polar night and polar day last for approximately 3 months each whereas at the North Pole it is 6 months (Berge et al., 2015b). There are also changes in light intensity throughout the diurnal cycle, even during the polar night and polar day. For instance, while the sun is always below the horizon during the polar night, it is closer to the horizon at solar noon, resulting in different levels of twilight depending on the latitude (Figure 1-4; Berge

et al., 2015b). This brightness around solar noon may be faint to the human eye, but Cronin et al. (2016) measured underwater light levels just below the ocean surface during the polar night and found levels comparable to those in the deep sea (500 m depth) during daytime (Kaartvedt et al., 2019a). While the polar night was thought to be a relatively dormant period for marine life, recent studies showed high biological activity occurring during that season (Berge et al., 2015a, 2015b, 2009; Hobbs et al., 2018).

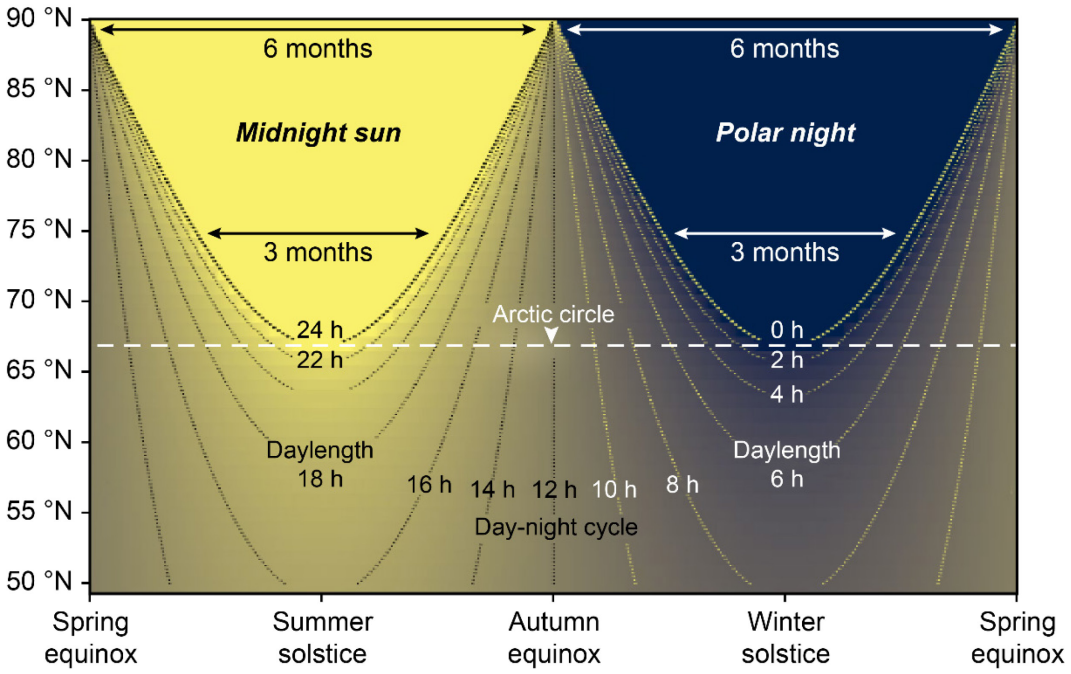

Figure 1-3. Duration of polar night (sun is always below the horizon) and polar day (also called midnight sun; sun is always above the horizon) in function of latitude. The photoperiod becomes increasingly extreme with latitude (modified from Ljungström et al., 2021).

Unlike sea ice cover, climate change does not affect photoperiod. The Earth's axial tilt cycle can modify the position of the polar circle and thus photoperiod, but this astronomical change occurs at a considerably longer time scale – 26,000 years – than that of climate change (Seidelmann, 1992). Its effect is thus negligible relative to the time scales considered within this thesis. Yet, the light available to biological process is indirectly impacted by climate change through decrease in sea ice and snow cover (Castellani et al.,

2022). Prior to the 21st century, the spring sea ice melt was restricted to the continental shelf seas, and the deep basins of the CAO were rarely exposed to direct sunlight. In more recent years, sea ice melt has extended past the shelf break and into the deep basins (Serreze and Meier, 2019). The effect of sea ice melt and increased light penetration on the marine ecosystem, e.g., on primary production or sympagic (ice-associated) organisms are still debated, and likely differ from one area of the Arctic Ocean to another (Ardyna and Arrigo, 2020; Steiner et al., 2021).

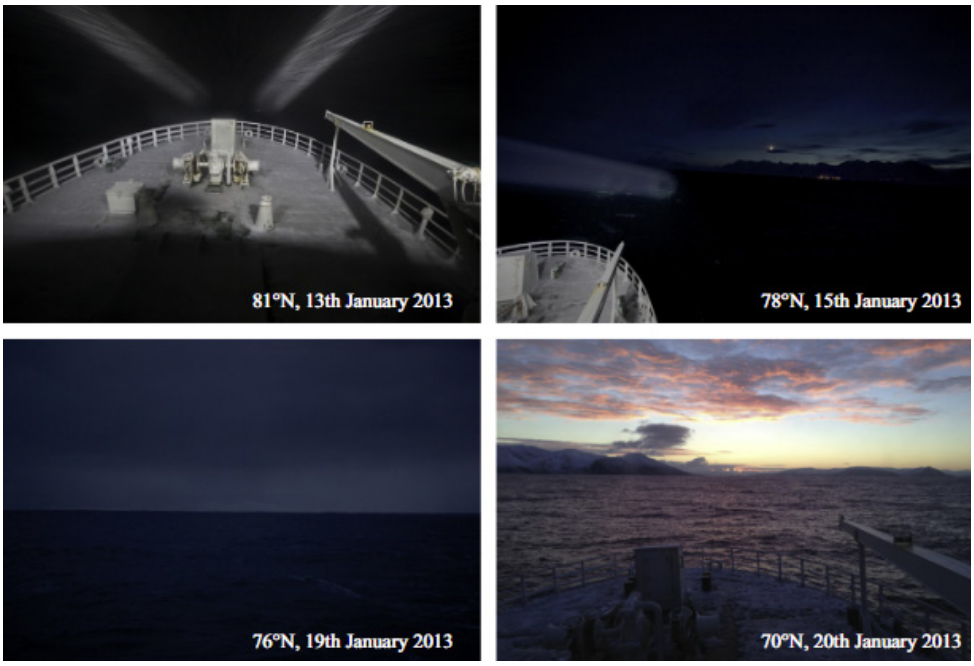

Figure 1-4. Light levels as seen by the human eye during the polar night at solar noon at 81 °N (upper left), 78 °N (upper right), 76 °N (lower left), and 70 °N (lower right; modified from Berge et al., 2015b).

1.2 The marine ecosystem of the Arctic Ocean

1.2.1 Primary production

Most of the annual primary production in the Arctic Ocean occurs during a relatively short period in spring and early summer, when enough sunlight and nutrients are available to allow for photosynthesis (Ardyna and Arrigo, 2020). The strong vertical stratification of

the water column of the Arctic Ocean, reduces vertical inputs of nutrients and winter nutrient concentrations strongly correlate with annual primary production in areas with low wind-driven or topographically-driven vertical mixing (Tremblay et al., 2015).

In ice-covered areas, the spring bloom generally starts with a sea ice algae bloom on the underside of the sea ice, followed by a short-lived pelagic phytoplankton bloom in the water column given appropriate growth conditions (Leu et al., 2015). The pelagic phytoplankton bloom can occur in open water and under the ice (Ardyna et al., 2020). It generally stops due to nutrient shortages in the euphotic zone in summer when a subsurface chlorophyll maximum develops (Ardyna et al., 2013; Martin et al., 2010). The delay in sea ice formation in autumn makes the upper ocean more vulnerable to mixing through wind stress, which can replenish surface waters in nutrients. These nutrient-rich waters, in combination with the increased light availability due to less sea ice, have increased the frequency of occurrence of autumn phytoplankton blooms over the last decades in the Arctic Ocean (Ardyna et al., 2014; Ardyna and Arrigo, 2020). During the polar night, primary production is small compared to the rest of the year and microalgal cell abundance is low (Randelhoff et al., 2020; Vader et al., 2015). Hence, seasonality in the Arctic light cycle and sea ice coverage stimulates seasonal pulses of primary production in spring – and sometime in autumn (depending on the time and location) – and constrains production to low levels during the winter months.

1.2.2 A specialized marine ecosystem

The extremely pulsed cycle of primary production combined with glacial temperatures, extreme photoperiod, and sea ice cover, have shaped unique marine ecosystems in the Arctic Ocean (Figure 1-5). Therefore, the Arctic fauna has developed a high degree of

specialization to its environment. While the upper trophic levels of the Arctic marine ecosystem generally have lower biodiversity than their tropical and temperate counterparts, the complexity and diversity of the planktonic and benthic food web is equivalent to that of temperate latitude ecosystems (Smetacek and Nicol, 2005).

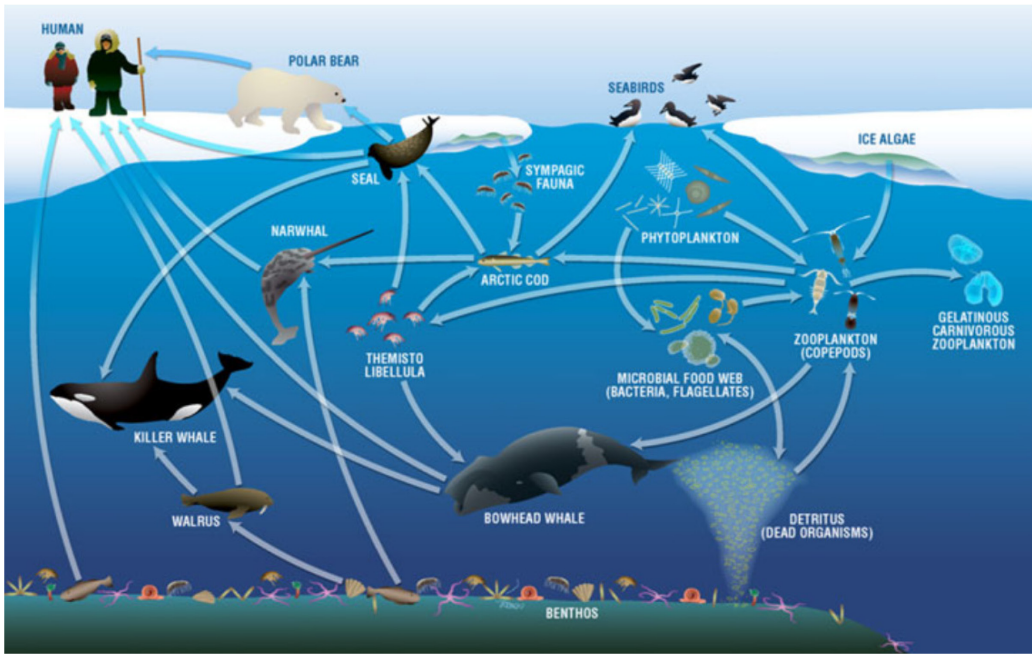

Figure 1-5. Schematic representation of an Arctic marine food web with a transition from a coastal (left) to an oceanic (right) ecosystem (from Darnis et al., 2012).

Among Arctic emblematic species, several top-predators endemic to the Arctic include polar bears (*Ursus maritimus*), narwhals (*Monodon monoceros*), and beluga whales (*Delphinapterus leucas*). These predators rely on energy channeled from primary production through lower trophic levels, including macrozooplankton and pelagic Arctic cod (*Boreogadus saida*), a central node within Arctic pelagic food webs (Bradstreet, 1986; Welch et al., 1992). Pelagic fish and large carnivorous zooplankton (e.g., *Themisto libellula*), feed on copepods which accumulate lipids synthesized by primary producers (Darnis et al., 2012). All these species have developed specific life history strategies and physiological adaptations to cope with the Arctic environment.

1.2.3 Pelagic vertical zonation and migrations

Light intensity decreases exponentially with depth due to absorption by the water itself, algae, inorganic and organic particulate matter (e.g., marine snow, sediments from river discharge), and dissolved organic compounds, and through scattering where suspended particles reflect light in different directions (Lalli and Parsons, 1997). The light attenuation coefficient measures this extinction of light through the water column. Traditionally, researchers have divided the upper water column of the ocean in vertical zones based on light penetration profiles (Figure 1-6). The epipelagic zone has sufficient light intensity to support primary production and generally corresponds to the upper 200 m of the water column. The mesopelagic zone – also referred to as the *"twilight zone"* – is located below the epipelagic between 200 and 1000 m depth; light levels are too low for photosynthesis, yet biological vision is possible (Kaartvedt et al., 2019a). The bathypelagic zone lies below the mesopelagic (> 1000 m depth) and light intensity is too low to support biological vision (Lalli and Parsons, 1997).

Fundamentally, light shapes the pelagic ecosystem with the strong vertical gradient in irradiance. Hence, pelagic fauna have developed life history strategies to take full advantage of that third dimension (Cohen and Forward, 2009; Darnis and Fortier, 2014; Hays, 2003). In the epi- and mesopelagic zone, many organisms rely on vision to forage. Thus, both visual predators and their prey have developed behaviours to accommodate diel or seasonal changes in light, mainly through vertical migrations (Hays, 2003). We can distinguish two types of vertical migrations: diel vertical migrations (DVM) occurring within a 24-h cycle, and seasonal vertical migrations (SVM) occurring within the annual cycle (Bandara et al., 2021).

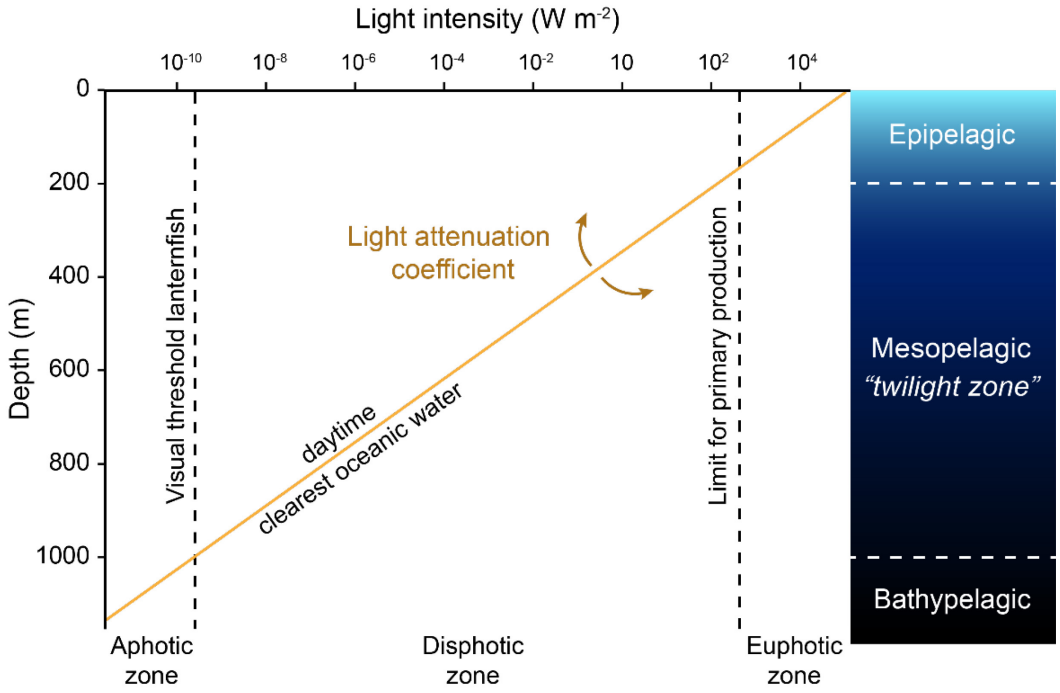

Figure 1-6. Light penetration from clear oceanic waters and corresponding ecological zones. Note the logarithmic scale of light intensity. The light attenuation coefficient changes the slope of light penetration into the water column, i.e., a high attenuation coefficient reduces light penetration (modified from Lalli and Parsons, 1997).

While predator-prey interactions and satiety levels are considered to be the ultimate drivers of DVM, diel changes in light intensity are considered to be the main proximate driver (Cohen and Forward, 2009; Hays, 2003; Pearre, 2003). Hence, an individual tries to balance predation risk while optimizing foraging – success is *"to see but not be seen"* (Ljungström et al., 2021). For example, herbivorous copepods can ascend to the surface layer at night to graze on algae when darkness limits mortality from visual predation, they then descend to greater depths during the day to avoid visual predators near the surface where light levels are high (Fortier, 2001). However, these behaviours are flexible and satiety levels or predation pressure may disrupt normal DVM patterns (Hays, 2003; Pearre, 2003; Urmy and Benoit-Bird, 2021). For example, reverse DVM, where fish or zooplankton ascend to shallower depths during the day and descend to greater depth during the night, has been

documented in both zooplankton and mesopelagic fish (Dypvik et al., 2012a; Irigoien et al., 2004).

In areas where there are strong seasonal variations in light availability or food supply, like the Arctic, SVM can occur. SVM is a common adaptation among Arctic zooplankton species which generally feed intensely during the peak in primary production near the surface in spring and spend the rest of the year overwintering at meso- or bathypelagic depths (Darnis and Fortier, 2014). During their overwintering phase, zooplankton benefit from the low light intensities prevailing at mesopelagic depth to maximize their survival by limiting visual predation (Bagøien et al., 2001; Dale et al., 1999).

DVM and SVM are not mutually exclusive, and DVM patterns may occur in addition to SVM. SVM and DVM are common in both pelagic nekton and zooplankton taxa (Cohen and Forward, 2009). These behaviours contribute to the biological carbon pump by actively transporting carbon from surface layers to greater depths (Siegel et al., 2023). There remain large uncertainties regarding the amount of carbon exported out of the euphotic zone by mesopelagic organisms, but recent studies estimated the global carbon flux due to migrating fish and zooplankton around 14-16 % (Archibald et al., 2019; Saba et al., 2021).

1.2.4 Zooplankton

Functional groups of zooplankton can be divided into size classes. Here I focus on mesozooplankton (0.2-20.0 mm length) and macrozooplankton (> 20.0 mm length) because they are important prey of the large stocks of fish, seabirds, and marine mammals in the Arctic Ocean (Darnis et al., 2012). The three herbivorous calanoid copepod species *Calanus hyperboreus*, *Calanus glacialis*, and *Calanus finmarchicus*, the omnivorous copepod *Metridia longa*, euphausiid (krill) species of the genus *Thysanoessa*, carnivorous

hyperiid amphipods of the genus *Themisto*, a few gelatinous taxa (ctenophore, cnidarian, siphonophores) and, in ice-covered areas, the ice-amphipods (mostly *Apherusa glacialis*) comprise most of the zooplankton biomass (Daase et al., 2021).

Arctic zooplankton have developed specific life history strategies to take full advantages of the high seasonality in primary production. In general, three types of strategies are realized by overwintering zooplankton (Hagen, 1999):

- *Type 1 – Diapause*: Accumulation of lipid reserves during the productive season and overwintering in a dormancy state.
- *Type 2 – Flexibility*: Accumulation of lipid reserves during the productive season and reduced metabolic activity the rest of the year but the organism remains active. Opportunistic feeding and/or dietary shift combined with body mass depletion during the polar night.
- *Type 3 – "Business as usual"*: No change in metabolic activity and opportunistic feeding throughout the year, including during the polar night.

1.2.4.1 Mesozooplankton

Among the mesozooplankton community in the Arctic, large copepods such as the Arctic *C. hyperboreus* and *C. glacialis*, and the boreal species *C. finmarchicus* and *M. longa* dominate the biomass (Choquet et al., 2017; Freer et al., 2022; Hirche and Mumm, 1992). However, small copepod species like *Oithona similis*, *Triconia borealis*, *Pseudocalanus* spp. and *Microcalanus pygmaeus* are the most abundant (Daase et al., 2021). While small copepods are an important link between the microbial food web and carnivorous zooplankton and fish larvae at some time of the year, their overall contribution to the energy

transfer from primary producers to upper trophic levels is negligible compared to that of large copepod species (Madsen et al., 2008).

Copepods - Calanus spp.

Calanus spp. are herbivorous filter feeders relying on the Type 1 – Diapause strategy for overwintering. The *Calanus* complex (*C. hyperboreus*, *C. glacialis*, and *C. finmarchicus*) performs extensive SVM (Darnis and Fortier, 2014). *Calanus* spp. graze on ice algae and pelagic phytoplankton at the surface in spring and accumulate large lipid reserves which can exceed 60 % of their dry mass (Falk-Petersen et al., 2009). They then descend to depths after the productive season where they overwinter in a state of dormancy, surviving on lipid reserves until next productive season (Ashjian et al., 2003; Daase et al., 2013; Darnis and Fortier, 2014). The overwintering depth depends on the species but also on other biotic factors such as the presence of predators which can deepen their overwintering depth (Dale et al., 1999). In addition to the SVM, *Calanus* generally undergo synchronous DVM during the light transition periods in spring and autumn. Synchronized DVM stop during the midnight sun period (Blachowiak-Samolyk et al., 2006), when asynchronous DVM, i.e., individual based DVM may instead prevail (Cottier et al., 2006).

During the polar night, the majority of the *Calanus* population is thought to be in diapause at depth. However, a number of recent studies challenge this paradigm given that aggregations of active *C. finmarchicus* have been observed at the surface during the polar night (Espinasse et al., 2022), and performing DVM (Berge et al., 2015a, 2015b; Darnis et al., 2017). Thus, the behaviour of *Calanus* species is more flexible and complex than previously assumed (Berge et al., 2015a; Daase et al., 2013). As climate warms and Atlantic water inflow increases, the prevalence of smaller and less lipid-rich *Calanus finmarchicus*

may increase in the Arctic Ocean, with cascading effects on the rest of the ecosystem (Renaud et al., 2018).

Copepods – Metridia longa

Another important copepod species in the Arctic Ocean is *Metridia longa*. This calanoid copepod is comparable in size to *Calanus finmarchicus* and also commonly occurs in the subarctic (Hays, 1995). However, in contrast to *Calanus* spp., *M. longa* are omnivorous and may possibly feed on *Calanus* eggs (Darnis and Fortier, 2014). The life history of *Metridia longa* differs from that of *Calanus* species and follows the Type 2 – Flexibility strategy for overwintering. This species does not exhibit strong SVM and is generally found in the deeper part of the water column, at mesopelagic depths (Ashjian et al., 2003; Darnis and Fortier, 2014; Wang et al., 2019). During the polar night, *M. longa* usually occur close to the surface, where they feed and reproduce (Berge et al., 2015a). This species is bioluminescent, like many other mesopelagic species, a trait that could explain their prevalence in surface waters during the polar night (Cronin et al., 2016).

1.2.4.2 Macrozooplankton

In addition to mesozooplankton, macrozooplankton (zooplankton taxa larger than 20.0 mm) are important nodes within Arctic marine food webs (Amiraux et al., 2023; Pedro et al., 2023; Welch et al., 1992). Macrozooplankton can be separated into two groups, sympagic (ice-associated) species that utilize the underside of sea ice and pelagic species found in the water column. Macrozooplankton can be herbivorous like euphausiids of the genus *Thyssanoessa*, or carnivorous, such as amphipods of the genus *Themisto*, or the ctenophore *Beroë cucumis*.

Sympagic amphipods

The sympagic macrozooplankton community is dominated by amphipods, and *Apherusa glacialis* are the most abundant (Arndt and Swadling, 2006). While knowledge gaps remain regarding their life history strategies, studies suggest that ice amphipods have a pelagic phase and an ice-associated phase (Berge et al., 2012b). Ice-amphipods graze on ice algae on the underside of sea ice in spring (Gulliksen and Lønne, 1991). Because their habitat disappears due to seasonal sea ice melt and drift, they have been hypothesized to descend to 200-900 m depth to use Atlantic water currents to redistribute poleward (Berge et al., 2012b), which could explain the occurrence of ice-amphipods in the mesopelagic zone (Werner et al., 1999). However, the life history strategy of *Apherusa glacialis* is complex and not well understood (Kunisch et al., 2020).

***Euphausiid - Thyssanoessa* spp.**

Euphausiids are an important pelagic taxa within the Arctic food web (Falk-Petersen et al., 1990). *Thyssanoessa inermis* are the most common krill species in areas influenced by Atlantic water (Buchholz et al., 2012; Dalpadado et al., 2016; Percy and Fife, 1985). In contrast to *Calanus* spp., *Thyssanoessa* remain active throughout the year, including the polar night (Type 2 – Flexibility). They tend to accumulate large lipid reserves in spring (Falk-Petersen et al., 2009) and shift their diet during the less productive time of season to be more opportunistic, and have the ability to shrink their body and regress their reproductive organs to conserve energy (Dalpadado and Ikeda, 1989; Huenerlage et al., 2015; Sargent and Falk-Petersen, 1981). Euphausiids perform DVM in spring and autumn and also during the polar night (Cottier et al., 2006; Darnis et al., 2017; Grenvald et al., 2016).

Hyperiid amphipod - Themisto spp.

Themisto libellula and *Themisto abyssorum* are the two most common species of pelagic hyperiid amphipods in the Arctic Ocean. *T. libellula* is endemic to the Arctic Ocean while *T. abyssorum* is boreal and considered a marker for the Atlantic water mass (Auel and Werner, 2003; Dalpadado, 2001). They are visual and opportunistic predators that follow the Type 3 – *"Business as usual"* overwintering strategy. *T. libellula* preferentially feed on *Calanus* spp. in summer whereas the more diverse *T. abyssorum* diet includes copepods and appendicularians (Dalpadado et al., 2008). Both species conduct DVM and feed on *Calanus* spp. during the polar night (Kraft et al., 2015, 2013), however, how these visual predators are able to feed during the polar night remains unknown. *Themisto* spp. are an important link between herbivorous copepods and higher trophic levels, and important prey for pelagic fish like Arctic cod (*Boreogadus saida*), seabirds, and seals (Cusa et al., 2019; Majewski et al., 2016; Vihtakari et al., 2018; Wathne et al., 2000).

Gelatinous macrozooplankton

Gelatinous predators, like ctenophores, hydromedusae, scyphomedusae, and siphonophores are other important carnivorous zooplankton within Arctic marine food webs. Their biology remain poorly understood in the Arctic because of the difficulties inherent to sampling fragile organisms which are hard to preserve (Kosobokova et al., 2011; Raskoff et al., 2005). The two main ctenophore species found in the Arctic Ocean are *Mertensia ovum* and *Beroë cucumis*. Physonect siphonophore species, i.e., siphonophores with a gas inclusion, such as *Rudjakovia plicata* and *Marrus orthocanna* can also occur within the Arctic Ocean at mesopelagic depths (Snoeijs-Leijonmalm et al., 2022).

1.2.5 Pelagic fish and cephalopods

Arctic fish communities, particularly those under perennial sea ice and in the deep basins of the CAO, are poorly studied because sea-ice conditions, remoteness, and costs limit sampling. Besides logistical constraints, the most serious difficulty to a comprehensive understanding of pelagic fish distribution and species richness in the Arctic Ocean is knowledge based on opportunistic and fragmentary observations, with no coherent time series. However, over the last decades, multiple scientific initiatives have started tackling this issue. For example, the scientific program conducted from the Canadian research icebreaker CCGS *Amundsen* has built a long-term time series of acoustic-trawl data within the Canadian Arctic which has been surveyed yearly since 2003. Furthermore, overwintering expeditions like the North Water Polynya Study (NOW) in 1997-1998 in northern Baffin Bay (CCGS *Amundsen*; Deming et al., 2002), the 2003-2004 Canadian Arctic Shelf Exchange Study (CASES) in the Beaufort Sea (CCGS *Amundsen*; Fortier and Cochran, 2008), the Circumpolar Flaw Lead System Study (CFL) in the Beaufort Sea during the 2007-2008 International Polar Year in 2007-2008 (CCGS *Amundsen*; Barber et al., 2010), or more recently the Multidisciplinary drifting Observatory for the Study of Arctic Climate (MOSAiC) in 2019-2020 in the CAO (R/V *Polarstern*; Shupe et al., (2020), have gathered crucial data which improved our knowledge of seasonality of Arctic ecosystems.

The most recent census on fish showed that 225 fish species occur in the Arctic Ocean, of which 21 % are considered Arctic, 71 % boreal, and 8 % widely distributed (Mecklenburg et al., 2018). Only 14 % of fish species found in the Arctic (regardless of their origin) are pelagic throughout their entire life cycle and the vast majority display ontogenetic changes with pelagic and demersal behaviours (Mecklenburg et al., 2018). However, considerable

knowledge gaps remain regarding the species composition and distribution of mesopelagic organisms in the Arctic Ocean. Here, I summarize the ecology of the most abundant taxa previously sampled in the mesopelagic zone of the Arctic Ocean including Arctic specialists and boreal species (Geoffroy et al., 2019). There are certainly other important species present in the Arctic Ocean, but if knowledge on the ecology of abundant mesopelagic species is scarce, that of rare species is elusive.

1.2.5.1 Arctic endemic species

Arctic cod (Boreogadus saida)

The Gadidae Arctic cod (*Boreogadus saida*; also known as polar cod in Europe) are likely the best studied pelagic fish in the Arctic due to their vast distribution and key role in the Arctic food web (Bradstreet, 1986; Mecklenburg et al., 2018; Welch et al., 1992). In the Canadian Arctic, these small forage fish (< 30 cm) represent > 90 % of the midwater fish community and occur in the CAO and surrounding Arctic shelf seas (Aune et al., 2021; David et al., 2016; Geoffroy et al., 2016; Nelson et al., 2020). Arctic cod associate with a wide variety of habitats including ice-free, nearshore marine waters, brackish lagoons, deeper shelf and slope areas, and in connection with anfractuosities in the sea-ice (Gradinger and Bluhm, 2004; Mecklenburg et al., 2018). Arctic cod can sustain sub-zeros temperatures because their blood contains antifreeze proteins synthesized in sub-zero temperatures (Nahrgang et al., 2010). Over its life cycle, this species occupies the entire water column – juveniles are found in the epipelagic and underside of the sea ice and larger congeners aggregate in the mesopelagic zone or near the seafloor (Geoffroy et al., 2016). Mature adults can conduct seasonal horizontal migrations (documented over at least 190 km) to their spawning ground in autumn (Aune et al., 2021; Kessel et al., 2017), where they

aggregate in the mesopelagic zone when sea ice cover has consolidated (Benoit et al., 2014; Geoffroy et al., 2011).

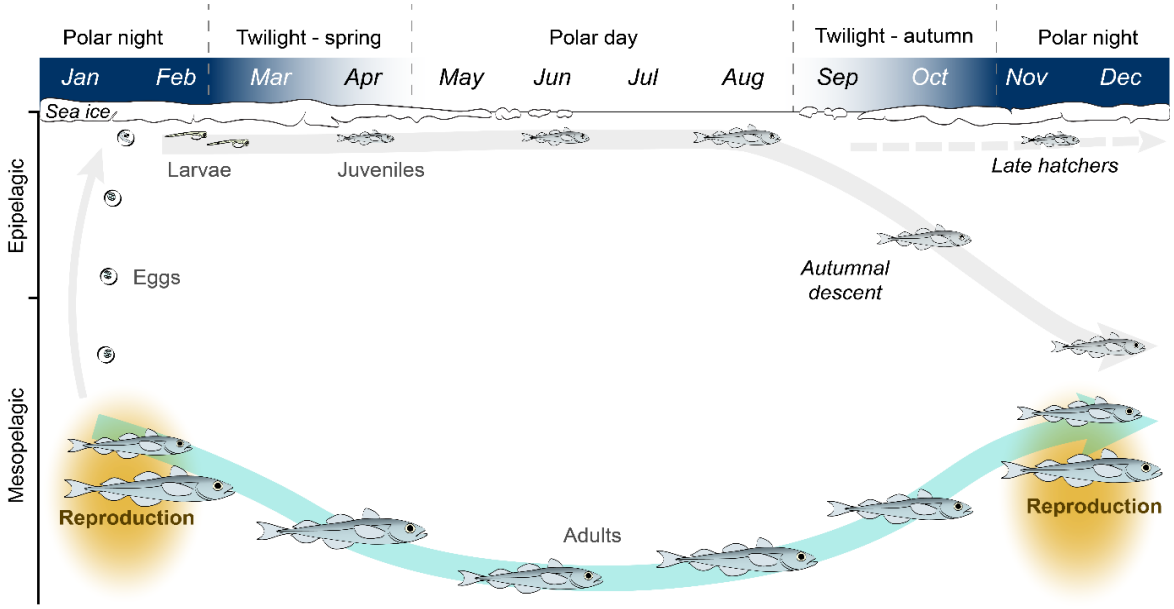

Figure 1-7. The life cycle of Arctic cod based on data from the Beaufort Sea (Geoffroy et al., 2016). Reproduction is suggested to occur at mesopelagic depth during the polar night, buoyant eggs rise to the surface and hatch under the ice. Juveniles stay under the ice during the productive season and descend to mesopelagic depths to join larger congeners in autumn. Late hatchers are hypothesized to stay in the epipelagic throughout the polar night to feed and descend to mesopelagic depth the following autumn.

Arctic cod are iteroparous (can spawn repeatedly over its life span), and, like many Arctic fishes, spawn in winter during the polar night (Figure 1-7; Geoffroy and Priou, 2020). After spawning, adults progressively migrate deeper in the water column as light intensity increases throughout the year, presumably to avoid diving marine mammals (Geoffroy et al., 2016). In autumn and spring, mesopelagic Arctic cod perform DVM within Atlantic waters and juveniles also perform DVM restricted to epipelagic depths (Benoit et al., 2010; Geoffroy et al., 2016). The occurrence of newly hatched larvae throughout the Arctic Ocean suggests spawning in several sites and habitats (Bouchard et al., 2015). Fertilized Arctic cod eggs are positively buoyant and ascend to the surface layer where fry hatch under the ice cover in late winter-early spring. The ice cover provides shelter from seabird and larger

fish predation, and Arctic cod larvae can feed on the under-ice zooplankton community (Bouchard et al., 2016). Hatching starts as early as December and last as late as July in areas with high freshwater discharge like the Laptev Sea or Beaufort Sea; hatch is limited to April-July in areas with little freshwater input such as northern Baffin Bay or the Canadian Archipelago, a pattern linked to warmer temperatures of brackish waters compared to seawater (Bouchard and Fortier, 2011). An early hatch date maximizes the growth season and pre-winter size, which increases survival and overwintering success leading to higher larval recruitment (Bouchard et al., 2015; Schembri et al., 2022).

As opportunistic planktivorous feeders, Arctic cod adapt their diet to spatial and temporal changes in prey availability (Cusa et al., 2019; Majewski et al., 2016). After yolk resorption, Arctic cod larvae feed on nauplii of small copepods (*Pseudocalanus* spp., *Oithona similis*, and *Triconia borealis)*, and on the eggs of larger copepod species (*Calanus hyperboreus* and *Metridia longa*) before shifting to copepodite stages of *Pseudocalanus* spp. and *Calanus glacialis* (Bouchard et al., 2016; Bouchard and Fortier, 2008). Juvenile Arctic cod (< 15 cm) mainly target calanoid copepods and amphipods whereas larger (> 15 cm) Arctic cod feed on larger prey like euphausiids, amphipods, and teleost fish (including cannibalism of juvenile Arctic cod; Hop and Gjøsæter 2013, McNicholl et al., 2016, Cusa et al., 2019).

Ice cod (Arctogadus glacialis)

In addition to Arctic cod, the other Gadidae endemic to the Arctic is the ice cod (*Arctogadus glacialis*; also sometime referred to as Arctic cod in literature, not to be confused with *Boreogadus saida*) which also has a circumpolar distribution (Aschan et al., 2009; Mecklenburg et al., 2018). Both species are morphologically similar, and are almost

impossible to differentiate as larvae and juveniles (Bouchard et al., 2013). *A. glacialis* distribution is poorly known but overlaps with that of Arctic cod on Arctic continental shelves, often in coastal habitats, and sometimes in brackish waters (Mecklenburg et al., 2018). Similarly to Arctic cod, ice cod possess antifreeze glycoproteins in their blood that allow them to survive in sub-zero temperatures (Præbel and Ramløv, 2005). Ice cod are generally less abundant than Arctic cod and, for example, represent < 9 % of juvenile Gadidae in the Amundsen Gulf (Bouchard et al., 2016; Madsen et al., 2016).

Similarly to Arctic cod, ice cod are opportunistic planktivorous feeders, consuming the most abundant prey available, with juvenile fish feeding on mesozooplankton (mostly *Calanus* spp. and *Metridia longa*), and adults on macrozooplankton, e.g., amphipods and mysids (Christiansen et al., 2012; Süfke et al., 1998). The life cycle of ice cod is poorly known, but their vertical distribution may resemble that of Arctic cod, with juveniles found under the ice (Bouchard et al., 2016), and adults at mesopelagic depths or near the seafloor (Aschan et al., 2009). The spawning period of ice cod varies greatly temporally, with reproduction in winter and hatching in March-July (Bouchard et al., 2013; Jordan et al., 2003).

Other Arctic species

Other Arctic species commonly found in the mesopelagic realm are snailfish (*Liparis* spp., mostly *Liparis fabricii*) and the cephalopod *Gonatus fabricii*. Interestingly, gelatinous snailfish (*Liparis fabricii*) are categorized as a continental shelf demersal fish (Mecklenburg et al., 2018) but adult specimens (> 20 cm) often inhabit the mesopelagic zone of the deep basins of the CAO and Arctic seas (Mecklenburg et al., 2007). Adult *Liparis fabricii* are also a common prey for pelagic predators including fish of commercial

interest like Greenland halibut (*Reinhardtius hippoglossoides*) and seals (Falk-Petersen et al., 2004; Giraldo et al., 2018). However, relatively little information exists on snailfish in the Arctic, with considerable knowledge gaps regarding their ecology and interactions with other trophic levels.

The boreo-Atlantic armhook squid (*Gonatus fabricii*), despite its name, is an Arctic species with a potential circumpolar distribution (Gardiner and Dick, 2010; Xavier et al., 2018). I categorize this species as Arctic because it is the only cephalopod species to complete its entire life cycle within the Arctic Ocean (Golikov et al., 2019). *Gonatus fabricii* has been documented in the Barents Sea, the Eurasian and Amerasian Basins of the CAO, Baffin Bay, and is also common to the North Atlantic. It is the most abundant cephalopod in the Arctic (Golikov et al., 2017).

Armhook squid generally spawn in winter (Bjørke and Hansen, 1996; Wiborg et al., 1984). *Gonatus fabricii* is lipid-rich (Hooker et al., 2001) and occupy a central position within the Arctic food web as both prey and predator (Chambers and Dick, 2007). Juveniles with length < 2 cm mostly feed on copepods in the epipelagic zone. As they grow larger (< 5 cm), armhook squid start exploiting a larger portion of the water column and shift their diet from copepod to macrozooplankton, fish, and other cephalopods (Golikov et al., 2022). When they reach 5 cm in length, *G. fabricii* migrate to the mesopelagic zone and mostly feed on fish and other cephalopods (Golikov et al., 2022). This species conducts DVM both as juveniles and adults (Kristensen, 1984; Moiseev, 1991). *Gonatus fabricii* is an important prey for predatory fish like Greenland halibut, seabirds (e.g., fulmar), and narwhals (Gardiner and Dick, 2010; Wold et al., 2011; Xavier et al., 2018).

1.2.5.2 Boreal species

In addition to Arctic specialists, boreal fish species are extending their distribution poleward following the rise in temperature and increasing spatial overlap with Arctic species in the Arctic gateway regions (Gordó-Vilaseca et al., 2023; Richardson et al., 2012). The northern range expansion of boreal species has resulted in lower abundances of Arctic specialists, which has retreated northward toward the cold Arctic water masses, a phenomenon known as the borealization of the Arctic ecosystem (Fossheim et al., 2015; Polyakov et al., 2020). For example, over the past two decades, capelin (*Mallotus villosus*) has gradually replaced Arctic cod as the main forage fish in northern Hudson Bay (Gaston and Elliott, 2014). Since the 1980s, juvenile beaked redfish (*Sebastes mentella*) have gradually replaced juvenile Arctic cod as the most abundant pelagic fish in the northwestern Barents Sea (Eriksen et al., 2015). Similarly, first sightings of boreal species have increased around the Arctic, including bluefin tuna (*Thunnus thynnus*) in eastern Greenland (MacKenzie et al., 2014) and Pacific sand lance (*Ammodytes hexapterus*) in the Beaufort Sea (Falardeau et al., 2017). Glacier lanternfish (*Benthosema glaciale*) and Atlantic cod (*Gadus morhua*) have also recently been sampled in the CAO (Ingvaldsen et al., 2023; Snoeijs-Leijonmalm et al., 2022; Zhang et al., 2022), yet, whether these observations relate to borealization or are representative of their normal distribution that was unreported until recently is unknown. Here, I summarise the ecology of the four most abundant boreal species sampled in offshore areas near Svalbard (76-81 °N) because this area has ongoing borealization (Fossheim et al., 2015; Geoffroy and Priou, 2020).

Beaked redfish (Sebastes mentella)

The Scorpaenidae beaked redfish (*Sebastes mentella*; also known as deepwater redfish) is the most widespread of the four redfish species that occur in the North Atlantic (Drevetnyak

and Nedreaas, 2009; Planque et al., 2013). They inhabit both continental shelves and deep basins of the North Atlantic, Barents Sea, Labrador Sea, and southern Baffin Bay (Cadrin et al., 2010). Beaked redfish perform extensive seasonal migrations from feeding to spawning grounds; however, there uncertainties remain regarding the migration paths and population connectivity (Drevetnyak and Nedreaas, 2009). Redfish also have a unique suite of life history characteristics, they are long-lived (maximum age of 40 y confirmed in the Barents Sea), slow growing, late maturing (50 % of specimens maturing by age 11-12), and iteroparous (i.e., they can spawn repeatedly; Planque et al., 2013). Instead of laying eggs, redfish are ovoviviparous, i.e. fertilization, egg development, and hatching occur internally, and fish larvae are extruded (St-Pierre and de Lafontaine, 1995). Recruitment varies greatly inter-annually, with strong year classes followed by years with very low recruitment (Drevetnyak and Nedreaas, 2009).

Larval extrusion occurs in winter along the continental slope of the Barents Sea and Irminger Sea; larvae ascend to the epipelagic zone where currents transport them to nursery grounds in the Barents Sea and eastern Greenland (Planque et al., 2013). In the Barents Sea, juvenile redfish occur further north and east than adults (Drevetnyak and Nedreaas, 2009). Juveniles spend the first years of their life in the nursery grounds and then migrate toward the continental slope to join the adult population (Drevetnyak and Nedreaas, 2009). Strong cohorts of juvenile redfish can also be found in both the epi- and mesopelagic zone where they can dominate the biomass (Geoffroy et al., 2019; Gjøsæter et al., 2020; Knutsen et al., 2017). Adult pelagic *S. mentella* are tightly coupled to the biological communities of the mesopelagic zone and are generally found between 300 and 600 m depth (Planque et al., 2013). The adults are restricted to Atlantic waters between 5-8 °C (Eriksen et al., 2015;

Ingvaldsen et al., 2003), while juveniles have been sampled within Arctic waters (0-2 °C) in the East Greenland Sea (Karamushko and Christiansen, 2021).

Redfish feed throughout the year, including during the polar night when they show some levels of stomach fullness (Geoffroy and Priou, 2020). The diet of juveniles is composed of meso- and macrozooplankton (mostly copepods, hyperiid amphipod and krill) while adults consume teleost fish, macrozooplankton, and various decapods (Brown-Vuillemin et al., 2023; Melnikov and Popov, 2009). The contribution of fish (capelin, herring, juvenile Atlantic cod, Arctic cod and cannibalism on juveniles) to the diet of adult redfish varies greatly among years, suggesting opportunistic feeding behaviour (Dolgov and Drevetnyak, 2011). Because of their life history characteristics, beaked redfish have high potential for poleward movement into the CAO with climate change (Hollowed et al., 2013).

Capelin (Mallotus villosus)

Capelin (*Mallotus villosus*) are members of the family Osmeridae with a circumpolar subarctic distribution. This short-lived (6-y maximum), relatively small (maximum size of 25 cm), pelagic, planktivorous, lipid-rich, and schooling species can be found from the surface down to 1,000 m. In comparison to Arctic cod, capelin are most abundant in subarctic regions but can occasionally tolerate colder temperatures (-1 °C) by entering a supercool state (Dalpadado and Mowbray, 2013; Raymond and Hassel, 2000). Capelin are linked to shelf seas and continental slopes and are rarely sampled beyond shelf breaks. In the Atlantic, they inhabit the Barents Sea, Iceland, and Greenland waters (including eastern Baffin Bay), the Labrador Sea, Hudson Bay and around Newfoundland (Dalpadado and Mowbray, 2013). Capelin are also found on the Pacific side, in the Bering, Chukchi, and Beaufort Seas (De Robertis et al., 2017; McNicholl et al., 2016). In the Barents Sea, capelin

are primarily distributed in the northern region along the polar front in both Atlantic and Arctic waters (Eriksen et al., 2017; Gjøsæter, 1998). Capelin migrate seasonally between feeding areas on the continental shelves and their shelf and coastal spawning grounds (Bliss et al., 2023; Carscadden et al., 2013; Gjøsæter, 1998). Capelin also perform DVM (Mowbray, 2002). Short-lived species, such as capelin, fluctuate substantially inter-annually in recruitment which is reflected in their total biomass, with cascading impacts on the entire ecosystem (Carscadden et al., 2013). For example, the decline in body condition of common murre (*Uria aalge*) in the early 1990s in Newfoundland was partly attributed to low recruitment of early spawning capelin due to colder than average sea temperatures (Davoren and Montevecchi, 2003).

Most capelin are semelparous, i.e., they spawn once in their lifetime. Spawning occurs from February to June with a peak in March-April in the Barents Sea and in June-August for the western Atlantic stock and Canadian Arctic (Carscadden et al., 2013; Christiansen et al., 2008; McNicholl et al., 2017). These demersal spawners lay sticky eggs on beaches or at depths < 30 m on the seabed, usually on gravel or sand (Carscadden et al., 2013). Hatching time varies between 80 days at 2 °C and 20 days at 7 °C (Gjøsæter, 1998), and better growth and condition generally characterizes early hatchers compared to late hatchers (Berg et al., 2021). Newly hatched larvae ascend to the surface where currents transport them toward their nursery grounds.

Similarly to Arctic cod, capelin are a forage species that occupies a central role within subarctic food webs, linking lower and higher trophic levels including piscivorous fish (e.g., Atlantic cod) and marine mammals (Hop and Gjøsæter, 2013). Small capelin (< 12 cm) primarily feed on calanoid copepods (*Calanus finmarchicus* in Atlantic waters and

Calanus glacialis in Arctic waters) whereas large capelin (> 12 cm) mostly target macrozooplankton (e.g., euphausiids; Dalpadado and Mowbray, 2013).

Atlantic cod (Gadus morhua)

The Gadidae Atlantic cod (*Gadus morhua*) are abundant in the North Atlantic and subarctic seas. Atlantic cod is a long-lived (maximum recorded age of 25 years), large (can grow longer than 100 cm), benthopelagic species that humans have harvested for centuries (Rose, 2004; Star et al., 2017). *G. morhua* is found south of the polar front in the Barents Sea, along the Norwegian coast, in the Baltic Sea and North Sea, around Iceland, in southeast and southwest Greenland (including eastern Davis Strait in Baffin Bay), along the coast of Labrador, and around Newfoundland south to Georges Bank (Drinkwater, 2005). Atlantic cod use both pelagic and demersal habitats and generally occur on continental shelves (Mecklenburg et al., 2018), although their distribution can extend past shelf breaks into the mesopelagic zone (Ingvaldsen et al., 2017; Snoeijs-Leijonmalm et al., 2022). This groundfish is most abundant between 100 m and 300 m and tolerates a wide range of temperatures (from -2 °C to 20 °C), but is usually restricted to Atlantic water masses between 0 and 8 ºC (Drinkwater, 2005). Like beaked redfish, juvenile Atlantic cod occur at a wider range of temperatures and salinities as adults. Atlantic cod perform extensive seasonal migrations from feeding to spawning grounds (Olsen et al., 2010; Robichaud and Rose, 2004). For example, in the Barents Sea adult Atlantic cod start migrating in January from their feeding grounds south of the polar front toward the coast of northern Norway where they spawn in spring, returning back to the polar front area after spawning (Olsen et al., 2010).

Atlantic cod are iteroparous and batch spawners. The spawning season is centred around February-June in Labrador and Greenland and around March-April on the Norwegian coast (Myers et al., 1993; Olsen et al., 2010). They aggregate on the shelf at temperatures between 4 and 6 °C during the spawning season. Eggs are neutrally buoyant and concentrate in the surface layer where currents transport them. Hatching occurs 2-3 weeks after fecundation, and larvae drift until late autumn when they settle on the seabed (Olsen et al., 2010).

Atlantic cod are generalist predators, feeding on both pelagic and benthic prey – a characteristic hypothesized to fuel their remarkable dominance within boreal regions (van Denderen et al., 2018). Juvenile Atlantic cod are planktivorous, primarily targeting copepods and macrozooplankton (Pedersen and Fossheim, 2008; Renaud et al., 2012). Adult *G. morhua* have a generalist diet but primarily target fish (mostly capelin) and decapods (Bogstad and Gjøsæter, 2001; Krumsick and Fisher, 2022). During years of low capelin abundance, Atlantic cod can feed on other pelagic fish such as Arctic cod, beaked redfish (*S. mentella*), juvenile haddock (*Melanogrammus aeglefinus*), American plaice (*Hippoglossoides platessoides*), and smaller Atlantic cod (Yaragina et al., 2009). Interestingly, Atlantic cod are both a competitor of Arctic cod, because juveniles of both species feed on the same prey, and a predator because adults feed on forage fish (Renaud et al., 2012).

Glacier lanternfish (Benthosema glaciale)

Glacier lanternfish (*Benthosema glaciale,* family Myctophidae) is a widely distributed mesopelagic species in the North Atlantic (Gjøsæter and Kawaguchi, 1980; Klevjer et al., 2020b). The northern extent of *B. glaciale* is eastern Baffin Bay around Davis Strait in the western Atlantic and around Svalbard in the eastern Atlantic. As a mesopelagic species,

they are absent from shelf seas (Geoffroy et al., 2019; Knutsen et al., 2017; Sameoto, 1989). However, recent observations of glacier lanternfish further north, within the Eurasian Basin and Amerasian Basin of the CAO, have challenged our current understanding of their distribution (Ingvaldsen et al., 2023; Snoeijs-Leijonmalm et al., 2022; Zhang et al., 2022). This species' swimming ability is limited and it is thus considered to mainly drift with currents (Kaartvedt et al., 2009). In the subarctic, *Benthosema glaciale* display flexible DVM behaviours and generally undergo synchronous DVM between meso- and epipelagic zones in spring and summer (Dypvik et al., 2012b; Kaartvedt et al., 2023).

Glacier lanternfish are a batch spawner and release up to five batches of eggs during a single spawning season (García-Seoane et al., 2014). The spawning season of glacier lanternfish ranges from April to October with a peak in June in the northwest Atlantic and in June-July in the northeast Atlantic (García-Seoane et al., 2014; Halliday et al., 2015). Past studies hypothesized that myctophids cannot reproduce at high latitudes, and that individuals caught in the CAO are sterile expatriates from the North Atlantic (Kaartvedt, 2008; Sameoto, 1989).

The main prey of lanternfish are copepods and macrozooplankton (euphausiids and amphipods; Knutsen et al., 2023; Pepin, 2013). Lanternfish have adapted their vision to low light levels that prevail at mesopelagic depths (Turner et al., 2009). As such, they can detect prey even at very low light levels. In the fjords of western Norway, *B. glaciale*, continue feeding during the winter although the population has a higher proportion of empty stomach than at other times of the year (Gjøsæter, 1973). This lipid-rich fish contains large subcutaneous and intramuscular lipid reserves that help it overwinter (Falk-Petersen et al., 1986)

1.3 The mesopelagic zone

1.3.1 Importance of the mesopelagic zone globally

Numerous pelagic species present in the Arctic Ocean conduct ontogenetic vertical migrations, exploiting different depth ranges throughout their life cycle. For example, Atlantic cod are demersal as adults but occur in the epi- and mesopelagic zones as juvenile (Geoffroy et al., 2019; Ingvaldsen et al., 2017; Knutsen et al., 2017). Similarly, species that undergo DVM may exploit both the mesopelagic zone during the day and the epipelagic at night. Despite its relevance to pelagic ecology, the mesopelagic zone has often been overlooked (Martin et al., 2020; St. John et al., 2016). Only within the last decade has the mesopelagic zone received increasing attention due to the high biomass it contains, potentially the largest fish biomass of the World's Ocean in the order of 1,000-10,000 million tons (Irigoien et al., 2014; Proud et al., 2019), and its role in biogeochemical cycling (Davison et al., 2013; Saba et al., 2021). The mesopelagic zone hosts many species of micronekton (2-20 cm) and zooplankton. Myctophidae (lanternfish) and Gonostomatidae (bristlemouths) are the most common mesopelagic taxa (Catul et al., 2011; Gjøsæter and Kawaguchi, 1980).

Because of the large mesopelagic biomass and the high lipid content of Myctophidae and Gonostomatidae, these resources have attracted commercial interests, and discussion of future commercial fisheries (Grimaldo et al., 2020). However, mesopelagic fishes are an important prey item to multiple commercial fish stocks and for charismatic megafauna including sharks, seals, and whales (Howey et al., 2016; Naito et al., 2013; Robinson et al., 2012). Furthermore, the rise in ocean temperature can lead to large shifts in mesopelagic biomass spatial distribution, which is predicted to decrease by 3-22 % at low and mid

latitudes by 2080-2100 due to the expansion of low productive systems (Ariza et al., 2022). Thus, baseline knowledge is required to understand all the risks and ecological impacts commercial fisheries of mesopelagic resources could have on marine ecosystems and their services (Fjeld et al., 2023).

1.3.2 Hydroacoustics to study the mesopelagic zone

Much of our knowledge on the vertical and spatial distribution of the mesopelagic fauna comes from remote observations with echosounders that image mesopelagic fish and zooplankton as deep sound scattering layers (DSL; Irigoien et al., 2014; Proud et al., 2019). These DSL are defined as a group of organisms scattering sound and appearing as a continuous layer on the echosounder. They were observed for the first time in the 1940s during World War II when the first echosounders were developed and installed on navy ships. At first, they were mistaken for the seabed because of their resemblance to seafloor backscatter. However, operators observed that the *"seabed"* was migrating upward at night and correctly concluded that this signal was instead of biological origin (Duvall and Christensen, 1946).

Hydroacoustics transmits a pulse of sound in the water, which is reflected by an acoustic target, e.g., a fish, and measures the amount of energy from this pulse received back (Simmonds and MacLennan, 2005). The temporal delay of the backscatter informs on the distance between the target and the echosounder. The amount of energy received, i.e., the backscatter intensity, is determined by a combination of physical parameters (such as source level and signal loss during propagation) and by factors associated with the nature of the biological scatterers. The efficiency at which an individual organism scatters sound varies according to its acoustic properties (e.g., a gas-inclusion such as a fish swimbladder

scatters more sound than flesh), its size, shape, orientation, and potentially other parameters like its physiological condition (Foote and Stanton, 2000; Simmonds and MacLennan, 2005). Backscatter intensity also varies according to the abundance of different types of animals present and the integration of acoustic backscatter, i.e., echo-integration, is now widely used to estimate the abundance and distribution of pelagic and semi-pelagic fish and macrozooplankton (Simmonds and MacLennan, 2005).

Table 1-1 Definition of acoustic parameters used in this thesis.

Symbol	Name	Quantity	Usage	Units
S_V	Volume backscattering strength	Density	Density of organisms within a volume	dB re 1 m^{-1}
S_A	Nautical area scattering strength (logarithmic)	Abundance	Abundance of organisms over an area	dB re 1 m^2 nmi^{-2}
s_A	Nautical area scattering coefficient (linear)	Abundance	Abundance of organisms over an area	m^2 nmi^{-2}
WMD	Weighted mean depth	Location	Mean depth of organisms in the water column	m
TS	Target strength	Signature	Acoustic signature of a single target	dB re 1 m^2

Several acoustic parameters can be derived from backscatter intensity, including the volume backscattering strength (S_V in dB re 1 m^{-1}) – a proxy for the density of scatterers – , nautical area scattering strength (S_A in dB re 1 m^2 nmi^{-2}) which can be depth integrated to give a proxy for the abundance of scatterers over an area, or the weighted mean depth (WMD in m) which describes the mean depth of scatterers within a depth interval (Table 1-1; Urmy et al., 2012).

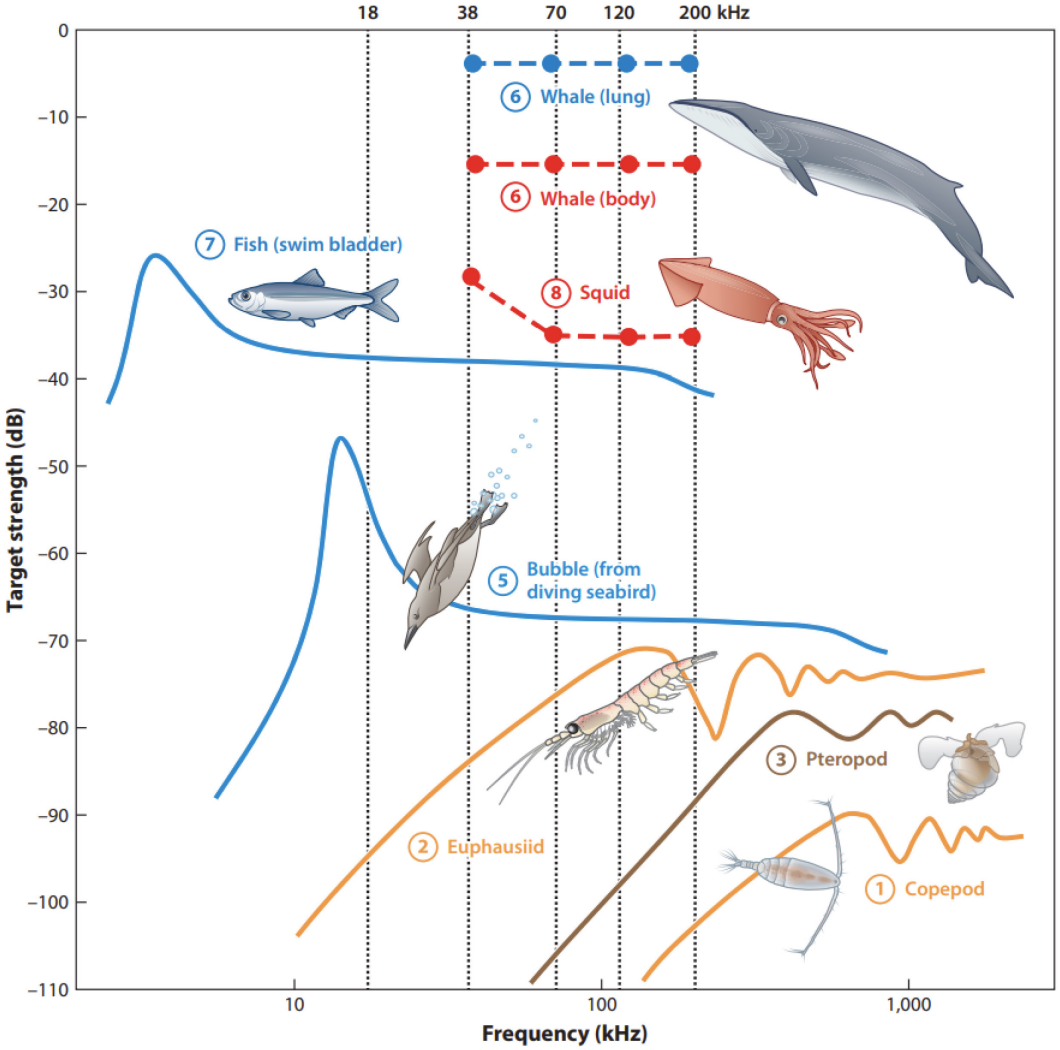

Figure 1-8. Characteristic frequency responses of different types of organisms (colors); orange: fluid-like scatterer; brown: shell-bearing scatterer; blue: gas-filled structure; red: fluid-like scatterer with hard-parts (cartilage or bones). The dashed lines show frequency response curves derived from empirical observations while solid lines indicate predictions based on scattering models validated through empirical measurements. The vertical dotted lines show typical sampling frequencies (18, 38, 70, 120, and 200 kHz; figure from (Benoit-Bird and Lawson, 2016).

Different types of organisms show characteristic frequency responses which can be used to remotely infer community composition using multifrequency echosounders (Figure 1-8; (Foote and Stanton, 2000; Holliday, 1977; Stanton et al., 1994). Typical frequencies of fisheries echosounders are 18, 38, 70, 120, 200, and 333 kHz (Chu, 2011) which can be used to partition acoustic backscatter into broad taxonomic levels, e.g., swimbladdered fish, non swimbladdered fish, or zooplankton (Korneliussen et al., 2018).

When sound is transmitted in the water it is partly dispersed through the acoustic beam spreading (e.g., the sound is emitted into a cone which increases in size with distance thus reducing the density of energy) and absorbed by water (Simmonds and MacLennan, 2005). Both these losses increase with range, i.e., the distance between the echosounder and the region of interest; if the echosounder is vertical at the surface of the ocean (0 m), then the range is equal to depth. A time-varied-gain function is used to compensate for absorption and spreading losses, (MacLennan, 1986). However, the amount of energy received back is not *"clean"*, in that it includes the backscatter of interest but also from other targets and noise. Common sources of noise are sounds generated by the vessel moving on the water (flow noise), environmental noise (e.g., wind entraining air bubbles at the surface of the ocean), and electrical interference (Simmonds and MacLennan, 2005). For instance, scattering from air bubbles of microstructure strongly attenuate both transmitted signal and echoes. Noise is also amplified by the time-varied-gain function, so that at long ranges, it dominates the amount of energy received. To ensure good quality data with little noise, the protocol involves calculating the signal-to-noise ratio (SNR) and excluding data with a low SNR, generally below 10 dB (De Robertis and Higginbottom, 2007).

Because sound absorption is frequency dependent, low frequencies (e.g., 18 and 38 kHz) have better SNR at long ranges than high frequencies (e.g., 120, 200, and 333 kHz; Simmonds and MacLennan, 2005). Hence, it is possible to *"see deeper"* with low frequencies than with high frequencies. However, low frequencies fail at detecting small acoustic targets like macrozooplankton but can detect them at high frequencies. For example, for a sound speed of 1450 m s^{-1}, the minimum target detection size is around 3.8 cm at 38 kHz and 0.7 cm at 200 kHz. Because mesopelagic layers are located relatively deep in the water column (> 200 m depth), most of the studies using hull-mounted

echosounders have relied on low frequencies to accurately characterize the DSL (e.g., Ariza et al., 2022; Irigoien et al., 2014; Proud et al., 2019). To overcome this issue, echosounders have been mounted on towed-bodies or probes that are submerged at mesopelagic depths (Dias Bernardes et al., 2020; Sawada et al., 2011). In this case, data has a good SNR, and the frequency choice is not dictated entirely by detection ranges. However, probe-mounted echosounders often require the research vessel to be stationary to collect data, in contrast to hull-mounted echosounders that can also collect data continuously across large areas.

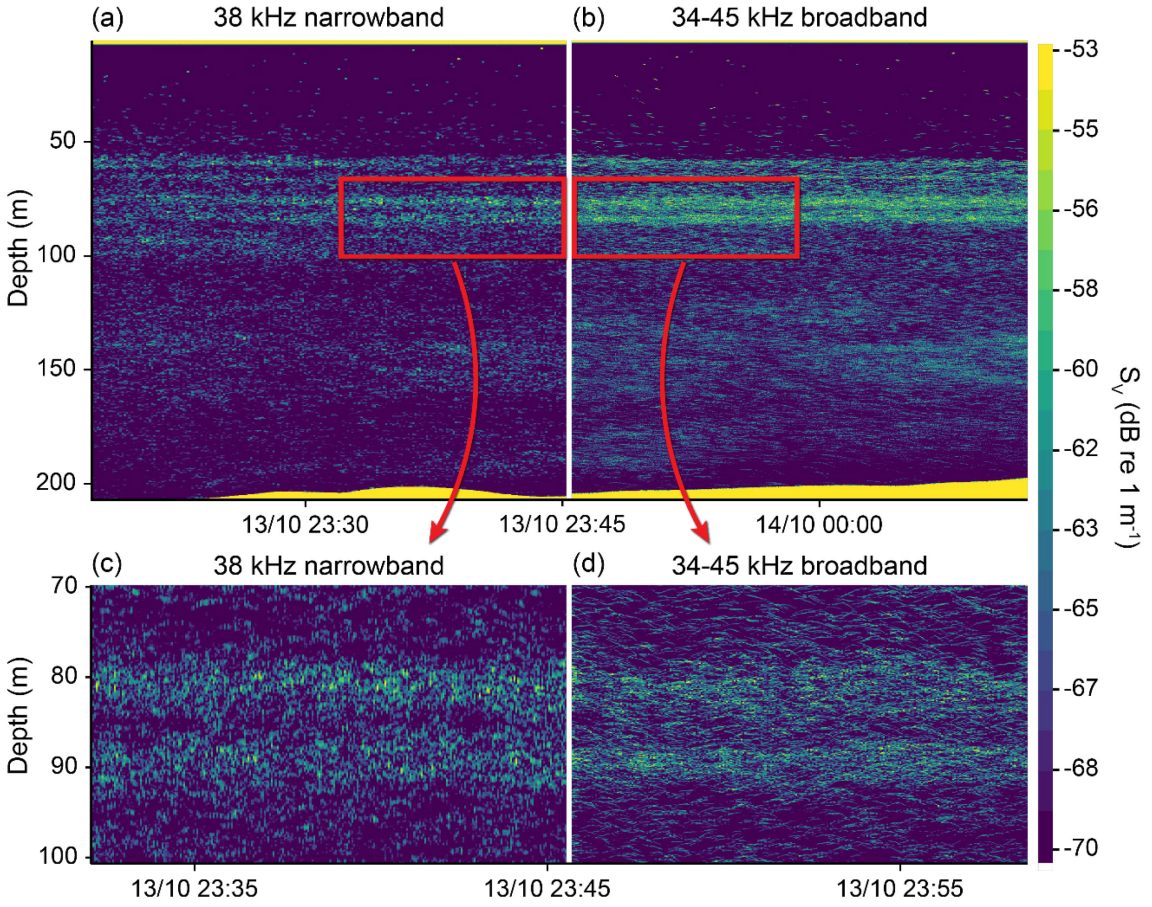

Figure 1-9. Echograms of volume backscattering strength (S_V in dB re 1 m^{-1}), a proxy for animal density (Simmonds and MacLennan, 2005), in (a) narrowband at 38 kHz and (b) broadband between 34-45 kHz. Zoom on the scattering layer between 70 and 100 m depth sampled with (c) narrowband and (d) broadband acoustics. The broadband data has a much higher vertical resolution than narrowband data which allows to distinguish single targets even in scattering layers. Acoustic data were collected in northern Baffin Bay in October 2021 with the hull-mounted echosounder of the CCGS *Amundsen*. The seafloor is visible as a yellow band at the bottom of the echogram.

The latest technological improvement in the field of fisheries acoustics is the development of frequency modulated scientific echosounders, also referred to as broadband or wideband echosounders (Figure 1-9a, b; Andersen et al., 2021). Instead of emitting a pulse of sound at a constant narrowband frequency – a ping, with a frequency bandwidth of a few kHz – the pulse of sound is emitted over a large frequency bandwidth – a chirp (currently with a spectrum up to 100 kHz). Using advanced signal processing techniques, broadband data enables much higher vertical resolution and an improved SNR (Figure 1-9c, d; Andersen et al., 2021). Broadband acoustics have the potential to achieve finer taxonomic classification (Benoit-Bird and Waluk, 2020; Chu and Stanton, 1998; Lavery et al., 2010).

Active acoustics provide a wealth of information regarding acoustic densities and vertical and spatial distributions of mesopelagic fish and zooplankton, but generally lack fine taxonomic resolution (Horne, 2000). Therefore, studies often combine acoustic data with other sampling methods to confirm scatterer identities. The most common method to ground-truth the acoustic signal is to use nets and trawls (e.g., Geoffroy et al., 2019; Ingvaldsen et al., 2023). Optical methods can also be used, like the Underwater Vision Profiler (UVP6), which photographs mesozooplankton in the water column (Picheral et al., 2022), or stereo-video cameras (Sawada et al., 2011). However, a perfect ground-truthing method does not exist. Nets and trawls have specific size selectivities and are subject to avoidance of fast-swimming individuals and taxa (Kaartvedt et al., 2012). Optical methods generally require additional sources of artificial light which can create avoidance problems (Geoffroy et al., 2021; Kaartvedt et al., 2019b; Peña et al., 2020). Furthermore, pelagic fauna also avoid artificial lights from ships at night (Berge et al., 2020). Hence, sampling the highly light-sensitive mesopelagic fauna requires careful consideration.

1.3.3 Light comfort zone and photoperiod constraint hypotheses

The central position of mesopelagic organisms in the food web as both prey and predator, and the strong vertical gradient in light intensity, make the ecology of the mesopelagic zone a large game of "hide and seek". Globally, the vertical distribution of mesopelagic organisms has been linked to temperature and oxygen concentrations patterns (Bianchi et al., 2013; Klevjer et al., 2016), but light penetration is considered to be one of the main proximate drivers (Aksnes et al., 2017). During daytime, light levels can span around ten order of magnitude within the mesopelagic zone (200-1000 m depth; Warrant and Locket, 2004), and most mesopelagic fish and zooplankton remain within a narrow range of specific light intensities (10^{-6} to 10^{-9} µmol quanta m^2 s^1; Aksnes et al., 2017). This range of light intensities is referred to as the light comfort zone of mesopelagic organisms (Langbehn et al., 2019; Røstad et al., 2016). Because mesopelagic fish and zooplankton are well attuned to dim light (Turner et al., 2009; Warrant and Locket, 2004), they may be able to exploit their light comfort zone as an antipredation window which would maximize prey searching efficiency relative to the mortality risk from visual predators (Clark and Levy, 1988).

The light comfort zone of mesopelagic organisms is affected by temporal variation in light intensity through changes in incoming solar or lunar radiation, which is further modulated by clouds, sea-ice, and latitudinal differences in photoperiod (Kaartvedt et al., 2019a; Langbehn et al., 2019). Consequently, DVM patterns are common among mesopelagic organisms that follow a light comfort zone. Across the temperate and tropical oceans, around 50 % of mesopelagic backscatter undergo DVM (Klevjer et al., 2016).

The extreme light climate that characterizes high latitudes violates the general framework of predator-prey interactions. Continuous irradiance during the polar day prevents safe

foraging near the surface where copepods accumulate to feed on algae, whereas continuous darkness during the polar night limits visual feeding at mesopelagic depths where copepods overwinter. This scenario is known as the photoperiod constraint hypothesis (Kaartvedt, 2008). The photoperiod constraint hypothesis predicts that mesopelagic organisms are depauperate in the Arctic Ocean, suggesting a decrease in mesopelagic fish abundance with increasing latitude. This decrease has been observed in the North Atlantic side of the Arctic (Chawarski et al., 2022; Gjøsæter et al., 2017; Knutsen et al., 2017; Siegelman-Charbit and Planque, 2016). However, this pattern may not be representative of the entire Arctic Ocean, because mesopelagic species may have different sensitivities to light and developed specific life history strategies (Jönsson et al., 2014).

Climate change has the potential to further disrupt the structure and dynamics of the Arctic mesopelagic zone through abiotic (e.g., sea ice melt affecting light comfort zones) and biotic changes (e.g., borealization; Fossheim et al., 2015). Whether Arctic or boreal species can cope with these changes is currently unknown. While the survival of some boreal mesopelagic species may depend on the light environment (Langbehn et al., 2022; Ljungström et al., 2021), plasticity in life history may allow survival in a changing Arctic environment. For example, winter reproduction is a key trait for coping with the Arctic seasonality because it allows first-feeding larvae to match with the peak in primary and pelagic production in spring. Hence, the ability to reproduce during polar night may further hamper colonisation of that habitat by boreal species (Berge et al., 2015b; Berge and Nahrgang, 2013).

The United Nations Decade of Ocean Science for Sustainable Development (2021-2030) has identified polar regions as priority areas for deep-sea research given their sensitivity to

climate change and limited knowledge on Arctic mesopelagic communities (Howell et al., 2020). Since June 2021, the International Agreement to Prevent Unregulated Fishing in the High Seas of the CAO has entered into force (FAO, 2021). The signing parties – the Arctic states of Canada, Denmark (Greenland), Norway, Russia, and the USA as well as the countries with fisheries interest in the Arctic Ocean, Iceland, the EU, Japan, South Korea, and China – have vowed not to develop fisheries activities within the CAO for 16 years (since the start of the treaty in 2021). The goal of that legislation is to ensure that adequate scientific information is collected and available to inform decision making about potential future commercial harvesting. The Arctic mesopelagic zone and its fauna are thus at the forefront of scientific and societal interests. Yet, large knowledge gaps remain regarding the spatio-temporal distribution, taxonomic composition, environmental drivers, and life history strategies allowing for year-round survival of mesopelagic fish and zooplankton in the Arctic.

1.4 Research objectives

1.4.1 Context of the study

The standing paradigms suggest that mesopelagic populations are depauperate in the Arctic Ocean because their foraging and reproductive successes are low (Berge and Nahrgang, 2013; Kaartvedt, 2008). Until recently, the presence of mesopelagic layers was only confirmed in western and northern of Svalbard, at the Arctic-Atlantic gateway (Geoffroy et al., 2019; Gjøsæter et al., 2017; Knutsen et al., 2017), and recent surveys have extended the presence of DSL in the CAO (mostly in the Eurasian Basin; Ingvaldsen et al., 2023; Snoeijs-Leijonmalm et al., 2021, 2022). Similarly, the species composition of mesopelagic layers was only scrutinized in Svalbard, where boreal and Arctic species co-occur

(Geoffroy et al., 2019; Knutsen et al., 2017), and partly in the CAO where the species composition inferred from DSL recordings was either speculated (Snoeijs-Leijonmalm et al., 2021), observed from cameras (Snoeijs-Leijonmalm et al., 2022), or ground-truthed with pelagic trawls (Ingvaldsen et al., 2023). Overall, uncertainties regarding the spatial extent and species composition of mesopelagic layers persist in the Arctic Ocean, in particular in the Canadian Arctic.

While DSL have been documented in the European Arctic and CAO, the mechanisms enabling their survival remain uncertain. Mechanistic models can highlight some of the key mechanisms necessary to succeed in the Arctic Ocean (Langbehn et al., 2019, 2022; Ljungström et al., 2021), but they rely on in situ data for adequate parametrization. To date, only models parametrized for the Arctic-Atlantic gateway exist and may not represent other regions of the Arctic appropriately. Hence, the limited observation from the Arctic Ocean hinders our ability to understand the underlying mechanisms, survival strategies, and environmental drivers of the Arctic mesopelagic biota that would allow better understanding of their fate in light of climate change.

The overall aim of this thesis is to provide a comprehensive overview of mesopelagic layers in the Arctic Ocean with regards to their spatial distribution, species composition, environmental drivers, and life history strategies. To achieve this aim, I focus on data collected at different spatial and temporal scales from multiple regions of the Arctic Ocean.

1.4.2 Chapter outlines

This thesis is divided into five chapters (including this introductory chapter) that explore different facets of the ecology of mesopelagic fauna in the Arctic Ocean (Figure 1-10). Chapter two focuses on the distribution and species composition patterns of mesopelagic

layers in multiple regions of the Arctic Ocean and tests whether those patterns relate to oceanic circulation, in particular Atlantic water advection. Chapter three investigates whether the mesopelagic layer performs DVM under constant daylight of the midnight sun in the ice-covered European Arctic. Chapter four explores the role of light penetration on the vertical structure and dynamics of the mesopelagic community and whether mesopelagic fish and zooplankton follow a light comfort zone at the critical time of sea-ice formation in northern Baffin Bay. Finally, chapter five synthesizes the findings of the three data chapters to provide a synopsis of the structure, dynamics, and mechanisms enabling mesopelagic fauna to succeed at high latitudes (Figure 1-10) and identifies possible future research questions.

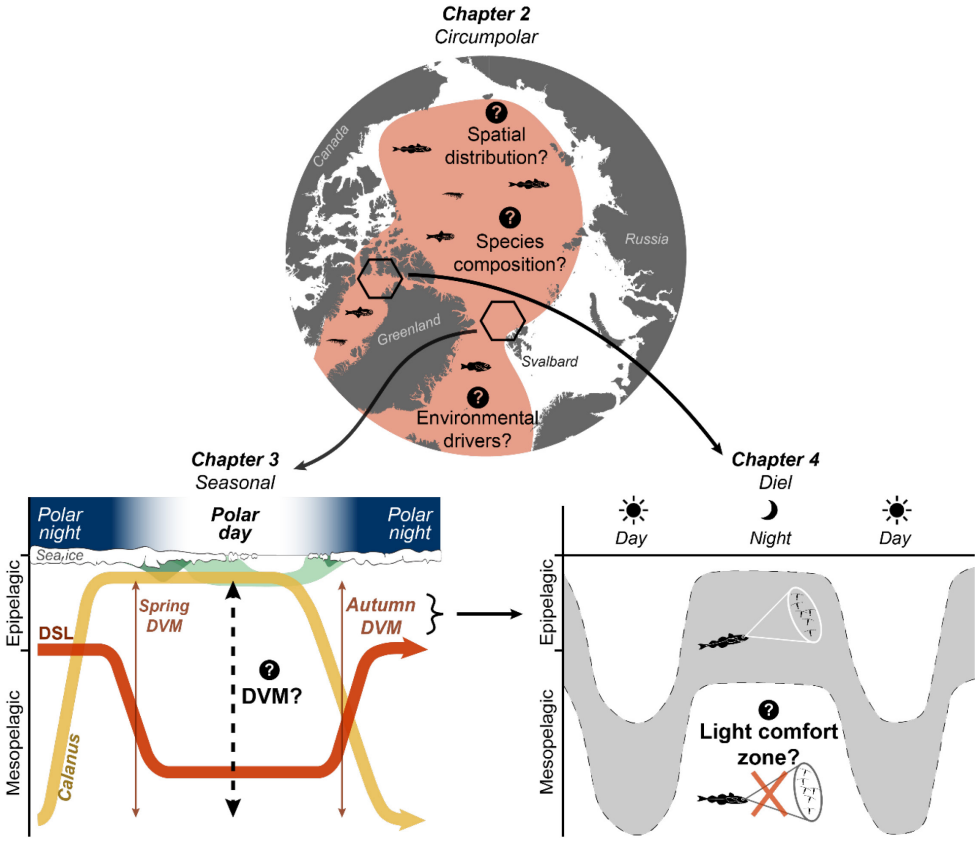

Figure 1-10. Structure and interplays of the different chapters of the thesis. Chapter two focuses on large spatial distributional patterns of mesopelagic fauna, chapter three on seasonal vertical distribution of the mesopelagic layer, and chapter four tests potential light-dependent mechanisms explaining the vertical distribution of mesopelagic fish and zooplankton.

1.4.3 Methods used during this study

All the core chapters (two to four) include data collected by hull-mounted echosounders. In chapter two, I used acoustic data collected by multiple research and fishing vessels, CCGS *Amundsen*, F/V *Frosti*, R/V *Helmer Hanssen*, and R/V *Polarstern*, in 2015-2017 around the Arctic Ocean and ground-truthed by mid-water trawls deployed in the DSL. Chapter three is based on data collected during a drift station of the R/V *Polarstern* in the Eurasian Basin of the CAO in 2017, where I used hull-mounted echosounder data (Simrad EK80; Kongsberg Discovery) at multiple frequencies, and two ice-tethered echosounders (Acoustic Zooplankton and Fish Profiler; ASL Environmental Sciences) installed at 15 m depth, one facing upward toward the sea ice and one facing downward toward the seafloor. Acoustic data collected on the underside of the sea was ground-truthed with a zooplankton net mounted on a ROV (ROVnet) which was deployed below the sea ice. In chapter four, I used hull-mounted data (Simrad EK80; Kongsberg Discovery) and an acoustic probe (Wideband Autonomous Transceiver, Kongsberg Discovery) deployed from the CCGS *Amundsen* in autumn 2021. Acoustic data were ground-truthed by mid-water trawls and by a UVP6 deployed in the mesopelagic layer. All acoustic data were processed using Echoview (Echoview Software Pty Ltd.), and other data streams, e.g., environmental (temperature, salinity, chlorophyll), oceanic circulation models, UVP6, nets and trawls were analyzed using R (R Core Team).

2 Chapter two: Mesopelagic fish and macrozooplankton are ubiquitous in high Arctic seas

2.1 Abstract

Mesopelagic fish rely on light-triggered diel vertical migrations for feeding. Because of the extreme light cycle prevailing at high latitudes, they are assumed to be depauperate in the Arctic Ocean. To test this hypothesis, we used acoustic and trawl data collected in four regions of the Arctic Ocean between 2012 and 2019. We observed consistent mesopelagic sound scattering layers in the Beaufort Sea, Baffin Bay, and northern Barents Sea. Median backscatter was 65.3 ± 90.5 m^2 nmi^{-2} across areas and years. Trawl catches showed that these layers were dominated by Arctic cod (*Boreogadus saida*) in the Beaufort Sea and in northern and western Baffin Bay, and by a combination of boreal and Arctic species in southern Baffin Bay and the northern Barents Sea. We conclude that, in contrast to the photoperiod constraint hypothesis, the mesopelagic zone constitutes a widespread ecological niche in the Arctic. Advection and species composition patterns further suggest asymmetric conditions across the Arctic Ocean, presumably representing distinct mesopelagic biogeographic provinces.

2.2 Introduction

Mesopelagic zooplankton and micronekton form deep scattering layers (DSL) between 200 and 1000 m depth in most of the global ocean and possibly host the highest biomass of fish in the world (Irigoien et al., 2014; Proud et al., 2019), mainly lanternfish (Myctophidae) and bristlemouths (Gonostomatidae; Gjøsæter and Kawaguchi, 1980). Mesopelagic organisms are highly attuned to light cues (Turner et al., 2009) which structure their vertical distribution and behaviour (Aksnes et al., 2017). It has been hypothesized that mesopelagic

taxa follow a light comfort zone (Røstad et al., 2016) – a range of isolumes that maximizes feeding chances while limiting mortality through visual predation (Clark and Levy, 1988). Every day, about 50 % of mesopelagic backscatter conduct diel vertical migrations (DVM; Klevjer et al., 2016). They move toward the surface during nighttime to feed on epipelagic prey and descend to mesopelagic depths to evade visual predators during daytime. Given their vast distribution and immense biomass, mesopelagic organisms fuel pelagic food webs and their DVM contribute to carbon export – estimated to be 14-17 % of the carbon flux out of the euphotic zone – as part of the biological carbon pump (Archibald et al., 2019; Davison et al., 2013; Saba et al., 2021).

The standing paradigm suggests that the extreme light regime prevailing at high latitudes hinders the establishment of viable mesopelagic fish populations in Arctic seas (Kaartvedt, 2008). Within this paradigm, during the Arctic polar night, continuous darkness prevents visual feeding, even for the dark-adapted mesopelagic fish. In summer, continuous illumination during the midnight sun reduces the amplitude of DVM, strengthening the vertical segregation between the DSL and the zooplankton prey at the surface of the ocean and increasing predation risks by visual predators for individuals conducting DVM (chapter three). Thus, it is assumed that mesopelagic fish cannot colonize the Arctic because of low energy acquisition during the midnight sun and polar night, and high predation mortality in summer makes individuals die faster than they can reproduce (Langbehn et al., 2022). These assumptions could explain the scarcity of common mesopelagic species, such as lanternfish and bristlemouths, in the Arctic Ocean. Yet, other fish species could be better adapted to the extreme light regime and occupy the mesopelagic niche of Arctic seas. If so, the mesopelagic niche would represent a largely overlooked component of Arctic marine ecosystems.

The United Nations Decade of Ocean Science for Sustainable Development (2021-2030) identified polar regions as priority areas for deep-sea research given their sensitivity to climate change and the limited amount of knowledge on their mid-water communities (Howell et al., 2020). Currently, the marine Arctic – including the Central Arctic Ocean and adjacent high-seas – is considered as a single mesopelagic province characterized by a depauperate micronekton fauna originating from the North Atlantic (Sutton et al., 2017). Accordingly, most of the research on mesopelagic fish communities in the Arctic has been conducted in areas under the influence of Atlantic water inflow – which is hypothesized to support the mesopelagic community in Svalbard (Geoffroy et al., 2019; Knutsen et al., 2017) – and in the Central Arctic Ocean (Ingvaldsen et al., 2023; Snoeijs-Leijonmalm et al., 2022, 2021). In contrast, observations of mesopelagic communities from the western Arctic seas and in regions not directly influenced by Atlantic water inflow remain scarce.

Here, we combine acoustic data collected over three years (2015-2017) and mid-water trawl data collected between 2012-2019 across a vast area covering the Beaufort Sea, Nares Strait, Baffin Bay, and the northern Barents Sea. We test the null hypothesis that mesopelagic fish and zooplankton are absent from Arctic seas. We also assess variations in taxonomic composition across regions. We further examine advection as a potential driver of the distribution of mesopelagic organism at high latitudes and consider the role of mesopelagic animals in the functioning of Arctic food webs.

2.3 Materials and Methods

2.3.1 Study area

Four regions of the Arctic Ocean – the Beaufort Sea, Nares Strait, Baffin Bay, and northern Barents Sea – were surveyed between 2012 and 2019. Surveys were conducted from the

CCGS *Amundsen*, F/V *Frosti*, R/V *Helmer Hanssen*, and R/V *Polarstern* (Figure 2-1). Each region was defined according to the Large Marine Ecosystems (LME) of the Arctic (PAME, 2013). Because we only sampled at the margins of the Central Arctic Ocean, the sites within the Central Arctic Ocean were attributed to either the northern Barents Sea or the Beaufort Sea based on their geographical proximity to these regions. Hereafter, we refer to the marine Arctic as the area including the Central Arctic Ocean and surrounding high seas.

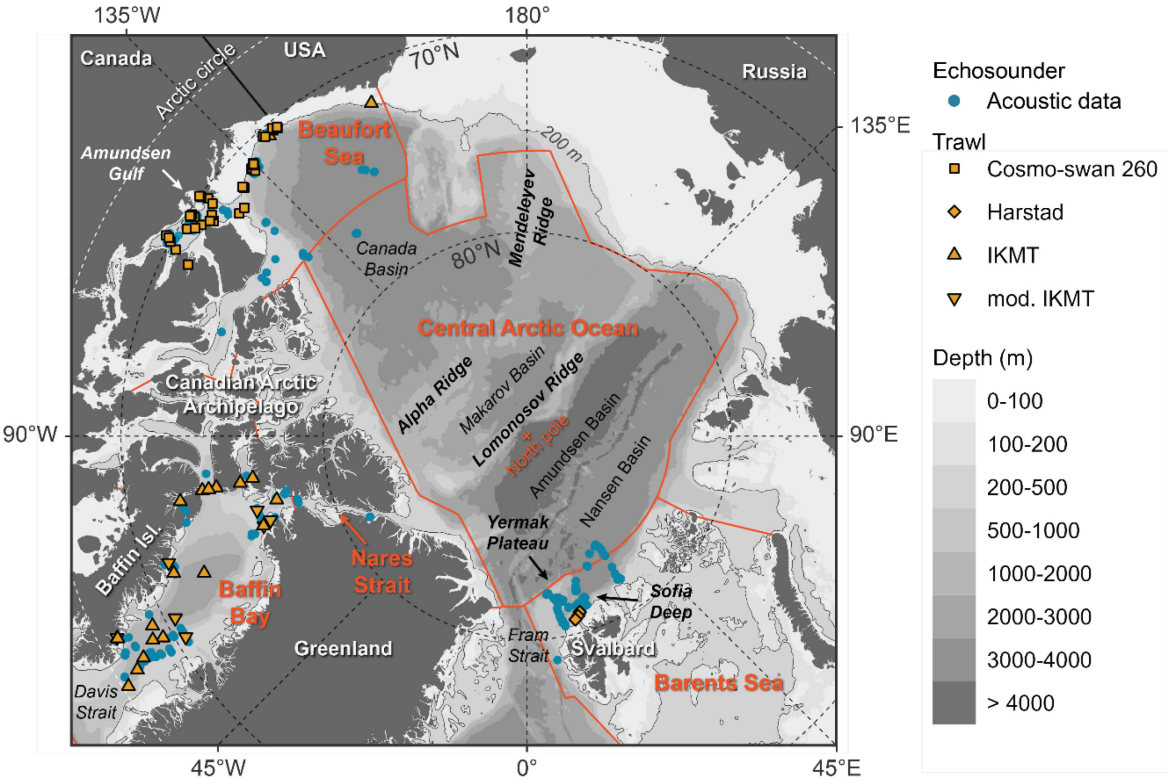

Figure 2-1. Study area with blue dots showing the location of acoustic data and orange diamonds the position of mid-water trawl deployments. The red polygons indicate the Central Arctic Ocean in addition to the four studied regions: the Beaufort Sea, Nares Strait, Baffin Bay, and northern Barents Sea. The red cross indicates the North Pole.

Baffin Bay and the northern Barents Sea can be distinguished from the Beaufort Sea and Nares Strait based on their connection to the subarctic. Both Baffin Bay and the northern Barents Sea have deep-sea connection to the North Atlantic through Davis Strait and Fram

Strait, respectively (Figure 2-1). The Barents Sea is the main gateway of Atlantic waters into the Central Arctic Ocean through the West Spitsbergen Current (Timmermans and Marshall, 2020). Atlantic water generally circulates cyclonically along the slope of the deep basins of the Central Arctic Ocean under the cold polar surface waters and exits through western Fram Strait (Rudels et al., 2013). The inflow of Atlantic water into Baffin Bay is ca. 7 times lower than in the Barents Sea and links the Labrador Sea and Baffin Bay (Cuny et al., 2005; Timmermans and Marshall, 2020). The main circulation feature of Baffin Bay is the Baffin Island Current, which carries Arctic water masses from Nares Strait and the Canadian Arctic Archipelago out of the marine Arctic. In contrast to Baffin Bay and the northern Barents Sea, the Beaufort Sea and Nares Strait are isolated from most subarctic waters by shallow sills.

2.3.2 Hydroacoustic sampling and processing

Each vessel was fitted with an echosounder (Simrad EK60/EK80, Kongsberg Discovery) and recorded acoustic data at 38 kHz in 2015, 2016, and 2017 (Figure 2-1). Although 18 kHz is also used to detect mesopelagic fish (Peña et al., 2020), we used 38 kHz data because it was the only frequency common to all surveys. A total of 1220 h of acoustic recordings were analyzed. For each survey, the closest available calibration factors in time were applied (Table S2-1), along with in situ speed of sound and absorption coefficient calculated from local CTD profiles (Demer et al., 2015). All ship echosounders were calibrated yearly prior to the surveys, except for the R/V *Polarstern* in 2015. Pulse length was set to 1.024 msec, ping rate varied to accommodate other acoustic instruments, and transmitted power differed between ships and years (Table S2-2).

Acoustic data were cleaned and edited using Echoview 12.1 (Echoview Software Pty Ltd.). we removed background noise (minimum 10 dB signal-to-noise ratio) and impulse noise with Echoview's algorithms (De Robertis and Higginbottom, 2007; Ryan et al., 2015). We only selected data recorded when ships were stationary (< 1 knot), because icebreaking prevented the collection of noise-free acoustic data. To select echograms that are deep enough for DSL to form, we constrained analyses to areas where the seafloor was at least 400 m deep. Acoustic backscatter was echo-integrated in 10 min per 5 m cells at a threshold of -82 dB re 1 m^{-1} from which the nautical area scattering coefficient (s_A in m^2 nmi^{-2}) was exported and analyzed in R (version 4.2.1, R Core Team).

Data were collected between May and September – when nights are short or nonexistent in the Arctic Ocean – but we nonetheless excluded data collected during nighttime (sun position < 0 ° below horizon) using the *suncalc* R package (version 0.5.0) to prevent any potential bias from diel vertical migrations. For each 10-min cell, we calculated the integrated s_A between 200 m and 1000 m depth or 10 m above seafloor and used it as a proxy for the abundance of mesopelagic organisms (Simmonds and MacLennan, 2005). We also calculated the weighted mean depth (WMD; Knutsen et al., 2017; Urmy et al., 2012) to compare the average depth of the mesopelagic layer between regions. To document the spatial distribution of mesopelagic backscatter over a large area, we calculated the mean integrated s_A and weighted mean depth per year for each 150 km x 150 km cell of a georeferenced grid (EASE-Grid 2.0 North; EPSG:6931). For visual comparisons, we calculated the integrated nautical area scattering strength (S_A in dB re 1 m^2 nmi^{-2}), a log-transformation of integrated mesopelagic s_A (Simmonds and MacLennan, 2005). All subsequent analyses used integrated s_A (hereafter referred to as mesopelagic backscatter) and WMD from the spatially averaged dataset.

2.3.3 Trawl sampling

Mesopelagic fish and zooplankton were sampled using mid-water trawls deployed in the mesopelagic zone from the CCGS *Amundsen*, F/V *Frosti*, and R/V *Helmer Hanssen* in 2015-2017 (Table 2-1). To strengthen the community analyses, we also included trawls from other years collected by the F/V *Frosti* in the Beaufort Sea (2012-2014 and 2017-2019) and by the CCGS *Amundsen* in Baffin Bay (2014-2016 and 2019) and Beaufort Sea (2014). The CCGS *Amundsen* was equipped with an Isaacs-Kidd Midwater Trawl (IKMT) with a 4.5 m x 3.0 m mouth opening and 5.0 mm mesh size in the codend for all years except in 2016 when a modified IKMT with a slightly smaller mouth opening (3.0 m x 3.0 m) and the same mesh size was used. The F/V *Frosti* was equipped with a Cosmo-swan 260 of 63.0 m door spread x 12.7 m vertical opening and a 12.7 mm codend mesh size and the R/V *Helmer Hanssen* with a Harstad pelagic trawl which had a 12 m x 11 m mouth opening and 10.0 mm mesh size in the codend. Tow speed was ca. 3-5 knots and tow duration varied between 20 and 74 min.

Table 2-1. Metadata of mid-water trawl deployments used by the CCGS *Amundsen*, R/V *Helmer Hanssen*, and F/V *Frosti*. * in 2016 a modified IKMT with a slightly smaller mouth opening was used in Baffin Bay. *n* indicates the number of trawl hauls.

Area	Years	Vessel	Trawl type	n	Tow duration (min)	Sampling depth (m)
Baffin Bay	2014, 2015, 2016*, 2019	CCGS *Amundsen*	IKMT	26	24–74	200–520
Barents Sea	2016	R/V *Helmer Hanssen*	Harstad	3	23–29	320–560
Beaufort Sea	2012, 2013, 2014, 2017, 2018, 2019	F/V *Frosti,* CCGS *Amundsen*	Cosmo-Swan 260, IKMT	46	20–72	200–500

The fish and cephalopod taxa caught were identified onboard to the lowest taxonomic level possible and counted. Because this study is based on data collected by vessels which used

different mid-water trawls, we standardized the data by calculating the relative abundance for each fish and cephalopod species per deployment to determine taxonomic composition by proportion of total catch. Unfortunately, macrozooplankton taxa were not routinely identified during the CCGS *Amundsen* surveys and F/V *Frosti* surveys. However, we present data from the two trawls of the F/V Frosti in 2019 and three trawls of the R/V *Helmer Hanssen* which recorded the total weight of each macrozooplankton taxa. For macrozooplankton, we calculated the relative biomass per deployment to determine taxonomic composition by proportion of total biomass.

2.3.4 Current velocity data

To contextualise mesopelagic backscatter data in relation to general oceanic circulation patterns, we extracted monthly current velocity and direction at 380 m depth from the Copernicus Marine Environmental Monitoring Service (CMEMS) Arctic Ocean Physics Reanalysis product (doi: 10.48670/moi-00007) over 2015-2017 at a resolution of 12.5 x 12.5 km. We matched the resolution of the current velocity data to that of the backscatter data by calculating the median current velocity per 150 x 150 km cell and then calculated the annual mean current velocity for each grid cell.

2.4 Results

2.4.1 Hydroacoustic observations

We consistently observed deep scattering layers (DSL) in the mesopelagic zone at latitudes ranging from 67 to 84 °N within three Arctic seas, in the Beaufort Sea, Baffin Bay, and northern Barents Sea, but not in Nares Strait (Figure 2-2a). Integrated mesopelagic backscatter (s_A) varied significantly between regions (Kruskal-Wallis, $H = 7.56$, $p = 0.022$) with the highest median mesopelagic s_A found in Baffin Bay (87.2 ± 63.8 m^2 nmi^{-2}),

followed by the northern Barents Sea (65.6 ± 88.0 m^2 nmi^{-2}), the Beaufort Sea (11.5 ± 15.0 m^2 nmi^{-2}), and Nares Strait (3.4 ± 2.5 m^2 nmi^{-2}; Table 2-2).

Table 2-2. Summary statistics of integrated mesopelagic backscatter (s_A in m^2 nmi^{-2}) and weighted mean depth (WMD) of the mesopelagic zone (200-1000 m depth) for each Arctic region. * Data from Nares Strait were excluded from statistical tests (Kruskal-Wallis and Dunn's tests) because of the low sample size.

		Integrated s_A (m^2 nmi^{-2})		**WMD (m)**
Region	**nb. cells**	Median (median absolute deviation)	Range (min-max)	Median (median absolute deviation)
Beaufort Sea	21	11.5 (15.0)	0.1 – 727.7	386 (71)
Nares Strait *	4	3.4 (2.5)	1.0 – 80.0	306 (41)
Baffin Bay	31	87.2 (63.8)	5.6 – 899.5	343 (32)
North. Barents Sea	15	65.6 (88.0)	1.4 – 40600.1	412 (44)
All areas	71	65.3 (90.5)	0.1 – 40600.1	364 (67)

Across all areas and years, the median backscatter was 65.3 ± 90.5 m^2 nmi^{-2}. We did not find interannual differences in mesopelagic backscatter within Baffin Bay (Kruskal-Wallis, $H = 4.27$, p-value = 0.118) and northern Barents Sea (Kruskal-Wallis, $H = 3.07$, $p = 0.216$). However, in the Beaufort Sea mesopelagic backscatter was significantly lower in 2015 than in 2017 (Kruskal-Wallis, $H = 14.23$, p-value < 0.001; Dunn's test, p-value < 0.001). Nares Strait was not sampled in 2015 and median backscatter was 4.3 ± 2.6 m^2 nmi^{-2} in 2016 and 1.0 ± 0.0 m^2 nmi^{-2} in 2017.

High s_A was recorded over the Yermak Plateau in the northern Barents Sea with values greater than 1000 m^2 nmi^{-2} (Figure 2-2a). High backscatter was also found in Lancaster Sound and in the Pikialasorsuaq (north water polynya) in northern Baffin Bay, and in the Amundsen Gulf of the Beaufort Sea with mean backscatter greater than 500 m^2 nmi^{-2}. In

contrast, mean backscatter was low (< 10 m^2 nmi^{-2}) in Nares Strait and at the margin of the CAO in the Canada Basin and Nansen Basin. Overall, we found a latitudinal decrease in mesopelagic backscatter in the Beaufort and Barents Sea, but not in Baffin Bay (Figure 2-2b). This pattern was consistent between years in Baffin Bay and in the Beaufort Sea, whereas we only observed a latitudinal decrease in the northern Barents Sea in 2017 when the sampling effort was larger and extended into the Nansen Basin (Figure S2-1, S2-2).

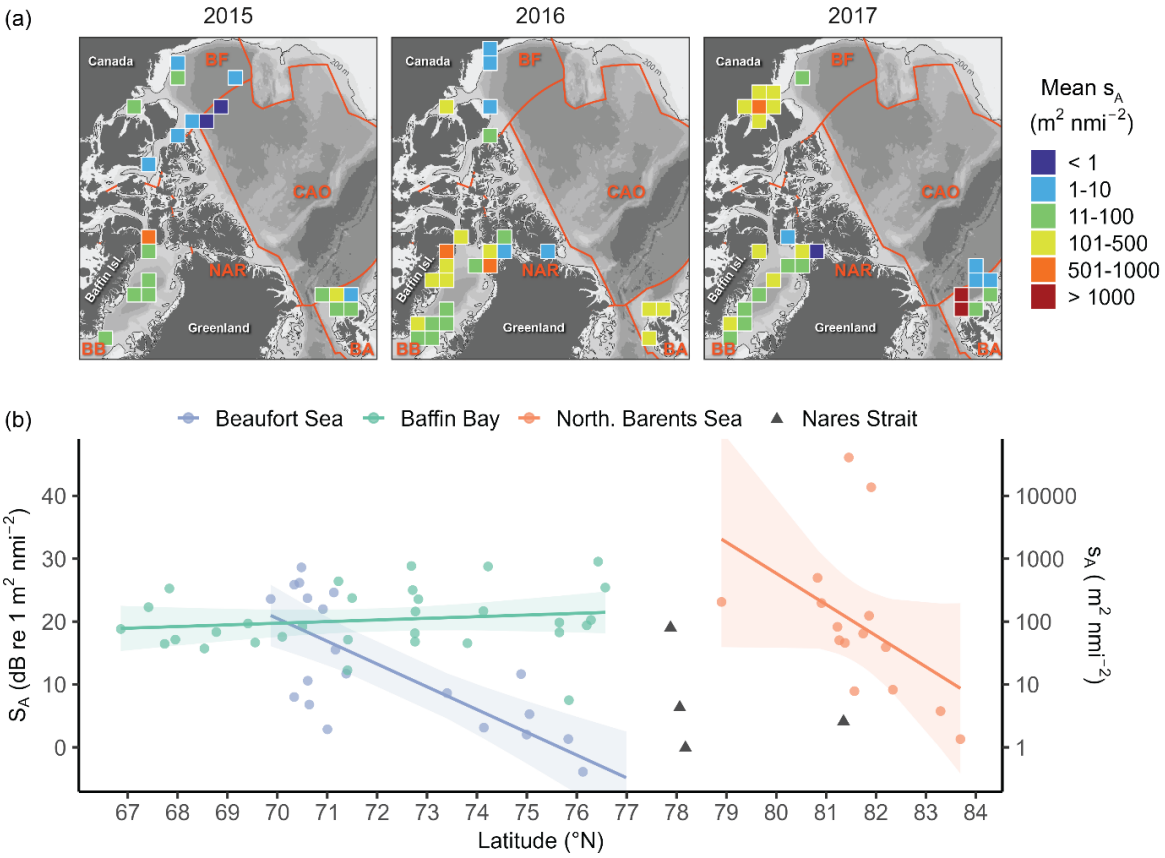

Figure 2-2. (a) Spatial distribution of the mean mesopelagic s_A (m^2 nmi^{-2}) in 2015, 2016, and 2017. Mean s_A are based on 2 to 1667 10-min acoustic echo-integration cells observations. The 200 m isobath is indicated on the maps. (b) Linear regressions of mesopelagic S_A (dB re 1 m^2 nmi^{-2}) as functions of latitude for each Arctic region and 95 % confidence interval (shaded areas). We did not calculate a regression for Nares Strait (triangles) because of the low sample size (n = 4). *BA*: northern Barents Sea; *BB*: Baffin Bay; *BF*: Beaufort Sea; *NAR*: Nares Strait; *CAO*: Central Arctic Ocean.

The mesopelagic layers occupied the upper mesopelagic zone with median WMD ranging between 343 ± 32 m in Baffin Bay and 412 ± 44 m in the northern Barents Sea. WMD

varied significantly between regions (Kruskal-Wallis, $H = 6.91$, p-value = 0.032; Table 2-2) but not years (Kruskal-Wallis, $H = 2.59$, p-value = 0.274). The shallowest mesopelagic layers were found in northern Baffin Bay (301 – 350 m) and the deepest in the Canada Basin of the Central Arctic Ocean (> 550 m; Figure S2-2).

2.4.2 Taxonomic composition

Using mid-water trawls deployed in the mesopelagic zone, we found that the endemic Arctic species Arctic cod (*Boreogadus saida*) was the most abundant mesopelagic fish in the western Arctic including the Beaufort Sea and western and northern Baffin Bay (Figure 2-3a). In contrast, lanternfish (mostly glacier lanternfish *Benthosema glaciale*) and juvenile redfish (*Sebastes* sp.) were the most abundant in southern and eastern Baffin Bay and north of Svalbard – two areas influenced by the advection of Atlantic water.

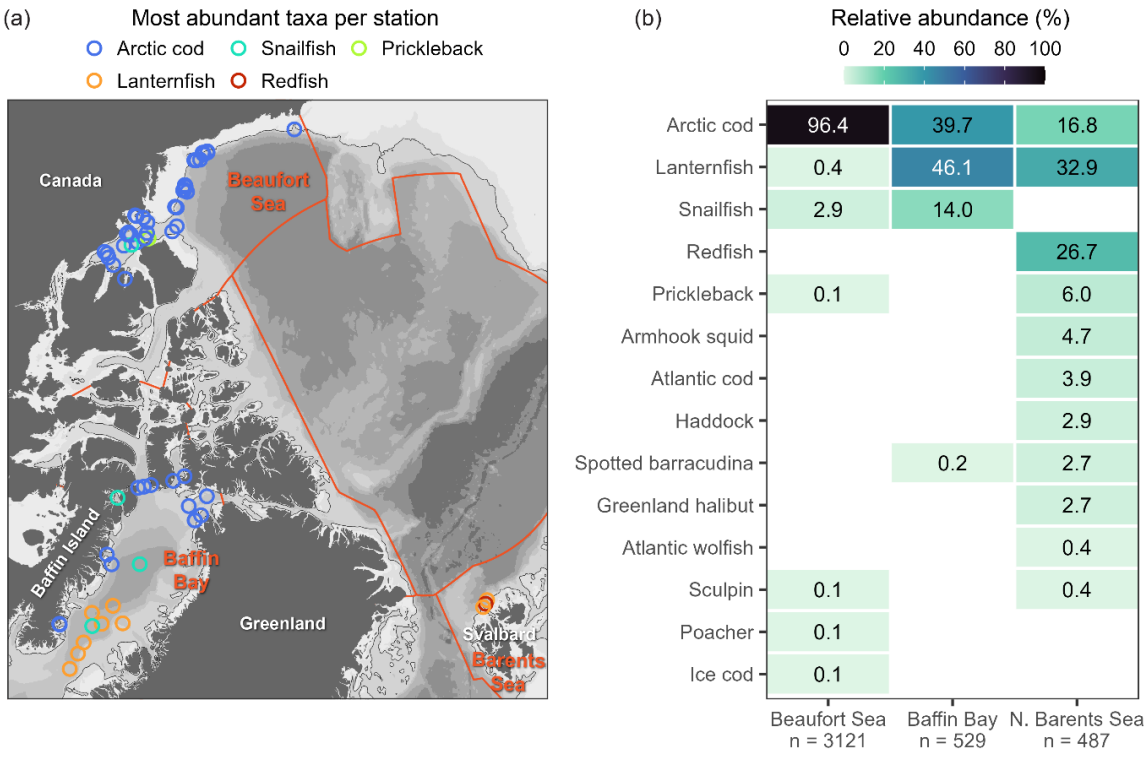

Figure 2-3. (a) The most abundant mesopelagic fish taxa per station and (b) relative abundance of mesopelagic fish taxa caught in the Beaufort Sea, Baffin Bay, and northern Barents Sea. n represents the total number of fish caught in each area.

Arctic cod represented 96.4 % of mesopelagic fish caught in the Beaufort Sea, the remaining being snailfish (2.9 %; *Liparis* sp.), glacier lanternfish (0.4 %), sculpins (0.1 %; *Triglops pingeli* and *Triglops nybelini*), the poacher Arctic alligatorfish (0.1 %; *Aspidophoroides olrikii*), and the prickleback slender eelblenny (0.1 %; *Lumpenus fabricii*; Figure 2-3b). We also found the Arctic gadidae, ice cod (*Arctogadus glacialis*) in low abundances (0.1 %) in the Beaufort Sea.

In Baffin Bay, the mesopelagic fish composition was dominated by glacier lanternfish in the south and by Arctic cod in the west and the north (Figure 2-3a). Over the entire Baffin Bay, Arctic cod represented 39.7 % of mesopelagic catches and lanternfish (46.1 %), the rest of the catch was made by snailfish (14.0 %) and the boreal species spotted barracudina (0.1 %; *Arctozenus risso*; Figure 2-3b).

We did not find a dominant mesopelagic species in the Northern Barents Sea, but rather a combination of different fish and cephalopods co-occurring. Overall, lanternfish (32.9 %), juvenile redfish (26.7 %; *Sebastes* sp.), and Arctic cod (16.8 %) were the most numerous there (Figure 2-3b). Other less abundant species were the prickleback daubed shanny (*Leptoclinus maculatus*), armhook squid (*Gonatus fabricii*), Atlantic cod (*Gadus morhua*), haddock (*Melanogrammus aeglefinus*), spotted barracudina (*Arctozenus risso*), Greenland halibut (*Reinhardtius hippoglossoides*), Atlantic wolfish (*Anarhichas lupus*), and twohorn sculpin (*Icelus bicornis*).

The main macrozooplankton species found in the Beaufort Sea and Svalbard were the hyperiid amphipods Themisto spp. (*Themisto libellula* and *Themisto abyssorum*), euphausiids (*Thyssanoessa* spp. and *Meganyctiphanes norvegica*), gelatinous zooplankton

(mostly *Cyanea capillata*; Figure S2-3). Mysids (*Boreomysis* sp.) were sampled in the Beaufort Sea but not in the northern Barents Sea.

2.4.3 Effects of advection and current velocity on mesopelagic backscatter

Current velocity in the Arctic Ocean was generally slower than in the North Atlantic (Figure 2-4a). In Baffin Bay, the Baffin Island Current flowed southward at high velocities in the northern part of the bay (3-4 cm s^{-1}) and slowed down as it progressed south (Figure 2-4b). We also observed the West Greenland Slope Current entering Baffin Bay on the eastern side of Davis Strait (2-3 cm s^{-1}; Figure 2-4b).

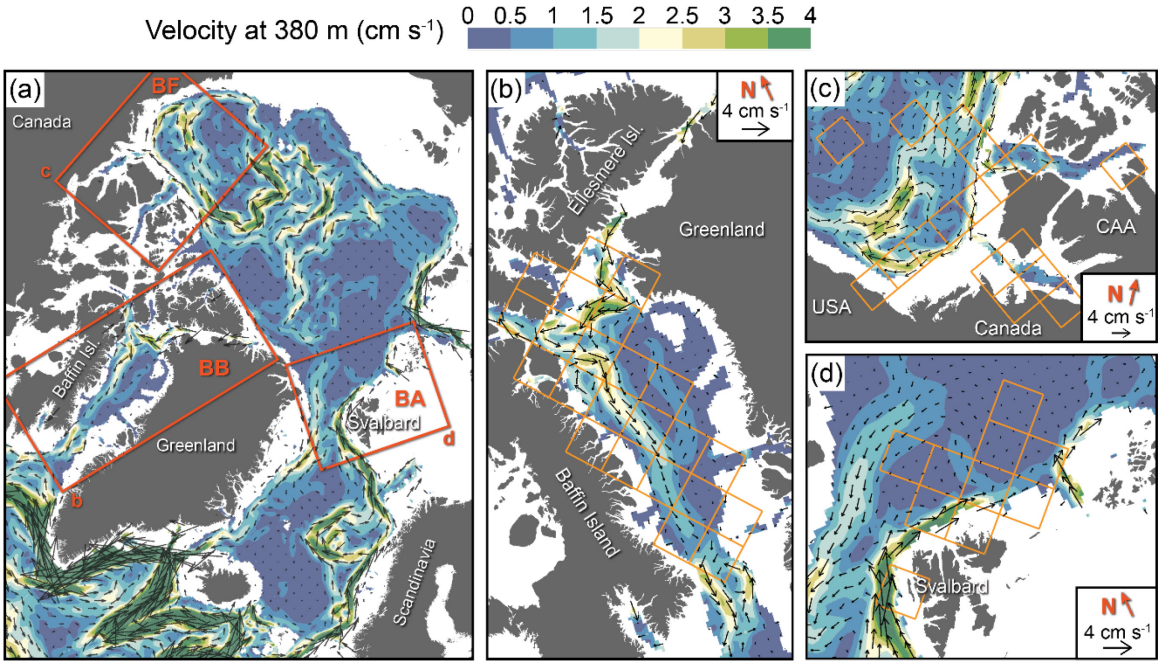

Figure 2-4. Oceanic currents in the marine Arctic with (a) the average current velocity and direction between 2015 and 2017 at 380 m depth, with focus on (b) Baffin Bay, (c) the Beaufort Sea, and (d) the northern Barents Sea. The length of the arrows is proportional to the current velocity. The orange grids indicate cells containing acoustic data. *BA*: northern Barents Sea; *BB*: Baffin Bay; *BF*: Beaufort Sea.

In the Beaufort Sea, the Beaufort Gyre resulted in a current flowing southward along the continental shelf of the Canadian Arctic Archipelago which entered the Amundsen Gulf (1-3 cm s^{-1}) and another current further offshore circulating in the opposite direction (1-2 cm

s^{-1}; Figure 2-4c). In the Amundsen Gulf and centre of the Canada Basin, the current velocities were low (< 1 cm s^{-1}).

The northern Barents Sea was characterized by the highest current velocities of all regions (Figure 2-4d). The West Spitsbergen Current originating from the North Atlantic flowed poleward at high velocities (up to 6 cm s^{-1}) in eastern Fram Strait and then eastward along the continental slope north of Svalbard at ca. 4 cm s^{-1} (Figure 2-4d). Further away from the continental slope, toward the Central Arctic Ocean, current velocities were low (< 1 cm s^{-1}), except to the east of Greenland and western Fram Strait where there was a slow southward current (1-2 cm s^{-1}) exiting the Central Arctic Ocean.

2.5 Discussion

2.5.1 Ubiquitous occurrence of mesopelagic layers in Arctic seas

Mesopelagic fish and zooplankton forming deep scattering layers were detected in three circumpolar Arctic seas. These observations challenge the current standing paradigm of depauperate mesopelagic fish populations at high latitudes (Kaartvedt, 2008; Langbehn et al., 2022). We found two clear fish communities across the study area. In the Canadian Arctic, species diversity was low and dominated by Arctic cod whereas in the European Arctic, species diversity was higher with a combination of Arctic and boreal species. Macrozooplankton were also present in the mesopelagic zone, in particular, the hyperiid amphipods *Themisto* spp., euphausiids, and gelatinous zooplankton (*Cyanea capillata*).

The capacity to feed year-round and a flexible life history that permits winter reproduction are two key traits necessary to survive in the Arctic Ocean (Berge and Nahrgang, 2013; Geoffroy and Priou, 2020). Feeding year-round is crucial for the build-up of sufficient energy reserves to invest in winter reproduction. This buildup of reserves allows first

feeding larvae to emerge during the productive season aligned with the peak in zooplankton nauplii and eggs, their main prey (Pepin et al., 2015). Arctic cod reproduce during the winter (Bouchard and Fortier, 2011). They also have highly sensitive eyes that can detect zooplankton even at very low light intensities (Jönsson et al., 2014), allowing them to continue feeding during the polar night (Berge et al., 2015a; Cusa et al., 2019; Larsen et al., 2023). Of the most abundant species caught in trawls, only Arctic cod met the two criteria of having the ability to feed year-round in the Arctic and reproducing during winter.

In comparison, most mesopelagic fishes of boreal origin captured in the study area do not possess the capacity to both feed and reproduce during winter. While redfish and juvenile boreal gadids – Atlantic cod and haddock – show varying levels of feeding during the polar night (Geoffroy and Priou, 2020; Snoeijs-Leijonmalm et al., 2022), they do not spawn in winter (Olsen et al., 2010; Planque et al., 2013). In contrast, glacier lanternfish spawn in winter in the northwest Atlantic (Halliday et al., 2015) but they reduce their foraging activity in winter (Gjøsæter, 1973). Even though mesopelagic boreal species advected into the Arctic may not survive a complete year-cycle (Wassmann et al., 2015), their presence in the European Arctic and eastern Baffin Bay suggests that they contribute to the mesopelagic niche in Arctic seas.

2.5.2 Advection can support regional fish assemblages

The dominance of boreal fish species in the eastern Arctic Ocean and southeastern Baffin Bay matched with the location of the main Atlantic water pathways into the Arctic Ocean (Curry et al., 2014; Rudels et al., 2013). Except for the spotted barracudina (mean length 23.4 ± 0.5 cm) and armhook squid (17.5 cm), all boreal mesopelagic nekton were small, with mean lengths ranging from 3.0 ± 0.1 cm for poacher Arctic alligatorfish to 8.0 ± 0.1

cm for ice cod (Figure S2-4). Generally, mesopelagic fish in the twilight zone are torpid during daytime (Barham, 1971; Belcher et al., 2020; Kaartvedt et al., 2009), although individual behaviours may diverge from this paradigm (Kaartvedt et al., 2023; Sobradillo et al., 2022). Hence, in areas of strong currents, e.g., Svalbard, small mesopelagic individuals of boreal origin could have been advected with Atlantic water currents. Alternatively, boreal mesopelagic fish and cephalopod could have followed their zooplankton prey which were advected into the Arctic seas (Basedow et al., 2018; Hunt et al., 2016).

In the Barents Sea, we observed high mesopelagic backscatter over the Sofia Deep to the east of the Yermak Plateau (Figure 2-1). This region has frequent anticyclonic eddies (Athanase et al., 2021), which concentrate zooplankton and micronekton and could be a hot spot for mesopelagic fish (Devine et al., 2021; Godø et al., 2012) and their predators (Arostegui et al., 2022). We also found elevated backscatter along the continental slope of the northern Barents Sea, where strong Atlantic currents can transport boreal species from the Norwegian Sea into the marine Arctic (Geoffroy et al., 2019; Gjøsæter et al., 2017; Knutsen et al., 2017). Atlantic water advection was not limited to the European Arctic. In southern Baffin Bay, lanternfish dominated the mesopelagic fish community and were likely transported by the West Greenland Slope Current originating in the North Atlantic. Our results suggest the importance of Atlantic water advection for sustaining local mesopelagic populations, at least, in the gateways to the marine Arctic, similarly to what is observed in the Southern Ocean (Saunders et al., 2017).

Unlike Atlantic water advection in the northern Barents Sea and southeast Baffin Bay, the Baffin Island Current transports cold Arctic waters from Nares Strait and the Canadian

Arctic Archipelago in western Baffin Bay (Cuny et al., 2005; Curry et al., 2014). There, Arctic cod dominate the mesopelagic assemblage. Adult Arctic cod are capable swimmers that conduct long horizontal migrations – the longest migration documented is 192 km (Kessel et al., 2017). Thus, it is the egg, larvae, and juvenile stages that are most prone to advection in currents. The Baffin Island Current acts as a vector for Arctic cod dispersal and structures Arctic cod populations along the entire eastern coast of Baffin Island (Nelson et al., 2020). Arctic cod are further advected out of Baffin Bay into the subarctic and carried southward along the Labrador coast where they dominate the continental slope fish community (Marsh and Mueter, 2020). Therefore, we conclude that both the advection of boreal species from the North Atlantic and the advection of Arctic species from the high Arctic contribute to the widespread occurrence of mesopelagic nekton in Arctic seas. While we focused analyses on large circulation patterns, smaller-scale processes such as mesoscale eddies could also play a role in the spatial distribution of mesopelagic fish (Boswell et al., 2020; Devine et al., 2021; Godø et al., 2012).

Fate of advected species

The geographical extent and survival of mesopelagic fish advected into the Arctic is likely to vary with the life history and ecology of each species. The general current circulation within the Central Arctic Ocean could theoretically transport boreal species from the European Arctic to the Canadian Arctic (Rudels et al., 2013). Yet, we did not catch North Atlantic species like redfish, Atlantic cod, or haddock in the Beaufort Sea, which corroborates previous studies (Majewski et al., 2017). The absence of redfish from the western Arctic could be explained by the ontogenetic migration of juveniles from the

nursery grounds around Svalbard to the southern Barents Sea and Norwegian Sea where they join the adult population of redfish (Drevetnyak and Nedreaas, 2009).

In comparison to redfish, there are no documented seasonal horizontal migration of glacier lanternfish which essentially act as passive drifters, e.g., moving with tidal currents or internal waves (Kaartvedt et al., 2009, 2008). Until recently, lanternfish were thought to be scarce at high latitudes because of challenging foraging conditions during the midnight sun and polar night (Kaartvedt, 2008; Langbehn et al., 2022), but recent observations have sampled *Benthosema glaciale* in low numbers in every region of the marine Arctic (Figure 2-6; Chernova and Neyelov, 1995; Geoffroy et al., 2019; Gjøsæter et al., 2017; Ingvaldsen et al., 2023; Knutsen et al., 2017; Majewski et al., 2017; Snoeijs-Leijonmalm et al., 2022; Zhang et al., 2022). Because glacier lanternfish are absent from the Pacific Ocean (Mecklenburg et al., 2018), the few specimens captured in the Siberian Seas and the Beaufort Sea were likely advected from the North Atlantic via the Fram Strait. Interestingly, in the North Atlantic the condition factor and liver indicator – metrics for the health of a fish (Le Cren, 1951) – of glacier lanternfish improved with increasing latitude (samples collected from 58.7 °N up to 68.4 °N; Knutsen et al., 2023). Whether the recent observations of glacier lanternfish in the Central Arctic Ocean and surrounding seas result from the strengthening of Atlantic water advection over the last decades (Polyakov et al., 2017) or from locally reproducing population of lanternfish discovered due to the recent increase in sampling effort in the Arctic Ocean is unknown. Nonetheless, these results confirm the circumpolar distribution of glacier lanternfish which remained to be confirmed (Mecklenburg et al., 2018). The life history strategies of lanternfish need to be established to understand their survival in the marine Arctic.

2.5.3 Mesopelagic species composition and biogeography

We identified two distinct mesopelagic assemblages in Arctic Seas. In the Beaufort Sea and in western and northern Baffin Bay, the mesopelagic nekton community was dominated by endemic Arctic cod whereas in south Baffin Bay and in the northern Barents Sea Arctic cod co-occurred with boreal expatriates. We could not assess interannual variations in the abundance of mesopelagic nekton because the spatial coverage differed among years, but Arctic cod was the most abundant fish in the sampled years in the Beaufort Sea, and western and northern Baffin Bay (Figure S2-5). While trawl sampling was restricted to 2016 in the northern Barents Sea, studies from 2014 and 2015 at the same time of the year in the same locations showed similar mesopelagic species composition (Gjøsæter et al., 2017; Knutsen et al., 2017). Both studies used multiple mid-water trawls and nets (Harstad trawl, Åkra trawl, and MIK-ring net), and the main mesopelagic nekton taxa catches were redfish (juveniles and adults), Atlantic cod (juveniles and adults), glacier lanternfish, armhook squid, and haddock. Hence, these data suggest that the separation of the mesopelagic nekton of Arctic seas into two distinct assemblages, one dominated by Arctic cod in the western Arctic and one in the eastern Arctic composed of a mix of boreal and Arctic species, was relatively stable in time and space.

The marine Arctic has been defined as a single mesopelagic province engulfing the Central Arctic Ocean and adjacent-high seas (Sutton et al., 2017). We argue that mesopelagic assemblages we observed in Arctic Seas may represent biogeographic provinces, namely the western Arctic province and eastern boreo-Arctic province (Figure 2-6). The western Arctic mesopelagic province is dominated by Arctic cod and encompasses the Beaufort Sea and western Baffin Bay, two areas characterized by the advection of cold water from the high Arctic (McLaughlin et al., 1996). In contrast, the eastern boreo-Arctic mesopelagic

province may be sustained by Atlantic water advection and is composed of a mix of boreal expatriates and endemic Arctic cod. Hydrographic fronts generally separate mesopelagic communities (Escobar-Flores et al., 2018), and the data supports the West Greenland Polar Front in Baffin Bay as the delineation between the eastern Arctic and western boreo-Arctic province (Chawarski et al., 2022). However, in the absence of data throughout much of the area north of 80 °N we cannot identify boundaries in the Central Arctic Ocean. The presence of DSL and observations of adult Atlantic cod, armhook squid, ice cod, and glacier lanternfish in the Amundsen and Nansen Basins of the Central Arctic Ocean suggest that the eastern boreo-Arctic province may extend in this area (Ingvaldsen et al., 2023; Snoeijs-Leijonmalm et al., 2022). Similarly, the western Arctic province may extend in the Canada and Makarov basins where a DSL has been observed but the species composition is currently unknown (Snoeijs-Leijonmalm et al., 2021). However, low abundances of fish were reported in the CAO, and they are probably not as abundant there as in peripheral seas.

In addition to fish and cephalopods sampled in this study, macrozooplankton also contribute to the mesopelagic niche in the Arctic. They are difficult to observe with shipboard acoustics because of their low contribution to acoustic backscatter at 38 kHz at mesopelagic depths. Yet, mesopelagic macrozooplankton can be abundant in Arctic waters and are an important prey for mesopelagic fish (Geoffroy et al., 2019). Important macrozooplankton taxa include hyperiid amphipods (*Themisto* spp.), euphausiids (*Thyssanoessa* spp.), mysids (*Boreomysis arctica*), and gelatinous zooplankton like *Cyanea capillata*. Gas-bearing siphonophores (physonect) like *Rudjakovia plicata* and *Marrus orthocanna* have also been sampled in the Central Arctic Ocean (Kosobokova et al., 2011; Raskoff et al., 2005; Snoeijs-Leijonmalm et al., 2022). Because of their gas-inclusions,

physonect siphonophores are much stronger acoustic targets compared to "fluid-like" zooplankton such as amphipods, euphausiids, and other gelatinous taxa (Lavery et al., 2007). The relative contribution of siphonophores to mesopelagic backscatter can be significant and, if not accounted for, can bias mesopelagic fish biomass estimates (Proud et al., 2019). Snoeijs-Leijonmalm et al. (2022) measured the size of the gas-inclusion of mesopelagic siphonophores in the Central Arctic Ocean and concluded that their contribution to the backscatter of the DSL was marginal in their data. The spatial distribution of macrozooplankton and their contribution to the mesopelagic biomass is limited in the Arctic Ocean, in particular in, the Canadian Arctic and Central Arctic Ocean, where it would need to be further scrutinized.

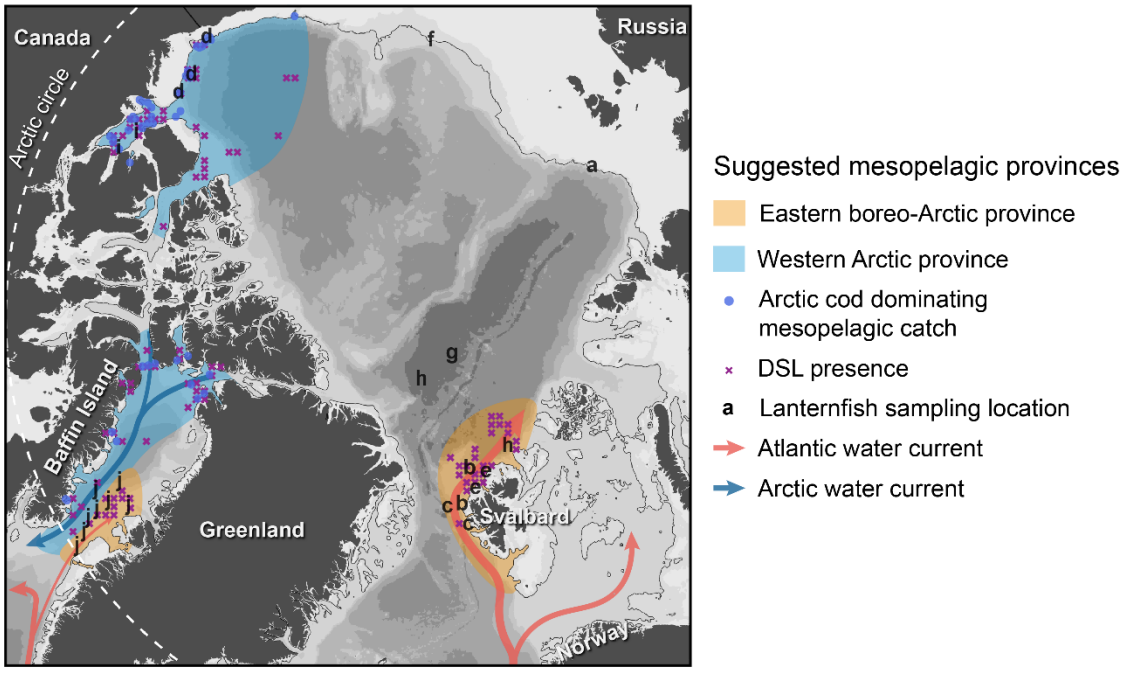

Figure 2-5. Suggested potential mesopelagic provinces Arctic high seas based on species composition, acoustic data, and environmental drivers (shaded areas). The dashed shaded area shows the potential extension of the provinces into the Central Arctic Ocean but remain to be confirmed. Arrows show the Atlantic water and Arctic water currents. The letters indicate sampling locations of lanternfish in the marine Arctic: a: Chernova and Neyelov (1995); b: Gjøsæter et al., (2017); c: Knutsen et al., (2017); d: Majewski et al., (2017); e: Geoffroy et al., (2019); f: Zhang et al., (2022); g: Snoeijs-Leijonmalm et al., (2022); h: Ingvaldsen et al., (2023); i: A. Majewski (unpublished); j: this study.

Because four mid-water trawls with different physical dimensions, mesh sizes, and tow durations were used in this study, the bias in catch composition is unknown. We caught mesopelagic nekton with similar length ranges with each mid-water trawl (Figure S2-4). However, large mesopelagic fish and cephalopods can avoid nets and small nets can more easily be avoided than larger nets because they create large pressure waves when towed fast (Kaartvedt et al., 2012). The small taxa and individuals may have been under sampled with the large mid-water trawl used, such as the Cosmo-swan 260 in the Beaufort Sea or Harstad trawl in the Barents Sea. Similarly, larger fish and cephalopod may have been under sampled with the IKMT and IKRMT, which have a small mouth opening compared to the Harstad and Cosmo-swan 260 trawls. Yet, the catch composition from the Cosmo-swan 260 and IKMT yielded similar results – dominance of Arctic cod in terms of

abundance – when they were deployed in the Beaufort Sea in August and September 2014 (Figure S2-6). Nonetheless, the catch composition should be interpreted with some caution.

2.5.4 Ecological significance of the mesopelagic niche in the Arctic

Given the intermediate trophic position of mesopelagic fish in the pelagic food web, they are an essential link for transferring energy from secondary consumers to top predators. Mesopelagic fish actively contribute to the biological carbon pump through DVM (Davison et al., 2013), although this contribution may be limited to brief periods between the polar night and midnight sun in the Arctic (Snoeijs-Leijonmalm et al., 2022). In the western Arctic province, mesopelagic fish diversity is low and Arctic cod may exert a wasp-waist control on the marine ecosystem, channeling most of the energy from secondary producers to top predators (Pedro et al., 2023; Welch et al., 1992). Arctic cod are lipid-rich fish (Hop and Gjøsæter, 2013) that sustain important populations of marine mammals, including endemic marine mammals like Beluga whales (*Delphinapterus leucas*) which forage on Arctic cod at mesopelagic depths in the Beaufort Sea (Choy et al., 2020; Storrie et al., 2022), bowhead whales (*Balaena mysticetus*), narwhals (*Monodon monoceros*), and ringed seals (*Phoca hispida*) which also forage on mesopelagic Arctic cod in the Pikialasorsuaq (north water polynya) in northern Baffin Bay (Heide-Jørgensen et al., 2013; Tremblay et al., 2006).

In the eastern boreo-Arctic province, lipid-rich boreal species like lanternfish and redfish (Olsen et al., 2020; Voronin et al., 2021) also support marine mammal populations. In contrast to the western Arctic province, aside from the three main Arctic endemic whale species – narwhals, beluga, and bowhead whales – most of the whales present in the eastern boreo-Arctic province are long-range migrants which spend the winter at lower latitudes

and migrate northward to their primary feeding grounds at high latitude in the spring and summer (MacKenzie et al., 2022). Mesopealgic fish also support commercially harvested fish species. For example, Atlantic cod uses the mesopelagic zone as both a nursery for its juveniles and as a foraging ground for adults (Geoffroy et al., 2019; Ingvaldsen et al., 2017; Knutsen et al., 2017). Although lanternfish represented 46 % of the assemblage in the northern Barents Sea, they only represent 2 % of the mesopelagic biomass (Geoffroy et al., 2019) and their abundance is presumably largely driven by variations in Atlantic water inflow (Langbehn et al., 2022). Because of this connectivity with the subarctic ecosystem through Atlantic water advection, perturbations in subarctic food webs, e.g., recruitment failures and successes, could have cascading effects on Arctic food webs. The higher biodiversity of the eastern boreo-Arctic province mesopelagic community could possibly result in higher resilience to biotic and abiotic environmental perturbations compared to the less diverse western Arctic province (Folke et al., 2004; Worm and Lotze, 2021).

Diminishing multi-year ice cover allows the expansion of anthropogenic activities in the Arctic Ocean, including oil and gas exploration, fisheries, mining, shipping, and tourism. Environmental impact surveys generally focus on marine mammals and benthos, often overlooking pelagic ecosystems (Drazen et al., 2020). Yet, to achieve ecosystem-based management approaches and efficient marine spatial planning, the biogeography of mid-water resources needs to be considered (Ceccarelli et al., 2021). The delineation of potential mesopelagic biogeographic provinces provided herein not only underpins the mesopelagic zone as a viable habitat for several fish, cephalopod, and macrozooplankton taxa, but also outlines the connectivity of mesopelagic communities between the Arctic and the subarctic. These suggested mesopelagic biogeographic provinces provide a basis for management and conservation planning for Arctic marine ecosystems.

3 Chapter three[2]: Dense mesopelagic sound scattering layer and vertical segregation of pelagic organisms at the Arctic-Atlantic gateway during the midnight sun

3.1 Abstract

Changes in vertical and spatial distributions of zooplankton and small pelagic fish impact the biological carbon pump and the distribution of larger piscivorous fish and marine mammal species. However, their distribution and abundance remain poorly documented at high latitudes because of the difficulties inherent to sampling relatively fast-moving organisms in ice-covered waters. This study documents the under-ice distribution of epipelagic and mesopelagic organisms at the Arctic-Atlantic gateway in spring, during the midnight sun period, using ice-tethered and ship-based echosounders. An epipelagic surface scattering layer composed of copepods consistently occupied the top 60 m and was associated with cold polar surface water (mean temperature of -1.5°C). A mesopelagic deep scattering layer (DSL), partly composed of fish, persisted between 280 m and 600 m and was associated with modified Atlantic water. Backscattering strength within the DSL was higher than previously reported in the Arctic and North Atlantic, and increased by two orders of magnitude over the continental slope where one of the Atlantic water pathways enters the Arctic Ocean. Mesopelagic organisms did not perform diel vertical migrations. The consistent segregation between copepods at the surface and their predators at mesopelagic depths suggests limited predator-prey interactions during the midnight sun period, even under the ice cover. Predation on copepods by mesopelagic organisms, including fish, could thus be limited to very pulsed events during the seasonal vertical

[2] A version of this chapter is published in *Progress in Oceanography 196 (102611)* doi:10.1016/j.pocean.2021.102611

migration of copepods to and from overwintering depths. This suggests that the arctic mesopelagic food web may be decoupled from secondary production in the epipelagic layer throughout most of the year.

3.2 Introduction

Macrozooplankton and small fish inhabit the mesopelagic zone, between 200 and 1,000 m, and play a crucial role in marine ecosystems by linking primary and secondary consumers to higher predators (Naito et al., 2013; Saunders et al., 2019) and contributing to the biological carbon pump (Davison et al., 2013). Mesopelagic organisms form deep sound scattering layers (DSL) that can be detected by hydroacoustic instruments and possibly represent the largest fish biomass of the world's oceans (Irigoien et al., 2014). As in most deep oceanic basins (Proud et al., 2017), recent investigations revealed that DSL also occur in the Arctic, although at lower acoustic densities than in temperate regions (Geoffroy et al., 2019; Gjøsæter et al., 2017; Knutsen et al., 2017; Snoeijs-Leijonmalm et al., 2021).

Globally, about half of the mesopelagic acoustic backscatter undergo diel vertical migrations (DVM; Klevjer et al., 2016). Migrating animals move to the epipelagic layer (0-200 m depth) to feed at night and descend at greater depths to shelter from predators during daytime. While the hunger state of the migrating individual and the trade-off between visual foraging and predation mortality are generally assumed to be the ultimate drivers of DVM (Hays, 2003; Pearre, 2003), other proximate factors such as light, temperature, or oxygen mediate the amplitude of the migrations (Bianchi et al., 2013; Cade and Benoit-Bird, 2015; Norheim et al., 2016). The relative importance of each of these factors vary spatially, but in situ irradiance is considered to play an essential role (Røstad et al., 2016). In the Arctic Ocean, pelagic organisms are attuned to strong seasonal changes in irradiance (Berge et al.,

2016). For example, most arctic copepods perform DVM when the photoperiod alternates between day and night, in spring and autumn, but the continuous irradiance and the resulting lack of nighttime refuge against visual predators usually stop DVM during the midnight sun period (Blachowiak-Samolyk et al., 2006; Cottier et al., 2006) when large copepods accumulate near the surface (Darnis and Fortier, 2014). DVM of mesopelagic organisms have been reported under the ice at the end of the midnight sun period and when the day-night cycle resumes in late summer, but these DVM did not reach the epipelagic zone (Gjøsæter et al., 2017).

The vertical segregation between mesopelagic communities and their zooplankton prey during the midnight sun period was suggested to be responsible for the absence of myctophids in northern Baffin Bay (Sameoto, 1989). The photoperiod constraint hypothesis suggests that by suppressing DVM during part of the year, the extreme photoperiod regime prevailing at high latitudes reduces the foraging success of mesopelagic communities and prevent their viable establishment in the Arctic Ocean (Kaartvedt, 2008). Studies later confirmed this hypothesis and showed a strong decrease in mesopelagic biomass toward the pole (Knutsen et al., 2017; Siegelman-Charbit and Planque, 2016). This latitudinal decrease in biomass was attributed to the reduced amplitude of DVM with the poleward increase in nighttime irradiance during spring-summer (Norheim et al., 2016). Theoretical modelling confirmed that the depth of the DSL in the Norwegian Sea could be predicted by in situ irradiance (Langbehn et al., 2019). However, observations of the migrating behaviour of the Arctic mesopelagic community during the midnight sun period remain scarce, especially under the ice, as previous studies were conducted in late summer, at the end of the midnight sun period and when the Arctic sea ice extent is at its lowest. Because sea ice and snow thickness strongly attenuate light transmittance to the ocean, in

particular prior to the summer melt (Perovich, 2005), they could sufficiently reduce under-ice in situ irradiance to modify the vertical distribution and migrating behaviour of mesopelagic organisms, similarly to what has been observed for copepods under the ice (Fortier, 2001). If mesopelagic animals perform DVM under the ice cover during the midnight sun period, it would keep the epipelagic and mesopelagic zones intertwined in a large part of the Arctic Ocean during that period. In contrast, if continuous segregation persists under the ice, it would greatly limit predator-prey interactions for most of the year.

In June 2017, in the midst of the midnight sun period, the R/V *Polarstern* conducted a drift station north of Svalbard over the eastern slope of the Yermak Plateau (> 900 m depth). Ice-tethered and ship-based echosounders recorded the vernal vertical distribution, DVM, and backscattering strength of pelagic organisms under the ice cover. Here, we test the hypothesis that there is no overlap between epipelagic prey and mesopelagic predators under the ice cover in spring, during the midnight sun period. We also investigate potential drivers of the variation in vertical distribution and backscattering strength of epipelagic and mesopelagic organisms.

3.3 Material and methods

3.3.1 Study area

The R/V *Polarstern* remained anchored to an ice floe over the Yermak Plateau, north of Svalbard, from June 3 to 15, 2017 (Figure 3-1). The mean sea ice and snow thickness of the ice floe was 1.90 m (Wollenburg et al., 2020) and was representative of the sea ice conditions prevailing in the area (Castellani et al., 2020). During this period, the vessel drifted ca. 100 km over bottom depths ranging from 930 to 1,608 m. The study area, at the northeast Atlantic gateway to the Arctic Ocean, represents a major deep-water connection

between the Atlantic and Arctic basins. The West Spitzbergen Current carries warm Atlantic water along the western slope of Svalbard and splits into three branches at the Yermak Plateau; the Svalbard Branch flowing along the northern slope of Svalbard, the Yermak Pass Branch flowing across the Yermak Plateau, and the Yermak Branch flowing around the Plateau (Figure 3-1; Athanase et al., 2021). Four main water masses co-occur in the study area: polar surface water (PSW; $\sigma_0 \leq 27.70$ and $\theta < 0$ °C), modified Atlantic water (MAW; $27.70 < \sigma_0 < 27.97$ and $\theta < 2$ °C; $\sigma_0 > 27.97$, $\sigma_{0.5} < 30.444$ and $\theta > 0$ °C), Atlantic water (AW; $27.70 < \sigma_0 < 27.97$ and $\theta > 2$ °C), and Arctic intermediate water (AIW; $\sigma_0 > 27.97$, $\sigma_{0.5} < 30.444$ and $\theta < 0$ °C; Meyer et al., 2017).

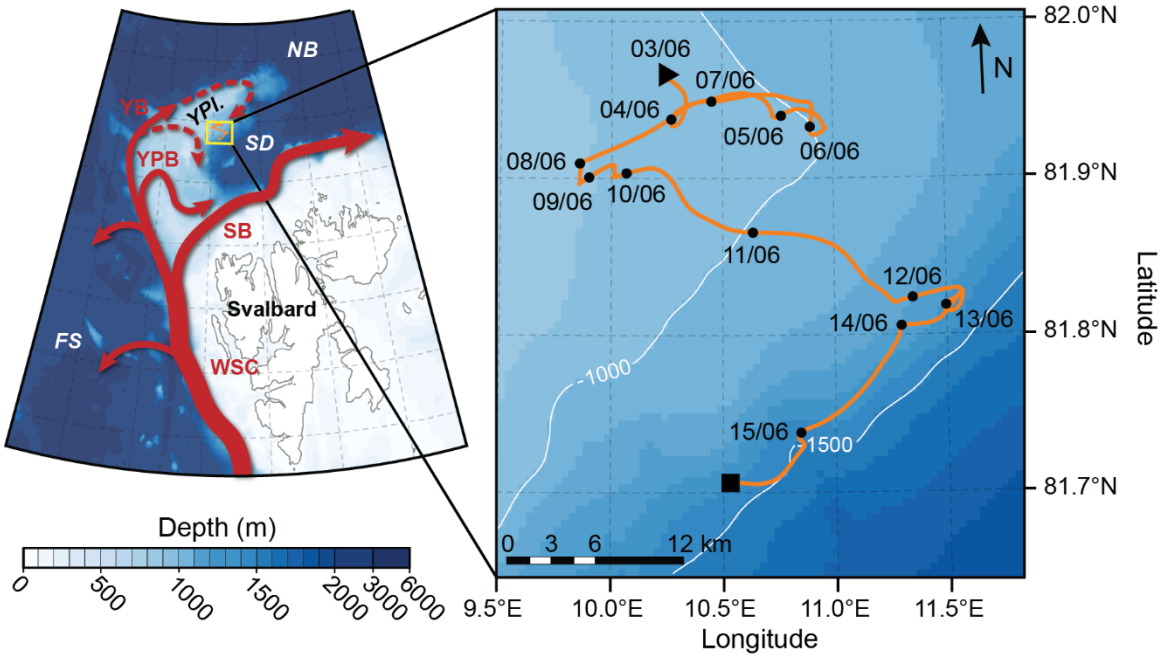

Figure 3-1. Bathymetric map of the Yermak Plateau, north of Svalbard, with regional circulation as suggested by Athanase et al. (2021). The yellow rectangle delimits the study area. Red solid arrows show the main pathways of Atlantic water into the Arctic Ocean and the dashed arrow indicates intermittent Atlantic water inflow. The orange line shows the drift trajectory between June 3 (black triangle) and June 15 (black rectangle), 2017. The 1,000 and 1,500 m isobaths are indicated. *YPl.*: Yermak Plateau; *SD*: Sofia Deep; *NB*: Nansen Basin; *FS*: Fram Strait; *WSC*: West Spitzbergen Current; *SB*: Svalbard Branch; *YPB*: Yermak Pass Branch; *YB*: Yermak Branch.

3.3.2 Environmental sampling

Temperature, salinity, dissolved oxygen, and fluorescence profiles were measured at least once per day with the shipborne Conductivity-Temperature-Depth system (CTD; Sea-Bird Electronics Inc, SBE-911+ plus) equipped with fluorescence (WETLabs, ECO-AFL/FL) and dissolved oxygen (SBE43) sensors. The temperature and salinity profiles from the ship CTD were used to calculate the speed of sound and absorption coefficients for hydroacoustic calculations. The fluorescence sensor was uncalibrated and only indicated relative values of chlorophyll *a* concentration (a proxy for phytoplankton biomass). Chlorophyll *a* in the top 50 m was also measured with a handheld CTD (Sea & Sun, CTD 75M) equipped with a calibrated fluorescence sensor (Turner, Cyclops-7) deployed from the sea ice. Additionally, an ice-tethered mooring equipped with three SBE37-IM MicroCAT sensors (Sea-Bird Electronics Inc.) recorded conductivity and temperature at 8, 56, and 141 m depth (and also pressure at 8 m), with a 30-second resolution between June 4 and 16.

A spectral radiation station was installed on the ice floe to measure above and under-ice irradiance. This station consisted of RAMSES hyperspectral radiometers (TriOS Gmbh) placed above the ice and at 50 cm below the ice-water interface which measured spectral irradiance (320 to 950 nm). In this study, we used the integrated irradiance over the 320-950 nm range. A snow buoy (Met Ocean, Snow Beacon) was also deployed between June 7 and July 12, which measured snow thickness at the surface of the ice floe.

3.3.3 Zooplankton sampling

Zooplankton and under-ice fauna were sampled with a plankton net (ROVnet; Wollenburg et al., 2020) mounted on the rear end of a remotely operated vehicle (ROV; Ocean Modules,

M500; Katlein et al., 2017). The ROVnet consisted of a polycarbonate frame with an opening of 40 cm by 60 cm, to which a zooplankton net with a mesh size of 500 µm was attached. After each ROVnet deployment, the net was rinsed with ambient seawater to concentrate the sample in the cod end. The ROVnet sampled horizontal profiles in the water below the sea ice. Standard ROVnet profiles were conducted at the ice-water interface, 5 m, and 10 m depth at 1 knot. The distance covered by each profile ranged between 300 and 600 m. Zooplankton were sorted in the laboratory to the lowest possible taxonomic level. We calculated abundances from the zooplankton counts and volume of water filtered by the net (Wollenburg et al., 2020). The ROV also carried a high-resolution video camera used to document the possible presence of fish under the ice.

3.3.4 Sampling and processing of hydroacoustic data

Acoustic backscatter was recorded using two ice-tethered single beam Autonomous Zooplankton and Fish Profilers (AZFP; ASL Environmental Sciences) operating at 38, 125, 200, and 455 kHz and a hull-mounted split beam EK60 (Simrad) echosounder operating at 18, 38, 70, 120, and 200 kHz. The AZFPs deployment was part of the developmental phase of an ice-tethered observatory for plankton and fish (Berge et al., 2016; Zolich et al., 2018). The AZFPs were deployed from June 9 until June 15, whereas the EK60 recorded during the entire drift station (June 3-15). The manufacturer calibrated the AZFPs before deployment, and all the frequencies of the hull-mounted echosounder but the 18 kHz were calibrated after the cruise (June 18) using the standard sphere method (Demer et al., 2015). Here, we show all echograms, including at 18 kHz, but we did not use that frequency for echo-integration because it was not calibrated. Due to the near stationary position of the ship drifting in the ice pack, the ambient noise levels were low, which increased the signal to noise ratio and detection ranges (Figure S3-1).

Each AZFP was positioned through holes in the sea ice approximately 100 m away from each other and 100 m away from the ship's echosounder and ADCP mooring to limit acoustic interference. The two AZFPs were moored at 15 m water depth within a stainless-steel frame supported by floats. To limit backscatter from the frame and floats, the AZFPs were mounted with a 15 ° angle relative to the vertical mooring line. One AZFP faced upward toward the sea ice, and the other faced downward toward the seafloor. The AZFP data were averaged internally with a 38.0 cm (upward-looking unit) or 95.5 cm (downward-looking unit) vertical resolution. Pulse length, ping rate, nominal beam angle, and nominal source-level varied between frequency and between the upward and downward facing AZFP (Table S3-1).

The ship-based hull-mounted echosounder EK60 was continuously operated during the drift period. The transducers were located at 11 m depth in the ship's hull and pulse length was set to 1.024 ms, the ping rate varied from 0.38 to 0.61 Hz to accommodate for other onboard acoustic instrumentation, and the beamwidth was 11 ° for the 18 kHz echosounder and 7 ° for the other transducers (Table S3-1). The higher transmitted power of the hull-mounted EK60 compared to the AZFP (Table S3-1) increased the signal to noise ratio and resulted in increased detection ranges for the EK60. The combination of these instruments thus ensonified the water column from ca. 0.5 m under the ice down to 786.0 m depth.

Acoustic data from the AZFPs and EK60 were scrutinized, cleaned, and edited using Echoview 11 (Echoview Software Pty Ltd.). We removed background (minimum 10 dB signal to noise ratio) and impulse noise with Echoview's algorithms (De Robertis and Higginbottom, 2007; Ryan et al., 2015). Little acoustic interference was observed on the upward and downward AZFPs. We echo-integrated the echograms in 10 min long x 1 m

deep cells for the upward looking AZFP and 10 min long x 3 m deep cells for the downward looking AZFP and hull-mounted EK60. The mean volume backscattering strength (MVBS in dB re 1 m^{-1}) and nautical area scattering coefficient (s_A in m^2 nmi^{-2}) were exported for each cell. To investigate the vertical migrations of the scatterers, we exported the weighted mean depth (WMD), also called centre of mass (Urmy et al., 2012), from 10 min long cells encompassing the full vertical extent of each sound scattering layer at 38 kHz for the EK60 and at 455 kHz for the AZFP data. Backscatter (MVBS and s_A) and vertical distribution data were then analyzed in R (version 4.0.3, R Core Team).

Acoustic backscatter (receiver signal strength indicator; RSSI) and water velocities underneath the ice floe were also recorded by an upward looking Acoustic Doppler Current Profilers (ADCP; Teledyne RD Instruments, 307.2 kHz) deployed at 101 m on the MicroCAT mooring line from June 4 to 16. The ADCP recorded data every 3 min in 50 s ensembles with one ping per second and averaged into 4 m depth cells. Data were post-cruise quality assessed with the IMOS Matlab toolbox provided by the Australian Ocean Data Network and Integrated Marine Observing System (AODN IMOS). An additional check was done on occurrences with substantially increased vertical velocities throughout the water column, found to be due to quick changes in tilt at strong winds and high ice-drifting speed (June 7, 10, and 11). For vertical velocity, the affected ensembles were manually removed, and for backscatter, these associated displacements were regarded small enough relative to the data averaging cell size (4 m) to keep. The final valid data range for the ADCP was 15-95 m depth. Further, the ADCP backscatter was extracted from each beam, checked for spurious values (affected ensembles were removed), and converted to mean volume backscattering strength (Gostiaux and van Haren (2010) and references therein). Both backscatter and vertical velocity data were interpolated linearly to 10 min

interval and used to calculate a 24 h *"model day"* composite averaged over days with good data. For vertical velocity, we used anomalies calculated for each cell by subtracting the record-average vertical velocity prior to synthesizing the composite (Cottier et al. (2006) and references therein). The vertical velocity anomaly 24 h composite was used to check if zooplankton performed asynchronous vertical migrations, as seen by net downward vertical velocities near the surface and net upward vertical velocities below (Cottier et al., 2006).

3.3.5 Acoustic classification of the scattering layers

To gain insights into the vertical distribution of different groups of scatterers in the epipelagic zone, we partitioned each echo-integration cell from the ice-tethered AZFPs following the multifrequency selection criteria listed in Darnis et al. (2017). In short, we applied the multifrequency classification on each echo-integration cell to reduce the inherent stochasticity of acoustic data (Korneliussen et al., 2018), and classified each given cell as being dominated by copepods if $MVBS_{125kHz} < MVBS_{200kHz} < MVBS_{455kHz}$, chaetognaths if $MVBS_{125kHz} < MVBS_{200kHz} > MVBS_{455kHz}$, or by euphausiids if $MVBS_{125kHz} > MVBS_{200kHz} < MVBS_{455kHz}$ (Darnis et al., 2017). The maximum range of the 455 kHz transducers limited the range of the dB-differencing analysis to 70 m depth. Although the abundance of zooplankton species varies across regions of Svalbard, e.g., between the Yermak Plateau north of Svalbard and Kongsfjorden on the west coast of Svalbard, both of these areas are influenced by Atlantic water masses and the diversity of zooplankton functional group remains similar (Daase and Eiane, 2007; Darnis et al., 2017). The classification algorithm from Darnis et al. (2017) is therefore applicable to the present study.

We scrutinized the target strength (TS) of single targets at 38 kHz from the hull-mounted split beam EK60. First, single targets were detected using Echoview's single-echo detection algorithm for split beam echosounders (method 2) with a maximum beam compensation of 3 dB which only retained single targets close to the beam axis (Table S3-2). To reduce the computing time, we detected single targets 4 h per day between 0-1, 6-7, 12-13, and 18-19 h from June 4 to 15. Second, we ran Echoview's fish track algorithm on the single target echograms and extracted single target tracks (named fish track in Echoview) to reduce the chances of detecting echoes from multiple targets. This algorithm finds single targets that can be tracked over consecutive pings which are assumed to be originating from a single object moving through time and space. As the R/V *Polarstern* was near stationary, we tracked single targets over at least 5 consecutive pings with no missed detection between pings (Table S3-3). The efficiency of the single target tracking increased with increasing depth due to the widening of the beam. We retained single targets found to be within a maximum horizontal diameter of 2 m (athwartship and alongship) and 1 m range from their position at the previous ping. The algorithm thus excluded animals swimming faster than 0.77 m s^{-1}, which is larger than the swimming speed of most mesopelagic animals (Peña et al., 2020 and references therein). We calculated the mean TS and mean depth for each single target track.

3.3.6 Statistical analyses

For each sound scattering layer, we used generalized additive models (GAM; Wood 2017) to explore the relationship between s_A (used as a proxy for animal density), WMD, and environmental drivers. We log transformed s_A to meet normality assumptions. Environmental drivers included bottom depth, the vertical extent of water masses of Atlantic origin (MAW and AW), temperature of polar surface water measured at 56 m

depth, temperature of modified Atlantic water measured at 141 m depth, time of day, and under-ice downwelling irradiance. To accommodate for the change in irradiance between days, for instance, due to cloud cover or snow melt, we used the interaction of under-ice downwelling irradiance and time of day modeled as a tensor product smooth.

We calculated the degree of collinearity between explanatory variables with the Spearman's correlation coefficient (ρ) and used a 0.80 cut-off value. GAMs were fitted with the *mgcv* package in R (version 1.8-33) using a Gaussian distribution with an identity link function. Time of day was modeled with a cyclic cubic regression spline and other explanatory variables were modeled using thin plate regression splines. We estimated the splines with the restricted maximum likelihood (REML) optimization method and limited the number of knots to 5 to prevent overfitting (Wood, 2017). Models were selected using null space penalization and we included a first order autoregressive error structure in the GAMs to accommodate for autocorrelation of residuals.

3.4 Results

3.4.1 Environmental conditions

The ice coverage was close to 100 % over the duration of the drift. Four water masses were superposed: polar surface water (PSW) from the surface down to ca. 110 m, modified Atlantic waters (MAW) from 110 m down to ca. 680 m with some intrusions of core Atlantic water (AW) between 120 and 300 m, and Arctic intermediate water (AIW) below MAW (Figure 3-2a, b). The vertical distribution of the water masses remained relatively constant in the first part of the drift (June 4-11) with MAW occupying 60 % of the upper 900 m water column. We observed a thickening of the MAW (down to ca. 725 m,

occupying 69 % of the top 900 m) after June 11, which coincided with the ice floe drifting southward toward the deeper continental slope (Figure 3-1, Figure 3-2a,b).

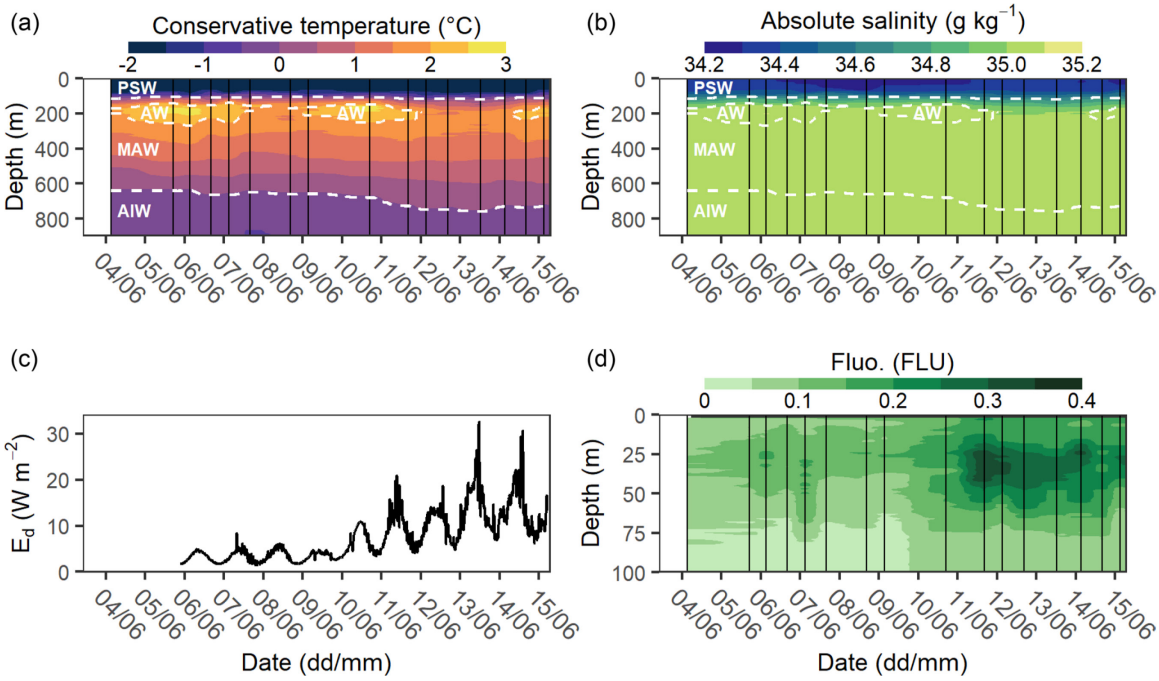

Figure 3-2. (a) Conservative temperature and (b) absolute salinity in the uppermost 900 m as measured during the R/V *Polarstern* drift by the ship CTD. Vertical black lines indicate the location of CTD casts and dashed white lines represent the boundaries between water masses. (c) Under-ice downwelling irradiance at 50 cm below the ice-water interface (E_d in W m^{-2}), and (d) fluorescence in the top 100 m (in arbitrary fluorescence units as the sensor was not calibrated). *PSW*: polar surface water; *AW*: Atlantic water; *MAW*: modified Atlantic water; *AIW*: Arctic intermediate water.

The sun never set below the horizon during the drift, but incident irradiance at the surface of the ice floe displayed a diurnal cycle (Figure S3-2a). The under-ice downwelling irradiance at 50 cm below the ice-water interface was ca. 4 % of the irradiance at the surface of the ice floe and exhibited a diurnal pattern with higher irradiance around local midday (UTC + 2 h) and lower irradiance around local midnight (Figure 3-2c). Thinner snow cover after June 11 increased under-ice downwelling irradiance and the diurnal variation in irradiance, which ranged between 0.7-10.9 W m^{-2} before June 11 and increased to 3.8-32.6 W m^{-2} afterwards (Figure 3-2c, Figure S3-2b). Following that increase in under-ice irradiance, the fluorescence and chlorophyll a concentration increased from 0.4-1.0 mg m^{-}

^{3} (average of 0.8 mg m^{-3}) to 0.4-1.8 mg m^{-3} (average of 1.1 mg m^{-3}) after June 11 (Figure 3-2d, Figure S3-2c). The subsurface chlorophyll a maximum was located at 34 m on June 11 (1.5 mg m^{-3}) and at 22 m on June 15 (1.8 mg m^{-3}).

3.4.2 Vertical distribution and backscattering strength of sound scatter layers

Two distinct acoustic sound scattering layers co-occurred under the ice cover; a shallow epipelagic surface scattering layer (SSL) in the top 60 m and a deep sound scattering layer (DSL) between 280 m and 600 m (Figure 3-3). We also observed intermittent scattered patches between the SSL and DSL (Figure 3-3, Figure S3-4). The backscatter of the SSL was higher at 455 kHz than at lower frequencies (Figure 3-3a), whereas the scattered intermediate patches and DSL volume backscattering strength was stronger at 38 kHz (Figure 3-3b), most likely because of lower signal-to-noise ratio at higher frequencies. We therefore focused the following analyses on the 455 kHz AZFP data for the SSL and 38 kHz EK60 data for the DSL.

In the epipelagic zone, the SSL had a median WMD of 31 m at 455 kHz and did not follow clear diel vertical migration patterns (DVM; Figure 3-4a). However, the lower limit of the SSL detected by the ADCP at 307 kHz was ca. 30 m deeper around midday (ca. 100 m) than at night (ca. 70 m), suggesting small-scale DVM of animals within the SSL (Figure S3-3a). These DVM were not detected at 455 kHz because the range of that transducer was limited to the top ca. 70 m. No asynchronous DVM pattern was detected within the SSL (Figure S3-3b). The s_A of the SSL remained relatively stable at a median of 18 m^2 nmi^{-2} at 455 kHz before June 11 and increased to a median of 28 m^2 nmi^{-2} at 455 kHz afterwards (Figure 3-4b).

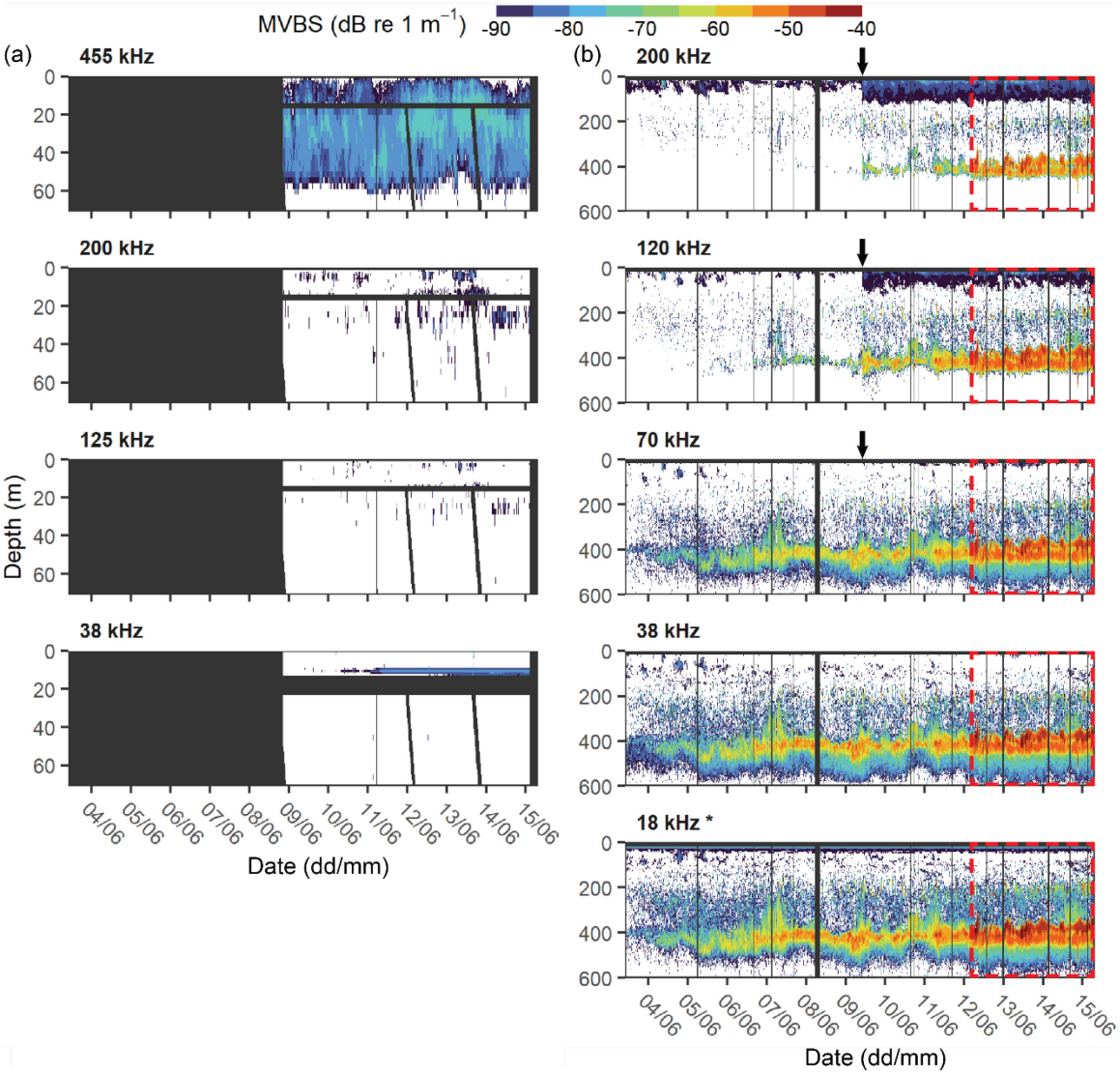

Figure 3-3. (a) Composite echograms of denoised mean volume backscattering strength (MVBS in dB re 1 m^{-1}) from the upward and downward facing ice-tethered AZFPs at 455, 200, 125, and 38 kHz. (b) Echogram of denoised MVBS from the hull-mounted EK60 at 200, 120, 70, 38, and 18 kHz (* not calibrated). The dashed red rectangle indicates the south-western part of the drift along the eastern slope of the Yermak Plateau (> 1,500 m), which coincides with an increase in backscattering strength within the DSL. The black arrows on the EK60 echograms at 200, 120, and 70 kHz on June 9 depicts the change in pulse length which was increased from 0.256 to 1.024 ms at 120 and 200 kHz, and from 0.512 to 1.024 ms at 70 kHz. Areas with bad acoustic data (due to acoustic interference with other instruments, near-field, or dead zone near the sea ice) or with no data are black.

The WMD of the DSL remained around 417 m depth (± 20 m) over the duration of the drift (Figure 3-4c). While animals within the DSL did not conduct DVM, they occasionally migrated vertically, for instance on June 5 and 6 when the WMD was deeper at midday than at midnight. The DSL and scattered intermediate patches were tightly connected, as

echoes from the DSL were observed migrating between these two scattering features, but did not conduct large amplitude DVM (Figure 3-4c, Figure S3-4). The backscattering strength of the DSL gradually increased from the beginning of the drift (daily median of 182 m^2 nmi^{-2} on June 4) until June 11 (daily median of 7,871 m^2 nmi^{-2}; Figure 3-4d). Thereafter, and until the end of the drift station, it peaked with daily medians ranging between 18,719 and 56,903 m^2 nmi^{-2}.

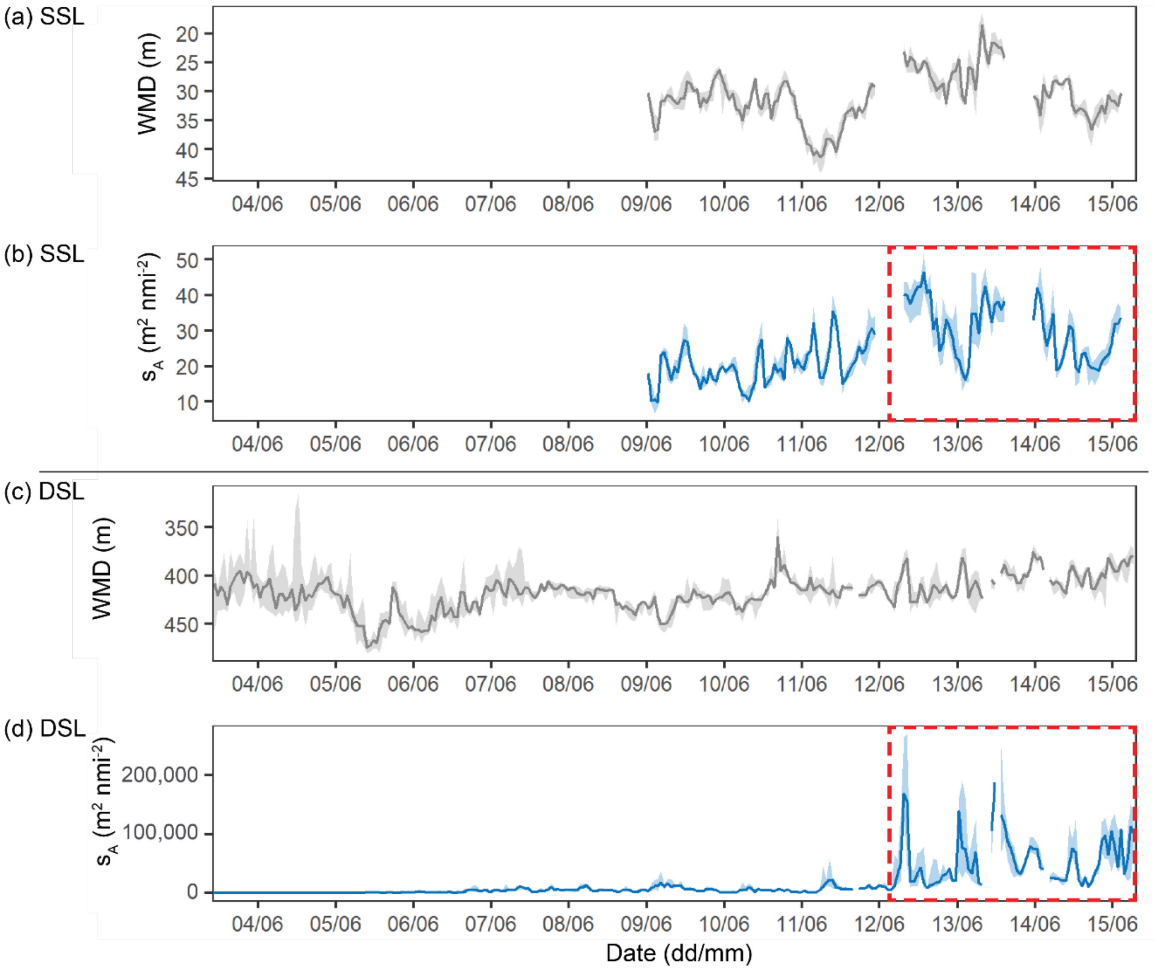

Figure 3-4. Weighted mean depth (WMD; grey) and nautical area scattering coefficient (s_A; blue) for the (a-b) SSL and (c-d) DSL during the drift station. Solid lines indicate the one-hour moving median, shading indicates the interval where 95 % of the data are located (2.5 and 97.5 percentiles). WMD and s_A medians were calculated at 455 kHz for the SSL and at 38 kHz for the DSL. The dashed red rectangle indicates the south-western part of the drift along the eastern slope of the Yermak Plateau (bottom depths > 1,500 m), which coincides with an increase in backscattering strength within the SSL and DSL.

3.4.3 Classification of the scatterers

The multifrequency analysis of the AZFP data classified 90 % of the echo-integration cells of the top 70 m as copepods (Figure S3-5). No fish were detected near the surface or in the SSL by the ice-tethered AZFP nor the hull-mounted EK60 at 38 kHz. The ROV video footage showed that only few juvenile Arctic cod (*Boreogadus saida*) were observed closely associated to the ice. *Calanus* spp. (*C. finmarchicus* and *C. glacialis*) dominated the ROVnet catches under the ice with 182 ind. m^{-3} on average (Figure S3-6). Other abundant epipelagic organisms were the calanoid copepod *Calanus hyperboreus*, hyperiid amphipods (*Themisto libellula* and *Themisto abyssorum*), and typically ice associated gammarid amphipods (mostly *Apherusa glacialis*). Copepods represented on average 91 % of the zooplankton abundance in the ROVnet, which corresponds to the multifrequency classification of AZFP data.

The single targets detected at 38 kHz in the DSL between 200 and 600 m depth had a dominating mode at -36 dB re 1 m^2 and a mode with less targets at -49 dB re 1 m^{-2} (Figure S3-7). These modes indicate that some strong targets, such as swimbladdered fish, were associated with the DSL. Weaker targets, such as macrozooplankton or gelatinous zooplankton, were likely present but eluded detection by the TS analysis because of the lower signal to noise ratio at these ranges (Figure S3-1).

3.4.4 Environmental factors driving the backscatter intensity of sound scattering layers

The SSL measured by the ice-tethered AZFP at 455 kHz showed that all of the backscatter was contained within the cold and less saline PSW (Figure 3-5a). In contrast, the backscatter in the scattered intermediate patches and DSL at 38 kHz from the hull-mounted EK60 was concentrated in waters above 0 °C, in the MAW and AW (Figure 3-5b).

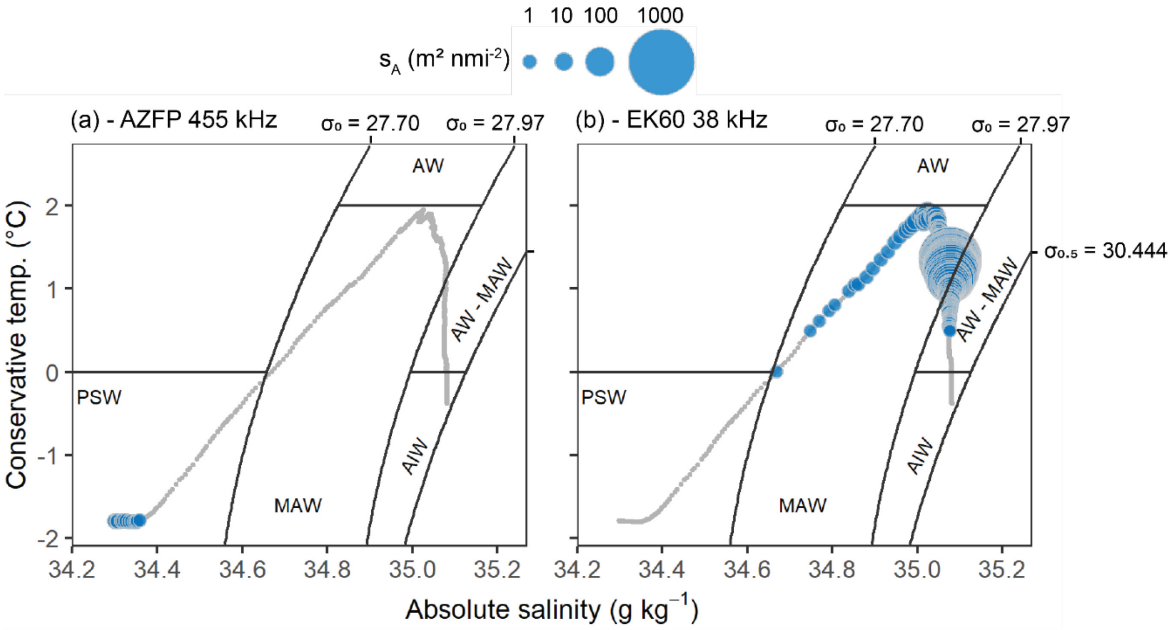

Figure 3-5. Nautical area scattering coefficient (s_A) overlaid on the average conservative temperature-absolute salinity profiles (grey dots; 3 m vertical resolution). The size of the bubbles is proportional to the s_A averaged per 3 m depth bin from the (a) ice-tethered AZFP at 455 kHz and (b) the hull-mounted EK60 at 38 kHz. The isopycnals (kg m^{-3}) used to define the water masses are included. *PSW*: polar surface water; *AW*: Atlantic water; *MAW*: modified Atlantic water; *AIW*: Arctic intermediate water.

The generalized additive models revealed that bottom depth was the main predictor for both backscattering strength and vertical distribution of the SSL and DSL (Table S3-4). Bottom depth was positively correlated to the vertical extent of MAW ($\rho > 0.85$, p-value < 0.001) and it was therefore impossible to distinguish the effects from these two covariates. The SSL was deepest (ca. 35 m depth) at 1,250 m bottom depth and the backscatter within the SSL increased with bottom depth (Figure 3-6a, b). The DSL remained at ca. 425 m depth where bottom depths were < 1,200 m and ascended to 410 m when the seafloor deepened (Figure 3-6c). Similarly, the backscattering strength within the DSL increased in deeper areas (Figure 3-6d).

Under-ice irradiance and temperature within the MAW were other significant predictors for the vertical distribution of the SSL and DSL, respectively (Table S3-4). The SSL was consistently deeper at low irradiance intensities, around midnight, and shallower at high

irradiance intensities, around midday (Figure 3-6a). This is possibly because copepods remaining outside the range of the 455 kHz during daytime, between 70 m and 100 m, moved within the top 60 m during nighttime (Figure S3-3a). The DSL deepened with decreasing temperature of the MAW (Figure 3-6c). Overall, the variation in vertical distribution of pelagic organisms remained small and the WMD of the SSL varied between 25 and 40 m and that of the DSL remained between 400 and 430 m.

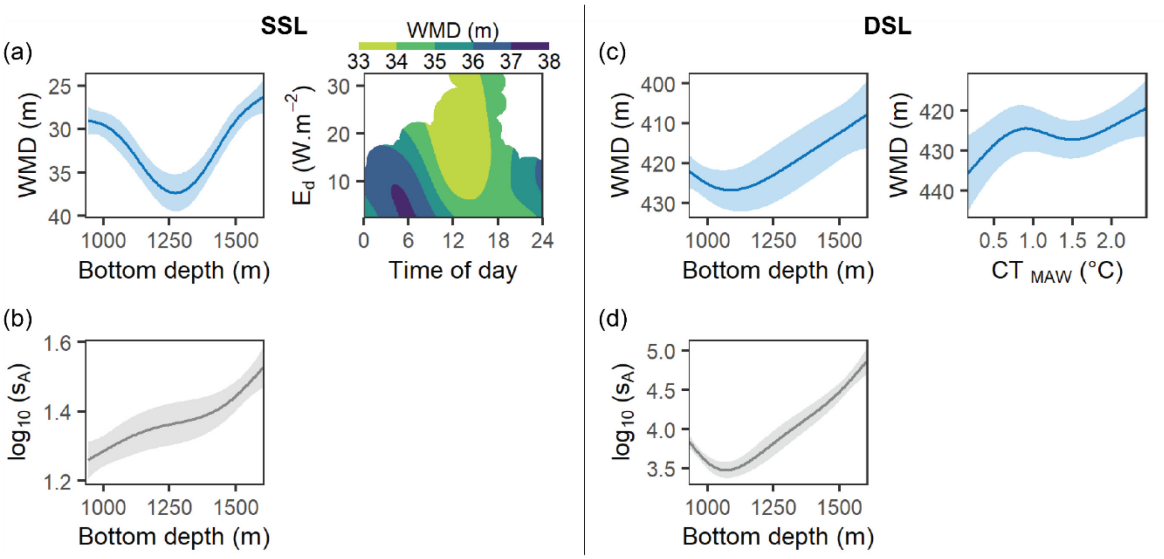

Figure 3-6. Significant smooth terms of generalized additive models showing the relationship between environmental drivers for the (a) weighted mean depth (WMD) of the SSL; (b) nautical area scattering coefficient (s_A) within the SSL; (c) WMD of the DSL; and (d) s_A within the DSL. Environmental variables that have been tested included bottom depth, temperature within the PSW (CT PSW), temperature within the MAW (CT MAW), and the interaction between under-ice irradiance (E_d) and time of day (cf. Table S3-4). Solid lines indicate the estimates of the smooths and shaded areas represent the 95 % confidence interval.

3.5 Discussion

3.5.1 Under-ice vertical segregation between epi- and mesopelagic organisms during the midnight sun

Despite the attenuation of up to 96 % of the surface irradiance by the ice and snow cover, the epipelagic SSL of copepods and the mesopelagic DSL, partly composed of fish, remained vertically segregated throughout the study. Copepods conducted DVM but never

descended deeper than 100 m, while the DSL remained in the Atlantic water masses, between 280 and 600 m (Figure 3-3). The segregation of epipelagic and mesopelagic organisms during the midnight sun period corroborates earlier observations from the Arctic in ice-free and partly ice-covered conditions at the end of the midnight sun period (Gjøsæter et al., 2017). However, contrary to Gjøsæter et al. (2017), we did not observe DVM of the mesopelagic community under the ice during the midnight sun period. The light conditions between this study in June, near the summer solstice, and that of Gjøsæter et al. (2017) in late August were likely very different and possibly explain this discrepancy. This study was conducted at the start of the melt season with an icescape characterized by few melt ponds and leads, and a relatively thick snow cover (Figure S3-2b). The prevailing ice cover (1.90 m thick) and constant illumination did not create an in situ light climate favouring large-scale DVM of mesopelagic organisms.

There was no significant relationship between under-ice irradiance and the depth of the DSL (Table S3-4). Although under-ice irradiance displayed a diurnal cycle, the difference between daytime and nighttime under-ice irradiance remained small (Figure 3-2c) and light attenuation by particles including phytoplankton, in particular after June 11 (Figure 3-2d, Figure S3-2c), likely resulted in relatively constant in situ light levels at mesopelagic depth. Norheim et al. (2016) observed a reduction in DVM amplitude of mesopelagic organisms with increased irradiance at night in the Norwegian Sea and attributed this pattern to the "light preferendum" hypothesis (Cohen and Forward, 2009). This hypothesis stipulates that animals occupying the mesopelagic realm seek a relatively constant ambient light environment and will adjust their vertical distribution accordingly to remain in their light comfort zone, the optimal environment for foraging while avoiding predation (Røstad et al., 2016). Using a dynamic state variable model validated with acoustic observations along

a latitudinal gradient in the Norwegian Sea, Langbehn et al. (2019) confirmed that light, rather than temperature, was the main driver of depth distribution in mesopelagic organisms. The absence of DVM by mesopelagic organisms under the ice during the midnight sun is thus likely resulting, at least in part, from relatively constant in situ light levels at mesopelagic depth.

Contrary to the Norwegian Sea, the surface waters of Baffin Bay are characterized by freezing temperatures in summer (Münchow et al., 2015), and Sameoto (1989) suggested that both constant irradiance and freezing temperatures of surface waters were responsible for the absence of myctophid in northern Baffin Bay in summer. A similar combination of factors could have been at play here because subzero temperatures prevailed in the epipelagic zone (mean temperature of -1.5 °C). Therefore, mesopelagic animals could have also avoided surface waters because of thermal stress, in addition to constant irradiance. Moreover, contrary to other regions such as the Norwegian Sea, the mesopelagic fish assemblage at the Arctic-Atlantic gateway is not dominated by lanternfish but rather by juveniles of demersal species such as Arctic cod, beaked redfish, Atlantic cod, and haddock (Geoffroy et al., 2019; Knutsen et al., 2017). Occasionally, large Atlantic cod (> 50 cm) are observed foraging within the DSL over the Fram Strait and northern Svalbard (Gjøsæter et al., 2020; Ingvaldsen et al., 2017). Except for Arctic cod, these species are not well adapted to freezing temperatures and would generally avoid the subzero temperatures of the epipelagic zone. Arctic cod, on the other hand, is adapted to subzero temperatures and individuals can be found under the ice (David et al., 2016), but most adult Arctic cod remain in warmer Atlantic waters, at least in the Beaufort Sea (Crawford et al., 2012; Geoffroy et al., 2016, 2011).

3.5.2 Ecological implications of the vertical segregation of pelagic organisms

Despite the importance of copepods as lipid-rich prey for fish within the DSL (e.g., Geoffroy et al., 2019), continuous vertical segregation limited predator-prey interactions between mesopelagic organisms and epipelagic copepods during the midnight sun. Hence, feeding on large copepods, such as *C. glacialis*, *C. finmarchicus*, and *C. hyperboreus*, by mesopelagic fish is likely limited to early spring and autumn in the Arctic during the seasonal vertical migration of *Calanus* (Figure 3-7). My findings thus partly support the photoperiod hypothesis, which explains the lower abundance of mesopelagic fish at higher latitudes by inferior feeding conditions imposed by the extreme light climate (Kaartvedt, 2008). When avoiding the strong light and freezing temperatures of the upper water column, mesopelagic organisms loose safe access to feed on lipid-rich prey at night. Some fish species may thus experience insufficient feeding conditions to survive (Norheim et al., 2016).

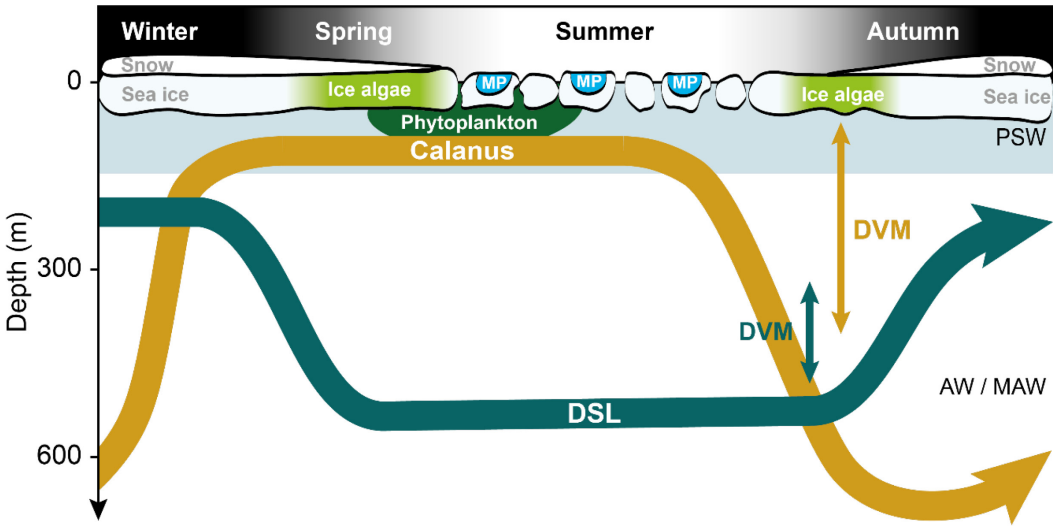

Figure 3-7. Schematic of the annual vertical distribution of the mesopelagic deep scattering layer (DSL) and *Calanus* spp. at the Arctic-Atlantic gateway. Based on Gjøsæter et al. (2017), Geoffroy et al. (2019), and the present study. Occurrence and relative amplitude of diel vertical migrations (DVM) are represented by vertical arrows. *PSW*: polar surface water; *AW* / *MAW*: Atlantic water / modified Atlantic water; *MP*: Melt pond.

In autumn, the day-night cycle increases the DVM amplitude of both mesopelagic organisms (Gjøsæter et al., 2017) and copepods (Daase et al., 2016), which then overlap vertically. This is also the period when large copepods start descending to overwintering depths after filling their lipid sacs by grazing on phytoplankton, and they thus represent lipid-rich prey for their predators (Falk-Petersen et al., 2009). By looking at the fatty acid trophic markers of mesopelagic organisms in the region, Geoffroy et al. (2019) confirmed that the mesopelagic food web is based on *Calanus* in early autumn. In winter, after large *Calanus* spp. descend to overwintering depths below the DSL (Dale et al., 1999; Hirche et al., 2006), mesopelagic organisms rather feed on euphausiids (e.g., *Thysanoessa* spp.; Geoffroy et al., 2019). In spring, the return of diapausing copepods and copepod eggs from deep overwintering depths to surface waters (Darnis and Fortier, 2014) could also provide a valuable food source for the mesopelagic fishes surviving at high latitudes. During both winter and summer, when large copepods are not ascending to or descending from the epipelagic layer, these fishes must feed on other prey, such as macrozooplankton (e.g., *Themisto* spp.), or mesopelagic copepods (e.g., *Metridia longa* or *Paraeuchaeta glacialis*; Kosobokova and Hopcroft, 2010). Although the species composition of the scattered intermediate patches is unknown, they were seen at times in close connection with the DSL and could represent another important food source (Figure S3-4).

3.5.3 High backscattering strength of the DSL at the Arctic-Atlantic gateway linked to Atlantic water masses

At the beginning of the drift station, the median integrated s_A (280-600 m) of the DSL at 38 kHz remained similar to previous mesopelagic values reported in the same area in August – September; a daily median of 182 m^2 nmi^{-2} on June 4 compared to 45-148 in Knutsen et al. (2017) and 351 m^2 nmi^{-2} in Geoffroy et al. (2019). The backscatter within

the DSL increased after June 5 and reached a daily median of 7,871 m^2 nmi^{-2} on June 11, which is slightly higher than the range for mesopelagic DSL in tropical and subtropical areas (158-7,617 m^2 nmi^{-2}; Irigoien et al., 2014). The backscatter continued to increase between June 12 and 15, over the eastern slope of the Yermak Plateau. There, the backscatter within the DSL reached a daily median of 56,903 m^2 nmi^{-2} on June 13, which is higher than all mesopelagic backscatter values previously documented in the Arctic Ocean and North Atlantic (Dias Bernardes et al., 2020; Fennell and Rose, 2015; Gjøsæter et al., 2017; Siegelman-Charbit and Planque, 2016; Snoeijs-Leijonmalm et al., 2021). The species likely forming the Arctic DSL exhibit a denser aggregating behaviour than lanternfish found in the North Atlantic. For instance, Arctic cod form dense aggregations at depth in the Atlantic water mass in the Beaufort Sea and the backscattering strength of these aggregations is similar to that measured over the slope of the Yermak Plateau (Benoit et al., 2010; Geoffroy et al., 2011). However, while the increase in backscattering strength can be related to an increase in mesopelagic biomass, it can also emerge from a change in species composition. Other potential contributors to the mesopelagic community at the Arctic-Atlantic gateway comprise macrozooplankton and gelatinous zooplankton (Geoffroy et al., 2019; Knutsen et al., 2017), including siphonophores (Raskoff et al., 2005).

The high backscattering strength observed within the DSL over the Yermak Plateau slope coincided with the regional AW circulation. On several occasions, the Yermak Branch that carries AW northward around the outer rim of the Yermak Plateau (Figure 3-1) has been identified recirculating southward along the eastern slope of the plateau (Athanase et al., 2021; Crews et al., 2019; Meyer et al., 2017). The DSL backscatter increased where MAW thickened, which corresponds to the location where the Yermak Branch flows. Most

mesopelagic fish encountered in the European Arctic are boreal species following their planktonic prey northward or advected with the inflow of Atlantic waters (Basedow et al., 2018; Geoffroy et al., 2019; Knutsen et al., 2017). Adult Arctic cod, the only abundant Arctic pelagic fish, also often associate with warmer Atlantic waters (Crawford et al., 2012; Geoffroy et al., 2016, 2011). We thus suggest that the convergence and concentration of mesopelagic fish and plankton advected with Atlantic waters at least partly explain the spatial variation in mesopelagic backscatter, with backscatter two orders of magnitude higher on the deeper continental slope of the Yermak Plateau than elsewhere.

3.6 Conclusion

In spring, mesopelagic organisms at the Arctic-Atlantic gateway can form aggregations with backscatter values comparable to or higher than in temperate regions. These mesopelagic organisms are concentrated in the Atlantic water masses. Hence, the increase in Atlantic water inflow into the Arctic (Athanase et al., 2021) could likely result in an increased advection of mesopelagic biota. However, the fate of the advected mesopelagic species into the deep basins of the Arctic Oceans is unknown. The clear vertical segregation between mesopelagic animals and large epipelagic copepods in June, during the midnight sun period, suggests that mesopelagic fish can only feed on the lipid-rich copepod prey for a short period of time in early spring and autumn. This confirms the very pulsed peaks in energy transfer prevailing in Arctic marine ecosystems.

4 Chapter four: Regular and inverse autumnal DVM by mesopelagic fish and zooplankton in Baffin Bay, eastern Canadian Arctic

4.1 Abstract

The distribution of mesopelagic fish and zooplankton extends into the Arctic Ocean. However, the mechanisms enabling their survival, in particular their foraging behaviour, in high latitude environments remain unknown. Here, we used acoustic and optical sensors together with trawl sampling to describe and quantify the vertical distribution and behaviour of mesopelagic organisms in northern Baffin Bay in autumn. We found that Arctic cod (*Boreogadus saida*), snailfish (*Liparis* sp.), mysids (*Boreomysis arctica*), and hyperiid amphipods (*Themisto libellula*) were the most abundant taxa, and that up to 21 % of the mesopelagic backscatter conducted DVM. The migrating organisms remained within the 10^{-6} and 10^{-9} µmol photons m^{-2} s^{-1} isolumes, similar to temperate and tropical regions. Arctic cod displayed a flexible DVM behaviour. Juveniles performed reverse and regular DVM whereas adults conducted regular DVM over a 200 m range or were non-migrating. These behaviours presumably emerged from intra-specific predation pressure and enhanced feeding conditions near surface. We conclude that autumn is a crucial period for mesopelagic fish foraging in the Arctic because it is one of the only seasons when their vertical distribution, following a light comfort zone, overlaps with that of their zooplankton prey.

4.2 Introduction

The mesopelagic zone, between 200 and 1000 m depth, hosts a large biomass of fish and zooplankton in all major oceanic basins (Irigoien et al., 2014; Proud et al., 2019). The

vertical distribution of mesopelagic animals has been linked to several environmental variables, including temperature and oxygen concentrations (Bianchi et al., 2013; Klevjer et al., 2016), but light penetration is considered to be one of the main environmental drivers (Aksnes et al., 2017). Aksnes et al. (2017) found that, in tropical and temperate regions, most of the mesopelagic backscatter was contained within a narrow range of ambient light (10^{-6} to 10^{-9} μmol quanta m^2 s^1). This range is thought to maximize feeding while minimizing mortality through visual predation, *"an antipredation window"* (Clark and Levy, 1988), and has been named the light comfort zone (Røstad et al., 2016). Because a large portion of mesopelagic organisms rely on diel vertical migrations (DVM) for feeding (Klevjer et al., 2020a, 2016), they contribute to active transport of carbon out of the euphotic zone (Davison et al., 2013; Saba et al., 2021). The intensity of this active carbon flux is linked to the amount of mesopelagic biomass migrating but also to the migration amplitude and predation rates, factors that currently carry large uncertainties (Bianchi et al., 2013; Irigoien et al., 2014; Klevjer et al., 2016; Proud et al., 2019) and are modified by climate change (Ariza et al., 2022; Flores et al., 2023).

The strong relationship between mesopelagic fish and their light environment was hypothesized to prevent them from establishing viable populations at high latitudes, where the photoperiod alternates between periods of constant darkness and constant brightness (Kaartvedt, 2008). While this latitudinal decrease in mesopelagic abundance has been documented in both hemispheres (Escobar-Flores et al., 2018; Siegelman-Charbit and Planque, 2016), recent studies have shown that the mesopelagic niche is not empty in high Arctic seas (chapter two) and in the Central Arctic Ocean (Ingvaldsen et al., 2023; Snoeijs-Leijonmalm et al., 2022, 2021). However, the mechanisms behind the year-round survival of mesopelagic fish and zooplankton in the Arctic remains uncertain because these animals

are vertically segregated from their prey for most of the year (Langbehn et al., 2022). The twilight periods, autumn and spring, have been proposed as critical periods for Arctic mesopelagic animals because their light comfort zone may overlap with the vertical distribution of their prey. Autumn may be a particularly critical period because it comes after the productive season during which copepods have accumulated lipid reserves (Falk-Petersen et al., 2009), making them a nutritious prey for mesopelagic predators. It is also the period of sea ice formation, which can absorb a substantial part of incoming irradiance (Castellani et al., 2022), and subsequently affect the light comfort zone of mesopelagic animals.

While temperature, salinity, and other water mass parameters are collected routinely, few mesopelagic studies collect direct underwater light measurements (Kaartvedt et al., 2019a). Here, we investigated the vertical distribution of mesopelagic organisms in relation to underwater light levels in autumn in the Arctic. The goals of this study were two-fold; (1) to document the vertical distribution and migratory behaviours of mesopelagic fish and zooplankton in autumn, and (2) verify if those patterns follow the same light levels as those mesopelagic assemblages from temperate and tropical environments. A combination of acoustic, optical, environmental sensors, and nets were deployed to describe the vertical distribution of pelagic fish and zooplankton in northern Baffin Bay in autumn during sea-ice formation. We test the hypothesis that mesopelagic organisms follow a light comfort zone that overlaps with the vertical distribution of their prey in autumn.

4.3 Methods

4.3.1 Survey design and study area

We conducted an acoustic-trawl survey in northern Baffin Bay from the CCGS *Amundsen* between 12 and 25 October 2021 (Figure 4-1). Northern Baffin Bay is connected to the Central Arctic Ocean through three shallow straits: Barrow Strait in Lancaster Sound, Hell's Gate in Jones Sound, and Kane Basin in Nares Strait – the smallest being Jones Sound and largest Nares Strait. This region is characterized by the presence of a large polynya forming in winter, the Pikialasorsuaq (north water polynya), encompassing Smith, Jones, and Lancaster Sounds (Dumont et al., 2009; Vincent, 2019). This highly productive area of the Canadian Arctic Archipelago (Ardyna et al., 2011; Marchese et al., 2017), concentrates zooplankton, fish, and top predators (Bouchard et al., 2018; Darnis et al., 2022; Heide-Jørgensen et al., 2016).

Two main water masses co-occur in the study region: cold and low salinity Arctic water ($\theta < 0$ °C, S ~ 33.7), generally in the top 200 m, results from the mixing of surface waters entering Baffin Bay in the Davis Strait with cold waters advected from the CAO, and warmer, more saline West Greenland Intermediate Water ($\theta > 0$ °C, $S > 34.0$) originating from advection of Atlantic water through Davis Strait flowing northward toward northern Baffin Bay (Tang et al., 2004). The temperature profiles from northern Baffin Bay are characterized by a minimum in Arctic waters resulting from winter cooling, which denotes the maximum depth of winter convection, and a temperature maximum marking West Greenland Intermediate Water (Tang et al., 2004).

We focus on two locations, Smith Sound and Jones Sound (Figure 4-1). The ship remained on station for 48-72 h at each location, with only minor displacements to deploy instruments or to prevent ship entrapment in the ice. Temperature and salinity profiles were measured with a Conductivity Temperature Depth (CTD; Seabird SBE 911+) sensor regularly

deployed from the ship. The CTD rosette was also equipped with a fluorometer (Seabird ECO triplet).

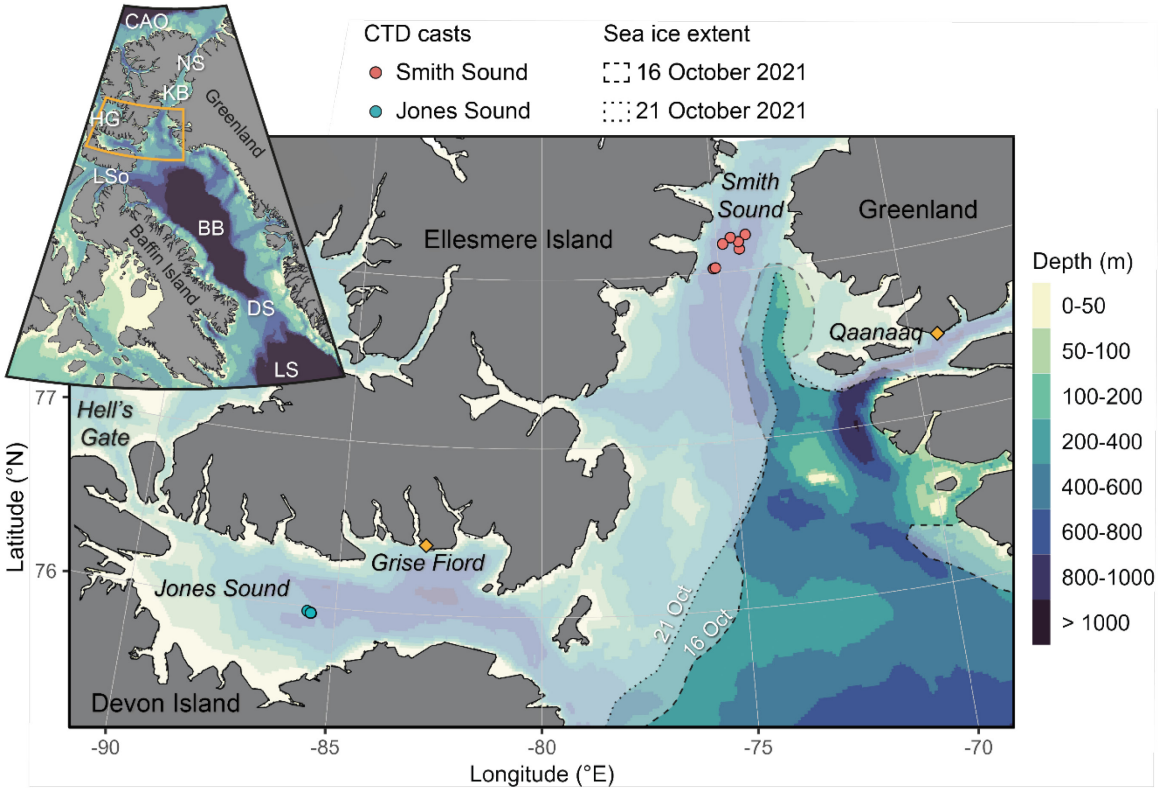

Figure 4-1. Study area (orange polygon) in northern Baffin Bay with the locations of the CTD casts (dots) colored by station. The white shaded area with dotted line indicates the sea ice edge on October 16th, 2021, when the ship was in Smith Sound, and the dotted line the ice edge on October 21st, 2021 when the ship was in Jones Sound. Sea ice extent data were exported from the U.S. National Ice Center (USNIC accessed on 22/03/2023). *BB*: Baffin Bay; *CAO*: Central Arctic Ocean; *DS*: Davis Strait; *HG*: Hell's Gate; *KB*: Kane Basin; *LS*: Labrador Sea; *LSo*: Lancaster Sound; *NS*: Nares Strait

4.3.2 Hydroacoustic data collection and processing

4.3.2.1 Hull-mounted echosounder

The behaviour of pelagic organisms was continuously monitored using a hull-mounted echosounder EK80 (Kongsberg Discovery) equipped with 38 kHz (ES38-7 split beam) and 120 kHz (ES120-7C split-beam) transducers operated in narrowband mode (see Table S4-1 for echosounder settings). Pulse length was set to 1.024 ms, ping rate varied between 0.5 and 0.25 Hz, and transmitted power was 2000 W at 38 kHz and 250 W at 120 kHz. The

ship echosounder was calibrated before the cruise following the standard sphere method (Demer et al., 2015). We applied in situ sound speed profile calculated from the average of all CTD casts taken from a station. For this study, we focused the analyses on data collected at 38 kHz because it was the only frequency that reached mesopelagic depths with a signal-to-noise ratio higher than 10 dB.

Echoview 13.1 (Echoview Software Pty Ltd) was used to process acoustic data. We removed background (10 dB signal-to-noise ratio) and impulse noise using Echoview's algorithms (De Robertis and Higginbottom, 2007; Ryan et al., 2015). The layer of entrained air bubbles near the surface and seafloor were excluded from further analyses and we added a 25 m offset to the seafloor exclusion line to remove backscatter originating from demersal organisms. We echo-integrated data in 20 min per 5 m depth cells from which we extracted volume backscattering strength (S_V in dB re 1 m^{-1}) and nautical area scattering coefficients (s_A in m^2 nmi^{-2}) at each frequency.

We analyzed processed acoustic data with R (version 4.2.3, R Core Team) and used the *suncalc* R package (version 0.5.1) to partition data into day and night. We defined day as the period between sunrise and sunset, and night, as the period between nautical dawn and nautical dusk, i.e., when the sun was at least 12° below the horizon. To investigate diurnal changes in the vertical distribution of scatterers, we calculated the s_A proportion as the contribution of each 5 m depth bin to the total backscatter profile for day and night profiles and assessed the migrating proportion (MP) of backscatter from the mesopelagic (defined as 200-1000 m depth range) to the epipelagic zone (above 200 m depth; Klevjer et al., 2016). Because we did not collect data in areas deeper than 700 m depth, any loss of backscatter during nighttime in the mesopelagic was interpreted as migration out of that

range into the epipelagic. We also calculated the weighted mean depth (WMD) and inertia of the epi- and mesopelagic zone during day and night (Urmy et al., 2012). WMD describes the average position of the scattering layer in the water column and inertia its spread around the weighted mean depth, respectively.

To investigate vertical migration behaviours of individual fish and zooplankton, we detected single targets with the ship echosounder at 38 kHz using the single target detection - split beam method 2 algorithm from Echoview (Table S4-2). We used a minimum compensated target strength (TS) threshold of -65 dB re 1 m^2 and constrained analyses to 500 m depth, where the signal-to-noise ratio for a -65 dB threshold remained above 6 dB (Figure S4-1). To minimize multiple target detections, which can lead to overestimations in TS, we calculated the Sawada index, i.e., the number of fish per acoustic sampling volume (Nv) and the ratio for multiple echoes (M) for cells of 50 pings x 2 m depth (Sawada et al., 1993). We selected cells that had $Nv < 0.04$ and $M < 0.70$, where the probability of multiple target detection was low. We only considered single targets detected close to the centre of the acoustic beam – within 3° of the off-axis angle, i.e., the angle between the single target relative to the axis of the acoustic beam. The depth and TS distribution of single targets were further scrutinized in R.

To verify whether the -65 dB TS threshold correctly separated single targets with gas inclusions, e.g., swimbladdered fish, from weaker scatterers e.g., non-swimbladdered fish and macrozooplankton, we ran scattering models for macrozooplankton and used species-specific published TS-length equations for fish (Gauthier and Horne, 2004; Geoffroy et al., 2016). We identified the most abundant species of each taxonomic group within the trawls and modelled fluid-like targets, such as mysids and amphipods, with the phase-

compensated distorted wave Born approximation (PC-DWBA) model of the *ZooScatR* R package (version 0.61; Gastauer et al., 2019). We varied shape, size, orientation, and material properties parameters based on literature values (for the detailed list of parameters used see Dunn et al., 2022), and used the length distribution calculated from the samples collected with the mid-water trawl at each station. For the PC-DWBA models, we ran 1000 simulations with random sampling within the distribution of each model parameter to calculate the mean and standard deviation in backscattering cross-section (m^2) within each taxonomic group, which were then converted to target strength (dB re 1 m^2).

To investigate whether specific groups of single targets displayed diel vertical migrations, we calculated the day-night difference in the frequency of occurrence of single target TS ($\Delta\nu_{TS}$ in %). The $\Delta\nu_{TS}$ metric describes the change in vertical distribution for a group of single targets (with similar TS properties) between day and night; a negative value indicates higher occurrence during nighttime than daytime, and a positive value the opposite. We only considered data during day and night, when organisms had finished their DVM, because during the twilight periods, when the organisms are migrating, their TS change significantly with their orientation and could bias this analysis (Kang et al., 2005; McQuinn and Winger, 2003). We first calculated the number of single targets within cells of 1 dB re 1 m^2 x 5 m vertical during daytime and nighttime at each station and excluded depth bins that contained less than a total of 30 targets. We then calculated the proportion of single targets within each cell per depth interval, which gave the daytime and nighttime frequency of occurrence of a given group of single targets resolved vertically. Finally, we calculated the day/night difference in frequency of occurrence for each depth bin.

4.3.2.2 Acoustic probe

One shortcoming of using hull-mounted echosounders for studying deep-living organisms is the reduced signal-to-noise ratio at greater depth, in particular at high frequencies. To tackle this issue, we recorded acoustic backscatter using a Wideband Autonomous Transceiver (WBAT, Kongsberg Discovery) equipped with a 38 (ES38-18DK split-beam) and a 333 kHz (ES333-7CDK single-beam) transducer mounted facing sideward on the CTD rosette – hereafter referred to as the acoustic probe. For this study, we focused on data collected by the 333 kHz transducer to focus on small acoustic targets such as mesozooplankton, which are prey for pelagic fish and carnivorous macrozooplankton. The acoustic probe operated in broadband mode between 283-383 kHz with a pulse length of 2.048 ms, power of 50 W, and with a ping rate of 0.5 Hz. The 333 kHz single-beam transducer was not calibrated. The absence of calibration of the acoustic probe likely had a limited impact on the qualitative analyses of this study. For each deployment the rosette was lowered at ca. 1 $m.s^{-1}$ and we only considered data from the downcast to avoid artefacts from when the rosette stopped to collect water samples in the upcast. This strategy resulted in backscatter profiles with the same sampling vertical resolution throughout the entire depth profile. Due to logistical constraints, we focused analyses on two casts collected during daytime, one in Smith Sound (CTD cast 13) and one in Jones Sound (CTD cast 28).

We constrained analyses to ranges from the transducers between 15 and 50 m, where avoidance by animals is limited (Geoffroy et al., 2021). We applied the in situ average sound speed and absorption coefficient at each frequency calculated from the temperature-salinity profile of the given CTD cast for each water mass. Using pulse-compressed data, we echo-integrated data in 1 ping per 1 m range cells between 283-383 kHz from which we extracted S_V. We then matched each acoustic ping to its corresponding depth and calculated

mean S_V for the 15-50 m range in 5 m depth bins. All acoustic calculations were done in the linear domain.

4.3.3 Trawl and net sampling

Micronekton and macrozooplankton were collected using an Isaacs-Kidd Midwater Trawl (IKMT). The trawl had a 4.5 m x 3 m mouth aperture (13.5 m^2) and was equipped with 5 mm mesh in the cod-end. The IKMT was lowered to the depth of the sound scattering layer and towed horizontally for 30 minutes at 3 knots. We chose the sampling depth based on the vertical distribution of the upper sound scattering layer. Once onboard, we identified the catch to the lowest taxonomic level possible and recorded the total number and weight of each species. For fish, we counted and measured (length and width) all individuals and estimated their weight based on length-weight relationships. For zooplankton, when > 20 specimens of a given species were collected, we measured and weighed a random subsample of 20 individuals. We did not include jellyfish (Hydrozoa) in abundance and biomass estimates because of their poor condition when collected from the net which prevented accurate identification, counting, and weighting.

4.3.4 Underwater vision profiler

An Underwater Vision Profiler 6 High Frequency (UVP6 HF; Picheral et al., 2022) mounted on the CTD rosette collected in situ images of mesozooplankton to describe their fine-scale vertical distribution and abundance, and to ground-truth backscatter from the acoustic probe. UVP6 HF used flashes of red light (635 nm) to illuminate a given volume of water and acquired images at a frequency of 20 Hz during its descent, which led to a sampling rate of 18.6 ± 7.0 images m^{-1} (ca. 1 image every 5 cm). Each image has a dimension of 15 x 18 x 2.3 cm (0.68 L sampled) and a resolution of 74 µm $pixel^{-1}$. The on-

board computer automatically segmented objects from initial images and resulting vignettes were saved when their major length was greater than 740 µm. The two casts from Jones Sound and Smith Sound produced 94813 vignettes.

The Ecotaxa Random Forest algorithm suggested a taxonomic classification for each object, which was then validated and corrected by a human annotator (Gorsky et al., 2010; Irisson et al., 2022; Picheral et al., 2010). Among all objects, 2022 were living organisms, including 962 copepods (most vignettes were non-living particles of marine snow). Because each image was taken at a known depth, we calculated the densities of copepods (ind m^{-3}) in 10 m depth bins by dividing the number of images assigned to the copepod taxa by the sampling volume within the depth bin. This concentration is generally inferior to estimations from net sampling because of the low volume sampled by images (Barth and Stone, 2022). However, the mostly constant sampling volume meant reliable relative variations in densities of organisms.

4.3.5 Light measurements and estimation of ambient light at depth

Surface irradiance (320-950 nm) was recorded every minute using a RAMSES hyperspectral irradiance sensor (TriOS) mounted on the ship. To match the resolution of acoustic data we calculated the average surface irradiance over 20 min. In general, the surface sensor was turned on prior to dawn and turned off after dusk, except in Jones Sound when it recorded irradiance near-continuously. At each station, light profiles were collected with a free-falling Compact-Optical Profiling System (C-OPS; Biospherical instruments, 19 wavelengths between 380 and 875 nm) in the upper 100 m as close to solar noon as possible.

We constrained analyses over the 400-700 nm range because data above and below those thresholds were noisy. Using C-OPS data, we estimated attenuation coefficients ($K_d(\lambda)$ in m^{-1}) in 10 m depth bins using the *Cops* R package (version 4.4-2, Bélanger et al., 2017). Because the spectral resolution of the C-OPS and RAMSES differed, we selected RAMSES wavelengths based on those recorded by the C-OPS. We used spectrally resolved surface irradiance from the ship-mounted RAMSES sensor and corresponding $K_d(\lambda)$ to estimate underwater downwelling irradiance ($E_d(z)$) over the 400-700 nm band in cells of 20 min per 10 m depth using:

$$E_d(z) = 0.97 \times \sum_{\lambda=400}^{700} E_0(\lambda) \times \exp\left(-\int_0^z K_d(\lambda, \sigma) d\sigma\right)$$

where $E_d(z)$ is the underwater irradiance at depth d, 0.97 is the constant for reluctance of irradiance at the water surface, $E_0(\lambda)$ is the surface irradiance at wavelength λ, and the exponential expression calculates the attenuation between surface and depth z (Klevjer et al., 2020a). For depths where $K_d(\lambda)$ was not determined (generally below 100 m depth), we used the average of the two deepest $K_d(\lambda)$ available. The estimated downwelling irradiance was then converted from energy units (W m^{-2}) to quantum fluxes (µmol photons m^{-2} s^{-1}).

4.4 Results

4.4.1 Environmental conditions in Smith Sound and Jones Sound

In October 2021, at the time of the research cruise, sea-ice formation was just beginning with ice thicknesses varying between 2 and 30 cm. In Smith Sound, sea ice was mainly composed of old ice floes surrounded by different types of new ice, while in Jones Sound, sampling started in open water and sea ice began forming while on station (Figure S4-2). The water mass vertical distribution was similar between Smith Sound and Jones Sound

with only slight changes in the extent and values (Figure 4-2). The surface waters (0-150 m depth in Smith Sound and 0-250 m depth in Jones Sound) were occupied by the Arctic Water mass layer, characterized by cold temperatures (< 0 °C) and low salinities (< 33.7; Figure 4-2a, b). Winter cooling and ice formation had started with the top 50 m of the water column, which was colder than the rest of the Arctic water mass. The temperature minimum was at 110 m in Smith Sound and between 100 and 200 m in Jones Sound. The warmer and more saline West Greenland Intermediate Water occurred below Arctic waters and extended down to the seafloor. The temperature maximum of Atlantic waters was deeper in Jones Sound (ca. 300 m depth) compared to Smith Sound (ca. 200 m depth). Fluorescence was restricted to the top 100 m of the water column with slightly higher values in Smith Sound compared to Jones Sound (Figure 4-2c).

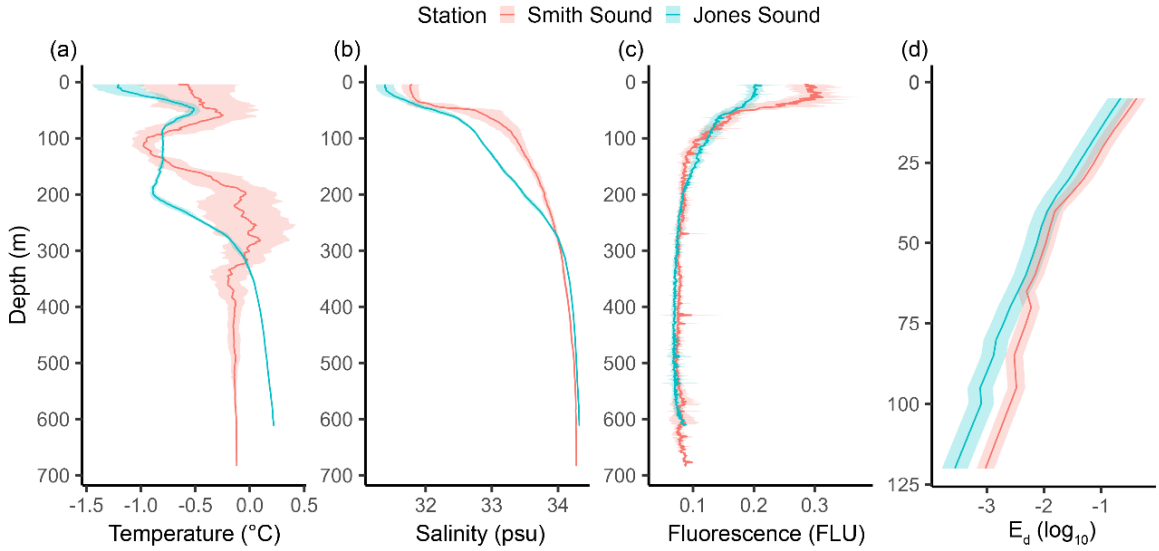

Figure 4-2. Mean profiles (solid line) with standard deviation of (a) temperature, (b) salinity, (c) fluorescence, and (d) underwater irradiance (log_{10}-transformed E_d in µmol photons m^2 s^{-1}, see methods) spectrally resolved and integrated for the 400-700 nm band in Smith Sound (red) and Jones Sound (teal). Note the different depth scale (y-axis) in (d), limited to the depth range where attenuation coefficients were estimated from light measurements.

The light penetration profiles were similar between the two areas, with slightly less attenuation in Jones Sound compared to Smith Sound, i.e., light penetrated slightly deeper

in Jones Sound than in Smith Sound (Figure 4-2d). For example, during daytime the 10^{-6} and 10^{-9} isolumes were reached at ca. 210 m and 340 m in Smith Sound and 220 m and 340 m in Jones Sound. The spectral distribution was broader near the surface than at depth, with the 450-520 nm range dominating below 300 m depth (Figure S4-3).

4.4.2 Species composition of scattering layers

Macrozooplankton dominated the mesopelagic trawl catches in Smith Sound and Jones Sound, both in terms of abundance (94-98% of the relative abundance) and biomass (53-83 % of the relative biomass; Table 4-1, Figure 4-3a, b). In terms of fish taxonomic composition, we only sampled two taxa, Arctic cod (*Boreogadus saida*) and snailfish (*Liparis* sp.). These two species occurred in similar abundance and biomass in both areas (Figure 4-3a, b). In Smith Sound, fish contributed to mesopelagic biomass more during daytime than during nighttime, averaging 47 % of biomass during day and 17 % during night (Figure 4-3b). The mesopelagic assemblage was only sampled during daytime in Jones Sound.

In Smith Sound, the hyperiid amphipod *Themisto libellula* dominated macrozooplankton (68-80 % in relative abundance and 44-65 % in relative biomass) whereas in Jones Sound the mysid *Boreomysis arctica* was most abundant (67 %) and represented the largest biomass (62 %). Other macrozooplankton taxa included the amphipods *Eusirus* sp., *Themisto abyssorum*, *Gammarus wilkitzkii*, and *Hyperia galba*, the pteropods *Clione limacina* and *Limacina helicina*, the chaetognath *Pseudosagitta maxima*, and the euphausiids *Thyssanoessa* spp. and *Meganyctiphanes norvegica*. Although jellyfish were not included in the abundance and biomass estimates, they were present at all stations.

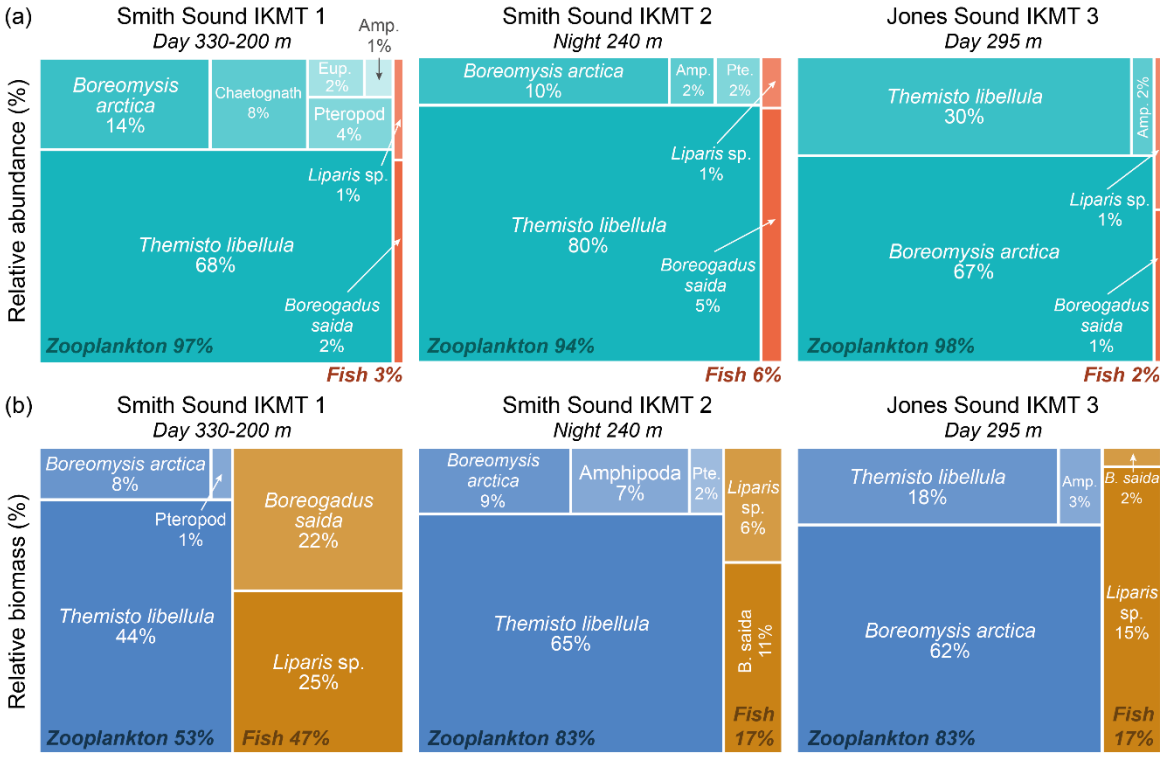

Figure 4-3. Species composition from IKMT trawls taken in the mesopelagic layer in Smith Sound and Jones Sound in terms of (a) relative abundance and (b) relative biomass. The area of the rectangles is proportional to the abundance or biomass of the taxa. *Amp.*: Diverse amphipod; *Eup.*: Euphausiids; *Pte.*: Pteropods.

4.4.3 Vertical distribution of scattering layers and vertical migrations

The daytime abundance of copepods was ca. 10 ind m^{-3} in the upper 100 m in Smith Sound and 120 m in Jones Sound and increased to ca. 20 ind m^{-3} below that depth down to 550 m depth (Figure 4-4a). The general shape of the mean volume backscattering strength profiles (S_V) collected by the acoustic probe during daytime were similar to that of the copepod distribution from the UVP6 (Figure 4-4b). S_V was lower in the upper water column (< -75 dB re 1 m^{-1}) and then increased with depth. we observed a peak in S_V at mesopelagic depths, ca. 280 m depth in Smith Sound and ca. 250 m depth in Jones Sound. Further analyses of the UVP and WBAT data will better quantify copepod vertical distribution. Yet, both instruments look at different size classes which can explain some of the discrepancies.

Table 4-1. Details of all mesopelagic taxa sampled with the IKMT in Smith Sound and Jones Sound. Weight was estimated with length-weight relationship for [a] Arctic cod (Geoffroy et al., 2016) and [b] snailfish (Smirnova et al., 2022). Mean length of *Boreomysis arctica* and *Themisto libellula* were not measured for IKMT 2 in Smith Sound so these values are from IKMT 1. Target strength at 38 kHz estimated with TS-length equations for [d] Arctic cod (Geoffroy et al., 2016), [e] wide non-swimbladdered fish (Gauthier and Horne, 2004), and with [f] scattering models PC-DWBA (see methods).

Net	Date-time (local)	Depth (m)	Species	Abundance (ind) *(relative abundance)*	Biomass (g) *(relative biomass)*	Mean length (cm) ± sd	Mean TS at 38 kHz (dB re 1 m^2) ± sd
Smith Sound IKMT 1	2021-10-16 12:51 (day)	330-200	Arctic cod *(Boreogadus saida)*	5 *(2 %)*	22 *(22 %)* [a]	6.7 ± 3.4	-53.0 ± 3.1 [d]
Smith Sound IKMT 1	2021-10-16 12:51 (day)	330-200	Snailfish *(Liparis* sp.*)*	2 *(1 %)*	25 *(25 %)* [b]	9.4 ± 1.9	-67.3 ± 2.4 [e]
Smith Sound IKMT 1	2021-10-16 12:51 (day)	330-200	Hyperiid amphipod *(Themisto libellula)*	176 *(68 %)*	43 *(44 %)*	1.8 ± 0.5	-69.2 ± 4.9 [f]
Smith Sound IKMT 1	2021-10-16 12:51 (day)	330-200	Mysid *(Boreomysis arctica)*	36 *(14 %)*	8 *(8 %)*	2.7 ± 0.6	-86.0 ± 4.4 [f]
Smith Sound IKMT 1	2021-10-16 12:51 (day)	330-200	Chaetognath (mostly *Pseudosagitta maxima*)	20 *(8 %)*	< 1 *(0 %)*		
Smith Sound IKMT 1	2021-10-16 12:51 (day)	330-200	Pteropod *(Limacina helicina)*	11 *(4 %)*	1 *(1 %)*		
Smith Sound IKMT 1	2021-10-16 12:51 (day)	330-200	Euphausiid *(Meganyctiphanes norvegica)*	5 *(2 %)*	< 1 *(0 %)*		
Smith Sound IKMT 1	2021-10-16 12:51 (day)	330-200	Amphipoda other *(Gammarus wilkitzkii* and *Hyperia galba)*	2 *(1 %)*	< 1 *(0 %)*		
Smith Sound IKMT 2	2021-10-17 22:12 (night)	240	Arctic cod *(Boreogadus saida)*	26 *(5 %)*	16 *(11 %)* [a]	4.2 ± 0.7	-56.2 ± 1.0 [d]

Smith Sound IKMT 2	2021-10-17 22:12 (night)	240	Snailfish *(Liparis* sp.*)*	3 *(1 %)*	9 *(6 %)* [b]	5.7 ± 2.2	-72.5 ± 4.7 [e]
Smith Sound IKMT 2	2021-10-17 22:12 (night)	240	Hyperiid amphipod *(Themisto libellula)*	408 *(80 %)*	97 *(65 %)*	1.8 ± 0.5 [c]	-69.2 ± 4.9 [f]
Smith Sound IKMT 2	2021-10-17 22:12 (night)	240	Mysid *(Boreomysis arctica)*	54 *(11 %)*	14 *(9 %)*	2.7 ± 0.6 [c]	-86.0 ± 4.4 [f]
Smith Sound IKMT 2	2021-10-17 22:12 (night)	240	Amphipoda other *(*mostly *Eusirus* sp. and *Gammarus wilkitzkii)*	10 *(2 %)*	11 *(7 %)*		
Smith Sound IKMT 2	2021-10-17 22:12 (night)	240	Pteropod *(Clione limacina)*	8 *(2 %)*	3 *(2 %)*		
Smith Sound IKMT 2	2021-10-17 22:12 (night)	240	Unidentified shrimp	1 *(0 %)*	< 1 *(0 %)*		
Smith Sound IKMT 2	2021-10-17 22:12 (night)	240	Euphausiid *(Thyssanoessa* sp.*)*	1 *(0 %)*	< 1 *(0 %)*		
Jones Sound IKMT 3	2021-10-17 22:16 (night)	295	Snailfish *(Liparis* sp.*)*	13 *(1 %)*	88 *(15 %)* [a]	7.6 ± 1.6	-69.6 ± 3.0 [d]
Jones Sound IKMT 3	2021-10-17 22:16 (night)	295	Arctic cod *(Boreogadus saida)*	10 *(1 %)*	9 *(1 %)* [b]	4.8 ± 0.4	-55.3 ± 0.6 [e]
Jones Sound IKMT 3	2021-10-17 22:16 (night)	295	Mysid *(Boreomysis arctica)*	1134 *(67 %)*	359 *(62 %)*	4.1 ± 0.9	-80.3 ± 4.7 [f]
Jones Sound IKMT 3	2021-10-17 22:16 (night)	295	Hyperiid amphipod *(Themisto libellula)*	507 *(30 %)*	103 *(18 %)*	2.3 ± 0.3	-65.8 ± 2.1 [f]
Jones Sound IKMT 3	2021-10-17 22:16 (night)	295	Amphipoda other (mostly *Eusirus* sp.)	29 *(2 %)*	20 *(3 %)*		
Jones Sound IKMT 3	2021-10-17 22:16 (night)	295	Pteropod *(Clione limacina* and *Limacina helicina)*	5 *(0 %)*	2 *(0 %)*		

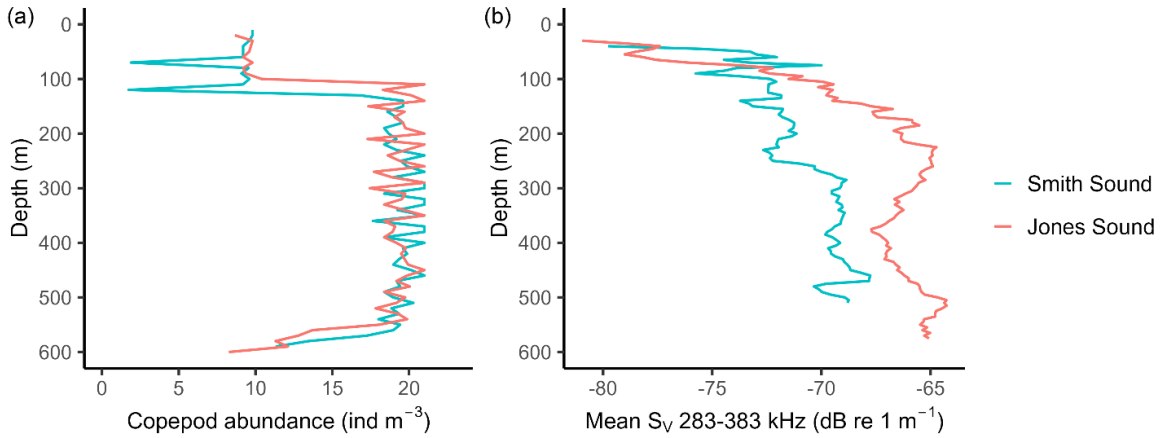

Figure 4-4. Daytime vertical distribution of (a) copepod abundance from UVP6 profiles and (b) volume backscattering strength (S_V 283-383 kHz) from the acoustic probe in Smith Sound and Jones Sound. The acoustic probe and UVP6 profiles were collected concurrently.

Using the hull mounted echosounder, we observed two main sound scattering layers in Smith Sound and Jones Sound, one in the epipelagic and one in the mesopelagic (Figure 4-5a, b). During daytime, the epipelagic layer occupied the top 100 m in Smith Sound and the top 180 m in Jones Sound whereas the mesopelagic layer was located deeper, i.e., 180-380 m in Smith Sound and 220-450 m depth in Jones Sound (Figure 4-5c, d). Mean S_V was higher in the epipelagic layer (-70 and -75 dB re 1 m^{-1} in Smith Sound and Jones Sound respectively) than in the mesopelagic layer (-80 dB re 1 m^{-1} in Smith Sound and -78 dB re 1 m^{-1} in Jones Sound). We observed diel vertical migration patterns (DVM) in both areas (Figure 4-5a, b). The mesopelagic layer clearly separated from the epipelagic layer during daytime and both layers merged during nighttime (Figure 4-5c, d). Twenty-one percent of the mesopelagic backscatter underwent DVM in Smith Sound and 4 % in Jones Sound (Table 4-2). Part of the mesopelagic sound scattering layer remained at depth throughout the day and did not conduct DVM, in particular in Jones Sound. In Jones Sound the inertia of the mesopelagic layer was lower during nighttime than during daytime, meaning that the mesopelagic layer was more dispersed vertically during the day than during the night, whereas inertia remained stable throughout the day in Smith Sound (Table 4-2).

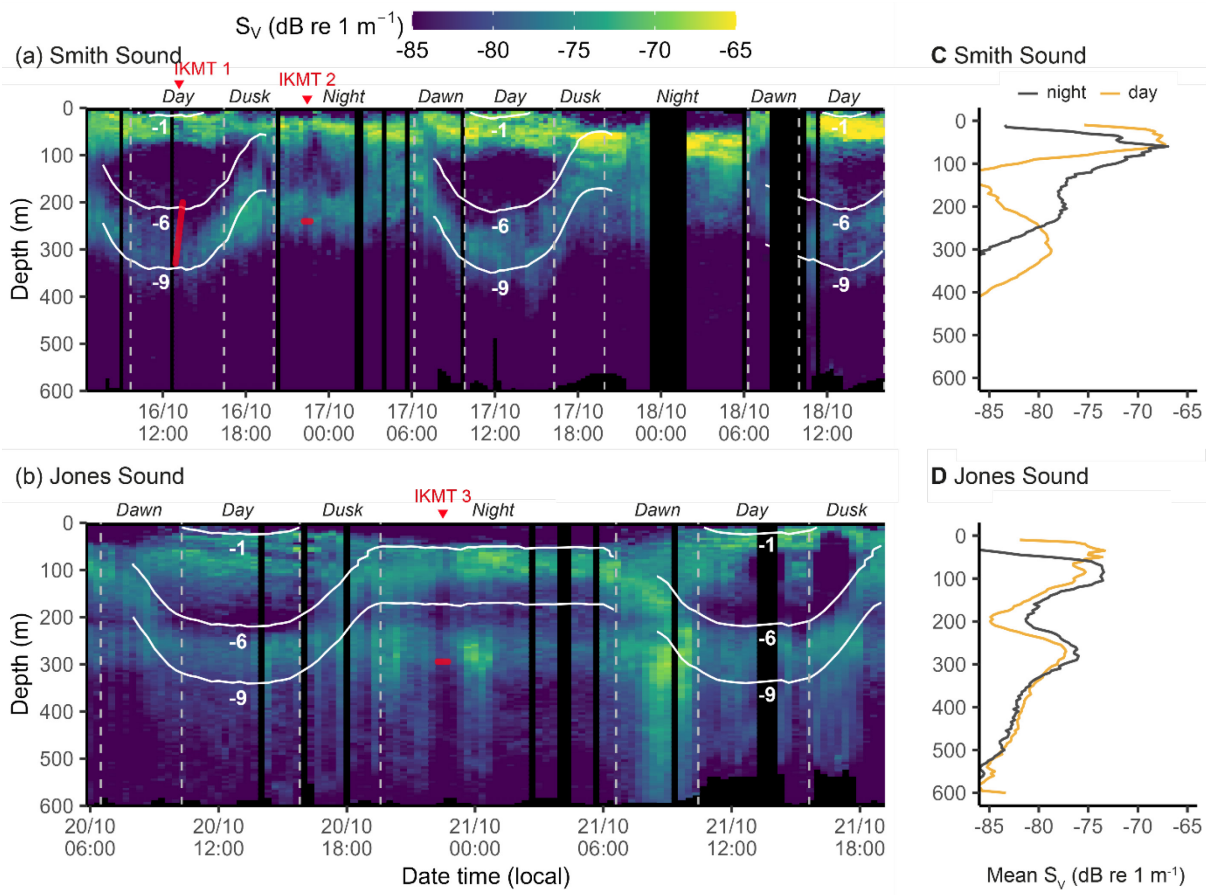

Figure 4-5. Echogram of volume backscattering strength (S_V in dB re 1 m^{-1}) at 38 kHz in (a) Smith Sound and (b) Jones Sound with (c, d) their respective mean S_V profiles during day and night. The white solid lines show the log_{10}-transformed ambient irradiance resolved for the 400-700 nm band at 10^{-1}, 10^{-6} and 10^{-9} µmol photons m^{-2} s^{-1}. The red lines indicate the sampling depths and timings of the IKMT trawls and the vertical grey dotted lines show nautical dawn, nautical dusk, sunrise and sunset times.

Interestingly, while the mesopelagic layer underwent DVM, the epipelagic layer was characterized by reverse DVM patterns, with shallower distributions during daytime than nighttime in both areas (Figure 4-5c, d). During nighttime, the top 20 m in Smith Sound and 40 m in Jones Sound were almost devoid of scatterers while during daytime the peak in S_V occurred just below the ocean's surface. The amplitude of reverse DVM was 35 m in Smith Sound and 26 m in Jones Sound (Table 4-2). The epipelagic layer was less dispersed during daytime (inertia of 691 m^{-2}) than during nighttime in Smith Sound (inertia of 1604 m^{-2}), while the opposite pattern occurred in Jones Sound (inertia of 1271 m^{-2} during day and 1838 m^{-2} during night).

Table 4-2. Summary of diel vertical migration (DVM) patterns of the epipelagic (0-200 m depth range) and mesopelagic layer (200-25 m above seafloor) in Smith Sound and Jones Sound at 38 kHz. MP represents the migratory proportion of mesopelagic backscatter, e.g., the percentage of mesopelagic backscatter that underwent DVM. WMD describes the weighted mean depth of the scattering layer and inertia the spread of the scattering layer around the WMD.

Station	**Depth layer (m)**	**Integrated s_A (m^2 nmi^{-2})**		**MP above 200 m (%)**	**WMD (m)**		**DVM amplitude (m)**	**Inertia (m^{-2})**	
		Night	*Day*		*Night*	*Day*		*Night*	*Day*
Smith Sound	Epipelagic	375	405	-	83	48	-35	1604	691
Jones Sound	Epipelagic	161	155	-	101	75	-26	1271	1838
Smith Sound	Mesopelagic	62	88	21	273	321	48	7347	7344
Jones Sound	Mesopelagic	150	133	4	330	353	23	9204	9901

The depth distribution of the mesopelagic layer aligned with the solar cycle, e.g., the mesopelagic layer started ascending to the epipelagic after sunset and ended around nautical dusk, while the descent to the mesopelagic zone started around nautical dawn and ended at sunrise (Figure 4-5a, b). During daytime, the ambient light at the top of the mesopelagic layer was ca. 10^{-6} µmol photons m^{-2} s^{-1} and ca. 10^{-9} µmol photons m^{-2} s^{-1} at the bottom of the mesopelagic layer (Figure 4-5a, b). This pattern also held during dawn and dusk – when part of the mesopelagic backscatter migrated vertically – the mesopelagic S_V peak remained between the 10^{-6} and 10^{-9} isolumes (Figure 4-6). During twilight and daytime, the mesopelagic S_V peak grouped around 10^{-8} µmol photons m^{-2} s^{-1} in Smith Sound whereas it occurred at slightly higher irradiance levels in Jones Sound (10^{-7} to 10^{-9} µmol photons m^{-2} s^{-1}; Figure 4-6a, b). During nighttime, mesopelagic backscatter was spread throughout the water column more so than during daytime, and some of the mesopelagic backscatter overlapped with the peak in epipelagic backscatter between 10^{-6} and 10^{-9} µmol photons m^{-2} s^{-1}. This pattern was more evident in Smith Sound where a larger proportion of the mesopelagic backscatter performed DVM compared to Jones Sound.

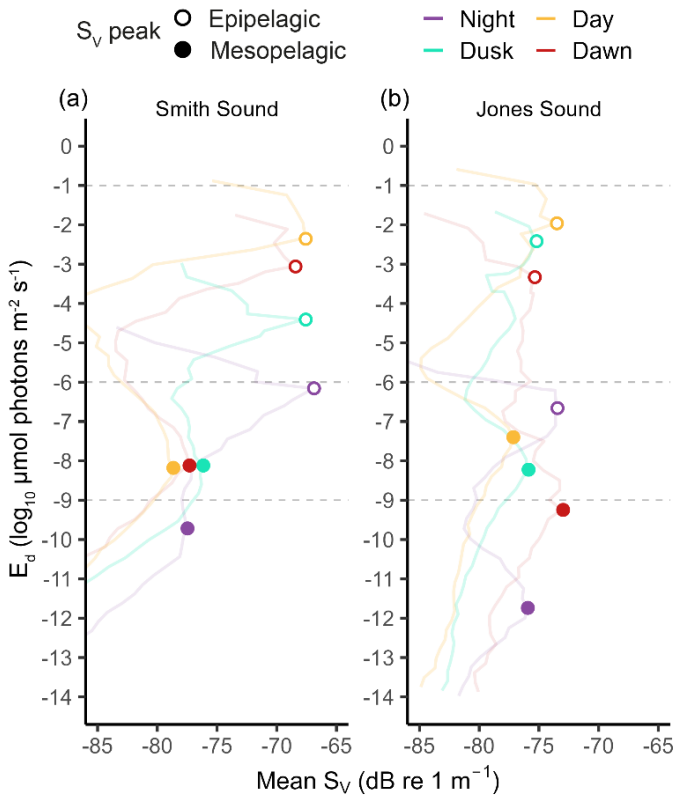

Figure 4-6. Vertical distribution of mean S_V (dB re 1 m^{-1}) in (a) Smith Sound and (b) Jones Sound throughout the day night cycle (colors) according to underwater irradiance availability (E_d in $\log_{10}$ µmol photons m^{-2} s^{-1}). Filled points show the S_V peak of the mesopelagic layer and circles the peak of the epipelagic layer.

The scattering models and target strength (TS) – length equations showed a higher TS in Arctic cod compared to snailfish, mysids, and amphipods – the co-occurring main taxa found in Smith Sound and Jones Sound (Table 4-1, Figure S4-4). Thus, the TS threshold at -65 dB re 1 m^2 used to detect single targets effectively separated Arctic cod of various sizes from the other main weaker scatterers. In both Smith Sound and Jones Sound, we found a vertical segregation in TS, with the epipelagic layer (< 250 m depth) composed of single targets with small TS (mode at ca. -55 dB re 1 m^2) – corresponding to young-of-the-year (age-0) and age-1 Arctic cod – and stronger targets (ca. -46 dB, age-1+ Arctic cod) found in the mesopelagic zone (> 250 m depth; Figure 4-7a, b).

While the vertical segregation in TS was similar between the two areas, the diel changes in vertical distribution of TS differed between Smith Sound and Jones Sound. In Smith Sound,

during daytime age-0 and age-1 Arctic cod split into a shallow group between 10-30 m depth and a deep group 70-230 m depth while at night they occurred between 30-60 m and 250-350 m depth (Figure 4-7c). The shallow group had a median TS of -53.7 dB (equivalent to 6.3 cm fish) mostly containing young-of-the-year Arctic cod and age-1, whereas the deep group was mostly composed of age-1 Arctic cod with some age-0 and small age-1+, with a mean TS 50.0 dB of for that group (equivalent to 11.4 cm fish). In contrast, strong single targets from age-1+ Arctic cod of length > 18 cm occupied the mesopelagic zone during the day (270-370 m depth) and ascended to the epipelagic layer at night (80-270 m).

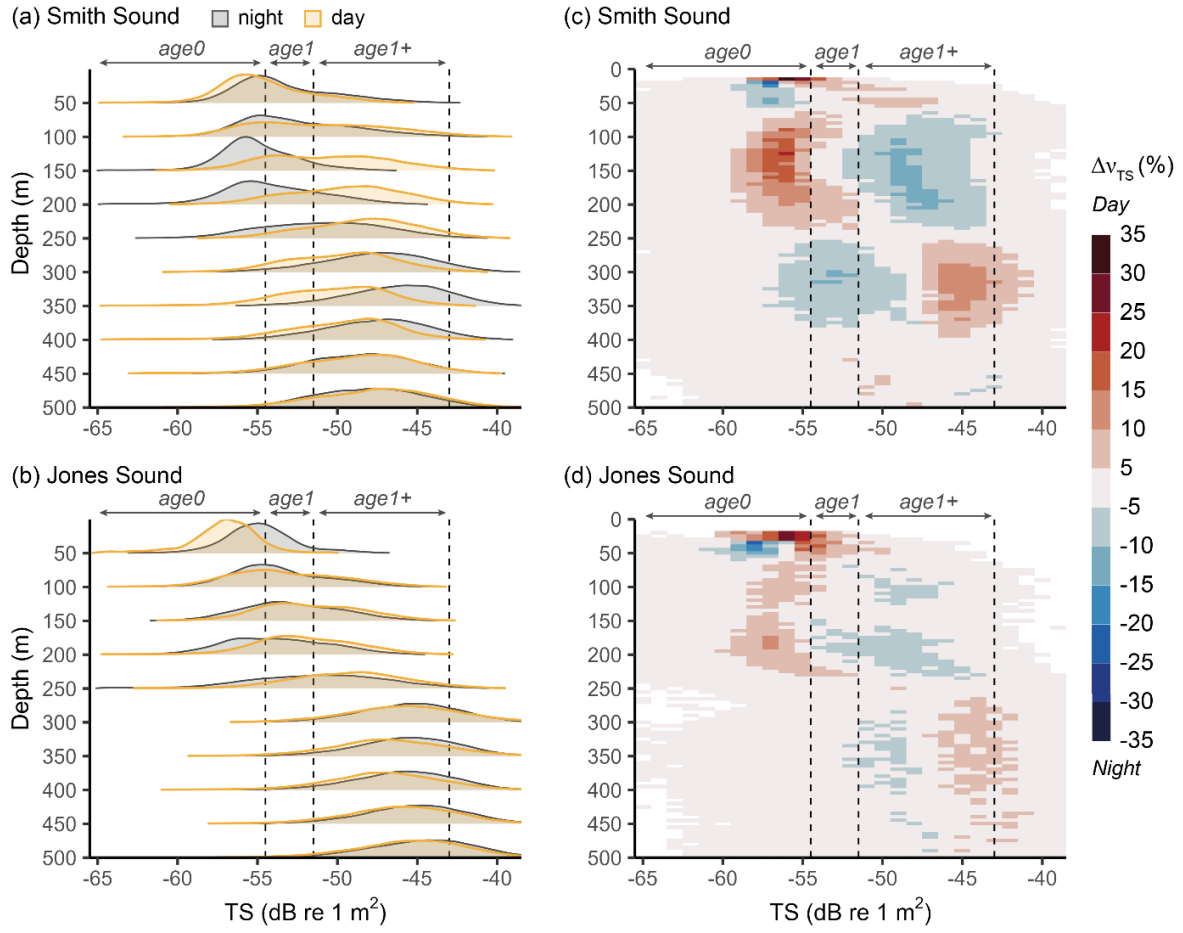

Figure 4-7. Frequency of distribution of target strength (TS; bandwidth of 0.41 dB) of single targets in 50 m depth bins detected in (a) Smith Sound and (b) Jones Sound during night (grey) and day (yellow). Day-night difference in frequency of occurrence of single targets (Δv_{TS}), the colors represent increased occurrence for a given group of single targets during daytime (red) and nighttime (blue) in (c) Smith Sound and (d) Jones Sound. The vertical dotted lines represent the maximum TS of age-0 (6 cm length), age-1 (9 cm length) and age-1+ Arctic cod (max 35 cm length) based on Geoffroy et al. (2016).

In Jones Sound, age-0 and age-1 Arctic cod were absent at mesopelagic depths and only occupied the upper 230 m of the water column (Figure 4-7b). During daytime, those small Arctic cod were split in a shallow group between 10-30 m depth and a deep group between 130-230 m depth, concentrating in the 30-60 m depth range at night (Figure 4-7d). Similarly to Smith Sound, age-1+ Arctic cod >18 cm (TS of -47 dB) were deeper during the day (250-450 m depth) than during night (150-230 m depth). The differences in day-night frequency of occurrence of age-1+ Arctic cod was smaller in Jones Sound (< 10 %) compared to Smith Sound (up to 15 %; Figure 4-7b, d).

4.5 Discussion

4.5.1 Ambient light and vertical distribution of mesopelagic animals

In the global ocean, the vertical distribution and migration amplitude of the mesopelagic scattering layer has been correlated with light penetration, oxygen levels, and temperature (Aksnes et al., 2017; Bianchi et al., 2013; Klevjer et al., 2016). However, light penetration shapes the daytime vertical distribution of mesopelagic organisms and their migrations (Aksnes et al., 2017; Klevjer et al., 2020a; Norheim et al., 2016). Aksnes et al. (2017) found that during daytime the average light intensity at the median depth of the mesopelagic sound scattering layer was 10^{-7} µmol quanta m^2 s^1, with the first and third quartiles depths ranging from 10^{-6} to 10^{-9} µmol quanta m^2 s^1. Klevjer et al. (2020a) found similar levels for multiple basins of the North Atlantic. We showed that the daytime depth of the mesopelagic layer in northern Baffin Bay corresponded to ambient light levels similar to those in temperate and tropical regions.

The daytime narrow range of light intensities at which the mesopelagic layer occurred, i.e., the light comfort zone (Røstad et al., 2016), may emerge from the "antipredation window" hypothesis (Clark and Levy, 1988). The antipredation window refers to a range of light levels

where the ratio of mortality risk to feeding rate is minimum, i.e., mesopelagic animals avoid high light intensities to limit predation risk and low light intensities to maximize feeding. Animals following a light comfort zone move vertically in synchrony with diel changes in surface irradiance (Bianchi and Mislan, 2016; Dupont et al., 2009; Siegelman-Charbit and Planque, 2016). Obviously, the non-migrating part of the mesopelagic layer experiences much larger daily variations in ambient light than experienced by migrating individuals. During the research cruise, the peak in mesopelagic backscatter during daytime, dusk, and dawn remained within a narrow range of light intensities that overlapped with the nighttime peak in epipelagic backscatter (Figure 4-6). This finding supports the hypothesis that the vertical distribution of migrating mesopelagic fauna follows a light comfort zone.

While migrating mesopelagic organisms remain within a specific light comfort zone, the spectral composition of ambient light varies throughout their migration, with a broader spectrum near the surface than at mesopelagic depths where downwelling irradiance peaks at ca. 475-490 nm (Figure S4-3; Li et al., 2014). Most deep-sea fishes, including lanternfish, possess visual pigments with a peak sensitivity centred around 468-494 nm, the deepest penetrating wavelengths (Warrant and Locket, 2004). This peak may result from evolution for maximum sensitivity to bioluminescence rather than to ambient light, because bioluminescence may be greater than downwelling light intensity at mesopelagic depths (Turner et al., 2009; Warrant and Locket, 2004). To understand how much light is "available" to mesopelagic organisms requires consideration of their spectral sensitivity. For example, in the Iceland Sea and Labrador Sea, lanternfish are one of the most important taxa in the mesopelagic zone and have a maximum sensitivity at 487 nm (Klevjer et al., 2020b; Turner et al., 2009). Klevjer et al. (2020a) estimated that a lanternfish in the Iceland Sea at 145 m depth could utilize around

80 % of the total light (400-600 nm) in contrast to about 25 % at 55 m in the Labrador Sea, due to differences in light absorption spectra.

The two main mesopelagic fish taxa caught in the samples were Arctic cod and snailfish. In contrast to the majority of lanternfish (Turner et al., 2009), Arctic cod have multifocal eye lenses (Jönsson et al., 2014) – considered necessary for sharp color vision – even during the polar night when mesopelagic irradiance levels prevail even at the ocean's surface (Cohen et al., 2020). Hence, Arctic cod are particularly well adapted to changing light conditions and this could allow them to take full advantage of the light spectrum during DVM. However, the lack of available detailed information on the eye sensitivity of Arctic cod points a need to assess how much light is "available" to Arctic cod at different depths. Similarly, the spectral sensitivity of snailfish has not been established.

Unlike the fish taxa, both the mysid (*Boreomysis arctica*) and hyperiid amphipod species (*Themisto libellula*) possess compound eyes (Land, 2000; Lindström, 2000). *T. libellula* is a visual predator of copepods and has large, double structured eyes with a specific upward-pointing region that may specialize on detecting prey against a background of downwelling light, whereas they may dedicate the lower part of the eyes to bioluminescent detections (Land, 2000, 1989). *T. libellula* forages during the polar night, suggesting that they can utilize very low light levels (Kraft et al., 2013). Noting the absence of information on *Boreomysis arctica* light sensitivity, two other pelagic species of mysids from the Baltic Sea (*Mysis mixta* and *M. relicta*) have light peak sensitivity at 505-520 nm (Lindström, 2000). Overall, because of the extreme photoperiod at high latitudes, Arctic-native taxa may have developed specific light spectrum sensitivities to utilize as much of the light field as possible throughout the year. Therefore, adaptations to low light levels during the polar night may favor occupation of mesopelagic habitat by Arctic species.

4.5.2 Mesopelagic DVM of adult Arctic cod

The mesopelagic niche in the Arctic is not as vacant as previously thought (Kaartvedt, 2008), and mesopelagic fish and macrozooplankton occupy this niche throughout the marine Arctic (chapter two; Ingvaldsen et al., 2023; Snoeijs-Leijonmalm et al., 2022). Because mesopelagic animals vertically segregate from their copepod prey for part of the year (chapter three), some uncertainties remain regarding foraging behaviour in the Arctic. Multiple studies identify twilight periods, spring, and autumn as critical times for mesopelagic organisms, because sufficient diel changes in light for the light comfort zone of mesopelagic animals to overlap in vertical distribution with copepods (Figure 4-6).

During the cruise, 21 % of the mesopelagic backscatter performed DVM in Smith Sound and 4 % in Jones Sound (Figure 4-5, Table 4-2). For Smith Sound, this proportion is similar to that of the Labrador Sea (18 %), higher than in the western Atlantic Ocean (Iceland and Irminger Sea with 9 % each respectively), and lower than the Norwegian Sea (78 %; Klevjer et al., 2020a). However, differences in backscatter migrating proportion between regions may not entirely reflect migrating biomass because of the dependence on the scattering characteristics of mesopelagic taxa. Here, the main scatterer at 38 kHz was Arctic cod (Figure S4-4) and, while large Arctic cod were not caught with the IKMT likely due to trawl avoidance, those large individuals were detected at depth > 250 m with the echosounder. Furthermore, we documented vertical migration behaviours of different size classes of Arctic cod with the day-night difference in frequency of occurrence of TS (Figure 4-7). However, the TS differencing method was only valid for studying strong acoustic targets because we were constrained to using the low frequency 38 kHz (Figure S4-1). Hence, we could not assess whether weak scatterers such as snailfish, mysids, and hyperiid amphipods were part of the DVM migrating assemblage. Yet, for strong targets like age-1+ Arctic cod, we showed that they conducted

regular DVM between meso- and epipelagic zones, and were thus the part of the migrating proportion following the 10^{-6} and 10^{-9} isolumes (Figure 4-6, Figure 4-7). Future studies could implement this approach on day-night data collected by an acoustic probe, resolving issues of low signal-to-noise ratio at depth and transducer choice. Ultimately, these data would improve understanding of vertical migration behaviour of weak scatterers, including macrozooplankton and non-swimbladdered fish.

We found that some adult Arctic cod conducted regular DVM to the epipelagic while the rest remained at depth (Figure 4-7). This pattern was particularly evident in Smith Sound compared to Jones Sound. DVM is a common feature in adult Arctic cod, for example in the Beaufort Sea where they conduct DVM during autumn, winter, and spring within the Atlantic water mass (Benoit et al., 2010; Geoffroy et al., 2016). If migrating Arctic cod follow their light comfort zone, their capacity to detect prey would not change throughout the diel cycle and would limit depth overlap with their prey. In contrast, given the shallowing of the isolumes, Arctic cod remaining at depth throughout the day would be visually impaired at night, and would thus not be able to detect prey during nighttime. This would restrict the feeding of non-migrating Arctic cod during daytime. Alternatively, rather than population wide DVM, the satiety level of each individual could trigger individual vertical migrations, where only "hungry" Arctic cod would conduct DVM (Pearre, 2003). The absence of DVM in adult Arctic cod in Jones Sound compared to Smith Sound could also reflect differences in top predator presence, e.g., marine mammals and seabirds, which can restrict vertical movements (Urmy and Benoit-Bird, 2021).

We observed consistent DVM of the mesopelagic fauna over the 8 days, even when the ship was transiting between stations, suggesting that this pattern persisted throughout the autumn period. It is impossible to infer the spatial extent of regular DVM behaviour from the data

because sampling was restricted to northern Baffin Bay. However, DVM of the mesopelagic layer has been observed under sea ice in the Central Arctic Ocean (Snoeijs-Leijonmalm et al., 2022), and near Svalbard in autumn (Gjøsæter et al., 2017), suggesting a pattern widespread within the Arctic Ocean where mesopelagic layers occur. In autumn, the large diurnal amplitude in irradiance allows the light comfort zone of mesopelagic organisms to span at least 300 m between 50 m and 350 m depth (Figure 4-5), potentially contributing to the biological carbon pump by actively transporting carbon from Arctic surface waters to the West Greenland intermediate waters (Davison et al., 2013). This migration maximizes the chances for a mesopelagic animal to encounter some of their prey as they search through a large part of the water column. This finding confirms that autumn is a critical period for Arctic mesopelagic organisms.

4.5.3 Flexible behaviour of juvenile Arctic cod: reverse and regular DVM

We observed flexible DVM patterns of juvenile Arctic cod, with both reverse and regular DVM, and distinguished between a deep and shallow group of juvenile Arctic cod based on their vertical distribution (Figure 4-7). Our data suggest that some juvenile Arctic cod conducted reverse DVM in the top 60 m of the water column, where they ascended to the surface during daytime and remained between 30-60 m at night. Similarly, we observed reverse DVM of the deep group in Smith Sound, which occurred at mesopelagic depths at night (250-370 m depth) and at epipelagic depths during day (70-230 m depth). Potentially, a portion of the juvenile Arctic cod population performed regular DVM, where they remained between 70-230 m during daytime and ascended to the subsurface at night.

While we could not assess the portion of juvenile Arctic cod conducting reverse and regular DVM, we showed that the vertical distribution of juvenile (age-0 and age-1) and adult Arctic cod do not overlap either during the day or the night (Figure 4-7). This lack of overlap suggests

intra-specific avoidance of adult Arctic cod by juvenile Arctic cod, noting that adults can feed on juvenile specimens in this cannibalistic species (Benoit et al., 2008; Rand et al., 2013). As a consequence, Arctic cod vertically segregate into size classes with younger and smaller fish occupying shallower depths than their older congeners (Geoffroy et al., 2016).

The reverse DVM patterns of juvenile Arctic cod did not conform to the light comfort zone hypothesis, particularly the shallow group that remained in the upper 60 m of the water column. During daytime they were presumably exposed to visual predators near the surface, however predation pressure near the surface was most likely low because seabirds had already migrated south (Frederiksen et al., 2016; Karnovsky and Hunt, 2002) and adult Arctic cod performing DVM did not reach the surface (Figure 4-7). Reverse DVM patterns in fish have seldom been observed and may result from improved feeding conditions during daytime (Annasawmy et al., 2020; Kaartvedt et al., 2009; Lebourges-Dhaussy et al., 2000; Staby et al., 2011). During daytime, data from the UVP6 and the acoustic probe showed that most of the mesozooplankton concentrated below 100 m depth (Figure 4-4). These instruments had a minimum detection size of ca. 0.7 mm and likely under sampled the abundant smaller mesozooplankton. Mesozooplankton net sampling indicated that young copepodites of *Calanus glacialis* (CI-CIII) occurred in the top 50 m of the water column (Malin Daase, unpublished data); those stages are one of the main prey of juvenile Arctic cod (Bouchard and Fortier, 2020). We suggest that the shallow group of juvenile Arctic cod conducting reverse DVM took advantage of the enhanced light conditions near the surface to feed on small copepodites. This corroborates the hypothesis of Geoffroy et al. (2016), who suggested that Arctic cod hatching late in the season remain near the surface to continue feeding throughout autumn and winter at a time when early hatchers have already descended to mesopelagic depths.

The deep group of juvenile Arctic cod displaying reverse DVM in Smith Sound were bigger than the shallow group (Figure 4-7). This group was most likely a mix of age-1 fish and age-0 early hatchers that already descended to mesopelagic depths. Their vertical distribution overlapped with that of their copepod prey, which was homogenous below 100 m depth (Figure 4-4), but was the exact opposite of that of adult Arctic cod (Figure 4-7). We thus suggest that reverse DVM of the deep group of juvenile Arctic cod was related to avoidance of their larger congeners. This conclusion is further supported by the absence of "deep" reverse DVM in Jones Sound where adult Arctic cod remained at depth throughout the day.

4.6 Conclusion

Arctic mesopelagic fish and macrozooplankton undergo DVM in autumn. One of the main fish species caught, Arctic cod, displayed flexible DVM behaviours. Juveniles performed reverse and regular DVM, whereas adults conducted regular DVM or were non-migrating. While mesopelagic adult Arctic cod conducting DVM support the light comfort zone hypothesis, predator-prey interactions likely drove the vertical distribution of juveniles. Our results confirm the importance of autumn as a key period for feeding in Arctic mesopelagic fauna. With ongoing sea ice decline due to climate change, the underwater light climate of Arctic waters is expected to change (Castellani et al., 2022). These changes will particularly be evident during twilight periods, and in autumn and spring, and may have consequences on the vertical distribution and behaviour of mesopelagic animals and their prey (Flores et al., 2023). This study supports the need for better understanding of the ecological processes controlling vertical migrations and biomass of mesopelagic organisms in a changing Arctic.

5 General conclusions

5.1 Thesis overview

The overall aim of this thesis was to provide a comprehensive overview of the spatial distribution, species composition, environmental drivers, and life history strategies of mesopelagic fauna in the Arctic Ocean. I addressed this objective by exploring different facets of the ecology of mesopelagic organisms in the Arctic Ocean. In chapter two, I demonstrated that mesopelagic layers composed of fish and macrozooplankton commonly occur in the European Arctic, Baffin Bay, and the Beaufort Sea. I identified two distinct mesopelagic fish assemblages, presumably representative of larger biogeographical provinces. The western Arctic province of the Canadian Arctic (Beaufort Sea, Baffin Bay, Canada Basin) was dominated by Arctic fish species – Arctic cod (*Boreogadus saida*) and snailfish (*Liparis* sp.) – and the eastern boreo-Arctic province (European Arctic and southeast Baffin Bay) was composed of a combination of boreal species and Arctic cod. The spatial extent of those provinces reflected advection patterns of Atlantic water (eastern boreo-Arctic) and Arctic water (western Arctic), possibly constrained by hydrographic fronts although the precise location and nature of these boundaries requires further investigation.

In chapter three and four I investigated the distribution of mesopelagic fish and macrozooplankton in relation to their main prey – copepods of the genus *Calanus* – during the midnight sun (chapter three) and in autumn (chapter four), to identify key periods of the year when feeding is possible. I showed that under the constant daylight of midnight sun, mesopelagic animals vertically segregated from *Calanus,* suggesting that spring and autumn are crucial periods for mesopelagic foraging (chapter three). Furthermore, the acoustic backscatter of the mesopelagic layer recorded in 2017 over the Sophia Deep north of Svalbard was the highest ever recorded in the Arctic Ocean. Mesopelagic densities were comparable to

temperate and tropical oceans. In autumn, some mesopelagic organisms performed diel vertical migrations (DVM; chapter four). These migrants tracked a light comfort zone, i.e., a narrow range of light intensities, and overlapped with the distribution of *Calanus*. This observation confirmed autumn as an important period when mesopelagic fish and macrozooplankton can feed on their copepod prey. In contrast, juvenile Arctic cod displayed reverse DVM patterns where they ascended in the water column during the day and descended at night, presumably to limit intraspecific predation and to exploit enhanced feeding opportunities. This pattern suggested that mesopelagic fish behaviours are flexible and underpin predator-prey interactions as an important driver of vertical distributions and behaviour of mesopelagic organisms.

Collectively, the three core chapters confirmed the widespread distribution of mesopelagic fish and macrozooplankton in the Arctic Ocean and the existence of a mesopelagic niche at high latitudes. These animals have developed specific life history strategies to cope with the extreme environment of the Arctic Ocean. Here, I pieced together the annual cycle of mesopelagic organisms in the Arctic Ocean, discussed the role of mesopelagic fauna in the Arctic marine food web, and the potential impacts of climate change and increasing human activities on their distribution. Finally, I detailed knowledge gaps that emerged from this work and identified future research questions.

5.2 The annual cycle of the mesopelagic layer

5.2.1 The light comfort zone constrains the vertical distribution of mesopelagic fauna throughout the year

The light comfort zone hypothesis provides a global and comprehensive framework explaining the behaviours of organisms that live in mesopelagic layers (Aksnes et al., 2017; Klevjer et al., 2020a; Røstad et al., 2016). The light comfort zone hypothesis likely also applies in the Arctic Ocean. The seasonal vertical migrations (Geoffroy et al., 2019), DVM in spring and autumn

(chapter four; Gjøsæter et al., 2017; Snoeijs-Leijonmalm et al., 2022), and the absence of large DVM excursions during the midnight sun and polar night (chapter three; Snoeijs-Leijonmalm et al., 2022), corroborate the light comfort zone hypothesis. Therefore, because mesopelagic sound scattering layers follow a light comfort zone throughout the year, I conclude that the annual vertical distribution of mesopelagic sound scattering layers contains four phases: two periods of overlap with *Calanus* in spring and autumn, separated by two periods of vertical segregation during the midnight sun and polar night (Figure 5-1). Hence, the results from this thesis suggests that the feeding and growth dynamics of mesopelagic fauna in the Arctic Ocean is characterized by two seasonal growth pulses in spring and autumn followed by two periods of lower growth. Yet, feeding could occur during the polar night and midnight sun.

5.2.2 How do mesopelagic fish and macrozooplankton survive a year in the Arctic?

Theoretically, if mesopelagic organisms adhere to a light comfort zone, they possess the same capacity to detect prey regardless of the time of day or season because their light environment remains constant (Kaartvedt et al., 2019a). In that case, only the vertical distribution of their prey limits feeding. Hence, I suggest that during the overlap periods in spring and autumn, mesopelagic fish and macrozooplankton prey on *Calanus* while during the midnight sun and polar night they enter an overwintering and oversummering phase, respectively, and feed on other prey found within their light comfort zone (Figure 5-1).

5.2.2.1 Spring and autumn vertical migration behaviours

Because the mesopelagic layer undergoes synchronous DVM in spring and autumn, their light comfort zone overlaps with the vertical distribution of *Calanus*. At these times of year, the large diurnal amplitude in irradiance maximizes the depth range covered by the light comfort zone compared to the polar night or midnight sun periods, e.g., ca. 300 m range (from 50 to 350 m depth) in Baffin Bay in October at the time of sea ice formation (Figure 5-1; chapter

four). This change in irradiance increases the chances for a mesopelagic fish or zooplankton to encounter *Calanus* at some point throughout the day.

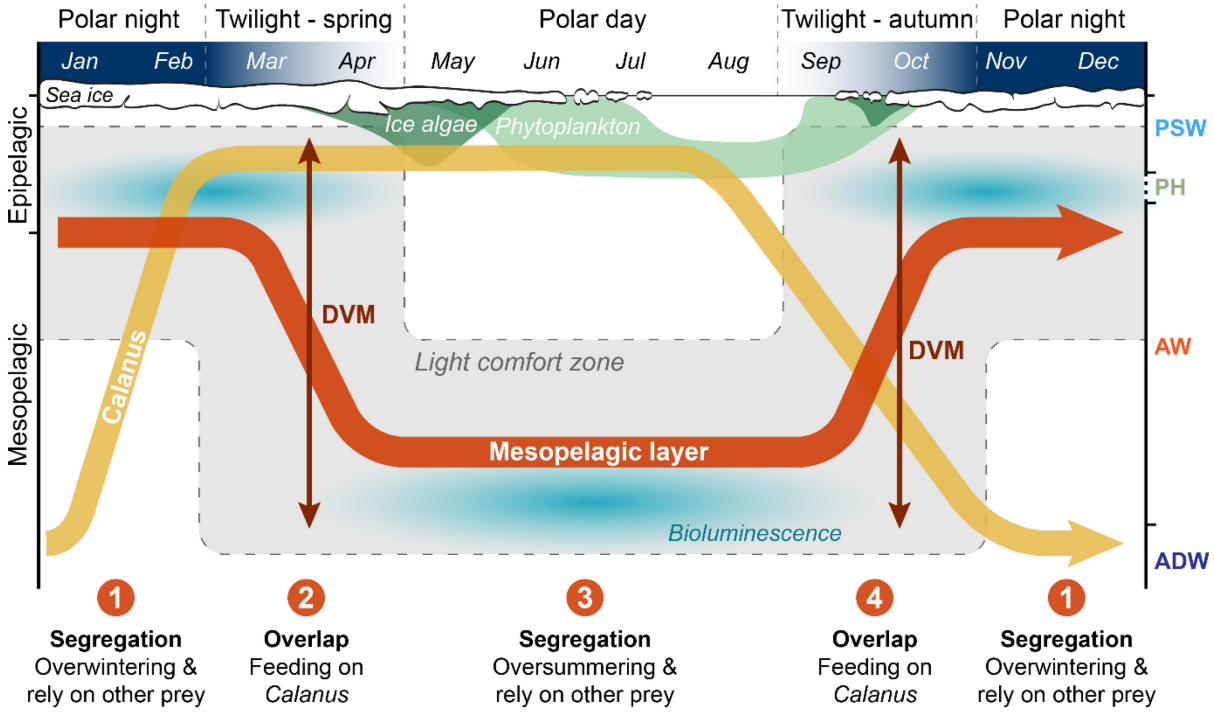

Figure 5-1. Annual vertical distribution of the mesopelagic layer in the Arctic Ocean. The mesopelagic layer follows a light comfort zone (chapter four). This annual cycle contains four phases: overwintering, active feeding in spring, oversummering, and active feeding in autumn. The light comfort zone has its largest extent in spring and autumn, and the distribution of mesopelagic organisms then overlaps with the distribution of the copepod *Calanus*, allowing active feeding. The mesopelagic layer is vertically segregated from *Calanus* during the polar day (chapter three), and at least during part of the polar night prior to the ascent of *Calanus*. During those periods of vertical segregation mesopelagic animals may forage on other prey within their light comfort zone (e.g., Ashjian et al., 2003; Darnis and Fortier, 2014). Bioluminescence is an important source of light in the light comfort zone of animals and may drive predator-prey interactions throughout the year (Cronin et al., 2016; Warrant, 2000). The vertical distribution of water masses is indicated on the right: *PSW*: Polar Surface Waters; *PH*: Pacific halocline; *AW*: Atlantic Water; *ADW*: Arctic Deep Water.

Autumn may be of particular importance, because *Calanus* have accumulated large lipid reserves that make them particularly nutritious prey compared to early spring when their lipid reserves are depleted (Falk-Petersen et al., 2009). However, these vertical migration behaviours can be flexible. They are modulated by individual behaviours (e.g., Kaartvedt et al., 2023) and predator-prey interactions – DVM pattern may change in the presence of predators (chapter four; Urmy and Benoit-Bird, 2021). The proportion of individuals undergoing DVM

determines the active transport of carbon to depth (Davison et al., 2013; Saba et al., 2021; Siegel et al., 2023). Hence, researchers must consider individual behaviours and flexible DVM patterns when evaluating the role of mesopelagic fish and zooplankton in marine food webs.

5.2.2.2 Strategies for overwintering and oversummering

The adaptations enabling overwintering and oversummering are poorly know in marine fish (Hurst, 2007). Overwintering in diapause (Type 1 - Diapause), like *Calanus*, is common among several species of Arctic freshwater fish, but has not been documented in marine fishes (Hurst, 2007; Reynolds, 1997). Therefore, fish that comprise the mesopelagic layer in the Arctic probably either reduce their metabolic activities while still active (Type 2 - Flexibility) or do not change their metabolic activities and remain active (Type 3 – *"Business as usual"*) during the midnight sun and polar night. Data from the polar night confirm that Arctic cod, Atlantic cod, and beaked redfish are active during that time of year, and show some level of feeding (Berge et al., 2015a; Cusa et al., 2019; Geoffroy and Priou, 2020; Larsen et al., 2023).

During the polar night, light intensity at the surface of the ocean resembles that of the mesopelagic zone during daytime (Cohen et al., 2020; Cronin et al., 2016; Kaartvedt et al., 2019a). This similarity means that the light comfort zone of mesopelagic animals is mostly located within the epipelagic zone, where copepods (*Metridia longa*) and macrozooplankton like euphausiids (*Thyssanoessa inermis*) and hyperiid amphipods (*Themisto libellula*) are active (Berge et al., 2015a, 2015b; Kraft et al., 2013). As a consequence, the pelagic ecosystem shifts from a *Calanus*-based food web in summer to a euphausiid-based during the polar night, at least in the eastern boreo-Arctic province (Geoffroy et al., 2019). By shifting their diet to larger species during the polar night, mesopelagic fish may not need to forage as often, e.g., a lanternfish may fill its daily energy requirement by capturing a single krill (Urmy and Horne, 2016). Because amphipods and krill remain active during the polar night (Grenvald et al., 2016;

Kraft et al., 2013), they may also be detected hydrodynamically with the lateral line of fish (Bassett et al., 2007; Kasumyan, 2003). Furthermore, the vertical segregation from *Calanus* only occurs at the beginning of the polar night because the ontogenetic ascent of *Calanus* from overwintering depth can finish by January (Berge et al., 2015a; Espinasse et al., 2022). Hence, during the polar night, the food supply for mesopelagic fish and macrozooplankton may be sufficient to ensure survival.

In contrast to the polar night, the polar day prevents foraging bouts into the productive epipelagic layer where *Calanus* graze on algae. Summer starvation has been proposed as the main factor limiting mesopelagic fish survival in the Arctic Ocean (Langbehn et al., 2022). Thus, mesopelagic fish must rely on other prey at mesopelagic depths within their light comfort zone. During the polar day, the copepod *Metridia longa*, krill, and amphipods are abundant at mesopelagic depth (Ashjian et al., 2003; Ingvaldsen et al., 2023; Kosobokova and Hopcroft, 2010). In gateway areas, advection of boreal zooplankton, which may surpass local growth from grazing on primary production (Kitamura et al., 2017), could also support mesopelagic fish stocks (Wassmann et al., 2015). However, zooplankton biomass estimates remain uncertain and vary spatially. Hence, better understanding of how mesopelagic taxa succeed in the Arctic Ocean requires seasonal investigations of the vertical distribution of prey within the light comfort zone of mesopelagic predator, as well as quantifying their biomass and documenting the diet of mesopelagic fish.

5.2.2.3 The role of bioluminescence

Bioluminescence is a widespread feature within mesopelagic taxa (Widder, 1999). Typically, these taxa use bioluminescence for conspecific identification, counterillumination to limit predation, or to lure prey (Young, 1983). During daytime at mesopelagic depth, bioluminescence intensity may surpass that of ambient light (Widder, 2002). In fact, Cronin et

al. (2016) found that bioluminescence was the main source of light below 30 m depth during the polar night. In contrast to diffuse ambient light, bioluminescence is a point source (Warrant and Locket, 2004). Numerous Arctic taxa are bioluminescent including the copepod *Metridia longa*, the euphausiid *Meganyctiphanes norvegica*, or the ctenophores *Mertensia ovum* and *Beroë cucumis* (Johnsen et al., 2014). The majority of mesopelagic taxa possess visual pigments with peak sensitivity around the deepest penetrating wavelength (ca. 480 nm) which also corresponds to the wavelength spectrum of bioluminescence (Turner et al., 2009; Warrant and Locket, 2004). While there is limited information on the peak eye sensitivity of many Arctic fish taxa from the mesopelagic zone, they may have developed maximum sensitivity to bioluminescence peaks, like other mesopelagic fish from temperate and tropical regions (Warrant and Locket, 2004). Hence, bioluminescence likely plays a functional role in shaping predator-prey interactions in the Arctic Ocean (Berge et al., 2012a; Cronin et al., 2016), but in situ measurements of bioluminescence intensity in the water column remain few (Cohen et al., 2020).

5.2.2.4 Possible seasonal horizontal migrations

Currents also transport some species horizontally. I suggest that Atlantic water advection at the Arctic gateway supports the mesopelagic food web by transporting boreal mesopelagic species into the Arctic Ocean (chapter two). Similarly, Arctic water current circulation in the western Arctic province connects populations of Arctic cod throughout Baffin Bay (Nelson et al., 2020). The effect of advection largely depends on taxa and life stages of mesopelagic micronekton, e.g., juvenile redfish extruded on Barents Sea shelf break are transported northward toward Svalbard whereas larger redfish can swim against currents to migrate southward to feeding grounds in the Barents and Norwegian Seas (Drevetnyak and Nedreaas, 2009; Planque et al., 2013).

Similarly, some taxa are more sensitive to advection than others. For example, adult glacier lanternfish that lack strong swimming capabilities are likely transported with currents more than, for example, adult Arctic cod which can perform extensive horizontal migrations (Kaartvedt et al., 2009, 2008; Kessel et al., 2017). Hence active migrations to favourable overwintering and oversummering habitats is a possible strategy for surviving the polar night and midnight sun period.

During the polar night, the light comfort zone is mostly limited to the epipelagic zone (Cohen et al., 2020; Cronin et al., 2016). Thus, it extends spatially to areas with shallower bathymetry, e.g., shelf seas and coastal areas, which are inaccessible to mesopelagic fish at other time of the year. In these areas, *Calanus* overwinters near the seafloor (e.g., Darnis and Fortier, 2014) within the light comfort zone of mesopelagic fish. However, this is a risky strategy because these species would need to leave the shallower shelf seas before the light returns in spring, to avoid being "trapped″ in an inappropriate light environment and becoming easy prey for visual predators. Species with strong swimming capabilities could undergo such seasonal migrations, e.g., Arctic cod (Kessel et al., 2017). Large knowledge gaps remain regarding potential seasonal migrations of mesopelagic species in the Arctic Ocean.

5.3 Possible implications of the mesopelagic fauna in the structure and function of Arctic marine ecosystems

Current global incentives seek to improve our comprehension of the biodiversity and biomass of organisms occupying the mesopelagic zone in polar environments, including their role in the biological carbon pump and as prey for top predators (Howell et al., 2020; Martin et al., 2020). This thesis covered some of the fundamental aspects of the biology and ecology of mesopelagic fish and zooplankton in the Arctic Ocean. The work from this thesis and recently published literature demonstrate that the mesopelagic zone constitutes a widespread ecological

niche in the Arctic Ocean (chapter two; Geoffroy et al., 2019; Ingvaldsen et al., 2023; Knutsen et al., 2017; Snoeijs-Leijonmalm et al., 2022). This niche is not vacant and is occupied by multiple trophic levels, including herbivorous and carnivorous macrozooplankton (e.g., euphausiid, mysids, and hyperiid amphipods), planktivorous fish (e.g., juveniles of Arctic cod, redfish, glacier lanternfish, and Atlantic cod), and piscivorous fish (adult Arctic cod, Atlantic cod, and armhook squid). Better understanding of their ecology is thus critical to quantifying accurately the biological carbon pump and energy pathways in Arctic marine ecosystems.

Because of the large seasonal variations in the behaviour of mesopelagic animals in the Arctic Ocean (Figure 5-1), the contribution of the mesopelagic layer to the biological carbon pump likely varies through the year. In spring and autumn, animals that undergo DVM actively contribute to the export of organic matter out of the epipelagic zone, whereas, during the polar day, the vertical segregation of mesopelagic fish and *Calanus* limit active transport of carbon from surface waters to the mesopelagic zone. Studies that quantify these contributions are currently ongoing in temperate areas but remain rare and need to be extended to other regions of the global ocean, including the in Arctic Ocean (Davison et al., 2013; Giering et al., 2014; Martin et al., 2020). Because of their central position within the Arctic food web and their role in the biological carbon pump, mesopelagic organisms should be included in future ecosystem and carbon budget studies.

5.4 The double pressure of climate change and increasing human activities in the Arctic Ocean

The Arctic Ocean provides many ecosystem services (i.e., the benefits humans obtain from ecosystems) for northerners and globally, e.g., food supply, climate regulation, cultural, and intrinsic values (Costanza et al., 1997; Eicken et al., 2009). Our ability to predict the response of the Arctic Ocean to the double pressure from climate change and increasing-human activities

and their effects on ecosystem services depend on understanding the functioning and structure of the Arctic marine ecosystem.

Currently, the mesopelagic zone remains a relative pristine environment, especially in the Arctic Ocean. The CAO is under a fisheries moratorium for the next 16 years (FAO, 2021) and human-activities mostly concentrate in shelf seas, e.g., the Barents and Bering Seas. However, this paradigm is changing rapidly. Sea ice extent, thickness, and duration has decreased drastically over the last decades (Kwok, 2018; Notz and Stroeve, 2018). Areas of the Arctic Ocean that were protected from human activities by ice cover are increasingly becoming more accessible to humans. Thus, it is crucial to study the mesopelagic zone now while it is still unexploited in order to understand and predict the wider consequences of climate change and potential commercial uses of that region of the Arctic Ocean (Howell et al., 2020; Martin et al., 2020).

5.4.1 Climate change impacts on the light environment

The decrease in sea ice extent, thickness, and duration allow more light to penetrate the Arctic Ocean, causing profound changes to key ecosystem functions such as shifts in the phenology of ice-algae and phytoplankton blooms and enhanced primary production in shelf seas (Ardyna and Arrigo, 2020; Castellani et al., 2022). While the effects of increased light penetration on primary producers are the subject of current investigations, their effects on pelagic taxa are largely unknown, especially on highly light-sensitive mesopelagic taxa.

Increasing light penetration could have two main effects on mesopelagic taxa. First, I predict a general deepening of the light comfort zone throughout the year. This change will be more evident during the midnight sun than during the polar night when small diel changes in light intensity occur (Johnsen et al., 2021). During the polar day, the vertical segregation between

mesopelagic fish and *Calanus* at the surface will increase but decrease slightly during the polar night. It is difficult to predict the consequences of this increased segregation on the survival of mesopelagic taxa, because they likely rely on other prey at these times of the year.

Second, I predict a temporal shift in the initiation and termination of DVM in spring and autumn. Sensitivity analyses of mechanistic models have shown that changes in the light regime are first-order drivers of mesopelagic fish DVM (Langbehn et al., 2019, 2022; Ljungström et al., 2021). Because of the delay in ice formation in autumn and early melt in spring, more light will be available in autumn and spring. Hence, DVM will begin later in the year in autumn and earlier in spring. One of the possible consequences of this change in DVM timing will be a mismatch with the vertical distribution of *Calanus* (Cushing, 1990; Durant et al., 2007), which could be detrimental to mesopelagic fish and macrozooplankton survival and recruitment.

The effects of increase light penetration on the vertical distribution of *Calanus* also merit consideration. *Calanus* are highly sensitive to light changes that structure their vertical migration behaviour in the Arctic Ocean (Hobbs et al., 2021, 2018), and changes in their migration behaviours could also contribute to a mismatch with mesopelagic predators. For example, Flores et al. (2023) identified a level of light intensity that triggered the seasonal migration of zooplankton to the under-ice layer in autumn and spring and applied this level to future underwater light environments derived from global climate models (CMIP6 models) under different climate change scenarios. They showed that the time spent by zooplankton under the ice during winter could decrease by up to a month within the next 30 years, which could have detrimental effects on mesopelagic predators. Application of this approach to mesopelagic sound scattering layers would help forecast the effects of decreasing sea ice cover on mesopelagic fish distribution.

Ljungström et al. (2021) used a mechanistic model to forecast the distributional change of an epipelagic planktivore (Atlantic herring, *Clupea harengus*) and a mesopelagic planktivore (glacier lanternfish, *Benthosema glaciale*) in the Arctic Ocean under different climate warming scenarios. They suggest that mesopelagic fish do not survive in the Arctic because of the lack of foraging opportunities during polar day and polar night. In contrast, they suggest that herring thrive during the polar day because they can forage on *Calanus* near the surface but would not be able to feed during the polar night. Hence, large herring with high migratory capacities may develop seasonal feeding migrations to the Arctic (Ljungström et al., 2021; Nøttestad et al., 1999). These modelling approaches are essential to achieve a comprehensive overview of the interplay between the physiology and ecology of mesopelagic fish and the light environment (Spence and Tingley, 2020; Twiname et al., 2020).

5.4.2 Anthropogenic impacts

Sea ice reduction has improved access to the Arctic Ocean, leading to increases in anthropogenic activities including maritime shipping, tourism, resource extractions, offshore wind, and fisheries. These activities come with substantial challenges regarding environmental impacts, economic viability, and safety (Haug et al., 2017; Ng et al., 2018; Palma et al., 2019; Petrick et al., 2017). The possible effects on mesopelagic taxa from increased human activities in the Arctic Ocean remain largely unknown.

5.4.2.1 Chemical and artificial light pollution

The risk of pollution from increasing human activities is an important threat to the Arctic Ocean (AMAP, 2021). For example, ship traffic on the northern sea route linking Asia to Europe through the Arctic Ocean and Russian Arctic has increased by ca. 60 % between 2016 and 2019 (Gunnarsson, 2021). With increased human activities in the Arctic Ocean comes an increase in risk of oil pollution from stranded or wrecked ships. Multiple spawning grounds for Arctic

species, like Arctic cod, are located along the shipping routes and thus at risk of oil pollution (Aune et al., 2021; Eriksen et al., 2020). Mesopelagic fish and zooplankton are most at risk of bioaccumulating adverse chemicals from oil spills or oil dispersants when they are close to the surface during the polar night, and in spring and autumn because pollutants accumulate at the sea ice-water interface (Aune et al., 2018). Studies on Arctic cod show that oil pollution has potential long-term consequences on the survival, growth, and reproduction of early life stages (Bender et al., 2021). Hence, chemical pollution can have cascading effect through the entire marine ecosystem of the entire Arctic Ocean.

Artificial light is also increasingly recognized as an important source of pollution in the marine environment, which can impact the vertical migration behaviour of pelagic and mesopelagic organisms (Marangoni et al., 2022). Coastal cities are an important source artificial light pollution on coastal environments whereas artificial lights from ships, oil and gas installations, offshore wind parks, and offshore aquaculture farms (e.g., Ocean Farm One from SalMar) are the main source of artificial light further away from the coast (Davies et al., 2014). For example, artificial lights from a ship can affect the vertical distribution of pelagic fish and zooplankton down to 200 m depth during the polar night (Berge et al., 2020). Avoidance patterns depends on light wavelength, intensity, and taxa (Geoffroy et al., 2021; Kaartvedt et al., 2019b; Peña et al., 2020). Artificial light could potentially inhibit DVM patterns or drastically reduce their amplitude (Marangoni et al., 2022). However, the effects of artificial light pollution in offshore remote area are difficult to assess, but experiments using active acoustics – which do not depend on light to collect data – are a useful tool for improving knowledge of the effect of light pollution on pelagic animals (Geoffroy et al., 2021).

5.4.2.2 Potential mesopelagic commercial fisheries

Given the immense biomass of mesopelagic fish globally, estimated to be above 10,000 million

tons (Irigoien et al., 2014; Proud et al., 2019) – representing more than 100 times the annual catch estimate of current commercial fisheries (Fjeld et al., 2023) – there are commercial interests in exploiting the mesopelagic zone. Potential fisheries targeting mesopelagic fish are often compared to the emerging fishery for *Calanus finmarchicus* (the *"redfeed"*) along the Norwegian coast because of similar characteristics (high biomass, species with low intrinsic commercial value but lipid- and protein-rich; Broms et al., 2016; Fjeld et al., 2023; Hansen et al., 2021; Olsen et al., 2020). The rhetoric for a commercial mesopelagic fishery is the same as for the *Calanus* fishery: mesopelagic organisms are heralded as a solution to reduce fishing pressures on overfished stocks because they could replace fish meal and oil in the aquaculture industry, be used for human consumption, and in nutraceuticals (Fjeld et al., 2023). The trial fishery for mesopelagic species in the North Atlantic targeted two species *Maurolicus muelleri* and *Benthosema glaciale* (Bjordal and Thorvaldsen, 2020). Results from this trail fishery raised multiple concerns regarding bycatch, fishing effort, lack of industrial-scale processing technology for mesopelagic species, markets, and knowledge on ecosystem impacts that remain to be addressed (Bjordal and Thorvaldsen, 2020; Fjeld et al., 2023; Grimaldo et al., 2020; Hidalgo and Browman, 2019; Prellezo, 2019).

In chapter two, I showed that mesopelagic fish and zooplankton are not homogeneously distributed in the Arctic Ocean. The species composition of those layers was diverse, in particular in the eastern boreo-Arctic province, where species of low commercial values (e.g., Arctic cod, glacier lanternfish, euphausiids, and amphipods) co-occur with juveniles of species with higher commercial value (e.g., Atlantic cod and beaked redfish). However, some mesopelagic species, such as like Arctic cod and glacier lanternfish, are rich in lipids and could potentially be of commercial interest (Grimaldo et al., 2020; Hop and Gjøsæter, 2013; Olsen et al., 2020). Because of the central position of mesopelagic fish and zooplankton in the food

web (Saunders et al., 2019), fishing for Arctic mesopelagic resources can have cascading effects on the rest of Arctic marine ecosystems. Many species rely on mesopelagic fish and zooplankton including beluga whales in the Beaufort Sea and Canada Basin (Bluhm and Gradinger, 2008; Storrie et al., 2022), and species targeted by commercial fisheries like the Greenland halibut stock in Baffin Bay (NAFO zone 0; DFO 2019). Because of the moratorium on fisheries in the CAO (FAO, 2021), potential future mesopelagic fisheries could only develop within the national waters of Arctic countries, mostly on shelf seas, where mesopelagic organisms are rare.

For all the above reasons, the development of a mesopelagic fishery in the Arctic Ocean would likely face the same issues of bycatch, fishing effort, economic viability, and environmental impacts as the trial mesopelagic fishery of the North Atlantic. Furthermore, the economic costs of operating such a fishery in the Arctic Ocean would almost certainly be higher than in temperate regions because of the remoteness and harsh environmental conditions (sea ice, darkness) that characterize the Arctic. Information on Arctic mesopelagic fauna is still limited and a much more thorough knowledge base, including on faunal population size, connectivity, and impacts from climate change, is required to make informed decisions on potential harvesting of mesopelagic species in the Arctic Ocean. Yet, to quote Fjeld et al. (2023): *"As technological advancements and ecological knowledge are increasing, […] time will tell whether your future diet will consist of mesopelagic fish, granted we are able to find and sustainably harvest the elusive treasure hidden in the twilight depths."*

5.5 Limitations of my approach and recommendations for future research

5.5.1 Limitations

While active acoustics provide a wealth of information regarding the distribution and behaviour

of pelagic organisms, it only suggests trophic interactions between mesopelagic species and their prey. Biological collections are required to establish those trophic links. The strength of the inferences that can be derived in the presence or absence of such information will be critical to progress in understanding the dynamics of Arctic food webs.

In chapter two, I used different mid-water trawls to sample the mesopelagic layer with different mesh sizes and openings that could have been a source of bias. Larger mesopelagic fish and cephalopods can avoid trawls (Kaartvedt et al., 2012). Smaller nets can also be more easily avoided than larger trawls or create larger pressure waves which when towed fast increase avoidance (Dewey and Moen, 1983). In addition, gelatinous taxa are not preserved well in trawls, and could thus be underrepresented (e.g., physonect siphonophores, which can contribute to acoustic backscatter at 38 kHz). Hence using other ground-truthing methods, such as environmental DNA, or optical sensors could help overcome this issue (Govindarajan et al., 2021; Picheral et al., 2022; Sawada et al., 2004).

In chapter three, I documented high backscatter of the mesopelagic layer, suggesting high mesopelagic biomass. However, because acoustic data was not ground-truthed it was not possible to convert backscatter into biomass estimates. The mesopelagic taxonomic composition north of Svalbard is diverse (chapter two) and the increase in acoustic backscatter could also reflect changes in taxonomic composition throughout the sampling period.

In chapter four, I documented the DVM patterns of Arctic cod through single echo detections on the hull-mounted echosounder data. However, because of the lower signal-to-noise ratio at depth, I could not investigate the migration patterns of the weaker scattering taxa, like mysids, hyperiid amphipods, and snailfish (a non-swimbladdered fish). The top 10 m of the water column were also not sampled accurately by the hull mounted echosounder (mounted at 7 m

depth) and the sideward-looking acoustic probe (interference with the ocean surface at shallow depths), and thus part of the juvenile Arctic cod population performing reverse DVM could have been overlooked. Using upward-facing echosounders would help determine the fraction of the Arctic cod near the ocean's surface. Furthermore, consistent day-night sampling with an acoustic probe could help identify the migration patterns of weak scattering taxa, e.g., mysids, amphipods, and non-swimbladdered fish. Nonetheless, echosounder data are extremely valuable in documenting the distribution and behaviour of pelagic organisms.

5.5.2 Recommendations for future research

The mesopelagic zone receives increasing attention from the scientific community, and yet, we currently know just enough to recognize its importance in maintaining a healthy ocean. The results from this thesis highlight two main knowledge gaps regarding the (i) spatial and seasonal distribution, biomass, and diversity estimates of Arctic mesopelagic taxa, (ii) their life history, trophic interactions, and contribution to the biological carbon pump. Here I synthesize some of the approaches that can be used to fill these knowledge gaps.

5.5.2.1 Biomass – Biodiversity – Spatial and seasonal distribution

Some uncertainties remain regarding the spatial distribution of mesopelagic fish and zooplankton in the Arctic Ocean. For example, the spatial extent of the biogeographic regions suggested in chapter two requires more data to refine their boundaries, in particular in the CAO. To achieve this objective, echosounders are particularly relevant because they can document variations both in vertical distribution and biomass of pelagic organisms. The deployment of autonomous sampling platforms, like moorings or ice-tethered observatories equipped with echosounders (chapter three) that drift with sea ice (Berge et al., 2016; Flores et al., 2023; Zolich et al., 2018), or the use of ships of opportunity (e.g., fishing vessel, cruise ships, supply ships; Escobar-Flores et al., 2018) would increase the spatial and temporal coverage of acoustic

data in the Arctic Ocean. These two sources of data are interesting because ice-tethered observatories drift in relatively data-poor areas with little ship traffic, and ships of opportunity often perform the same journey across seasons and years providing time-series of specific transects.

The amount of acoustic data collected is increasing rapidly due to the multiplication of echosounder deployment and their technological improvements (e.g., broadband), requiring more efficient data treatment methods. Recent advancements in open-source, machine learning algorithms for scrutinizing acoustic data have the potential to improve greatly the processing efficiency and classification accuracy of large acoustic databases in a systematic and reproducible way (Choi et al., 2021; Handegard et al., 2021).

The development of broadband acoustics offer promising results to classify acoustic data at a finer taxonomic resolution than previously achieved with narrowband acoustics (Benoit-Bird and Waluk, 2020; Dunn et al., 2022; Korneliussen et al., 2018). The use of acoustic probes or towed echosounder lowered to mesopelagic depths is particularly pertinent to broadband acoustics, in that they collect good quality (with high signal-to-noise ratio) data near mesopelagic individuals (Figure 5-2). Several of these platforms already exist, such as the Deep-See (Zhuang and Lavery, 2021), the TS Probe (Andersen et al., 2013), or J-QUEST (Sawada et al., 2004). Furthermore, these platforms can be paired with ground-truthing methods like stereo-cameras for identifying the scatterer and measuring their size and orientation within the acoustic beam. Data from these platforms are essential to understand the backscatter of mesopelagic fish and zooplankton, which can then be used to refine scattering models (i.e., mathematical models of the acoustic backscatter of a species which is used to transform backscatter into biomass). In addition, the length-weight and target strength-length relationships must be established for all mesopelagic species commonly found in the Arctic

Ocean, including non-swimbladdered fish like snailfish. However, this is a challenging objective because some species change ontogenetically, affecting their scattering. For example some lanternfish shift from a gas-filled to a lipid-filled swimbladder (Neighbors and Nafpaktitis, 1982; Peña et al., 2023). The depth-dependence of swimbladder size and target strength also needs consideration (Bassett et al., 2020). All these data would help to improve mesopelagic biomass estimates in the Arctic Ocean.

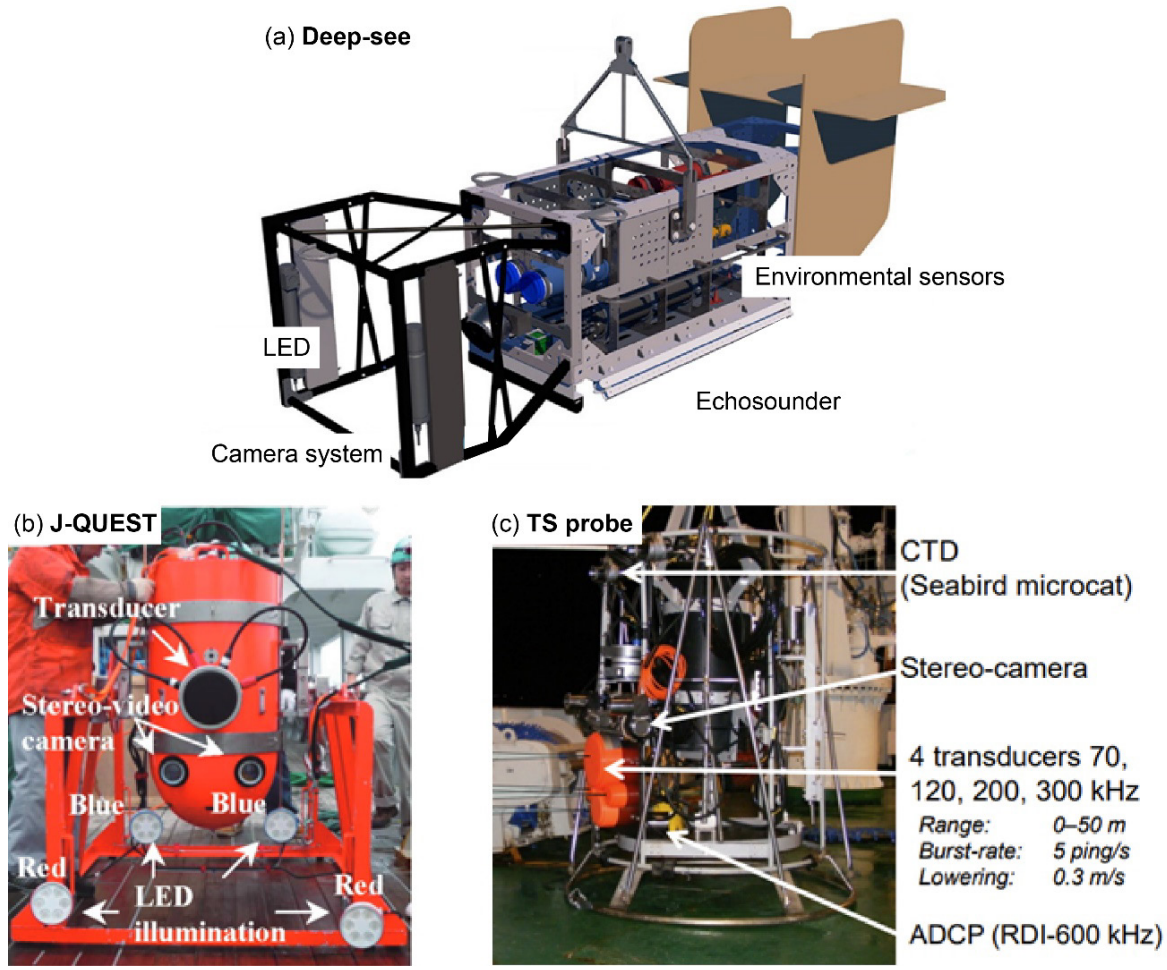

Figure 5-2. Platform developed to study the mesopelagic layer combining echosounder, optics, and environmental sensors, (a) the Deep-See, (b) the J-QUEST, and (c) the TS probe. Pictures and drawing modified from WHOI website, Sawada et al. (2011), and IMR website.

Other optical sensors like the Underwater Vision Profiler 6 (Picheral et al., 2022), environmental DNA (Govindarajan et al., 2021; McClenaghan et al., 2020), or bathyphotometers measuring bioluminescence – which can infer some level of taxonomic

composition (Cronin et al., 2016; Johnsen et al., 2014) – are increasingly paired with echosounder data for ground-truthing. However, nets and trawls are still important (e.g., diet studies) and cannot be entirely replaced by these less invasive technologies. Thus, collecting and combining data from different instruments is required to better estimate mesopelagic diversity.

5.5.2.2 Life history strategies and contribution to the biological carbon pump

Refining the annual cycle of mesopelagic fish and zooplankton in the Arctic Ocean and better understanding their life history strategies requires seasonal data. Researchers should increase sampling effort during the traditionally under studied times of the year like during the polar night (Berge et al., 2015b), in particular in the Canadian Arctic and CAO where little data are available. Seasonal time series from autonomous echosounders installed on moorings or ice-tethered echosounders can help define and quantify seasonal behaviours of the mesopelagic layer. Research cruises and overwintering expeditions are thus required to gather biological collection.

How mesopelagic fish and zooplankton survive during the polar night and midnight sun remains unclear. Studies focusing on the diet and trophic position of the marine food web (using stable isotopes, isoprenoids, and fatty acids) with a focus on mesopelagic fish as well as macrozooplankton would help in understanding survival strategies at times of vertical segregation with *Calanus* (Geoffroy et al., 2019; Woods et al., 2020) and identify energy pathways through the Arctic marine food web (Amiraux et al., 2023).

This thesis suggests that the contribution of mesopelagic fish and zooplankton to the biological carbon pump varies throughout the year. While active acoustics cannot directly quantify organic matter, time-series can quantify the periods during which DVM occur and document

their amplitude and the proportion of migrating versus non-migrating individuals. All of these data are relevant to parametrize the contribution of mesopelagic organisms to the biological carbon pump (Saba et al., 2021).

This thesis emphasizes the importance of light for structuring the dynamics of the mesopelagic zone. However, our understanding of vision in Arctic fauna is restricted to a few taxa (Cohen et al., 2021; Jönsson et al., 2014). Physiological studies establishing the spectral eye sensitivities are required to calculate how much light is available to mesopelagic organisms and identify levels of light-triggered behaviours (Flores et al., 2023; Hobbs et al., 2021). In addition, light levels and light attenuation in the water column can now be quantified with highly sensitive light sensors (e.g., chapter four). Collecting such light profiles is extremely relevant to understand the light environment in which mesopelagic fauna dwell. Bioluminescence is also an important source of light in the mesopelagic zone, which also needs to be quantified (Cronin et al., 2016; Johnsen et al., 2014). Scrutinizing bioluminescence could help understand the structure of the mesopelagic zone and its predator-prey dynamics.

Finally, because of the vast size and complexity of the mesopelagic zone, enhanced international cooperation through research projects and networks, e.g., Joint Exploration of the Twilight Zone Ocean Network (JETZON), is key in advancing knowledge of the mesopelagic zone in the Arctic Ocean and globally. Thus, given the magnitude of the challenge in front of us, it appears pertinent to repeat the message of Martin et al (2020): *"We cannot let climate warming and human exploitation fundamentally alter the twilight zone before we even begin to understand the potential consequences for the health of the planet"*.

6 Bibliography

Aksnes, D.L., Røstad, A., Kaartvedt, S., Martinez, U., Irigoien, X., 2017. Light penetration structures the deep acoustic scattering layers in the global ocean. Sci. Adv. 3. https://doi.org/10.1126/sciadv.1602468

AMAP, 2021. AMAP assessment 2020: POPs and chemicals of emerging Arctic concern: influence of climate change, AMAP Assessment. Arctic Monitoring and Assessment Programme (AMAP), Tromsø, Norway.

Amiraux, R., Mundy, C.J., Pierrejean, M., Niemi, A., Hedges, K.J., Brown, T.A., Ehn, J.K., Elliott, K.H., Ferguson, S.H., Fisk, A.T., Gilchrist, G., Harris, L.N., Iken, K., Jacobs, K.B., Johnson, K.F., Kuzyk, Z.A., Limoges, A., Loewen, T.N., Love, O.P., Matthews, C.J.D., Ogloff, W.R., Rosenberg, B., Søreide, J.E., Watt, C.A., Yurkowski, D.J., 2023. Tracing carbon flow and trophic structure of a coastal Arctic marine food web using highly branched isoprenoids and carbon, nitrogen and sulfur stable isotopes. Ecol. Indic. 147, 109938. https://doi.org/10.1016/j.ecolind.2023.109938

Andersen, L.N., Chu, D., Heimvoll, H., Korneliussen, R., Macaulay, G.J., Ona, E., 2021. Quantitative processing of broadband data as implemented in a scientific splitbeam echosounder. https://doi.org/10.48550/arXiv.2104.07248

Andersen, L.N., Ona, E., Macaulay, G., 2013. Measuring fish and zooplankton with a broadband split beam echo sounder, in: 2013 MTS/IEEE OCEANS - Bergen. Presented at the 2013 MTS/IEEE OCEANS - Bergen, pp. 1–4. https://doi.org/10.1109/OCEANS-Bergen.2013.6850133

Annasawmy, P., Ternon, J.-F., Lebourges-Dhaussy, A., Roudaut, G., Cotel, P., Herbette, S., Ménard, F., Marsac, F., 2020. Micronekton distribution as influenced by mesoscale eddies, Madagascar shelf and shallow seamounts in the south-western Indian Ocean: an acoustic approach. Deep Sea Res. Part II Top. Stud. Oceanogr. 176, 104812. https://doi.org/10.1016/j.dsr2.2020.104812

Archibald, K.M., Siegel, D.A., Doney, S.C., 2019. Modeling the impact of zooplankton diel vertical migration on the carbon export flux of the biological pump. Glob. Biogeochem. Cycles 33, 181–199. https://doi.org/10.1029/2018GB005983

Ardyna, M., Arrigo, K.R., 2020. Phytoplankton dynamics in a changing Arctic Ocean. Nat. Clim. Change 10, 892–903. https://doi.org/10.1038/s41558-020-0905-y

Ardyna, M., Babin, M., Gosselin, M., Devred, E., Bélanger, S., Matsuoka, A., Tremblay, J.-É., 2013. Parameterization of vertical chlorophyll *a* in the Arctic Ocean: impact of the subsurface chlorophyll maximum on regional, seasonal, and annual primary production estimates. Biogeosciences 10, 4383–4404. https://doi.org/10.5194/bg-10-4383-2013

Ardyna, M., Babin, M., Gosselin, M., Devred, E., Rainville, L., Tremblay, J.-É., 2014. Recent Arctic Ocean sea ice loss triggers novel fall phytoplankton blooms. Geophys. Res. Lett. 41, 6207–6212. https://doi.org/10.1002/2014GL061047

Ardyna, M., Gosselin, M., Michel, C., Poulin, M., Tremblay, J., 2011. Environmental forcing of phytoplankton community structure and function in the Canadian high Arctic: contrasting oligotrophic and eutrophic regions. Mar. Ecol. Prog. Ser. 442, 37–57. https://doi.org/10.3354/meps09378

Ardyna, M., Mundy, C.J., Mills, M.M., Oziel, L., Grondin, P.-L., Lacour, L., Verin, G., van Dijken, G., Ras, J., Alou-Font, E., Babin, M., Gosselin, M., Tremblay, J.-É., Raimbault, P., Assmy, P., Nicolaus, M., Claustre, H., Arrigo, K.R., 2020. Environmental drivers of under-ice phytoplankton bloom dynamics in the Arctic Ocean. Elem. Sci. Anthr. 8, 30. https://doi.org/10.1525/elementa.430

Ariza, A., Lengaigne, M., Menkes, C., Lebourges-Dhaussy, A., Receveur, A., Gorgues, T., Habasque, J., Gutiérrez, M., Maury, O., Bertrand, A., 2022. Global decline of pelagic fauna in a warmer ocean. Nat. Clim. Change 12, 928–934. https://doi.org/10.1038/s41558-022-01479-2

Arndt, C.E., Swadling, K.M., 2006. Crustacea in Arctic and Antarctic sea ice: distribution, diet and life history strategies, in: Advances in Marine Biology. Academic Press, pp. 197–315. https://doi.org/10.1016/S0065-2881(06)51004-1

Arostegui, M.C., Gaube, P., Woodworth-Jefcoats, P.A., Kobayashi, D.R., Braun, C.D., 2022. Anticyclonic eddies aggregate pelagic predators in a subtropical gyre. Nature 609, 535–540. https://doi.org/10.1038/s41586-022-05162-6

Årthun, M., Eldevik, T., Smedsrud, L.H., Skagseth, Ø., Ingvaldsen, R.B., 2012. Quantifying the influence of atlantic heat on Barents Sea ice variability and retreat. J. Clim. 25, 4736–4743. https://doi.org/10.1175/JCLI-D-11-00466.1

Aschan, M., Karamushko, O., Byrkjedal, I., Wienerroither, R., Borkin, I., Christiansen, J., 2009. Records of the gadoid fish *Arctogadus glacialis* (Peters, 1874) in the European Arctic. Polar Biol. 32, 963–970. https://doi.org/10.1007/s00300-009-0595-4

Ashjian, C.J., Campbell, R.G., Welch, H.E., Butler, M., Van Keuren, D., 2003. Annual cycle in abundance, distribution, and size in relation to hydrography of important copepod species in the western Arctic Ocean. Deep Sea Res. Part Oceanogr. Res. Pap. 50, 1235–1261. https://doi.org/10.1016/S0967-0637(03)00129-8

Athanase, M., Provost, C., Artana, C., Pérez-Hernández, M.D., Sennéchael, N., Bertosio, C., Garric, G., Lellouche, J.-M., Prandi, P., 2021. Changes in Atlantic water circulation patterns and volume transports north of Svalbard over the last 12 years (2008–2020). J. Geophys. Res. Oceans 126. https://doi.org/10.1029/2020JC016825

Auel, H., Werner, I., 2003. Feeding, respiration and life history of the hyperiid amphipod *Themisto libellula* in the Arctic marginal ice zone of the Greenland Sea. J. Exp. Mar. Biol. Ecol. 296, 183–197. https://doi.org/10.1016/S0022-0981(03)00321-6

Aune, M., Aniceto, A.S., Biuw, M., Daase, M., Falk-Petersen, S., Leu, E., Ottesen, C.A.M., Sagerup, K., Camus, L., 2018. Seasonal ecology in ice-covered Arctic seas - considerations for spill response decision making. Mar. Environ. Res. 141, 275–288. https://doi.org/10.1016/j.marenvres.2018.09.004

Aune, M., Raskhozheva, E., Andrade, H., Augustine, S., Bambulyak, A., Camus, L., Carroll, J., Dolgov, A.V., Hop, H., Moiseev, D., Renaud, P.E., Varpe, Ø., 2021. Distribution and ecology of polar cod (*Boreogadus saida*) in the eastern Barents Sea: a review of historical literature. Mar. Environ. Res. 166, 105262. https://doi.org/10.1016/j.marenvres.2021.105262

Bagøien, E., Kaartvedt, S., Aksnes, D.L., Eiane, K., 2001. Vertical distribution and mortality of overwintering *Calanus*. Limnol. Oceanogr. 46, 1494–1510. https://doi.org/10.4319/lo.2001.46.6.1494

Bandara, K., Varpe, Ø., Wijewardene, L., Tverberg, V., Eiane, K., 2021. Two hundred years of zooplankton vertical migration research. Biol. Rev. 96, 1547–1589. https://doi.org/10.1111/brv.12715

Barber, D.G., Asplin, M.G., Gratton, Y., Lukovich, J.V., Galley, R.J., Raddatz, R.L., Leitch, D., 2010. The international polar year (IPY) circumpolar flaw lead (CFL) system study: overview and the physical system. Atmosphere-Ocean 48, 225–243. https://doi.org/10.3137/OC317.2010

Barham, E.G., 1971. Deep-sea fishes: lethargy and vertical orientation, in: Proceedings of an International Symposium on Biological Sound Scattering in the Ocean. U.S. Government Printing Office, Washington, DC, pp. 100–118.

Barth, A., Stone, J., 2022. Comparison of an in situ imaging device and net-based method to study mesozooplankton communities in an oligotrophic system. Front. Mar. Sci. 9, 898057. https://doi.org/10.3389/fmars.2022.898057

Basedow, S.L., Sundfjord, A., von Appen, W.-J., Halvorsen, E., Kwasniewski, S., Reigstad, M., 2018. Seasonal variation in transport of zooplankton into the Arctic basin through the Atlantic gateway, Fram Strait. Front. Mar. Sci. 5, 194. https://doi.org/10.3389/fmars.2018.00194

Bassett, C., Lavery, A.C., Stanton, T.K., Cotter, E.D., 2020. Frequency- and depth-dependent target strength measurements of individual mesopelagic scatterers. J. Acoust. Soc. Am. 148, EL153–EL158. https://doi.org/10.1121/10.0001745

Bassett, D.K., Carton, A.G., Montgomery, J.C., 2007. Saltatory search in a lateral line predator. J. Fish Biol. 70, 1148–1160. https://doi.org/10.1111/j.1095-8649.2007.01380.x

Bélanger, S., Carrascal-Leal, C., Jaegler, T., Larouche, P., Galbraith, P., 2017. Assessment of radiometric data from a buoy in the St. Lawrence estuary. J. Atmospheric Ocean. Technol. 34, 877–896. https://doi.org/10.1175/JTECH-D-16-0176.1

Belcher, A., Cook, K., Bondyale-Juez, D., Stowasser, G., Fielding, S., Saunders, R.A., Mayor, D.J., Tarling, G.A., 2020. Respiration of mesopelagic fish: a comparison of respiratory electron transport system (ETS) measurements and allometrically calculated rates in the Southern Ocean and Benguela Current. ICES J. Mar. Sci. 77, 1672–1684. https://doi.org/10.1093/icesjms/fsaa031

Bender, M., Giebichenstein, J., Teisrud, R., Laurent, J., Frantzen, M., Meador, J., Sørensen, L., Hansen, B., Reinardy, H., Laurel, B., Nahrgang, J., 2021. Combined effects of crude oil exposure and warming on eggs and larvae of an Arctic forage fish. Sci. Rep. 11, 8410. https://doi.org/10.1038/s41598-021-87932-2

Benoit, D., Simard, Y., Fortier, L., 2014. Pre-winter distribution and habitat characteristics of polar cod (*Boreogadus saida*) in southeastern Beaufort Sea. Polar Biol. 37, 149–163. https://doi.org/10.1007/s00300-013-1419-0

Benoit, D., Simard, Y., Fortier, L., 2008. Hydroacoustic detection of large winter aggregations of Arctic cod (*Boreogadus saida*) at depth in ice-covered Franklin Bay (Beaufort Sea). J. Geophys. Res. Oceans 113. https://doi.org/10.1029/2007JC004276

Benoit, D., Simard, Y., Gagné, J., Geoffroy, M., Fortier, L., 2010. From polar night to midnight sun: photoperiod, seal predation, and the diel vertical migrations of polar cod (*Boreogadus saida*) under landfast ice in the Arctic Ocean. Polar Biol. 33, 1505–1520. https://doi.org/10.1007/s00300-010-0840-x

Benoit-Bird, K.J., Lawson, G.L., 2016. Ecological insights from pelagic habitats acquired using active acoustic techniques. Annu. Rev. Mar. Sci. 8, 463–490. https://doi.org/10.1146/annurev-marine-122414-034001

Benoit-Bird, K.J., Waluk, C.M., 2020. Exploring the promise of broadband fisheries echosounders for species discrimination with quantitative assessment of data processing effects. J. Acoust. Soc. Am. 147, 411–427. https://doi.org/10.1121/10.0000594

Berg, F., Shirajee, S., Folkvord, A., Godiksen, J.A., Skaret, G., Slotte, A., 2021. Early life growth is affecting timing of spawning in the semelparous Barents Sea capelin (*Mallotus villosus*). Prog. Oceanogr. 196, 102614. https://doi.org/10.1016/j.pocean.2021.102614

Berge, J., Båtnes, A.S., Johnsen, G., Blackwell, S.M., Moline, M.A., 2012a. Bioluminescence in the high Arctic during the polar night. Mar. Biol. 159, 231–237. https://doi.org/10.1007/s00227-011-1798-0

Berge, J., Cottier, F., Last, K.S., Varpe, Ø., Leu, E., Søreide, J., Eiane, K., Falk-Petersen, S., Willis, K., Nygård, H., Vogedes, D., Griffiths, C., Johnsen, G., Lorentzen, D., Brierley, A.S., 2009. Diel vertical migration of Arctic zooplankton during the polar night. Biol. Lett. 5, 69–72. https://doi.org/10.1098/rsbl.2008.0484

Berge, J., Daase, M., Renaud, P.E., Ambrose, W.G., Darnis, G., Last, K.S., Leu, E., Cohen, J.H., Johnsen, G., Moline, M.A., Cottier, F., Varpe, Ø., Shunatova, N., Bałazy, P., Morata, N., Massabuau, J.-C., Falk-Petersen, S., Kosobokova, K., Hoppe, C.J.M., Węsławski, J.M., Kukliński, P., Legeżyńska, J., Nikishina, D., Cusa, M., Kędra, M., Włodarska-Kowalczuk, M., Vogedes, D., Camus, L., Tran, D., Michaud, E., Gabrielsen, T.M., Granovitch, A., Gonchar, A., Krapp, R., Callesen, T.A., 2015a. Unexpected levels of biological activity during the polar night offer new perspectives on a warming Arctic. Curr. Biol. 25, 2555–2561. https://doi.org/10.1016/j.cub.2015.08.024

Berge, J., Geoffroy, M., Daase, M., Cottier, F., Priou, P., Cohen, J.H., Johnsen, G., McKee, D., Kostakis, I., Renaud, P.E., Vogedes, D., Anderson, P., Last, K.S., Gauthier, S., 2020. Artificial light during the polar night disrupts Arctic fish and zooplankton behaviour down to 200 m depth. Commun. Biol. 3, 1–8. https://doi.org/10.1038/s42003-020-0807-6

Berge, J., Geoffroy, M., Johnsen, G., Cottier, F., Bluhm, B., Vogedes, D., 2016. Ice-tethered observational platforms in the Arctic Ocean pack ice. IFAC-Pap., 10th IFAC Conference on

Control Applications in Marine Systems 49, 494–499. https://doi.org/10.1016/j.ifacol.2016.10.484
Berge, J., Nahrgang, J., 2013. The Atlantic spiny lumpsucker *Eumicrotremus spinosus*: life history traits and the seemingly unlikely interaction with the pelagic amphipod *Themisto libellula*. Pol. Polar Res. 34, 279–287. https://doi.org/10.2478/popore-2013-0013
Berge, J., Renaud, P.E., Darnis, G., Cottier, F., Last, K., Gabrielsen, T.M., Johnsen, G., Seuthe, L., Weslawski, J.M., Leu, E., Moline, M., Nahrgang, J., Søreide, J.E., Varpe, Ø., Lønne, O.J., Daase, M., Falk-Petersen, S., 2015b. In the dark: a review of ecosystem processes during the Arctic polar night. Prog. Oceanogr., Overarching perspectives of contemporary and future ecosystems in the Arctic Ocean 139, 258–271. https://doi.org/10.1016/j.pocean.2015.08.005
Berge, J., Varpe, Ø., Moline, M.A., Wold, A., Renaud, P.E., Daase, M., Falk-Petersen, S., 2012b. Retention of ice-associated amphipods: possible consequences for an ice-free Arctic Ocean. Biol. Lett. 8, 1012–1015. https://doi.org/10.1098/rsbl.2012.0517
Beszczynska-Möller, A., Fahrbach, E., Schauer, U., Hansen, E., 2012. Variability in Atlantic water temperature and transport at the entrance to the Arctic Ocean, 1997–2010. ICES J. Mar. Sci. 69, 852–863. https://doi.org/10.1093/icesjms/fss056
Bianchi, D., Galbraith, E.D., Carozza, D.A., Mislan, K. a. S., Stock, C.A., 2013. Intensification of open-ocean oxygen depletion by vertically migrating animals. Nat. Geosci. 6, 545–548. https://doi.org/10.1038/ngeo1837
Bianchi, D., Mislan, K. a. S., 2016. Global patterns of diel vertical migration times and velocities from acoustic data. Limnol. Oceanogr. 61, 353–364. https://doi.org/10.1002/lno.10219
Bjordal, Å., Thorvaldsen, K.G., 2020. Trial fishing for mesopelagic species 2019 (No. 2020–5), Rapport far havforskningen. Institute of Marine Research, Bergen, Norway.
Bjørke, H., Hansen, K., 1996. Recordings of mature *Gonatus fabricii* (Lichtenstein) off the Norwegian coast (Working paper No. CM1996/K:17). International Council for the exploration of the Sea.
Blachowiak-Samolyk, K., Kwasniewski, S., Richardson, K., Dmoch, K., Hansen, E., Hop, H., Falk-Petersen, S., Mouritsen, L., 2006. Arctic zooplankton do not perform diel vertical migration (DVM) during periods of midnight sun. Mar. Ecol. Prog. Ser. 308, 101–116. https://doi.org/10.3354/meps308101
Bliss, L.M., Dawe, N., Carruthers, E.H., Murphy, H.M., Davoren, G.K., 2023. Using fishers' knowledge to determine the spatial extent of deep-water spawning of capelin (Mallotus villosus) in Newfoundland, Canada. Front. Mar. Sci. 9.
Bluhm, B.A., Gradinger, R., 2008. Regional variability in food availability for Arctic marine mammals. Ecol. Appl. 18, S77–S96. https://doi.org/10.1890/06-0562.1
Bluhm, B.A., Kosobokova, K.N., Carmack, E.C., 2015. A tale of two basins: an integrated physical and biological perspective of the deep Arctic Ocean. Prog. Oceanogr. 139, 89–121. https://doi.org/10.1016/j.pocean.2015.07.011
Bogstad, B., Gjøsæter, H., 2001. Predation by cod (*Gadus morhua*) on capelin (*Mallotus villosus*) in the Barents Sea: implications for capelin stock assessment. Fish. Res. 53, 197–209. https://doi.org/10.1016/S0165-7836(00)00288-5
Boswell, K.M., D'Elia, M., Johnston, M.W., Mohan, J.A., Warren, J.D., Wells, R.J.D., Sutton, T.T., 2020. Oceanographic Structure and Light Levels Drive Patterns of Sound Scattering Layers in a Low-Latitude Oceanic System. Front. Mar. Sci. 7. https://doi.org/10.3389/fmars.2020.00051
Bouchard, C., Fortier, L., 2020. The importance of *Calanus glacialis* for the feeding success of young polar cod: a circumpolar synthesis. Polar Biol. 43, 1095–1107. https://doi.org/10.1007/s00300-020-02643-0
Bouchard, C., Fortier, L., 2011. Circum-arctic comparison of the hatching season of polar cod *Boreogadus saida*: a test of the freshwater winter refuge hypothesis. Prog. Oceanogr., Arctic Marine Ecosystems in an Era of Rapid Climate Change 90, 105–116. https://doi.org/10.1016/j.pocean.2011.02.008
Bouchard, C., Fortier, L., 2008. Effects of polynyas on the hatching season, early growth and survival of polar cod *Boreogadus saida* in the Laptev Sea. Mar. Ecol. Prog. Ser. 355, 247–256. https://doi.org/10.3354/meps07335

Bouchard, C., Geoffroy, M., LeBlanc, M., Fortier, L., 2018. Larval and adult fish assemblages along the Northwest Passage: the shallow Kitikmeot and the ice-covered Parry Channel as potential barriers to dispersal. Arct. Sci. 4, 781–793. https://doi.org/10.1139/as-2018-0003

Bouchard, C., Mollard, S., Suzuki, K., Robert, D., Fortier, L., 2016. Contrasting the early life histories of sympatric Arctic gadids *Boreogadus saida* and *Arctogadus glacialis* in the Canadian Beaufort Sea. Polar Biol. 39, 1005–1022. https://doi.org/10.1007/s00300-014-1617-4

Bouchard, C., Robert, D., Nelson, R., Fortier, L., 2013. The nucleus of the lapillar otolith discriminates the early life stages of *Boreogadus saida* and *Arctogadus glacialis*. Polar Biol. 36, 1537–1542. https://doi.org/10.1007/s00300-013-1371-z

Bouchard, C., Thorrold, S., Fortier, L., 2015. Spatial segregation, dispersion and migration in early stages of polar cod *Boreogadus saida* revealed by otolith chemistry. Mar. Biol. 162, 855–868. https://doi.org/10.1007/s00227-015-2629-5

Bradstreet, M.S., 1986. Aspects of the biology of Arctic cod (*Boreogadus saida*) and its importance in Arctic marine food chains, Canadian Technical Report of Fisheries and Aquatic Sciences. Department of Fisheries and Oceans, Central and Arctic Region.

Broms, C., Strand, E., Utne, K.R., Hjøllo, S., Sundby, S., Melle, W., 2016. Vitenskapelig bakgrunnsmateriale for forvaltningsplan for raudåte. 37.

Brown-Vuillemin, S., Tremblay, R., Chabot, D., Sirois, P., Robert, D., 2023. Feeding ecology of redfish (*Sebastes* sp.) inferred from the integrated use of fatty acid profiles as complementary dietary tracers to stomach content analysis. J. Fish Biol. 102, 1049–1066. https://doi.org/10.1111/jfb.15348

Buchholz, F., Werner, T., Buchholz, C., 2012. First observation of krill spawning in the high Arctic Kongsfjorden, west Spitsbergen. Polar Biol. 35, 1273–1279. https://doi.org/10.1007/s00300-012-1186-3

Cade, D.E., Benoit-Bird, K.J., 2015. Depths, migration rates and environmental associations of acoustic scattering layers in the Gulf of California. Deep Sea Res. Part Oceanogr. Res. Pap. 102, 78–89. https://doi.org/10.1016/j.dsr.2015.05.001

Cadrin, S.X., Bernreuther, M., Daníelsdóttir, A.K., Hjörleifsson, E., Johansen, T., Kerr, L., Kristinsson, K., Mariani, S., Nedreaas, K., Pampoulie, C., Planque, B., Reinert, J., Saborido-Rey, F., Sigurðsson, T., Stransky, C., 2010. Population structure of beaked redfish, *Sebastes mentella*: evidence of divergence associated with different habitats. ICES J. Mar. Sci. 67, 1617–1630. https://doi.org/10.1093/icesjms/fsq046

Carmack, E., Wassmann, P., 2006. Food webs and physical–biological coupling on pan-Arctic shelves: unifying concepts and comprehensive perspectives. Prog. Oceanogr., Structure and function of contemporary food webs on Arctic shelves: a pan-Arctic comparison 71, 446–477. https://doi.org/10.1016/j.pocean.2006.10.004

Carmack, E., Winsor, P., Williams, W., 2015. The contiguous panarctic riverine coastal domain: a unifying concept. Prog. Oceanogr., Overarching perspectives of contemporary and future ecosystems in the Arctic Ocean 139, 13–23. https://doi.org/10.1016/j.pocean.2015.07.014

Carmack, E.C., 2007. The alpha/beta ocean distinction: a perspective on freshwater fluxes, convection, nutrients and productivity in high-latitude seas. Deep Sea Res. Part II Top. Stud. Oceanogr. 54, 2578–2598. https://doi.org/10.1016/j.dsr2.2007.08.018

Carmack, E.C., Yamamoto-Kawai, M., Haine, T.W.N., Bacon, S., Bluhm, B.A., Lique, C., Melling, H., Polyakov, I.V., Straneo, F., Timmermans, M.-L., Williams, W.J., 2016. Freshwater and its role in the Arctic marine system: sources, disposition, storage, export, and physical and biogeochemical consequences in the Arctic and global oceans. J. Geophys. Res. Biogeosciences 121, 675–717. https://doi.org/10.1002/2015JG003140

Carscadden, J., Gjøsæter, H., Vilhjálmsson, H., 2013. Recruitment in the Barents Sea, Icelandic, and Eastern Newfoundland/Labrador capelin (*Mallotus villosus*) stocks. Prog. Oceanogr. 114. https://doi.org/10.1016/j.pocean.2013.05.006

Castellani, G., Schaafsma, F.L., Arndt, S., Lange, B.A., Peeken, I., Ehrlich, J., David, C., Ricker, R., Krumpen, T., Hendricks, S., Schwegmann, S., Massicotte, P., Flores, H., 2020. Large-scale

variability of physical and biological sea-ice properties in polar oceans. Front. Mar. Sci. 7, 536. https://doi.org/10.3389/fmars.2020.00536
Castellani, G., Veyssière, G., Karcher, M., Stroeve, J., Banas, S.N., Bouman, A.H., Brierley, S.A., Connan, S., Cottier, F., Große, F., Hobbs, L., Katlein, C., Light, B., McKee, D., Orkney, A., Proud, R., Schourup-Kristensen, V., 2022. Shine a light: under-ice light and its ecological implications in a changing Arctic Ocean. Ambio 51, 307–317. https://doi.org/10.1007/s13280-021-01662-3
Catul, V., Gauns, M., Karuppasamy, P.K., 2011. A review on mesopelagic fishes belonging to family Myctophidae. Rev. Fish Biol. Fish. 21, 339–354. https://doi.org/10.1007/s11160-010-9176-4
Ceccarelli, D.M., Davey, K., Jones, G.P., Harris, P.T., Matoto, S.V., Raubani, J., Fernandes, L., 2021. How to meet new global targets in the offshore realms: biophysical guidelines for offshore networks of no-take marine protected areas. Front. Mar. Sci. 8, 634574. https://doi.org/10.3389/fmars.2021.634574
Chambers, C.A., Dick, T.A., 2007. Using environmental variables to predict the structure of deep-sea Arctic fish communities: implications for food web construction. Arct. Antarct. Alp. Res. 39, 2–8. https://doi.org/10.1657/1523-0430(2007)39[2:UEVTPT]2.0.CO;2
Chawarski, J., Klevjer, T.A., Coté, D., Geoffroy, M., 2022. Evidence of temperature control on mesopelagic fish and zooplankton communities at high latitudes. Front. Mar. Sci. 9, 917985. https://doi.org/10.3389/fmars.2022.917985
Chernova, N.V., Neyelov, A.V., 1995. Fish caught in the Laptev Sea during the cruise of R/V "*Polarstern*" in 1993. Ber Polarforsch 176, 222–227.
Choi, C., Kampffmeyer, M., Handegard, N.O., Salberg, A.-B., Brautaset, O., Eikvil, L., Jenssen, R., 2021. Semi-supervised target classification in multi-frequency echosounder data. ICES J. Mar. Sci. 78, 2615–2627. https://doi.org/10.1093/icesjms/fsab140
Choquet, M., Hatlebakk, M., Dhanasiri, A.K.S., Kosobokova, K., Smolina, I., Søreide, J.E., Svensen, C., Melle, W., Kwaśniewski, S., Eiane, K., Daase, M., Tverberg, V., Skreslet, S., Bucklin, A., Hoarau, G., 2017. Genetics redraws pelagic biogeography of *Calanus*. Biol. Lett. 13. https://doi.org/10.1098/rsbl.2017.0588
Choy, E.S., Giraldo, C., Rosenberg, B., Roth, J.D., Ehrman, A.D., Majewski, A., Swanson, H., Power, M., Reist, J.D., Loseto, L.L., 2020. Variation in the diet of beluga whales in response to changes in prey availability: insights on changes in the Beaufort Sea ecosystem. Mar. Ecol. Prog. Ser. 647, 195–210. https://doi.org/10.3354/meps13413
Christiansen, J., Hop, H., Nilssen, E., Joensen, J., 2012. Trophic ecology of sympatric Arctic gadoids, *Arctogadus glacialis* (Peters, 1872) and *Boreogadus saida* (Lepechin, 1774), in NE Greenland. Polar Biol. 35. https://doi.org/10.1007/s00300-012-1170-y
Christiansen, J.S., Præbel, K., Siikavuopio, S.I., Carscadden, J.E., 2008. Facultative semelparity in capelin *Mallotus villosus* (Osmeridae)-an experimental test of a life history phenomenon in a sub-Arctic fish. J. Exp. Mar. Biol. Ecol. 360, 47–55. https://doi.org/10.1016/j.jembe.2008.04.003
Chu, D., 2011. Technology evolution and advances in fisheries acoustics. J. Mar. Sci. Technol. 19, 245–252. https://doi.org/10.51400/2709-6998.2188
Chu, D., Stanton, T.K., 1998. Application of pulse compression techniques to broadband acoustic scattering by live individual zooplankton. J. Acoust. Soc. Am. 104, 39–55. https://doi.org/10.1121/1.424056
Clark, C.W., Levy, D.A., 1988. Diel vertical migrations by juvenile sockeye salmon and the antipredation window. Am. Nat. 131, 271–290. https://doi.org/10.1086/284789
Cohen, J., Forward, R., 2009. Zooplankton diel vertical migration - a review of proximate control, in: Oceanography and Marine Biology. pp. 77–109. https://doi.org/10.1201/9781420094220.ch2
Cohen, J.H., Berge, J., Moline, M.A., Johnsen, G., Zolich, A.P., 2020. Light in the polar night, in: Berge, J., Johnsen, G., Cohen, J.H. (Eds.), Polar Night Marine Ecology: Life and Light in the Dead of Night, Advances in Polar Ecology. Springer International Publishing, Cham, pp. 37–66. https://doi.org/10.1007/978-3-030-33208-2_3

Cohen, J.H., Last, K.S., Charpentier, C.L., Cottier, F., Daase, M., Hobbs, L., Johnsen, G., Berge, J., 2021. Photophysiological cycles in Arctic krill are entrained by weak midday twilight during the polar night. PLOS Biol. 19, e3001413. https://doi.org/10.1371/journal.pbio.3001413

Costanza, R., d'Arge, R., de Groot, R., Farber, S., Grasso, M., Hannon, B., Limburg, K., Naeem, S., O'Neill, R.V., Paruelo, J., Raskin, R.G., Sutton, P., van den Belt, M., 1997. The value of the world's ecosystem services and natural capital. Nature 387, 253–260. https://doi.org/10.1038/387253a0

Cottier, F.R., Tarling, G.A., Wold, A., Falk-Petersen, S., 2006. Unsynchronised and synchronised vertical migration of zooplankton in a high Arctic fjord. Limnol. Oceanogr. 51, 2586–2599. https://doi.org/10.4319/lo.2006.51.6.2586

Crawford, R.E., Vagle, S., Carmack, E.C., 2012. Water mass and bathymetric characteristics of polar cod habitat along the continental shelf and slope of the Beaufort and Chukchi seas. Polar Biol. 35, 179–190. https://doi.org/10.1007/s00300-011-1051-9

Crews, L., Sundfjord, A., Hattermann, T., 2019. How the Yermak Pass branch regulates Atlantic water inflow to the Arctic Ocean. J. Geophys. Res. Oceans 124, 267–280. https://doi.org/10.1029/2018JC014476

Cronin, H.A., Cohen, J.H., Berge, J., Johnsen, G., Moline, M.A., 2016. Bioluminescence as an ecological factor during high Arctic polar night. Sci. Rep. 6, 36374. https://doi.org/10.1038/srep36374

Cuny, J., Rhines, P.B., Ron Kwok, 2005. Davis Strait volume, freshwater and heat fluxes. Deep Sea Res. Part Oceanogr. Res. Pap. 52, 519–542. https://doi.org/10.1016/j.dsr.2004.10.006

Curry, B., Lee, C.M., Petrie, B., Moritz, R.E., Kwok, R., 2014. Multiyear Volume, Liquid Freshwater, and Sea Ice Transports through Davis Strait, 2004–10*. J. Phys. Oceanogr. 44, 1244–1266. https://doi.org/10.1175/JPO-D-13-0177.1

Cusa, M., Berge, J., Varpe, Ø., 2019. Seasonal shifts in feeding patterns: individual and population realized specialization in a high Arctic fish. Ecol. Evol. 9, 11112–11121. https://doi.org/10.1002/ece3.5615

Cushing, D.H., 1990. Plankton production and year-class strength in fish populations: an update of the match/mismatch hypothesis, in: Blaxter, J.H.S., Southward, A.J. (Eds.), Advances in Marine Biology. Academic Press, pp. 249–293. https://doi.org/10.1016/S0065-2881(08)60202-3

Daase, M., Berge, J., Søreide, J., Falk-Petersen, S., 2021. Ecology of Arctic pelagic communities, in: Arctic Ecology. 219-259, pp. 219–259.

Daase, M., Eiane, K., 2007. Mesozooplankton distribution in northern Svalbard waters in relation to hydrography. Polar Biol. 30, 969–981. https://doi.org/10.1007/s00300-007-0255-5

Daase, M., Falk-Petersen, S., Varpe, Ø., Darnis, G., Søreide, J.E., Wold, A., Leu, E., Berge, J., Philippe, B., Fortier, L., 2013. Timing of reproductive events in the marine copepod *Calanus glacialis*: a pan-Arctic perspective. Can. J. Fish. Aquat. Sci. 70, 871–884. https://doi.org/10.1139/cjfas-2012-0401

Daase, M., Hop, H., Falk-Petersen, S., 2016. Small-scale diel vertical migration of zooplankton in the high Arctic. Polar Biol. 39, 1213–1223. https://doi.org/10.1007/s00300-015-1840-7

Dale, T., Bagøien, E., Melle, W., Kaartvedt, S., 1999. Can predator avoidance explain varying overwintering depth of *Calanus* in different oceanic water masses? Mar. Ecol. Prog. Ser. 179, 113–121. https://doi.org/10.3354/meps179113

Dalpadado, P., 2001. Distribution of *Themisto* (Amphipoda) spp. in the Barents Sea and predator-prey interactions. ICES J. Mar. Sci. 58, 876–895. https://doi.org/10.1006/jmsc.2001.1078

Dalpadado, P., Hop, H., Rønning, J., Pavlov, V., Sperfeld, E., Buchholz, F., Rey, A., Wold, A., 2016. Distribution and abundance of euphausiids and pelagic amphipods in Kongsfjorden, Isfjorden and Rijpfjorden (Svalbard) and changes in their relative importance as key prey in a warming marine ecosystem. Polar Biol. 39, 1765–1784. https://doi.org/10.1007/s00300-015-1874-x

Dalpadado, P., Ikeda, T., 1989. Some observations on moulting, growth and maturation of krill (*Thysanoessa inermis*) from the Barents Sea. J. Plankton Res. 11, 133–139. https://doi.org/10.1093/plankt/11.1.133

Dalpadado, P., Mowbray, F., 2013. Comparative analysis of feeding ecology of capelin from two shelf ecosystems, off Newfoundland and in the Barents Sea. Prog. Oceanogr. 114, 97–105. https://doi.org/10.1016/j.pocean.2013.05.007

Dalpadado, P., Yamaguchi, A., Ellertsen, B., Johannessen, S., 2008. Trophic interactions of macro-zooplankton (krill and amphipods) in the marginal ice zone of the Barents Sea. Deep Sea Res. Part II Top. Stud. Oceanogr. 55, 2266–2274. https://doi.org/10.1016/j.dsr2.2008.05.016

Darnis, G., Fortier, L., 2014. Temperature, food and the seasonal vertical migration of key arctic copepods in the thermally stratified Amundsen Gulf (Beaufort Sea, Arctic Ocean). J. Plankton Res. 36, 1092–1108. https://doi.org/10.1093/plankt/fbu035

Darnis, G., Geoffroy, M., Dezutter, T., Aubry, C., Massicotte, P., Brown, T., Babin, M., Cote, D., Fortier, L., 2022. Zooplankton assemblages along the North American Arctic: ecological connectivity shaped by ocean circulation and bathymetry from the Chukchi Sea to Labrador Sea. Elem. Sci. Anthr. 10, 00053. https://doi.org/10.1525/elementa.2022.00053

Darnis, G., Hobbs, L., Geoffroy, M., Grenvald, J.C., Renaud, P.E., Berge, J., Cottier, F., Kristiansen, S., Daase, M., E. Søreide, J., Wold, A., Morata, N., Gabrielsen, T., 2017. From polar night to midnight sun: diel vertical migration, metabolism and biogeochemical role of zooplankton in a high Arctic fjord (Kongsfjorden, Svalbard). Limnol. Oceanogr. 62, 1586–1605. https://doi.org/10.1002/lno.10519

Darnis, G., Robert, D., Pomerleau, C., Link, H., Archambault, P., Nelson, R.J., Geoffroy, M., Tremblay, J.-É., Lovejoy, C., Ferguson, S.H., Hunt, B.P.V., Fortier, L., 2012. Current state and trends in Canadian Arctic marine ecosystems: II. Heterotrophic food web, pelagic-benthic coupling, and biodiversity. Clim. Change 115, 179–205. https://doi.org/10.1007/s10584-012-0483-8

David, C., Lange, B., Krumpen, T., Schaafsma, F., van Franeker, J.A., Flores, H., 2016. Under-ice distribution of polar cod *Boreogadus saida* in the Central Arctic Ocean and their association with sea-ice habitat properties. Polar Biol. 39, 981–994. https://doi.org/10.1007/s00300-015-1774-0

Davies, T.W., Duffy, J.P., Bennie, J., Gaston, K.J., 2014. The nature, extent, and ecological implications of marine light pollution. Front. Ecol. Environ. 12, 347–355. https://doi.org/10.1890/130281

Davison, P.C., Checkley, D.M., Koslow, J.A., Barlow, J., 2013. Carbon export mediated by mesopelagic fishes in the northeast Pacific Ocean. Prog. Oceanogr. 116, 14–30. https://doi.org/10.1016/j.pocean.2013.05.013

Davoren, G., Montevecchi, W., 2003. Signals from seabirds indicate changing biology of capelin stocks. Mar. Ecol. Prog. Ser. 258, 253–261. https://doi.org/10.3354/meps258253

De Robertis, A., Higginbottom, I., 2007. A post-processing technique to estimate the signal-to-noise ratio and remove echosounder background noise. ICES J. Mar. Sci. 64, 1282–1291. https://doi.org/10.1093/icesjms/fsm112

De Robertis, A., Taylor, K., Wilson, C.D., Farley, E.V., 2017. Abundance and distribution of Arctic cod (*Boreogadus saida*) and other pelagic fishes over the U.S. Continental Shelf of the Northern Bering and Chukchi Seas. Deep Sea Res. Part II Top. Stud. Oceanogr. 135, 51–65. https://doi.org/10.1016/j.dsr2.2016.03.002

Demer, D., Berger, L., Bernasconi, M., Bethke, E., Boswell, K., Chu, D., Domokos, R., Dunford, A., Fässler, S., Gauthier, S., Hufnagle, L.T., Jech, M.J., Bouffant, N., Lebourges-Dhaussy, A., Lurton, X., Macaulay, G.J., Perrot, Y., Ryan, T., Parker-Stetter, S.L., Stienessen, S., Weber, T.C., Williamson, N., 2015. Calibration of acoustic instruments. https://doi.org/10.17895/ICES.PUB.5494

Deming, J.W., Fortier, L., Fukuchi, M., 2002. The International north water polynya study (NOW). Deep Sea Res. Part II Top. Stud. Oceanogr. 49. https://doi.org/10.1016/S0967-0645(02)00168-6

Devine, B., Fennell, S., Themelis, D., Fisher, J.A.D., 2021. Influence of anticyclonic, warm-core eddies on mesopelagic fish assemblages in the Northwest Atlantic Ocean. Deep Sea Res. Part Oceanogr. Res. Pap. 173, 103555. https://doi.org/10.1016/j.dsr.2021.103555

Dewey, M.R., Moen, T.E., 1983. Evaluation of a frame trawl and Tucker trawl for sampling young-of-the-year fish. J. Ark. Acad. Sci. 37.

DFO, 2019. Greenland halibut - Northwest Atlantic Fisheries Organization Subarea 0, Integrated Fishery Management Plan. Department of Fisheries and Oceans Canada, Winnipeg, Canada.

Dias Bernardes, I., Ona, E., Gjøsæter, H., 2020. Study of the Arctic mesopelagic layer with vessel and profiling multifrequency acoustics. Prog. Oceanogr. 182, 102260. https://doi.org/10.1016/j.pocean.2019.102260

Dolgov, A., Drevetnyak, K., 2011. Feeding of three species from the genus *Sebastes* in the Barents Sea. Presented at the Joint ICES/PICES Theme Session on Atlantic redfish and Pacific rockfish: Comparing biology, ecology, assessment and management.

Drazen, J.C., Smith, C.R., Gjerde, K.M., Haddock, S.H.D., Carter, G.S., Choy, C.A., Clark, M.R., Dutrieux, P., Goetze, E., Hauton, C., Hatta, M., Koslow, J.A., Leitner, A.B., Pacini, A., Perelman, J.N., Peacock, T., Sutton, T.T., Watling, L., Yamamoto, H., 2020. Midwater ecosystems must be considered when evaluating environmental risks of deep-sea mining. Proc. Natl. Acad. Sci. 117, 17455–17460. https://doi.org/10.1073/pnas.2011914117

Drevetnyak, K., Nedreaas, K.H., 2009. Historical movement pattern of juvenile beaked redfish (*Sebastes mentella* Travin) in the Barents Sea as inferred from long-term research survey series. Mar. Biol. Res. 5, 86–100. https://doi.org/10.1080/17451000802534865

Drinkwater, K.F., 2005. The response of Atlantic cod (*Gadus morhua*) to future climate change. ICES J. Mar. Sci. 62, 1327–1337. https://doi.org/10.1016/j.icesjms.2005.05.015

Dumont, D., Gratton, Y., Arbetter, T.E., 2009. Modeling the dynamics of the north water polynya ice bridge. J. Phys. Oceanogr. 39, 1448–1461. https://doi.org/10.1175/2008JPO3965.1

Dunn, M., Pedersen, G., Basedow, S.L., Daase, M., Falk-Petersen, S., Bachelot, L., Camus, L., Geoffroy, M., 2022. Inverse method applied to autonomous broadband hydroacoustic survey detects higher densities of zooplankton in near-surface aggregations than vessel-based net survey. Can. J. Fish. Aquat. Sci. 00, 1–17. https://doi.org/10.1139/cjfas-2022-0105

Dupont, N., Klevjer, T.A., Kaartvedt, S., Aksnesa, D.L., 2009. Diel vertical migration of the deep-water jellyfish *Periphylla periphylla* simulated as individual responses to absolute light intensity. Limnol. Oceanogr. 54, 1765–1775. https://doi.org/10.4319/lo.2009.54.5.1765

Durant, J., Hjermann, D., Ottersen, G., Stenseth, N., 2007. Climate and the match or mismatch between predator requirements and resource availability. Clim. Res. 33, 271–283. https://doi.org/10.3354/cr033271

Duvall, G.E., Christensen, R.J., 1946. Stratification of sound scatterers in the ocean. J. Acoust. Soc. Am. 18, 254. https://doi.org/10.1121/1.1902470

Dypvik, E., Klevjer, T.A., Kaartvedt, S., 2012a. Inverse vertical migration and feeding in glacier lanternfish (*Benthosema glaciale*). Mar. Biol. 159, 443–453. https://doi.org/10.1007/s00227-011-1822-4

Dypvik, E., Røstad, A., Kaartvedt, S., 2012b. Seasonal variations in vertical migration of glacier lanternfish, *Benthosema glaciale*. Mar. Biol. 159, 1673–1683. https://doi.org/10.1007/s00227-012-1953-2

Eicken, H., Lovecraft, A.L., Druckenmiller, M.L., 2009. Sea-ice system services: a framework to help identify and meet information needs relevant for Arctic observing networks. Arctic 62, 119–136.

Eriksen, E., Huserbråten, M., Gjøsæter, H., Vikebø, F., Albretsen, J., 2020. Polar cod egg and larval drift patterns in the Svalbard archipelago. Polar Biol. 43, 1029–1042. https://doi.org/10.1007/s00300-019-02549-6

Eriksen, E., Ingvaldsen, R.B., Nedreaas, K., Prozorkevich, D., 2015. The effect of recent warming on polar cod and beaked redfish juveniles in the Barents Sea. Reg. Stud. Mar. Sci. 2, 105–112. https://doi.org/10.1016/j.rsma.2015.09.001

Eriksen, E., Skjoldal, H.R., Gjøsæter, H., Primicerio, R., 2017. Spatial and temporal changes in the Barents Sea pelagic compartment during the recent warming. Prog. Oceanogr. 151, 206–226. https://doi.org/10.1016/j.pocean.2016.12.009

Escobar-Flores, P.C., O'Driscoll, R.L., Montgomery, J.C., 2018. Spatial and temporal distribution patterns of acoustic backscatter in the New Zealand sector of the Southern Ocean. Mar. Ecol. Prog. Ser. 592, 19–35. https://doi.org/10.3354/meps12489

Espinasse, B., Daase, M., Halvorsen, E., Reigstad, M., Berge, J., Basedow, S.L., 2022. Surface aggregations of *Calanus finmarchicus* during the polar night. ICES J. Mar. Sci. 79, 803–814. https://doi.org/10.1093/icesjms/fsac030

Falardeau, M., Bouchard, C., Robert, D., Fortier, L., 2017. First records of Pacific sand lance (*Ammodytes hexapterus*) in the Canadian Arctic Archipelago. Polar Biol. 40, 2291–2296. https://doi.org/10.1007/s00300-017-2141-0

Falk-Petersen, I.-B., Falk-Petersen, S., Sargent, J.R., 1986. Nature, origin and possible roles of lipid deposits in *Maurolicus muelleri* (Gmelin) and *Benthosema glaciale* (Reinhart) from Ullsfjorden, northern Norway. Polar Biol. 5, 235–240. https://doi.org/10.1007/BF00446091

Falk-Petersen, S., Haug, T., Nilssen, K.T., Wold, A., Dahl, T.M., 2004. Lipids and trophic linkages in harp seal (*Phoca groenlandica*) from the eastern Barents Sea. Polar Res. 23, 43–50. https://doi.org/10.3402/polar.v23i1.6265

Falk-Petersen, S., Hopkins, C., Sargent, J.R., 1990. Trophic relationships in the pelagic, Arctic food web. Trophic Relatsh. Mar. Environ. 315–333.

Falk-Petersen, S., Mayzaud, P., Kattner, G., Sargent, J.R., 2009. Lipids and life strategy of Arctic *Calanus*. Mar. Biol. Res. 5, 18–39. https://doi.org/10.1080/17451000802512267

FAO, 2021. Agreement to prevent unregulated high seas fisheries in the Central Arctic Ocean (No. LEX-FAOC199323).

Fennell, S., Rose, G., 2015. Oceanographic influences on deep scattering layers across the North Atlantic. Deep Sea Res. Part Oceanogr. Res. Pap. 105, 132–141. https://doi.org/10.1016/j.dsr.2015.09.002

Fjeld, K., Tiller, R., Grimaldo, E., Grimsmo, L., Standal, I.-B., 2023. Mesopelagics–new gold rush or castle in the sky? Mar. Policy 147, 105359. https://doi.org/10.1016/j.marpol.2022.105359

Flores, H., Veyssière, G., Castellani, G., Wilkinson, J., Hoppmann, M., Karcher, M., Valcic, L., Cornils, A., Geoffroy, M., Nicolaus, M., Niehoff, B., Priou, P., Schmidt, K., Stroeve, J., 2023. Sea-ice decline could keep zooplankton deeper for longer. Nat. Clim. Change 1–9. https://doi.org/10.1038/s41558-023-01779-1

Folke, C., Carpenter, S., Walker, B., Scheffer, M., Elmqvist, T., Gunderson, L., Holling, C.S., 2004. Regime shifts, resilience, and biodiversity in ecosystem management. Annu. Rev. Ecol. Evol. Syst. 35, 557–581. https://doi.org/10.1146/annurev.ecolsys.35.021103.105711

Foote, K.G., Stanton, T.K., 2000. 6 - Acoustical methods, in: Harris, R., Wiebe, P., Lenz, J., Skjoldal, H.R., Huntley, M. (Eds.), ICES Zooplankton Methodology Manual. Academic Press, London, pp. 223–258. https://doi.org/10.1016/B978-012327645-2/50007-4

Fortier, L., Cochran, J.K., 2008. Introduction to special section on annual cycles on the Arctic Ocean shelf. J. Geophys. Res. Oceans 113. https://doi.org/10.1029/2007JC004457

Fortier, M., 2001. Visual predators and the diel vertical migration of copepods under Arctic sea ice during the midnight sun. J. Plankton Res. 23, 1263–1278. https://doi.org/10.1093/plankt/23.11.1263

Fossheim, M., Primicerio, R., Johannesen, E., Ingvaldsen, R., Aschan, M., Dolgov, A., 2015. Recent warming leads to a rapid borealization of fish communities in the Arctic. Nat. Clim. Change 5. https://doi.org/10.1038/nclimate2647

Frederiksen, M., Descamps, S., Erikstad, K.E., Gaston, A.J., Gilchrist, H.G., Grémillet, D., Johansen, K.L., Kolbeinsson, Y., Linnebjerg, J.F., Mallory, M.L., McFarlane Tranquilla, L.A., Merkel, F.R., Montevecchi, W.A., Mosbech, A., Reiertsen, T.K., Robertson, G.J., Steen, H., Strøm, H., Thórarinsson, T.L., 2016. Migration and wintering of a declining seabird, the thick-billed murre *Uria lomvia*, on an ocean basin scale: conservation implications. Biol. Conserv. 200, 26–35. https://doi.org/10.1016/j.biocon.2016.05.011

Freer, J.J., Daase, M., Tarling, G.A., 2022. Modelling the biogeographic boundary shift of *Calanus finmarchicus* reveals drivers of Arctic atlantification by subarctic zooplankton. Glob. Change Biol. 28, 429–440. https://doi.org/10.1111/gcb.15937

García-Seoane, E., Bernal, A., Saborido-Rey, F., 2014. Reproductive ecology of the glacier lanternfish *Benthosema glaciale*. Hydrobiologia 727, 137–149. https://doi.org/10.1007/s10750-013-1796-y

Gardiner, K., Dick, T.A., 2010. Arctic cephalopod distributions and their associated predators. Polar Res. 29, 209–227. https://doi.org/10.1111/j.1751-8369.2010.00146.x

Gastauer, S., Chu, D., Cox, M.J., 2019. ZooScatR—An R package for modelling the scattering properties of weak scattering targets using the distorted wave Born approximation. J. Acoust. Soc. Am. 145, EL102–EL108. https://doi.org/10.1121/1.5085655

Gaston, A., Elliott, K., 2014. Seabird diet changes in northern Hudson Bay, 1981-2013, reflect the availability of schooling prey. Mar. Ecol. Prog. Ser. 513, 211–223. https://doi.org/10.3354/meps10945

Gauthier, S., Horne, J.K., 2004. Potential acoustic discrimination within boreal fish assemblages. ICES J. Mar. Sci. 61, 836–845. https://doi.org/10.1016/j.icesjms.2004.03.033

Geoffroy, M., Daase, M., Cusa, M., Darnis, G., Graeve, M., Santana Hernández, N., Berge, J., Renaud, P.E., Cottier, F., Falk-Petersen, S., 2019. Mesopelagic sound scattering layers of the high Arctic: seasonal variations in biomass, species assemblage, and trophic relationships. Front. Mar. Sci. 6, 364. https://doi.org/10.3389/fmars.2019.00364

Geoffroy, M., Langbehn, T., Priou, P., Varpe, Ø., Johnsen, G., Le Bris, A., Fisher, J.A.D., Daase, M., McKee, D., Cohen, J., Berge, J., 2021. Pelagic organisms avoid white, blue, and red artificial light from scientific instruments. Sci. Rep. 11, 14941. https://doi.org/10.1038/s41598-021-94355-6

Geoffroy, M., Majewski, A., LeBlanc, M., Gauthier, S., Walkusz, W., Reist, J.D., Fortier, L., 2016. Vertical segregation of age-0 and age-1+ polar cod (*Boreogadus saida*) over the annual cycle in the Canadian Beaufort Sea. Polar Biol. 39, 1023–1037. https://doi.org/10.1007/s00300-015-1811-z

Geoffroy, M., Priou, P., 2020. Fish ecology during the polar night, in: Polar Night Marine Ecology: Life and Light in the Dead of Night, Advances in Polar Ecology. Springer International Publishing, Cham, pp. 181–216. https://doi.org/10.1007/978-3-030-33208-2_7

Geoffroy, M., Robert, D., Darnis, G., Fortier, L., 2011. The aggregation of polar cod (*Boreogadus saida*) in the deep Atlantic layer of ice-covered Amundsen Gulf (Beaufort Sea) in winter. Polar Biol. 34, 1959–1971. https://doi.org/10.1007/s00300-011-1019-9

Giering, S.L.C., Sanders, R., Lampitt, R.S., Anderson, T.R., Tamburini, C., Boutrif, M., Zubkov, M.V., Marsay, C.M., Henson, S.A., Saw, K., Cook, K., Mayor, D.J., 2014. Reconciliation of the carbon budget in the ocean's twilight zone. Nature 507, 480–483. https://doi.org/10.1038/nature13123

Giraldo, C., Stasko, A., Walkusz, W., Majewski, A., Rosenberg, B., Power, M., Swanson, H., Reist, J.D., 2018. Feeding of Greenland halibut (*Reinhardtius hippoglossoides*) in the Canadian Beaufort Sea. J. Mar. Syst. 183, 32–41. https://doi.org/10.1016/j.jmarsys.2018.03.009

Gjøsæter, H., 1998. The population biology and exploitation of capelin (*Mallotus villosus*) in the Barents Sea. Sarsia 83, 453–496. https://doi.org/10.1080/00364827.1998.10420445

Gjøsæter, H., Ingvaldsen, R., Christiansen, J.S., 2020. Acoustic scattering layers reveal a faunal connection across the Fram Strait. Prog. Oceanogr. 185, 102348. https://doi.org/10.1016/j.pocean.2020.102348

Gjøsæter, H., Wiebe, P.H., Knutsen, T., Ingvaldsen, R.B., 2017. Evidence of diel vertical migration of mesopelagic sound-scattering organisms in the Arctic. Front. Mar. Sci. 4, 332. https://doi.org/10.3389/fmars.2017.00332

Gjøsæter, J., 1973. The food of the myctophid fish, *Benthosema glaciale* (Reinhardt), from western Norway. Sarsia 52, 53–58. https://doi.org/10.1080/00364827.1973.10411231

Gjøsæter, J., Kawaguchi, K., 1980. A review of the world resources of mesopelagic fish. Food and Agriculture Organsiation, Rome, Italy.

Godø, O.R., Samuelsen, A., Macaulay, G.J., Patel, R., Hjøllo, S.S., Horne, J., Kaartvedt, S., Johannessen, J.A., 2012. Mesoscale eddies are oases for higher trophic marine life. PLoS ONE 7, e30161. https://doi.org/10.1371/journal.pone.0030161

Golikov, A.V., Blicher, M.E., Jørgensen, L.L., Walkusz, W., Zakharov, D.V., Zimina, O.L., Sabirov, R.M., 2019. Reproductive biology and ecology of the boreoatlantic armhook squid *Gonatus*

fabricii (Cephalopoda: Gonatidae). J. Molluscan Stud. 85, 287–299. https://doi.org/10.1093/mollus/eyz023

Golikov, A.V., Ceia, F.R., Hoving, H.J.T., Queirós, J.P., Sabirov, R.M., Blicher, M.E., Larionova, A.M., Walkusz, W., Zakharov, D.V., Xavier, J.C., 2022. Life history of the Arctic squid *Gonatus fabricii* (Cephalopoda: Oegopsida) reconstructed by analysis of individual ontogenetic stable isotopic trajectories. Animals 12, 3548. https://doi.org/10.3390/ani12243548

Golikov, A.V., Sabirov, R.M., Lubin, P.A., 2017. First assessment of biomass and abundance of cephalopods *Rossia palpebrosa* and *Gonatus fabricii* in the Barents Sea. J. Mar. Biol. Assoc. U. K. 97, 1605–1616. https://doi.org/10.1017/S0025315416001004

Gordó-Vilaseca, C., Stephenson, F., Coll, M., Lavin, C., Costello, M.J., 2023. Three decades of increasing fish biodiversity across the northeast Atlantic and the Arctic Ocean. Proc. Natl. Acad. Sci. 120, e2120869120. https://doi.org/10.1073/pnas.2120869120

Gorsky, G., Ohman, M.D., Picheral, M., Gasparini, S., Stemmann, L., Romagnan, J.-B., Cawood, A., Pesant, S., García-Comas, C., Prejger, F., 2010. Digital zooplankton image analysis using the ZooScan integrated system. J. Plankton Res. 32, 285–303. https://doi.org/10.1093/plankt/fbp124

Gostiaux, L., van Haren, H., 2010. Extracting meaningful information from uncalibrated backscattered echo intensity data. J. Atmospheric Ocean. Technol. 27, 943–949. https://doi.org/10.1175/2009JTECHO704.1

Govindarajan, A.F., Francolini, R.D., Jech, J.M., Lavery, A.C., Llopiz, J.K., Wiebe, P.H., Zhang, W. (Gordon), 2021. Exploring the use of environmental DNA (eDNA) to detect animal taxa in the mesopelagic zone. Front. Ecol. Evol. 9. https://doi.org/10.3389/fevo.2021.574877

Gradinger, R.R., Bluhm, B.A., 2004. In-situ observations on the distribution and behavior of amphipods and Arctic cod (*Boreogadus saida*) under the sea ice of the high Arctic Canada Basin. Polar Biol. 27, 595–603. https://doi.org/10.1007/s00300-004-0630-4

Grenvald, J.C., Callesen, T.A., Daase, M., Hobbs, L., Darnis, G., Renaud, P.E., Cottier, F., Nielsen, T.G., Berge, J., 2016. Plankton community composition and vertical migration during polar night in Kongsfjorden. Polar Biol. 39, 1879–1895. https://doi.org/10.1007/s00300-016-2015-x

Grimaldo, E., Grimsmo, L., Alvarez, P., Herrmann, B., Møen Tveit, G., Tiller, R., Slizyte, R., Aldanondo, N., Guldberg, T., Toldnes, B., Carvajal, A., Schei, M., Selnes, M., 2020. Investigating the potential for a commercial fishery in the Northeast Atlantic utilizing mesopelagic species. ICES J. Mar. Sci. 77, 2541–2556. https://doi.org/10.1093/icesjms/fsaa114

Gulliksen, B., Lønne, O.J., 1991. Sea ice macrofauna in the Antarctic and the Arctic. J. Mar. Syst. 2, 53–61. https://doi.org/10.1016/0924-7963(91)90013-K

Gunnarsson, B., 2021. Recent ship traffic and developing shipping trends on the northern sea route—policy implications for future arctic shipping. Mar. Policy 124, 104369. https://doi.org/10.1016/j.marpol.2020.104369

Hagen, W., 1999. Reproductive strategies and energetic adaptations of polar zooplankton. Invertebr. Reprod. Dev. 36, 25–34. https://doi.org/10.1080/07924259.1999.9652674

Haine, T.W.N., Curry, B., Gerdes, R., Hansen, E., Karcher, M., Lee, C., Rudels, B., Spreen, G., De Steur, L., Stewart, K.D., Woodgate, R., 2015. Arctic freshwater export: Status, mechanisms, and prospects. Glob. Planet. Change 125, 13–35. https://doi.org/10.1016/j.gloplacha.2014.11.013

Halliday, R.G., Clark, K.J., Themelis, D.E., 2015. The biology of *Benthosema glaciale* and *Ceratoscopelus maderensis* (Myctophidae) in the Slope Sea off Nova Scotia, Canada. J. Northwest Atl. Fish. Sci. 47, 75–89. https://doi.org/10.2960/J.v47.m708

Handegard, N.O., Tonje, F.N., Johnsen, E., Pedersen, G., Tenningen, M., Korneliussen, R., Ona, E., 2021. Fisheries acoustics in Norway—wide band data, autonomous platforms and deep learning. J. Acoust. Soc. Am. 150, A254. https://doi.org/10.1121/10.0008196

Hansen, C., Skogen, M.D., Utne, K.R., Broms, C., Strand, E., Hjøllo, S.S., 2021. Patterns, efficiency and ecosystem effects when fishing *Calanus finmarchicus* in the Norwegian Sea—using an individual-based model. Mar. Ecol. Prog. Ser. 680, 15–32. https://doi.org/10.3354/meps13942

Haug, T., Bogstad, B., Chierici, M., Gjøsæter, H., Hallfredsson, E.H., Høines, Å.S., Hoel, A.H., Ingvaldsen, R.B., Jørgensen, L.L., Knutsen, T., Loeng, H., Naustvoll, L.-J., Røttingen, I., Sunnanå, K., 2017. Future harvest of living resources in the Arctic Ocean north of the Nordic and Barents seas: a review of possibilities and constraints. Fish. Res. 188, 38–57. https://doi.org/10.1016/j.fishres.2016.12.002

Hays, G.C., 2003. A review of the adaptive significance and ecosystem consequences of zooplankton diel vertical migrations, in: Jones, M.B., Ingólfsson, A., Ólafsson, E., Helgason, G.V., Gunnarsson, K., Svavarsson, J. (Eds.), Migrations and Dispersal of Marine Organisms, Developments in Hydrobiology. Springer Netherlands, Dordrecht, pp. 163–170. https://doi.org/10.1007/978-94-017-2276-6_18

Hays, G.C., 1995. Ontogenetic and seasonal variation in the diel vertical migration of the copepods *Metridia lucens* and *Metridia longa*. Limnol. Oceanogr. 40, 1461–1465. https://doi.org/10.4319/lo.1995.40.8.1461

Heide-Jørgensen, M.P., Burt, L.M., Hansen, R.G., Nielsen, N.H., Rasmussen, M., Fossette, S., Stern, H., 2013. The significance of the north water polynya to Arctic top predators. AMBIO 42, 596–610. https://doi.org/10.1007/s13280-012-0357-3

Heide-Jørgensen, M.P., Sinding, M.-H.S., Nielsen, N.H., Rosing-Asvid, A., Hansen, R.G., 2016. Large numbers of marine mammals winter in the north water polynya. Polar Biol. 39, 1605–1614. https://doi.org/10.1007/s00300-015-1885-7

Hidalgo, M., Browman, H.I., 2019. Developing the knowledge base needed to sustainably manage mesopelagic resources. ICES J. Mar. Sci. 76, 609–615. https://doi.org/10.1093/icesjms/fsz067

Hirche, H.-J., Mumm, N., 1992. Distribution of dominant copepods in the Nansen Basin, Arctic Ocean, in summer. Deep Sea Res. Part Oceanogr. Res. Pap. 39, S485–S505. https://doi.org/10.1016/S0198-0149(06)80017-8

Hirche, H.J., Muyakshin, S., Klages, M., Auel, H., 2006. Aggregation of the Arctic copepod *Calanus hyperboreus* over the ocean floor of the Greenland Sea. Deep Sea Res. Part Oceanogr. Res. Pap. 53, 310–320. https://doi.org/10.1016/j.dsr.2005.08.005

Hobbs, L., Banas, N.S., Cohen, J.H., Cottier, F.R., Berge, J., Varpe, Ø., 2021. A marine zooplankton community vertically structured by light across diel to interannual timescales. Biol. Lett. 17, 20200810. https://doi.org/10.1098/rsbl.2020.0810

Hobbs, L., Cottier, F.R., Last, K.S., Berge, J., 2018. Pan-Arctic diel vertical migration during the polar night. Mar. Ecol. Prog. Ser. 605, 61–72. https://doi.org/10.3354/meps12753

Hoegh-Guldberg, O., Bruno, J.F., 2010. The impact of climate change on the world's marine ecosystems. Science 328, 1523–1528. https://doi.org/10.1126/science.1189930

Holliday, D., 1977. Extracting bio-physical information from the acoustic signature of marine organisms. Ocean. Sound Scatt. Predict.

Hollowed, A., Benjamin, P., Loeng, H., 2013. Potential movement of fish and shellfish stocks from the sub-Arctic to the Arctic Ocean. Fish. Oceanogr. 22, 355–370. https://doi.org/10.1111/fog.12027

Hooker, S.K., Iverson, S.J., Ostrom, P., Smith, S.C., 2001. Diet of northern bottlenose whales inferred from fatty-acid and stable-isotope analyses of biopsy samples. Can. J. Zool. 79, 1442–1454. https://doi.org/10.1139/z01-096

Hop, H., Gjøsæter, H., 2013. Polar cod (*Boreogadus saida*) and capelin (*Mallotus villosus*) as key species in marine food webs of the Arctic and the Barents Sea. Mar. Biol. Res. 9, 878–894. https://doi.org/10.1080/17451000.2013.775458

Horne, J.K., 2000. Acoustic approaches to remote species identification: a review. Fish. Oceanogr. 9, 356–371. https://doi.org/10.1046/j.1365-2419.2000.00143.x

Howell, K.L., Hilário, A., Allcock, A.L., Bailey, D.M., Baker, M., Clark, M.R., Colaço, A., Copley, J., Cordes, E.E., Danovaro, R., Dissanayake, A., Escobar, E., Esquete, P., Gallagher, A.J., Gates, A.R., Gaudron, S.M., German, C.R., Gjerde, K.M., Higgs, N.D., Le Bris, N., Levin, L.A., Manea, E., McClain, C., Menot, L., Mestre, N.C., Metaxas, A., Milligan, R.J., Muthumbi, A.W.N., Narayanaswamy, B.E., Ramalho, S.P., Ramirez-Llodra, E., Robson, L.M., Rogers, A.D., Sellanes, J., Sigwart, J.D., Sink, K., Snelgrove, P.V.R., Stefanoudis, P.V., Sumida, P.Y.,

Taylor, M.L., Thurber, A.R., Vieira, R.P., Watanabe, H.K., Woodall, L.C., Xavier, J.R., 2020. A blueprint for an inclusive, global deep-sea ocean decade field program. Front. Mar. Sci. 7, 584861. https://doi.org/10.3389/fmars.2020.584861

Howey, L.A., Tolentino, E.R., Papastamatiou, Y.P., Brooks, E.J., Abercrombie, D.L., Watanabe, Y.Y., Williams, S., Brooks, A., Chapman, D.D., Jordan, L.K.B., 2016. Into the deep: the functionality of mesopelagic excursions by an oceanic apex predator. Ecol. Evol. 6, 5290–5304. https://doi.org/10.1002/ece3.2260

Huenerlage, K., Graeve, M., Buchholz, C., Buchholz, F., 2015. The other krill: overwintering physiology of adult *Thysanoessa inermis* (Euphausiacea) from the high-Arctic Kongsfjord. Aquat. Biol. 23, 225–235. https://doi.org/10.3354/ab00622

Hunt, G.L., Drinkwater, K.F., Arrigo, K., Berge, J., Daly, K.L., Danielson, S., Daase, M., Hop, H., Isla, E., Karnovsky, N., Laidre, K., Mueter, F.J., Murphy, E.J., Renaud, P.E., Smith, W.O., Trathan, P., Turner, J., Wolf-Gladrow, D., 2016. Advection in polar and sub-polar environments: impacts on high latitude marine ecosystems. Prog. Oceanogr. 149, 40–81. https://doi.org/10.1016/j.pocean.2016.10.004

Hurst, T.P., 2007. Causes and consequences of winter mortality in fishes. J. Fish Biol. 71, 315–345. https://doi.org/10.1111/j.1095-8649.2007.01596.x

Ingvaldsen, R., Loeng, H., Ottersen, G., Ådlandsvik, B., 2003. Climate variability in the Barents Sea during the 20th century with a focus on the 1990s. ICES Mar. Sci. Symp. 219, 160–168. https://doi.org/10.17895/ices.pub.19271780

Ingvaldsen, R.B., Eriksen, E., Gjøsæter, H., Engås, A., Schuppe, B.K., Assmann, K.M., Cannaby, H., Dalpadado, P., Bluhm, B.A., 2023. Under-ice observations by trawls and multi-frequency acoustics in the Central Arctic Ocean reveals abundance and composition of pelagic fauna. Sci. Rep. 13, 1000. https://doi.org/10.1038/s41598-023-27957-x

Ingvaldsen, R.B., Gjøsæter, H., Ona, E., Michalsen, K., 2017. Atlantic cod (*Gadus morhua*) feeding over deep water in the high Arctic. Polar Biol. 40, 2105–2111. https://doi.org/10.1007/s00300-017-2115-2

Irigoien, X., Conway, D., Harris, R., 2004. Flexible diel vertical migration behaviour of zooplankton in the Irish Sea. Mar. Ecol. Prog. Ser. 267, 85–97. https://doi.org/10.3354/meps267085

Irigoien, X., Klevjer, T.A., Røstad, A., Martinez, U., Boyra, G., Acuña, J.L., Bode, A., Echevarria, F., Gonzalez-Gordillo, J.I., Hernandez-Leon, S., Agusti, S., Aksnes, D.L., Duarte, C.M., Kaartvedt, S., 2014. Large mesopelagic fishes biomass and trophic efficiency in the open ocean. Nat. Commun. 5, 3271. https://doi.org/10.1038/ncomms4271

Irisson, J.-O., Ayata, S.-D., Lindsay, D.J., Karp-Boss, L., Stemmann, L., 2022. Machine learning for the study of plankton and marine snow from images. Annu. Rev. Mar. Sci. 14, 277–301. https://doi.org/10.1146/annurev-marine-041921-013023

Jakobsson, M., Mayer, L.A., Bringensparr, C., Castro, C.F., Mohammad, R., Johnson, P., Ketter, T., Accettella, D., Amblas, D., An, L., Arndt, J.E., Canals, M., Casamor, J.L., Chauché, N., Coakley, B., Danielson, S., Demarte, M., Dickson, M.-L., Dorschel, B., Dowdeswell, J.A., Dreutter, S., Fremand, A.C., Gallant, D., Hall, J.K., Hehemann, L., Hodnesdal, H., Hong, J., Ivaldi, R., Kane, E., Klaucke, I., Krawczyk, D.W., Kristoffersen, Y., Kuipers, B.R., Millan, R., Masetti, G., Morlighem, M., Noormets, R., Prescott, M.M., Rebesco, M., Rignot, E., Semiletov, I., Tate, A.J., Travaglini, P., Velicogna, I., Weatherall, P., Weinrebe, W., Willis, J.K., Wood, M., Zarayskaya, Y., Zhang, T., Zimmermann, M., Zinglersen, K.B., 2020. The international bathymetric chart of the Arctic Ocean version 4.0. Sci. Data 7, 176. https://doi.org/10.1038/s41597-020-0520-9

Johnsen, G., Candeloro, M., Berge, J., Moline, M., 2014. Glowing in the dark: discriminating patterns of bioluminescence from different taxa during the Arctic polar night. Polar Biol. 37, 707–713. https://doi.org/10.1007/s00300-014-1471-4

Johnsen, G., Zolich, A., Grant, S., Bjørgum, R., Cohen, J.H., McKee, D., Kopec, T.P., Vogedes, D., Berge, J., 2021. All-sky camera system providing high temporal resolution annual time series of irradiance in the Arctic. Appl. Opt. 60, 6456. https://doi.org/10.1364/AO.424871

Jönsson, M., Varpe, Ø., Kozłowski, T., Berge, J., Kröger, R.H.H., 2014. Differences in lens optical plasticity in two gadoid fishes meeting in the Arctic. J. Comp. Physiol. A 200, 949–957. https://doi.org/10.1007/s00359-014-0941-z

Jordan, A.D., Møller, P.R., Nielsen, J.G., 2003. Revision of the Arctic cod genus *Arctogadus*. J. Fish Biol. 62, 1339–1352. https://doi.org/10.1046/j.1095-8649.2003.00115.x

Kaartvedt, S., 2008. Photoperiod may constrain the effect of global warming in Arctic marine systems. J. Plankton Res. 30, 1203–1206. https://doi.org/10.1093/plankt/fbn075

Kaartvedt, S., Christiansen, S., Titelman, J., 2023. Mid-summer fish behavior in a high-latitude twilight zone. Limnol. Oceanogr. 9999, 1–16. https://doi.org/10.1002/lno.12374

Kaartvedt, S., Langbehn, T.J., Aksnes, D.L., 2019a. Enlightening the ocean's twilight zone. ICES J. Mar. Sci. 76, 803–812. https://doi.org/10.1093/icesjms/fsz010

Kaartvedt, S., Røstad, A., Klevjer, T., Staby, A., 2009. Use of bottom-mounted echo sounders in exploring behavior of mesopelagic fishes. Mar. Ecol. Prog. Ser. 395, 109–118. https://doi.org/10.3354/meps08174

Kaartvedt, S., Røstad, A., Opdal, A., Aksnes, D., 2019b. Herding mesopelagic fish by light. Mar. Ecol. Prog. Ser. 625, 225–231. https://doi.org/10.3354/meps13079

Kaartvedt, S., Staby, A., Aksnes, D.L., 2012. Efficient trawl avoidance by mesopelagic fishes causes large underestimation of their biomass. Mar. Ecol. Prog. Ser. 456, 1–6. https://doi.org/10.3354/meps09785

Kaartvedt, S., Torgersen, T., Klevjer, T., Røstad, A., Devine, J., 2008. Behavior of individual mesopelagic fish in acoustic scattering layers of Norwegian fjords. Mar. Ecol. Prog. Ser. 360, 201–209. https://doi.org/10.3354/meps07364

Kang, D., Mukai, T., Iida, K., Hwang, D., Myoung, J.-G., 2005. The influence of tilt angle on the acoustic target strength of the Japanese common squid (*Todarodes pacificus*). ICES J. Mar. Sci. 62, 779–789. https://doi.org/10.1016/j.icesjms.2005.02.002

Karamushko, O., Christiansen, J., 2021. New data on the distribution of beaked redfish *Sebastes mentella* (Sebastidae) in the Greenland Sea. J. Ichthyol. 61, 96–102. https://doi.org/10.1134/S0032945221010082

Karnovsky, N.J., Hunt, G.L., 2002. Estimation of carbon flux to dovekies (*Alle alle*) in the North Water. Deep Sea Res. Part II Top. Stud. Oceanogr. 49, 5117–5130. https://doi.org/10.1016/S0967-0645(02)00181-9

Kasumyan, A., 2003. The lateral line in fish: structure, function, and role in behavior. J. Ichthyol. 43, S175–S213.

Katlein, C., Schiller, M., Belter, H.J., Coppolaro, V., Wenslandt, D., Nicolaus, M., 2017. A new remotely operated sensor platform for interdisciplinary observations under sea ice. Front. Mar. Sci. 4, 281. https://doi.org/10.3389/fmars.2017.00281

Kessel, S.T., Hussey, N.E., Crawford, R.E., Yurkowski, D.J., Webber, D.M., Dick, T.A., Fisk, A.T., 2017. First documented large-scale horizontal movements of individual Arctic cod (*Boreogadus saida*). Can. J. Fish. Aquat. Sci. 74, 292–296. https://doi.org/10.1139/cjfas-2016-0196

Kim, Y.-H., Min, S.-K., Gillett, N.P., Notz, D., Malinina, E., 2023. Observationally-constrained projections of an ice-free Arctic even under a low emission scenario. Nat. Commun. 14, 3139. https://doi.org/10.1038/s41467-023-38511-8

Kitamura, M., Amakasu, K., Kikuchi, T., Nishino, S., 2017. Seasonal dynamics of zooplankton in the southern Chukchi Sea revealed from acoustic backscattering strength. Cont. Shelf Res. 133, 47–58. https://doi.org/10.1016/j.csr.2016.12.009

Klevjer, T.A., Irigoien, X., Røstad, A., Fraile-Nuez, E., Benítez-Barrios, V.M., Kaartvedt., S., 2016. Large scale patterns in vertical distribution and behaviour of mesopelagic scattering layers. Sci. Rep. 6, 19873. https://doi.org/10.1038/srep19873

Klevjer, T.A., Melle, W., Knutsen, T., Aksnes, D.L., 2020a. Vertical distribution and migration of mesopelagic scatterers in four north Atlantic basins. Deep Sea Res. Part II Top. Stud. Oceanogr. 180, 104811. https://doi.org/10.1016/j.dsr2.2020.104811

Klevjer, T.A., Melle, W., Knutsen, T., Strand, E., Korneliussen, R., Dupont, N., Salvanes, A.G.V., Wiebe, P.H., 2020b. Micronekton biomass distribution, improved estimates across four north Atlantic basins. Deep Sea Res. Part II Top. Stud. Oceanogr. 180, 104691. https://doi.org/10.1016/j.dsr2.2019.104691

Knutsen, T., Strand, E., Klevjer, T.A., Salvanes, A.G.V., Broms, C., Sunde, S.M., Aksnes, D.L., García-Seoane, E., Melle, W., 2023. Feeding ecology of *Benthosema glaciale* across the North Atlantic. Front. Mar. Sci. 10, 1086607. https://doi.org/10.3389/fmars.2023.1086607

Knutsen, T., Wiebe, P.H., Gjøsæter, H., Ingvaldsen, R.B., Lien, G., 2017. High latitude epipelagic and mesopelagic scattering layers—a reference for future Arctic ecosystem change. Front. Mar. Sci. 4, 334. https://doi.org/10.3389/fmars.2017.00334

Korneliussen, R., Berger, L., Campanilla, F., Chu, D., Demer, D., De Robertis, A., Domokos, R., Doray, M., Fielding, S., Fässler, S.M.M., Gauthier, S., Gastauer, S., Horne, J., Hutton, B., Iriarte, F., Jech, J.M., Kloser, R., Lawson, G., Lebourges-Dhaussy, A., McQuinn, I., Peña, M., Scoulding, B., Sakinan, S., Schaber, M., Taylor, J.C., Thompson, C.H., 2018. Acoustic target classification. ICES Coop. Res. Rep. 344, 104. https://doi.org/10.17895/ICES.PUB.4567

Kosobokova, K., Hopcroft, R., Hirche, H.-J., 2011. Patterns of zooplankton diversity through the depths of the Arctic's central basins. Mar. Biodivers. 41, 29–50. https://doi.org/10.1007/s12526-010-0057-9

Kosobokova, K.N., Hopcroft, R.R., 2010. Diversity and vertical distribution of mesozooplankton in the Arctic's Canada Basin. Deep Sea Res. Part II Top. Stud. Oceanogr. 57, 96–110. https://doi.org/10.1016/j.dsr2.2009.08.009

Kraft, A., Berge, J., Varpe, Ø., Falk-Petersen, S., 2013. Feeding in Arctic darkness: mid-winter diet of the pelagic amphipods *Themisto abyssorum* and *T. libellula*. Mar. Biol. 160, 241–248. https://doi.org/10.1007/s00227-012-2065-8

Kraft, A., Graeve, M., Janssen, D., Greenacre, M., Falk-Petersen, S., 2015. Arctic pelagic amphipods: lipid dynamics and life strategy. J. Plankton Res. 37, 790–807. https://doi.org/10.1093/plankt/fbv052

Kristensen, T., 1984. Biology of the Squid *Gonatus fabricii* (Lichtenstein, 1818) from West Greenland Waters, Bioscience (Meddelelser om Grønland). Museum Tusculanum Press, University of Copenhagen.

Krumsick, K.J., Fisher, J.A.D., 2022. Spatial variation in food web structure in a recovering marine ecosystem. PLOS ONE 17, e0268440. https://doi.org/10.1371/journal.pone.0268440

Kunisch, E.H., Bluhm, B.A., Daase, M., Gradinger, R., Hop, H., Melnikov, I.A., Varpe, Ø., Berge, J., 2020. Pelagic occurrences of the ice amphipod *Apherusa glacialis* throughout the Arctic. J. Plankton Res. 42, 73–86. https://doi.org/10.1093/plankt/fbz072

Kwok, R., 2018. Arctic sea ice thickness, volume, and multiyear ice coverage: losses and coupled variability (1958–2018). Environ. Res. Lett. 13, 105005. https://doi.org/10.1088/1748-9326/aae3ec

Lalli, C.M., Parsons, T.R., 1997. Biological oceanography: an introduction, 2nd ed. ed, Open University oceanography series. Butterworth Heinemann, Oxford, England.

Land, M.F., 2000. On the functions of double eyes in midwater animals. Philos. Trans. R. Soc. B Biol. Sci. 355, 1147–1150. https://doi.org/10.1098/rstb.2000.0656

Land, M.F., 1989. The eyes of hyperiid amphipods: relations of optical structure to depth. J. Comp. Physiol. A 164, 751–762. https://doi.org/10.1007/BF00616747

Langbehn, T., Aksnes, D., Kaartvedt, S., Fiksen, Ø., Jørgensen, C., 2019. Light comfort zone in a mesopelagic fish emerges from adaptive behaviour along a latitudinal gradient. Mar. Ecol. Prog. Ser. 623, 161–174. https://doi.org/10.3354/meps13024

Langbehn, T.J., Aksnes, D.L., Kaartvedt, S., Fiksen, Ø., Ljungström, G., Jørgensen, C., 2022. Poleward distribution of mesopelagic fishes is constrained by seasonality in light. Glob. Ecol. Biogeogr. 31, 546–561. https://doi.org/10.1111/geb.13446

Lange, B.A., Beckers, J.F., Casey, J.A., Haas, C., 2019. Airborne observations of summer thinning of multiyear sea ice originating from the Lincoln Sea. J. Geophys. Res. Oceans 124, 243–266. https://doi.org/10.1029/2018JC014383

Larsen, L.-H., Cusa, M., Eglund-Newby, S., Berge, J., Renaud, P.E., Varpe, Ø., Geoffroy, M., Falk-Petersen, S., 2023. Diets of gadoid fish in Arctic waters of Svalbard fjords during the polar night. Polar Biol. https://doi.org/10.1007/s00300-023-03167-z

Lavery, A.C., Chu, D., Moum, J.N., 2010. Measurements of acoustic scattering from zooplankton and oceanic microstructure using a broadband echosounder. ICES J. Mar. Sci. 67, 379–394. https://doi.org/10.1093/icesjms/fsp242

Lavery, A.C., Wiebe, P.H., Stanton, T.K., Lawson, G.L., Benfield, M.C., Copley, N., 2007. Determining dominant scatterers of sound in mixed zooplankton populations. J. Acoust. Soc. Am. 122, 3304–3326. https://doi.org/10.1121/1.2793613

Le Cren, E.D., 1951. The length-weight relationship and seasonal cycle in gonad weight and condition in the perch (*Perca fluviatilis*). J. Anim. Ecol. 20, 201–219. https://doi.org/10.2307/1540

Lebourges-Dhaussy, A., Marchal, É., Menkès, C., Champalbert, G., Biessy, B., 2000. *Vinciguerria nimbaria* (micronekton), environment and tuna: their relationships in the eastern Tropical Atlantic. Oceanol. Acta 23, 515–528. https://doi.org/10.1016/S0399-1784(00)00137-7

Leu, E., Mundy, C.J., Assmy, P., Campbell, K., Gabrielsen, T.M., Gosselin, M., Juul-Pedersen, T., Gradinger, R., 2015. Arctic spring awakening – steering principles behind the phenology of vernal ice algal blooms. Prog. Oceanogr. 139, 151–170. https://doi.org/10.1016/j.pocean.2015.07.012

Li, L., Stramski, D., Reynolds, R.A., 2014. Characterization of the solar light field within the ocean mesopelagic zone based on radiative transfer simulations. Deep Sea Res. Part Oceanogr. Res. Pap. 87, 53–69. https://doi.org/10.1016/j.dsr.2014.02.005

Lindström, M., 2000. Eye function of Mysidacea (Crustacea) in the northern Baltic Sea. J. Exp. Mar. Biol. Ecol. 246, 85–101. https://doi.org/10.1016/S0022-0981(99)00178-1

Ljungström, G., Langbehn, T.J., Jørgensen, C., 2021. Light and energetics at seasonal extremes limit poleward range shifts. Nat. Clim. Change 11, 530–536. https://doi.org/10.1038/s41558-021-01045-2

MacKenzie, B.R., Payne, M.R., Boje, J., Høyer, J.L., Siegstad, H., 2014. A cascade of warming impacts brings bluefin tuna to Greenland waters. Glob. Change Biol. 20, 2484–2491. https://doi.org/10.1111/gcb.12597

MacKenzie, K.M., Lydersen, C., Haug, T., Routti, H., Aars, J., Andvik, C.M., Borgå, K., Fisk, A.T., Meier, S., Biuw, M., Lowther, A.D., Lindstrøm, U., Kovacs, K.M., 2022. Niches of marine mammals in the European Arctic. Ecol. Indic. 136, 108661. https://doi.org/10.1016/j.ecolind.2022.108661

MacLennan, D.N., 1986. Time varied gain functions for pulsed sonars. J. Sound Vib. 110, 511–522. https://doi.org/10.1016/S0022-460X(86)80151-1

Madsen, M.L., Nelson, R.J., Fevolden, S.-E., Christiansen, J.S., Præbel, K., 2016. Population genetic analysis of Euro-Arctic polar cod *Boreogadus saida* suggests fjord and oceanic structuring. Polar Biol. 39, 969–980. https://doi.org/10.1007/s00300-015-1812-y

Madsen, S.D., Nielsen, T.G., Hansen, B.W., 2008. Annual population development and production by small copepods in Disko Bay, western Greenland. Mar. Biol. 155, 63–77. https://doi.org/10.1007/s00227-008-1007-y

Majewski, A., Walkusz, W., Lynn, B., Atchison, S., Eert, J., Reist, J., 2016. Distribution and diet of demersal Arctic Cod, *Boreogadus saida*, in relation to habitat characteristics in the Canadian Beaufort Sea. Polar Biol. 39. https://doi.org/10.1007/s00300-015-1857-y

Majewski, A.R., Atchison, S., MacPhee, S., Eert, J., Niemi, A., Michel, C., Reist, J.D., 2017. Marine fish community structure and habitat associations on the Canadian Beaufort shelf and slope. Deep Sea Res. Part Oceanogr. Res. Pap. 121, 169–182. https://doi.org/10.1016/j.dsr.2017.01.009

Marangoni, L.F.B., Davies, T., Smyth, T., Rodríguez, A., Hamann, M., Duarte, C., Pendoley, K., Berge, J., Maggi, E., Levy, O., 2022. Impacts of artificial light at night in marine ecosystems—a review. Glob. Change Biol. 28, 5346–5367. https://doi.org/10.1111/gcb.16264

Marchese, C., Albouy, C., Tremblay, J.-E., Dumont, D., D'Ortenzio, F., Vissault, S., Bélanger, S., 2017. Changes in phytoplankton bloom phenology over the north water (NOW) polynya: a response

to changing environmental conditions. Polar Biol. 40. https://doi.org/10.1007/s00300-017-2095-2
Marsh, J.M., Mueter, F.J., 2020. Influences of temperature, predators, and competitors on polar cod (*Boreogadus saida*) at the southern margin of their distribution. Polar Biol. 43, 995–1014. https://doi.org/10.1007/s00300-019-02575-4
Martin, A., Boyd, P., Buesseler, K., Cetinic, I., Claustre, H., Giering, S., Henson, S., Irigoien, X., Kriest, I., Memery, L., Robinson, C., Saba, G., Sanders, R., Siegel, D., Villa-Alfageme, M., Guidi, L., 2020. The oceans' twilight zone must be studied now, before it is too late. Nature 580, 26–28. https://doi.org/10.1038/d41586-020-00915-7
Martin, J., Tremblay, J., Gagnon, J., Tremblay, G., Lapoussière, A., Jose, C., Poulin, M., Gosselin, M., Gratton, Y., Michel, C., 2010. Prevalence, structure and properties of subsurface chlorophyll maxima in Canadian Arctic waters. Mar. Ecol. Prog. Ser. 412, 69–84. https://doi.org/10.3354/meps08666
McClenaghan, B., Fahner, N., Cote, D., Chawarski, J., McCarthy, A., Rajabi, H., Singer, G., Hajibabaei, M., 2020. Harnessing the power of eDNA metabarcoding for the detection of deep-sea fishes. PLOS ONE 15, e0236540. https://doi.org/10.1371/journal.pone.0236540
McLaughlin, F.A., Carmack, E.C., Macdonald, R.W., Bishop, J.K.B., 1996. Physical and geochemical properties across the Atlantic/Pacific water mass front in the southern Canadian Basin. J. Geophys. Res. Oceans 101, 1183–1197. https://doi.org/10.1029/95JC02634
McNicholl, D., Walkusz, W., Davoren, G., Majewski, A., Reist, J., 2016. Dietary characteristics of co-occurring polar cod (*Boreogadus saida*) and capelin (*Mallotus villosus*) in the Canadian Arctic, Darnley Bay. Polar Biol. 39. https://doi.org/10.1007/s00300-015-1834-5
McNicholl, D., Wolki, B., Ostertag, S., 2017. Traditional ecological knowledge and local observations of capelin (*Mallotus villosus*) in Darnley Bay, NT (No. 3144), Canadian Manuscript Report of Fisheries and Aquatic Sciences. Department of Fisheries and Oceans Canada, Winnipeg, Canada.
McQuinn, I.H., Winger, P.D., 2003. Tilt angle and target strength: target tracking of Atlantic cod (*Gadus morhua*) during trawling. ICES J. Mar. Sci. 60, 575–583. https://doi.org/10.1016/S1054-3139(03)000390
Mecklenburg, C., Stein, D., Sheiko, B., Chernova, N., Mecklenburg, T., Holladay, B., 2007. Russian-American long-term census of the Arctic: benthic fishes trawled in the Chukchi Sea and Bering Strait, August 2004. Northwest. Nat. 88, 168–187. https://doi.org/10.1898/1051-1733(2007)88[168:RLCOTA]2.0.CO;2
Mecklenburg, C.W., Lynghammar, A., Johannesen, E., Byrkjedal, I., Christiansen, J.S., Dolgov, A.V., Karamushko, O.V., Mecklenburg, T.A., Møller, P.R., Steinke, D., Wienerroither, R.M., 2018. Marine fishes of the Arctic region: volume 1 and 2 (Technical Report), CAFF Monitoring Series Reports. Conservation of Arctic Flora and Fauna.
Melnikov, S., Popov, V., 2009. The distribution and specific features of the biology of deepwater redfish *Sebastes mentella* (Scorpaenidae) during mating in the pelagial of the northern Atlantic. J. Ichthyol. 49, 300–312. https://doi.org/10.1134/S0032945209040031
Meyer, A., Sundfjord, A., Fer, I., Provost, C., Villacieros Robineau, N., Koenig, Z., Onarheim, I.H., Smedsrud, L.H., Duarte, P., Dodd, P.A., Graham, R.M., Schmidtko, S., Kauko, H.M., 2017. Winter to summer oceanographic observations in the Arctic Ocean north of Svalbard. J. Geophys. Res. Oceans 122, 6218–6237. https://doi.org/10.1002/2016JC012391
Moiseev, S.I., 1991. Observation of the vertical distribution and behavior of nektonic squids using manned submersibles. Bull. Mar. Sci. 49, 446–456.
Mowbray, F.K., 2002. Changes in the vertical distribution of capelin (*Mallotus villosus*) off Newfoundland. ICES J. Mar. Sci. 59, 942–949. https://doi.org/10.1006/jmsc.2002.1259
Münchow, A., Falkner, K.K., Melling, H., 2015. Baffin Island and West Greenland Current systems in northern Baffin Bay. Prog. Oceanogr. 132, 305–317. https://doi.org/10.1016/j.pocean.2014.04.001

Münchow, A., Melling, H., Falkner, K.K., 2006. An observational estimate of volume and freshwater flux leaving the Arctic Ocean through Nares Strait. J. Phys. Oceanogr. 36, 2025–2041. https://doi.org/10.1175/JPO2962.1

Myers, R.A., Mertz, G., Bishop, C.A., 1993. Cod spawning in relation to physical and biological cycles of the northern North-west Atlantic. Fish. Oceanogr. 2, 154–165. https://doi.org/10.1111/j.1365-2419.1993.tb00131.x

Nahrgang, J., Camus, L., Broms, F., Christiansen, J.S., Hop, H., 2010. Seasonal baseline levels of physiological and biochemical parameters in polar cod (*Boreogadus saida*): implications for environmental monitoring. Mar. Pollut. Bull. 60, 1336–1345. https://doi.org/10.1016/j.marpolbul.2010.03.004

Naito, Y., Costa, D.P., Adachi, T., Robinson, P.W., Fowler, M., Takahashi, A., 2013. Unravelling the mysteries of a mesopelagic diet: a large apex predator specializes on small prey. Funct. Ecol. 27, 710–717. https://doi.org/10.1111/1365-2435.12083

Neighbors, M.A., Nafpaktitis, B.G., 1982. Lipid compositions, water contents, swimbladder morphologies and buoyancies of nineteen species of midwater fishes (18 myctophids and 1 neoscopelid). Mar. Biol. 66, 207–215. https://doi.org/10.1007/BF00397024

Nelson, R.J., Bouchard, C., Fortier, L., Majewski, A.R., Reist, J.D., Præbel, K., Madsen, M.L., Rose, G.A., Kessel, S.T., Divoky, G.J., 2020. Circumpolar genetic population structure of polar cod, *Boreogadus saida*. Polar Biol. 43, 951–961. https://doi.org/10.1007/s00300-020-02660-z

Ng, A.K.Y., Andrews, J., Babb, D., Lin, Y., Becker, A., 2018. Implications of climate change for shipping: opening the Arctic seas. Wiley Interdiscip. Rev. Clim. Change 9, e507. https://doi.org/10.1002/wcc.507

Nicolaus, M., Katlein, C., Maslanik, J., Hendricks, S., 2012. Changes in Arctic sea ice result in increasing light transmittance and absorption. Geophys. Res. Lett. 39. https://doi.org/10.1029/2012GL053738

Norheim, E., Klevjer, T.A., Aksnes, D.L., 2016. Evidence for light-controlled migration amplitude of a sound scattering layer in the Norwegian Sea. Mar. Ecol. Prog. Ser. 551, 45–52. https://doi.org/10.3354/meps11731

Nøttestad, L., Giske, J., Holst, J.C., Huse, G., 1999. A length-based hypothesis for feeding migrations in pelagic fish. Can. J. Fish. Aquat. Sci. 56, 26–34. https://doi.org/10.1139/f99-222

Notz, D., Stroeve, J., 2018. The trajectory towards a seasonally ice-free Arctic Ocean. Curr. Clim. Change Rep. 4, 407–416. https://doi.org/10.1007/s40641-018-0113-2

Olsen, E., Aanes, S., Mehl, S., Holst, J.C., Aglen, A., Gjøsæter, H., 2010. Cod, haddock, saithe, herring, and capelin in the Barents Sea and adjacent waters: a review of the biological value of the area. ICES J. Mar. Sci. 67, 87–101. https://doi.org/10.1093/icesjms/fsp229

Olsen, R.E., Strand, E., Melle, W., Nørstebø, J.T., Lall, S.P., Ringø, E., Tocher, D.R., Sprague, M., 2020. Can mesopelagic mixed layers be used as feed sources for salmon aquaculture? Deep Sea Res. Part II Top. Stud. Oceanogr. 180, 104722. https://doi.org/10.1016/j.dsr2.2019.104722

Onarheim, I.H., Årthun, M., 2017. Toward an ice-free Barents Sea. Geophys. Res. Lett. 44, 8387–8395. https://doi.org/10.1002/2017GL074304

Oziel, L., Sirven, J., Gascard, J.C., 2016. The Barents Sea frontal zones and water masses variability (1980-2011). Ocean Sci. 12, 169–184. https://doi.org/10.5194/os-12-169-2016

Palma, D., Varnajot, A., Dalen, K., Basaran, I.K., Brunette, C., Bystrowska, M., Korablina, A.D., Nowicki, R.C., Ronge, T.A., 2019. Cruising the marginal ice zone: climate change and Arctic tourism. Polar Geogr. 42, 215–235. https://doi.org/10.1080/1088937X.2019.1648585

PAME, 2013. Large Marine Ecosystems (LME's) of the Arctic, PAME-led group of experts on the ecosystem approach to management. Protection of the Arctic Environment.

Pearre, S., 2003. Eat and run? The hunger/satiation hypothesis in vertical migration: history, evidence and consequences. Biol. Rev. Camb. Philos. Soc. 78, 1–79. https://doi.org/10.1017/S146479310200595X

Pedersen, T., Fossheim, M., 2008. Diet of 0-group stages of capelin (*Mallotus villosus*), herring (*Clupea harengus*) and cod (*Gadus morhua*) during spring and summer in the Barents Sea. Mar. Biol. 153, 1037–1046. https://doi.org/10.1007/s00227-007-0875-x

Pedro, S., Lemire, M., Hoover, C., Saint-Béat, B., Janjua, M.Y., Herbig, J., Geoffroy, M., Yunda-Guarin, G., Moisan, M.-A., Boissinot, J., Tremblay, J.-É., Little, M., Chan, L., Babin, M., Kenny, T.-A., Maps, F., 2023. Structure and function of the western Baffin Bay coastal and shelf ecosystem. Elem. Sci. Anthr. 11, 00015. https://doi.org/10.1525/elementa.2022.00015

Peña, M., Andrès, L., González-Quirós, R., 2023. Target strength of *Cyclothone species* with fat-filled swimbladders. J. Mar. Syst. 240, 103884. https://doi.org/10.1016/j.jmarsys.2023.103884

Peña, M., Cabrera-Gámez, J., Domínguez-Brito, A.C., 2020. Multi-frequency and light-avoiding characteristics of deep acoustic layers in the North Atlantic. Mar. Environ. Res. 154, 104842. https://doi.org/10.1016/j.marenvres.2019.104842

Pepin, P., 2013. Distribution and feeding of *Benthosema glaciale* in the western Labrador Sea: Fish–zooplankton interaction and the consequence to calanoid copepod populations. Deep Sea Res. Part Oceanogr. Res. Pap. 75, 119–134. https://doi.org/10.1016/j.dsr.2013.01.012

Pepin, P., Robert, D., Bouchard, C., Dower, J.F., Falardeau, M., Fortier, L., Jenkins, G.P., Leclerc, V., Levesque, K., Llopiz, J.K., Meekan, M.G., Murphy, H.M., Ringuette, M., Sirois, P., Sponaugle, S., 2015. Once upon a larva: revisiting the relationship between feeding success and growth in fish larvae. ICES J. Mar. Sci. 72, 359–373. https://doi.org/10.1093/icesjms/fsu201

Percy, J.A., Fife, F.J., 1985. Energy distribution in an Arctic coastal macrozooplankton community. Arctic 38, 39–42.

Perovich, D.K., 2005. On the aggregate-scale partitioning of solar radiation in Arctic sea ice during the surface heat budget of the Arctic Ocean (SHEBA) field experiment. J. Geophys. Res. Oceans 110. https://doi.org/10.1029/2004JC002512

Petrick, S., Riemann-Campe, K., Hoog, S., Growitsch, C., Schwind, H., Gerdes, R., Rehdanz, K., 2017. Climate change, future Arctic sea ice, and the competitiveness of European Arctic offshore oil and gas production on world markets. Ambio 46, 410–422. https://doi.org/10.1007/s13280-017-0957-z

Picheral, M., Catalano, C., Brousseau, D., Claustre, H., Coppola, L., Leymarie, E., Coindat, J., Dias, F., Fevre, S., Guidi, L., Irisson, J.O., Legendre, L., Lombard, F., Mortier, L., Penkerch, C., Rogge, A., Schmechtig, C., Thibault, S., Tixier, T., Waite, A., Stemmann, L., 2022. The Underwater Vision Profiler 6: an imaging sensor of particle size spectra and plankton, for autonomous and cabled platforms. Limnol. Oceanogr. Methods 20, 115–129. https://doi.org/10.1002/lom3.10475

Picheral, M., Guidi, L., Stemmann, L., Karl, D.M., Iddaoud, G., Gorsky, G., 2010. The Underwater Vision Profiler 5: an advanced instrument for high spatial resolution studies of particle size spectra and zooplankton. Limnol. Oceanogr. Methods 8, 462–473. https://doi.org/10.4319/lom.2010.8.462

Planque, B., Kristinsson, K., Astakhov, A., Bernreuther, M., Bethke, E., Drevetnyak, K., Nedreaas, K., Reinert, J., Rolskiy, A., Sigurðsson, T., Stransky, C., 2013. Monitoring beaked redfish (*Sebastes mentella*) in the North Atlantic, current challenges and future prospects. Aquat. Living Resour. 26, 293–306. https://doi.org/10.1051/alr/2013062

Polyakov, I.V., Alkire, M.B., Bluhm, B.A., Brown, K.A., Carmack, E.C., Chierici, M., Danielson, S.L., Ellingsen, I., Ershova, E.A., Gårdfeldt, K., Ingvaldsen, R.B., Pnyushkov, A.V., Slagstad, D., Wassmann, P., 2020. Borealization of the Arctic Ocean in response to anomalous advection from sub-Arctic seas. Front. Mar. Sci. 7, 491. https://doi.org/10.3389/fmars.2020.00491

Polyakov, I.V., Pnyushkov, A.V., Alkire, M.B., Ashik, I.M., Baumann, T.M., Carmack, E.C., Goszczko, I., Guthrie, J., Ivanov, V.V., Kanzow, T., Krishfield, R., Kwok, R., Sundfjord, A., Morison, J., Rember, R., Yulin, A., 2017. Greater role for Atlantic inflows on sea-ice loss in the Eurasian Basin of the Arctic Ocean. Science 356, 285–291. https://doi.org/10.1126/science.aai8204

Præbel, K., Ramløv, H., 2005. Antifreeze activity in the gastrointestinal fluids of *Arctogadus glacialis* (Peters 1874) is dependent on food type. J. Exp. Biol. 208, 2609–2613. https://doi.org/10.1242/jeb.01666

Prellezo, R., 2019. Exploring the economic viability of a mesopelagic fishery in the Bay of Biscay. ICES J. Mar. Sci. 76, 771–779. https://doi.org/10.1093/icesjms/fsy001

Proud, R., Cox, M.J., Brierley, A.S., 2017. Biogeography of the global ocean's mesopelagic zone. Curr. Biol. 27, 113–119. https://doi.org/10.1016/j.cub.2016.11.003

Proud, R., Handegard, N.O., Kloser, R.J., Cox, M.J., Brierley, A.S., 2019. From siphonophores to deep scattering layers: uncertainty ranges for the estimation of global mesopelagic fish biomass. ICES J. Mar. Sci. 76, 718–733. https://doi.org/10.1093/icesjms/fsy037

Rabe, B., Karcher, M., Kauker, F., Schauer, U., Toole, J.M., Krishfield, R.A., Pisarev, S., Kikuchi, T., Su, J., 2014. Arctic Ocean basin liquid freshwater storage trend 1992–2012. Geophys. Res. Lett. 41, 961–968. https://doi.org/10.1002/2013GL058121

Rand, K.M., Whitehouse, A., Logerwell, E.A., Ahgeak, E., Hibpshman, R., Parker-Stetter, S., 2013. The diets of polar cod (*Boreogadus saida*) from August 2008 in the US Beaufort Sea. Polar Biol. 36, 907–912. https://doi.org/10.1007/s00300-013-1303-y

Randelhoff, A., Lacour, L., Marec, C., Leymarie, E., Lagunas, J., Xing, X., Darnis, G., Penkerc'h, C., Sampei, M., Fortier, L., D'Ortenzio, F., Claustre, H., Babin, M., 2020. Arctic mid-winter phytoplankton growth revealed by autonomous profilers. Sci. Adv. 6, eabc2678. https://doi.org/10.1126/sciadv.abc2678

Raskoff, K.A., Purcell, J.E., Hopcroft, R.R., 2005. Gelatinous zooplankton of the Arctic Ocean: in situ observations under the ice. Polar Biol. 28, 207–217. https://doi.org/10.1007/s00300-004-0677-2

Raymond, J.A., Hassel, A., 2000. Some characteristics of freezing avoidance in two osmerids, rainbow smelt and capelin. J. Fish Biol. 57, 1–7. https://doi.org/10.1111/j.1095-8649.2000.tb02240.x

Renaud, P.E., Berge, J., Varpe, Ø., Lønne, O.J., Nahrgang, J., Ottesen, C., Hallanger, I., 2012. Is the poleward expansion by Atlantic cod and haddock threatening native polar cod, *Boreogadus saida*? Polar Biol. 35, 401–412. https://doi.org/10.1007/s00300-011-1085-z

Renaud, P.E., Daase, M., Banas, N.S., Gabrielsen, T.M., Søreide, J.E., Varpe, Ø., Cottier, F., Falk-Petersen, S., Halsband, C., Vogedes, D., Heggland, K., Berge, J., 2018. Pelagic food-webs in a changing Arctic: a trait-based perspective suggests a mode of resilience. ICES J. Mar. Sci. 75, 1871–1881. https://doi.org/10.1093/icesjms/fsy063

Reynolds, J.B., 1997. Ecology of overwintering fishes in Alaskan freshwaters, in: Milner, A.M., Oswood, M.W. (Eds.), Freshwaters of Alaska: Ecological Syntheses, Ecological Studies. Springer, New York, NY, pp. 281–302. https://doi.org/10.1007/978-1-4612-0677-4_11

Richardson, A.J., Brown, C.J., Brander, K., Bruno, J.F., Buckley, L., Burrows, M.T., Duarte, C.M., Halpern, B.S., Hoegh-Guldberg, O., Holding, J., Kappel, C.V., Kiessling, W., Moore, P.J., O'Connor, M.I., Pandolfi, J.M., Parmesan, C., Schoeman, D.S., Schwing, F., Sydeman, W.J., Poloczanska, E.S., 2012. Climate change and marine life. Biol. Lett. 8, 907–909. https://doi.org/10.1098/rsbl.2012.0530

Robichaud, D., Rose, G.A., 2004. Migratory behaviour and range in Atlantic cod: inference from a century of tagging. Fish Fish. 5, 185–214. https://doi.org/10.1111/j.1467-2679.2004.00141.x

Robinson, P.W., Costa, D.P., Crocker, D.E., Gallo-Reynoso, J.P., Champagne, C.D., Fowler, M.A., Goetsch, C., Goetz, K.T., Hassrick, J.L., Hückstädt, L.A., Kuhn, C.E., Maresh, J.L., Maxwell, S.M., McDonald, B.I., Peterson, S.H., Simmons, S.E., Teutschel, N.M., Villegas-Amtmann, S., Yoda, K., 2012. Foraging behavior and success of a mesopelagic predator in the Northeast Pacific Ocean: insights from a data-rich species, the northern elephant seal. PLOS ONE 7, e36728. https://doi.org/10.1371/journal.pone.0036728

Rose, G.A., 2004. Reconciling overfishing and climate change with stock dynamics of Atlantic cod (*Gadus morhua*) over 500 years. Can. J. Fish. Aquat. Sci. 61, 1553–1557. https://doi.org/10.1139/f04-173

Røstad, A., Kaartvedt, S., Aksnes, D.L., 2016. Light comfort zones of mesopelagic acoustic scattering layers in two contrasting optical environments. Deep Sea Res. Part Oceanogr. Res. Pap. 113, 1–6. https://doi.org/10.1016/j.dsr.2016.02.020

Rudels, B., 2015. Arctic Ocean circulation, processes and water masses: a description of observations and ideas with focus on the period prior to the international polar year 2007–2009. Prog. Oceanogr., Oceanography of the Arctic and North Atlantic Basins 132, 22–67. https://doi.org/10.1016/j.pocean.2013.11.006

Rudels, B., Schauer, U., Björk, G., Korhonen, M., Pisarev, S., Rabe, B., Wisotzki, A., 2013. Observations of water masses and circulation with focus on the Eurasian Basin of the Arctic Ocean from the 1990s to the late 2000s. Ocean Sci. 9, 147–169. https://doi.org/10.5194/os-9-147-2013

Ryan, T.E., Downie, R.A., Kloser, R.J., Keith, G., 2015. Reducing bias due to noise and attenuation in open-ocean echo integration data. ICES J. Mar. Sci. 72, 2482–2493. https://doi.org/10.1093/icesjms/fsv121

Saba, G.K., Burd, A.B., Dunne, J.P., Hernández-León, S., Martin, A.H., Rose, K.A., Salisbury, J., Steinberg, D.K., Trueman, C.N., Wilson, R.W., Wilson, S.E., 2021. Toward a better understanding of fish-based contribution to ocean carbon flux. Limnol. Oceanogr. 66, 1639–1664. https://doi.org/10.1002/lno.11709

Sameoto, D., 1989. Feeding ecology of the lantern fish *Benthosema glaciale* in a subarctic region. Polar Biol. 9, 169–178. https://doi.org/10.1007/BF00297172

Sargent, J.R., Falk-Petersen, S., 1981. Ecological investigations on the zooplankton community in Balsfjorden, northern Norway: lipids and fatty acids in *Meganyctiphanes norvegica*, *Thysanoessa raschi* and *T. inermis* during mid-winter. Mar. Biol. 62, 131–137. https://doi.org/10.1007/BF00388175

Saunders, R.A., Collins, M.A., Stowasser, G., Tarling, G.A., 2017. Southern Ocean mesopelagic fish communities in the Scotia Sea are sustained by mass immigration. Mar. Ecol. Prog. Ser. 569, 173–185. https://doi.org/10.3354/meps12093

Saunders, R.A., Hill, S.L., Tarling, G.A., Murphy, E.J., 2019. Myctophid fish (Family Myctophidae) are central consumers in the food web of the Scotia Sea (Southern Ocean). Front. Mar. Sci. 6, 530. https://doi.org/10.3389/fmars.2019.00530

Sawada, K., Furusawa, M., Williamson, N.J., 1993. Conditions for the precise measurement of fish target strength in situ. J. Mar. Acoust. Soc. Jpn. 20, 73–79. https://doi.org/10.3135/jmasj.20.73

Sawada, K., Takahashi, H., Takao, Y., Watanabe, K., Horne, John.K., McClatchie, S., Abe, K., 2004. Development of an acoustic-optical system to estimate target-strengths and tilt angles from fish aggregations, in: MTS/IEEE Techno-Ocean 2004. pp. 395–400. https://doi.org/10.1109/OCEANS.2004.1402949

Sawada, K., Uchikawa, K., Matsuura, T., Sugisaki, H., Amakasu, K., Abe, K., 2011. In situ and ex situ target strength measurement of mesopelagic lanternfish, *Diaphys theta* (Family Myctophidae). J. Mar. Sci. Technol. 19. https://doi.org/10.51400/2709-6998.2196

Schauer, U., Fahrbach, E., Osterhus, S., Rohardt, G., 2004. Arctic warming through the Fram Strait: oceanic heat transport from 3 years of measurements. J. Geophys. Res. Oceans 109. https://doi.org/10.1029/2003JC001823

Schauer, U., Loeng, H., Rudels, B., Ozhigin, V.K., Dieck, W., 2002. Atlantic water flow through the Barents and Kara seas. Deep Sea Res. Part Oceanogr. Res. Pap. 49, 2281–2298. https://doi.org/10.1016/S0967-0637(02)00125-5

Schembri, S., Deschepper, I., Myers, P.G., Sirois, P., Fortier, L., Bouchard, C., Maps, F., 2022. Arctic cod (*Boreogadus saida*) hatching in the Hudson Bay system: testing of the freshwater winter refuge hypothesis. Elem. Sci. Anthr. 9, 00042. https://doi.org/10.1525/elementa.2021.00042

Seidelmann, P.K., 1992. Explanatory supplement to the astronomical almanac. University Science Books, Washington, DC.

Serreze, M.C., Barry, R.G., 2011. Processes and impacts of Arctic amplification: a research synthesis. Glob. Planet. Change 77, 85–96. https://doi.org/10.1016/j.gloplacha.2011.03.004

Serreze, M.C., Meier, W.N., 2019. The Arctic's sea ice cover: trends, variability, predictability, and comparisons to the Antarctic. Ann. N. Y. Acad. Sci. 1436, 36–53. https://doi.org/10.1111/nyas.13856

Shupe, M.D., Rex, M., Dethloff, K., Damm, E., Fong, A.A., Gradinger, R., Heuzé, C., Loose, B., Makarov, A., Maslowski, W., Nicolaus, M., Perovich, D., Rabe, B., Rinke, A., Sokolov, V., Sommerfeld, A., 2020. The MOSAiC expedition: a year drifting with the Arctic sea ice. NOAA Arct. Rep. Card 2020. https://doi.org/10.25923/9G3V-XH92

Siegel, D.A., DeVries, T., Cetinić, I., Bisson, K.M., 2023. Quantifying the ocean's biological pump and its carbon cycle impacts on global scales. Annu. Rev. Mar. Sci. 15, 329–356. https://doi.org/10.1146/annurev-marine-040722-115226

Siegelman-Charbit, L., Planque, B., 2016. Abundant mesopelagic fauna at oceanic high latitudes. Mar. Ecol. Prog. Ser. 546, 277–282. https://doi.org/10.3354/meps11661

Simmonds, J., MacLennan, D.N., 2005. Fisheries acoustics: theory and practice. John Wiley & Sons.

Smetacek, V., Nicol, S., 2005. Polar ocean ecosystems in a changing world. Nature 437, 362–368. https://doi.org/10.1038/nature04161

Smirnova, E.V., Chernova, N.V., Karamushko, O.V., 2022. Species composition, abundance, distribution features and size characteristics of fish of the Genus *Liparis* (Cottiformes: Liparidae) in the East-Siberian and Laptev Seas. J. Ichthyol. 62, 850–862. https://doi.org/10.1134/S0032945222050174

Snoeijs-Leijonmalm, P., Flores, H., Sakinan, S., Hildebrandt, N., Svenson, A., Castellani, G., Vane, K., Mark, F.C., Heuzé, C., Tippenhauer, S., Niehoff, B., Hjelm, J., Hentati Sundberg, J., Schaafsma, F.L., Engelmann, R., The EFICA-MOSAiC team, 2022. Unexpected fish and squid in the central Arctic deep scattering layer. Sci. Adv. 8, eabj7536. https://doi.org/10.1126/sciadv.abj7536

Snoeijs-Leijonmalm, P., Gjøsæter, H., Ingvaldsen, R.B., Knutsen, T., Korneliussen, R., Ona, E., Skjoldal, H.R., Stranne, C., Mayer, L., Jakobsson, M., Gårdfeldt, K., 2021. A deep scattering layer under the North Pole pack ice. Prog. Oceanogr. 194, 102560. https://doi.org/10.1016/j.pocean.2021.102560

Sobradillo, B., Christiansen, S., Røstad, A., Kaartvedt, S., 2022. Individual daytime swimming of mesopelagic fishes in the world's warmest twilight zone. Deep Sea Res. Part Oceanogr. Res. Pap. 190, 103897. https://doi.org/10.1016/j.dsr.2022.103897

Spence, A.R., Tingley, M.W., 2020. The challenge of novel abiotic conditions for species undergoing climate-induced range shifts. Ecography 43, 1571–1590. https://doi.org/10.1111/ecog.05170

St. John, M.A., Borja, A., Chust, G., Heath, M., Grigorov, I., Mariani, P., Martin, A.P., Santos, R.S., 2016. A dark hole in our understanding of marine ecosystems and their services: perspectives from the mesopelagic community. Front. Mar. Sci. 3, 31. https://doi.org/10.3389/fmars.2016.00031

Staby, A., Røstad, A., Kaartvedt, S., 2011. Long-term acoustical observations of the mesopelagic fish *Maurolicus muelleri* reveal novel and varied vertical migration patterns. Mar. Ecol. Prog. Ser. 441, 241–255. https://doi.org/10.3354/meps09363

Stanton, T.K., Wiebe, P.H., Chu, D., Benfield, M.C., Scanlon, L., Martin, L., Eastwood, R.L., 1994. On acoustic estimates of zooplankton biomass. ICES J. Mar. Sci. 51, 505–512. https://doi.org/10.1006/jmsc.1994.1051

Star, B., Boessenkool, S., Gondek, A.T., Nikulina, E.A., Hufthammer, A.K., Pampoulie, C., Knutsen, H., André, C., Nistelberger, H.M., Dierking, J., Petereit, C., Heinrich, D., Jakobsen, K.S., Stenseth, N.C., Jentoft, S., Barrett, J.H., 2017. Ancient DNA reveals the Arctic origin of Viking Age cod from Haithabu, Germany. Proc. Natl. Acad. Sci. 114, 9152–9157. https://doi.org/10.1073/pnas.1710186114

Steiner, N.S., Bowman, J., Campbell, K., Chierici, M., Eronen-Rasimus, E., Falardeau, M., Flores, H., Fransson, A., Herr, H., Insley, S.J., Kauko, H.M., Lannuzel, D., Loseto, L., Lynnes, A., Majewski, A., Meiners, K.M., Miller, L.A., Michel, L.N., Moreau, S., Nacke, M., Nomura, D., Tedesco, L., van Franeker, J.A., van Leeuwe, M.A., Wongpan, P., 2021. Climate change impacts on sea-ice ecosystems and associated ecosystem services. Elem. Sci. Anthr. 9, 1–55. https://doi.org/10.1525/elementa.2021.00007

Storrie, L., Hussey, N.E., MacPhee, S.A., O'Corry-Crowe, G., Iacozza, J., Barber, D.G., Nunes, A., Loseto, L.L., 2022. Year-round dive characteristics of male beluga whales from the eastern Beaufort Sea population indicate seasonal shifts in foraging strategies. Front. Mar. Sci. 8, 715412. https://doi.org/10.3389/fmars.2021.715412

St-Pierre, J.-F., de Lafontaine, Y., 1995. Fecundity and reproduction characteristics of beaked redfish (*Sebastes fasciatus* and *S. mentella*) in the Gulf of St. Lawrence (No. 2059), Can Tech Rep Fish Aquat Sci.

Stroeve, J., Notz, D., 2018. Changing state of Arctic sea ice across all seasons. Environ. Res. Lett. 13, 103001. https://doi.org/10.1088/1748-9326/aade56

Süfke, L., Piepenburg, D., Von Dorrien, C.F., 1998. Body size, sex ratio and diet composition of *Arctogadus glacialis* (Peters, 1874) (Pisces: Gadidae) in the northeast water polynya (Greenland). Polar Biol. 20, 357–363. https://doi.org/10.1007/s003000050314

Sutton, T.T., Clark, M.R., Dunn, D.C., Halpin, P.N., Rogers, A.D., Guinotte, J., Bograd, S.J., Angel, M.V., Perez, J.A.A., Wishner, K., Haedrich, R.L., Lindsay, D.J., Drazen, J.C., Vereshchaka, A., Piatkowski, U., Morato, T., Błachowiak-Samołyk, K., Robison, B.H., Gjerde, K.M., Pierrot-Bults, A., Bernal, P., Reygondeau, G., Heino, M., 2017. A global biogeographic classification of the mesopelagic zone. Deep Sea Res. Part Oceanogr. Res. Pap. 126, 85–102. https://doi.org/10.1016/j.dsr.2017.05.006

Tang, C.C.L., Ross, C.K., Yao, T., Petrie, B., DeTracey, B.M., Dunlap, E., 2004. The circulation, water masses and sea-ice of Baffin Bay. Prog. Oceanogr. 63, 183–228. https://doi.org/10.1016/j.pocean.2004.09.005

Timmermans, M.-L., Marshall, J., 2020. Understanding Arctic Ocean circulation: a review of ocean dynamics in a changing climate. J. Geophys. Res. Oceans 125, 1–35. https://doi.org/10.1029/2018JC014378

Tremblay, J.-É., Anderson, L.G., Matrai, P., Coupel, P., Bélanger, S., Michel, C., Reigstad, M., 2015. Global and regional drivers of nutrient supply, primary production and CO2 drawdown in the changing Arctic Ocean. Prog. Oceanogr. 139, 171–196. https://doi.org/10.1016/j.pocean.2015.08.009

Tremblay, J.-É., Hattori, H., Michel, C., Ringuette, M., Mei, Z.-P., Lovejoy, C., Fortier, L., Hobson, K.A., Amiel, D., Cochran, K., 2006. Trophic structure and pathways of biogenic carbon flow in the eastern north water polynya. Prog. Oceanogr. 71, 402–425. https://doi.org/10.1016/j.pocean.2006.10.006

Tremblay, J.-É., Simpson, K., Martin, J., Miller, L., Gratton, Y., Barber, D., Price, N.M., 2008. Vertical stability and the annual dynamics of nutrients and chlorophyll fluorescence in the coastal, southeast Beaufort Sea. J. Geophys. Res. Oceans 113. https://doi.org/10.1029/2007JC004547

Turner, J.R., White, E.M., Collins, M.A., Partridge, J.C., Douglas, R.H., 2009. Vision in lanternfish (Myctophidae): adaptations for viewing bioluminescence in the deep-sea. Deep Sea Res. Part Oceanogr. Res. Pap. 56, 1003–1017. https://doi.org/10.1016/j.dsr.2009.01.007

Twiname, S., Audzijonyte, A., Blanchard, J.L., Champion, C., de la Chesnais, T., Fitzgibbon, Q.P., Fogarty, H.E., Hobday, A.J., Kelly, R., Murphy, K.J., Oellermann, M., Peinado, P., Tracey, S., Villanueva, C., Wolfe, B., Pecl, G.T., 2020. A cross-scale framework to support a mechanistic understanding and modelling of marine climate-driven species redistribution, from individuals to communities. Ecography 43, 1764–1778. https://doi.org/10.1111/ecog.04996

Urmy, S.S., Benoit-Bird, K.J., 2021. Fear dynamically structures the ocean's pelagic zone. Curr. Biol. 31, 5086-5092.e3. https://doi.org/10.1016/j.cub.2021.09.003

Urmy, S.S., Horne, J.K., 2016. Multi-scale responses of scattering layers to environmental variability in Monterey Bay, California. Deep Sea Res. Part Oceanogr. Res. Pap. 113, 22–32. https://doi.org/10.1016/j.dsr.2016.04.004

Urmy, S.S., Horne, J.K., Barbee, D.H., 2012. Measuring the vertical distributional variability of pelagic fauna in Monterey Bay. ICES J. Mar. Sci. 69, 184–196. https://doi.org/10.1093/icesjms/fsr205

Vader, A., Marquardt, M., Meshram, A.R., Gabrielsen, T.M., 2015. Key Arctic phototrophs are widespread in the polar night. Polar Biol. 38, 13–21. https://doi.org/10.1007/s00300-014-1570-2

van Denderen, P.D., Lindegren, M., MacKenzie, B.R., Watson, R.A., Andersen, K.H., 2018. Global patterns in marine predatory fish. Nat. Ecol. Evol. 2, 65–70. https://doi.org/10.1038/s41559-017-0388-z

Vihma, T., 2014. Effects of Arctic sea ice decline on weather and climate: a review. Surv. Geophys. 35, 1175–1214. https://doi.org/10.1007/s10712-014-9284-0
Vihtakari, M., Welcker, J., Moe, B., Chastel, O., Tartu, S., Hop, H., Bech, C., Descamps, S., Gabrielsen, G.W., 2018. Black-legged kittiwakes as messengers of Atlantification in the Arctic. Sci. Rep. 8, 1178. https://doi.org/10.1038/s41598-017-19118-8
Vincent, R.F., 2019. A study of the north water polynya ice arch using four decades of satellite data. Sci. Rep. 9, 20278. https://doi.org/10.1038/s41598-019-56780-6
Voronin, V.P., Nemova, N.N., Ruokolainen, T.R., Artemenkov, D.V., Rolskii, A.Y., Orlov, A.M., Murzina, S.A., 2021. Into the deep: new data on the lipid and fatty acid profile of redfish *Sebastes mentella* inhabiting different depths in the Irminger Sea. Biomolecules 11, 704. https://doi.org/10.3390/biom11050704
Wang, Y.-G., Tseng, L.-C., Lin, M., Hwang, J.-S., 2019. Vertical and geographic distribution of copepod communities at late summer in the Amerasian Basin, Arctic Ocean. PLOS ONE 14, e0219319. https://doi.org/10.1371/journal.pone.0219319
Warrant, E., 2000. The eyes of deep-sea fishes and the changing nature of visual scenes with depth. Philos. Trans. R. Soc. B Biol. Sci. 355, 1155–1159.
Warrant, E.J., Locket, N.A., 2004. Vision in the deep sea. Biol. Rev. 79, 671–712. https://doi.org/10.1017/S1464793103006420
Wassmann, P., Kosobokova, K.N., Slagstad, D., Drinkwater, K.F., Hopcroft, R.R., Moore, S.E., Ellingsen, I., Nelson, R.J., Carmack, E., Popova, E., Berge, J., 2015. The contiguous domains of Arctic Ocean advection: trails of life and death. Prog. Oceanogr. 139, 42–65. https://doi.org/10.1016/j.pocean.2015.06.011
Wathne, J.A., Haug, T., Lydersen, C., 2000. Prey preference and niche overlap of ringed seals *Phoca hispida* and harp seals *P. groenlandica* in the Barents Sea. Mar. Ecol. Prog. Ser. 194, 233–239. https://doi.org/10.3354/meps194233
Wekerle, C., Wang, Q., Danilov, S., Jung, T., Schröter, J., 2013. The Canadian Arctic Archipelago throughflow in a multiresolution global model: model assessment and the driving mechanism of interannual variability. J. Geophys. Res. Oceans 118, 4525–4541. https://doi.org/10.1002/jgrc.20330
Welch, H.E., Bergmann, M.A., Siferd, T.D., Martin, K.A., Curtis, M.F., Crawford, R.E., Conover, R.J., Hop, H., 1992. Energy flow through the marine ecosystem of the Lancaster Sound region, Arctic Canada. Arctic 45, 343–357.
Werner, I., Auel, H., Garrity, C., Hagen, W., 1999. Pelagic occurrence of the sympagic amphipod *Gammarus wilkitzkii* in ice-free waters of the Greenland Sea – dead end or part of life-cycle? Polar Biol. 22, 56–60. https://doi.org/10.1007/s003000050390
Wiborg, K.F., Gjøsæter, J., Beck, I.M., 1984. The squid *Gonatus fabricii* (Lichtenstein) investigations in the Norwegian Sea and Western Barents Sea 1982-1983 (Report), ICES Council Meeting Papers. ICES.
Widder, E., 2002. Bioluminescence and the pelagic visual environment. Mar. Freshw. Behav. Physiol. 35, 1–26. https://doi.org/10.1080/10236240290025581
Widder, E.A., 1999. Bioluminescence, in: Archer, S.N., Djamgoz, M.B.A., Loew, E.R., Partridge, J.C., Vallerga, S. (Eds.), Adaptive Mechanisms in the Ecology of Vision. Springer Netherlands, Dordrecht, pp. 555–581. https://doi.org/10.1007/978-94-017-0619-3_19
Wold, A., Jæger, I., Hop, H., Gabrielsen, G.W., Falk-Petersen, S., 2011. Arctic seabird food chains explored by fatty acid composition and stable isotopes in Kongsfjorden, Svalbard. Polar Biol. 34, 1147–1155. https://doi.org/10.1007/s00300-011-0975-4
Wollenburg, J.E., Iversen, M., Katlein, C., Krumpen, T., Nicolaus, M., Castellani, G., Peeken, I., Flores, H., 2020. New observations of the distribution, morphology and dissolution dynamics of cryogenic gypsum in the Arctic Ocean. The Cryosphere 14, 1795–1808. https://doi.org/10.5194/tc-14-1795-2020
Wood, S.N., 2017. Generalized additive models: an introduction with R, second edition, 2nd ed. Chapman and Hall/CRC, Boca Raton. https://doi.org/10.1201/9781315370279

Woodgate, R., Peralta-Ferriz, C., 2021. Warming and freshening of the Pacific inflow to the Arctic from 1990-2019 implying dramatic shoaling in Pacific winter water ventilation of the Arctic water column. Geophys. Res. Lett. 48, 1–11. https://doi.org/10.1029/2021GL092528

Woods, B., Walters, A., Hindell, M., Trebilco, R., 2020. Isotopic insights into mesopelagic niche space and energy pathways on the southern Kerguelen Plateau. Deep Sea Res. Part II Top. Stud. Oceanogr., Ecosystem drivers of food webs on the Kerguelen Axis of the Southern Ocean 174, 104657. https://doi.org/10.1016/j.dsr2.2019.104657

Worm, B., Lotze, H.K., 2021. Chapter 21 - Marine biodiversity and climate change, in: Letcher, T.M. (Ed.), Climate Change (Third Edition). Elsevier, pp. 445–464. https://doi.org/10.1016/B978-0-12-821575-3.00021-9

Xavier, J., Cherel, Y., Allcock, A., Rosa, R., Sabirov, R., Blicher, M., Golikov, A., 2018. A review on the biodiversity, distribution and trophic role of cephalopods in the Arctic and Antarctic marine ecosystems under a changing ocean. Mar. Biol. 165, 1–26. https://doi.org/10.1007/s00227-018-3352-9

Yaragina, N.A., Bogstad, B., Kovalev, Y.A., 2009. Variability in cannibalism in northeast Arctic cod (*Gadus morhua*) during the period 1947–2006. Mar. Biol. Res. 5, 75–85. https://doi.org/10.1080/17451000802512739

Young, R.E., 1983. Oceanic bioluminescence: an overview of general functions. Bull. Mar. Sci. 33, 829–845.

Zhang, R., Li, Y., Liu, Q., Puqing, S., Li, H., Wang, R., Ding, S., Lin, L., 2022. Glacier lanternfish (*Benthosema glaciale*) first found on the continental slope of the Pacific Arctic. Polar Biol. 45. https://doi.org/10.1007/s00300-021-02988-0

Zhuang, Z., Lavery, A.C., 2021. Target density estimation of mesopelagic fish using a towed, broadband, split-beam, acoustic scattering system. J. Acoust. Soc. Am. 150, A255. https://doi.org/10.1121/10.0008200

Zolich, A., De La Torre, P.R., Rodwell, S., Geoffroy, M., Johnsen, G., Berge, J., 2018. An ice-tethered buoy for fish and plankton research, in: OCEANS 2018 MTS/IEEE Charleston. IEEE, Charleston, SC, pp. 1–7. https://doi.org/10.1109/OCEANS.2018.8604603

Appendices

Supplementary material for Chapter 2

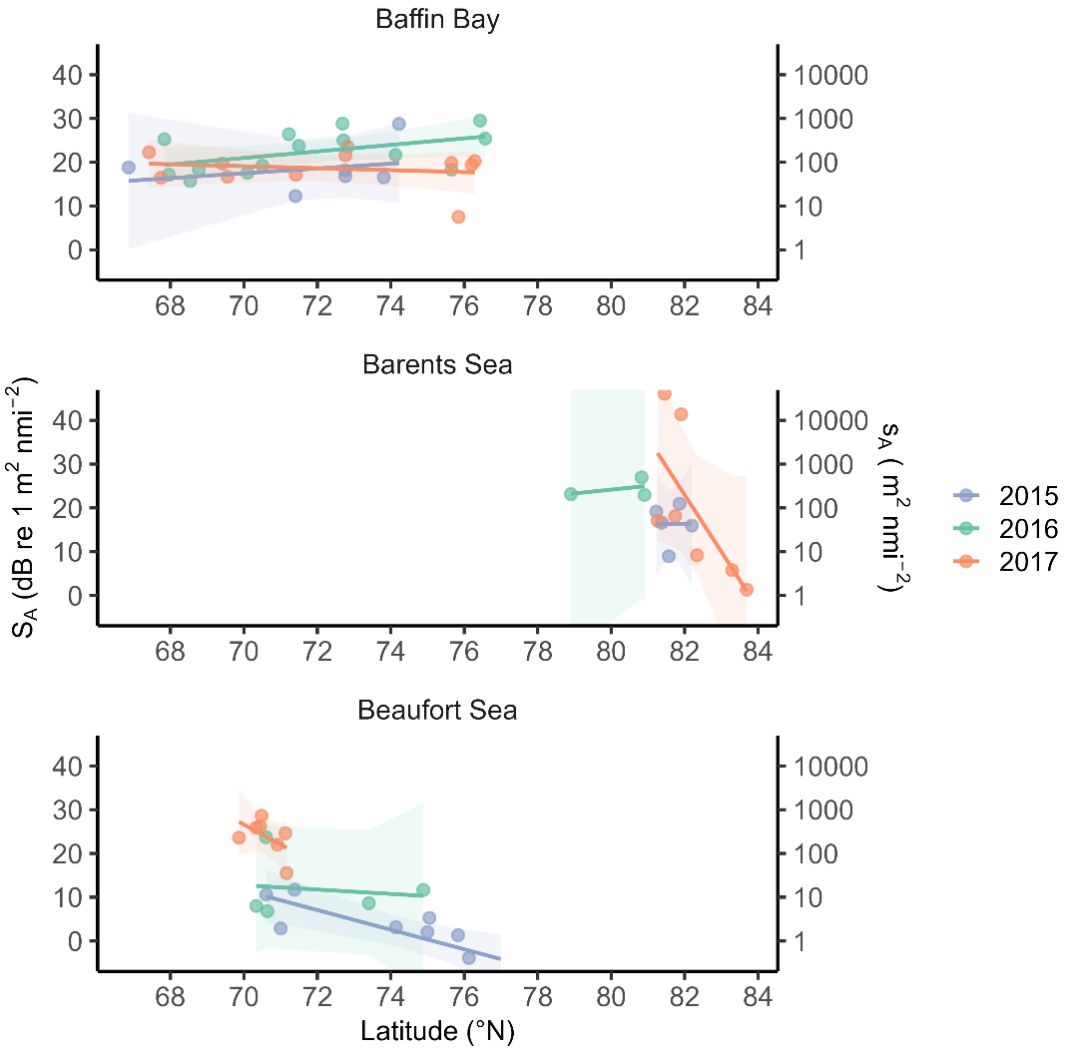

Figure S2-1. Linear regressions of mesopelagic S_A (dB re 1 m^2 nmi^{-2}) in function of latitude for each Arctic region per year and 95 % confidence interval (shaded areas).

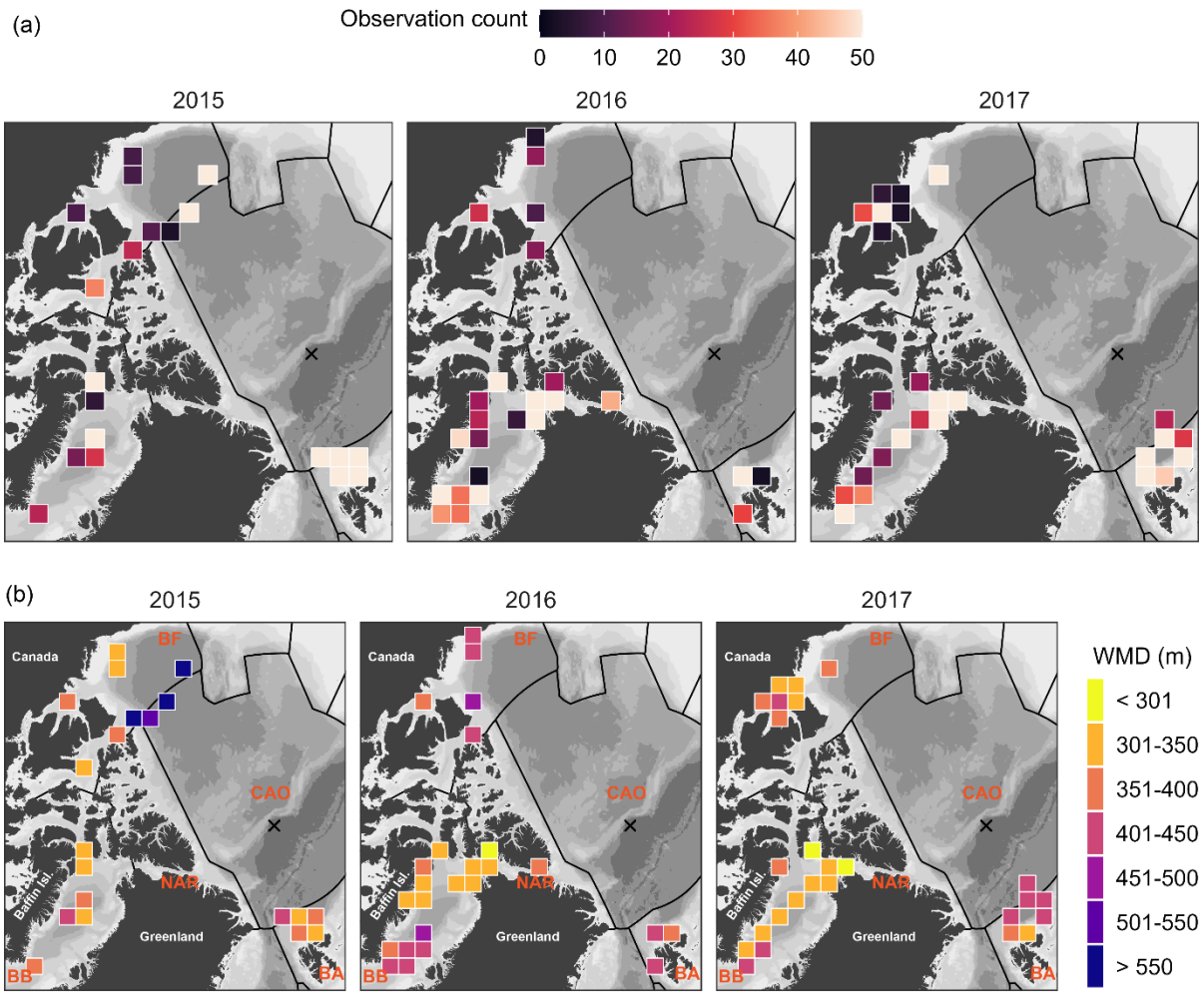

Figure S2-2. (a) Number of 10-min acoustic sample per 150 km grid cell per year and (b) weighted mean depth (WMD) of the mesopelagic layer in 2015, 2016, and 2017.

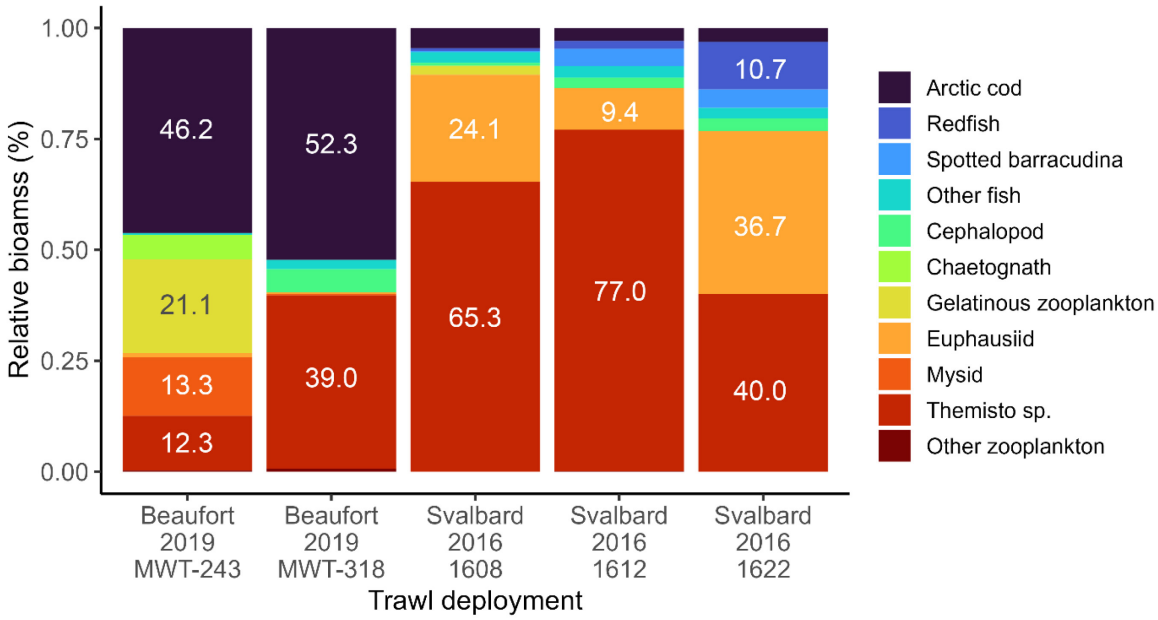

Figure S2-3. Relative biomass of mesopelagic organisms in the Beaufort Sea in 2019 and in the northern Barents Sea in 2016.

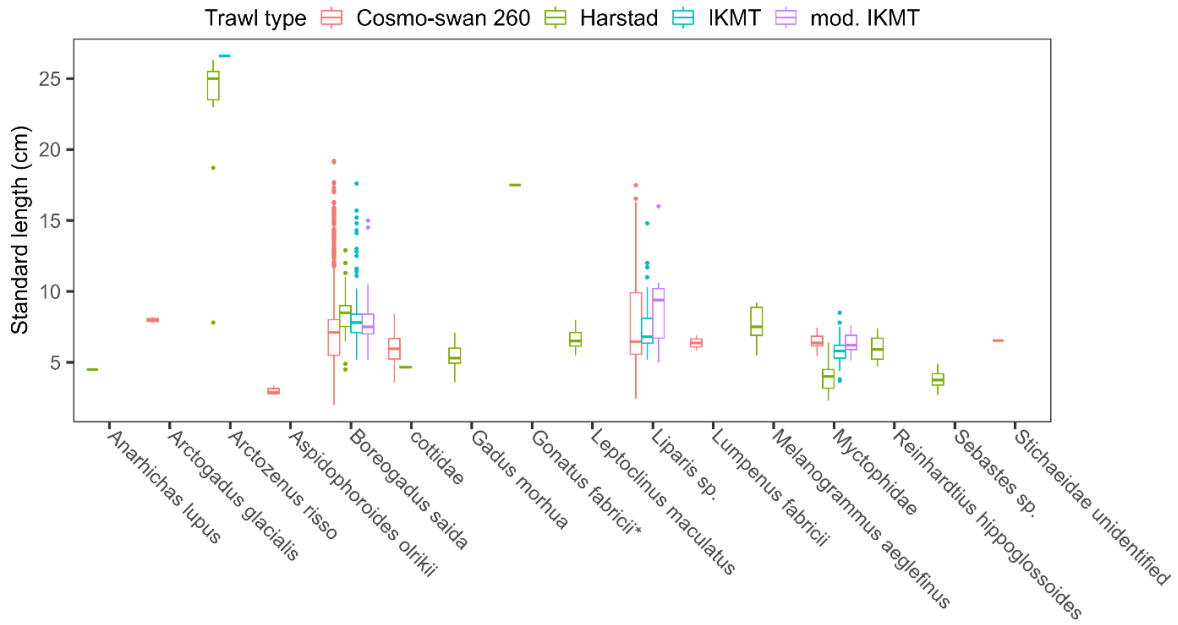

Figure S2-4. Length distribution of mesopelagic fish per trawl type across all regions and years. The Cosmo-swan 260 trawl was deployed from the F/V *Frosti* in the Beaufort Sea, Harstad trawl from the R/V *Helmer Hanssen* in the northern Barents Sea, and IKMT and modified IKMT from the CCGS *Amundsen* in Baffin Bay. *only one *Gonatus fabricii* was measured.

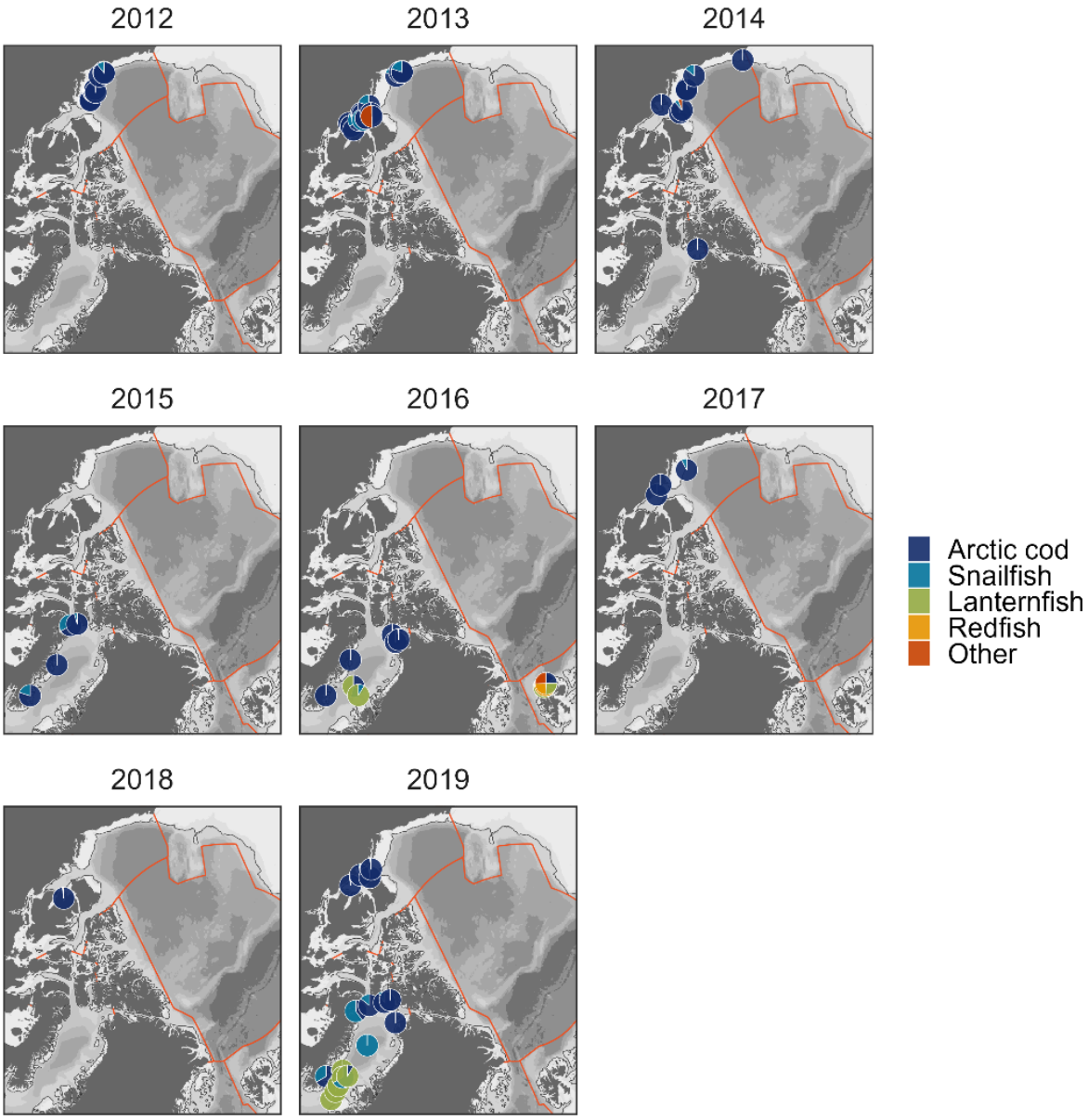

Figure S2-5. Map of the relative abundance of mesopelagic fish at each station per year.

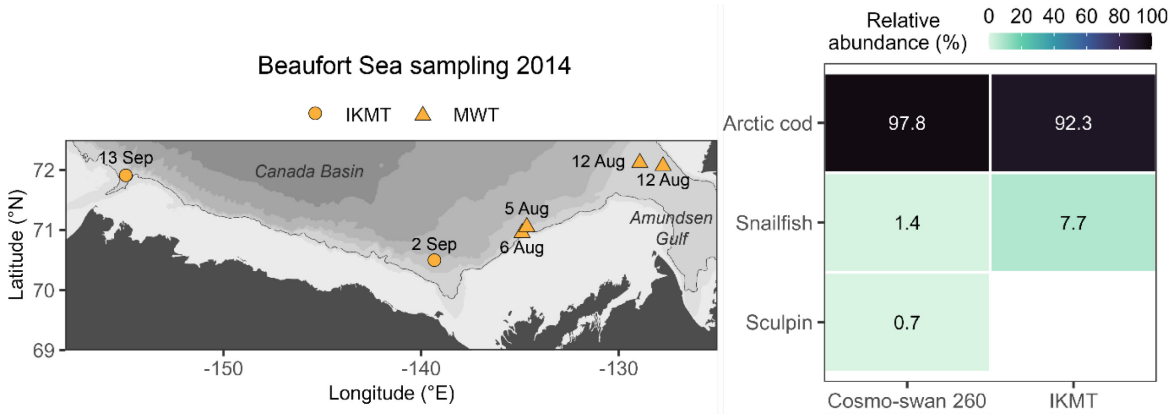

Figure S2-6. Comparison of the relative abundance calculated from the Cosmo-swan 260 and IKMT mid-water trawls deployed in the Beaufort Sea in 2014. I selected deployments were on the continental break of the Beaufort Sea. The IKMT deployments occurred the 2-13 September 2014 and the Cosmo-swan between 5-12 August 2014.

Table S2-1 Calibration parameters of the ship-borne echosounders used in the study.

Ship	**CCGV *Amundsen***	**CCGV *Amundsen***	**CCGV *Amundsen***	**F/V *Frosti***	**R/V *Helmer Hanssen***	**R/V *Polarstern***	**R/V *Polarstern***
Year	2015	2016	2017	2017	2016	2015	2017
Frequency (kHz)	38	38	38	38	38	38	38
Sa correction (dB)	-0.53	-0.57	-0.49	-0.32	-0.63	NA	-0.44
Gain (dB)	21.53	21.79	22.13	25.76	26.77	NA	24.84
Major axis 3 dB beam angle (°)	7.60	6.93	6.57	6.68	7.03	NA	6.92
Major axis angle offset (°)	-0.07	0.06	0.16	0.14	-0.11	NA	0.07
Major axis angle sensitivity (°)	22.0	21.9	21.9	18.0	21.9	NA	21.9
Minor axis 3 dB beam angle (°)	6.94	6.67	6.59	6.56	7.08	NA	6.92
Minor axis angle offset (°)	-0.16	0.23	0.03	-0.09	-0.09	NA	0.07
Minor axis angle sensitivity (°)	22.0	21.9	21.9	18.0	21.9	NA	21.9
Two way beam angle (dB re 1 sr)	-20.5	-20.6	-20.6	-20.7	-20.8	NA	-20.6

Table S2-2. Echosounder settings used for acoustic-trawl surveys in 2015, 2016, and 2017.

Year	Area	Vessel	Pulse length (msec)	Power (W)	Records duration (h)
2015	Beaufort Sea	CCGS *Amundsen*	1.024	2000	93
	Baffin Bay	CCGS *Amundsen*	1.024	2000	60
	Barents Sea	R/V *Polarstern*	1.024	1000	230
2016	Beaufort Sea	CCGS *Amundsen*	1.024	2000	48
	Baffin Bay	CCGS *Amundsen*	1.024	2000	142
	Barents Sea	R/V *Helmer Hanssen*	1.024	2000	11
2017	Beaufort Sea	F/V *Frosti*	1.024	2000	116
	Baffin Bay	CCGS *Amundsen*	1.024	2000	99
	Barents Sea	R/V *Polarstern*	1.024	1000	421

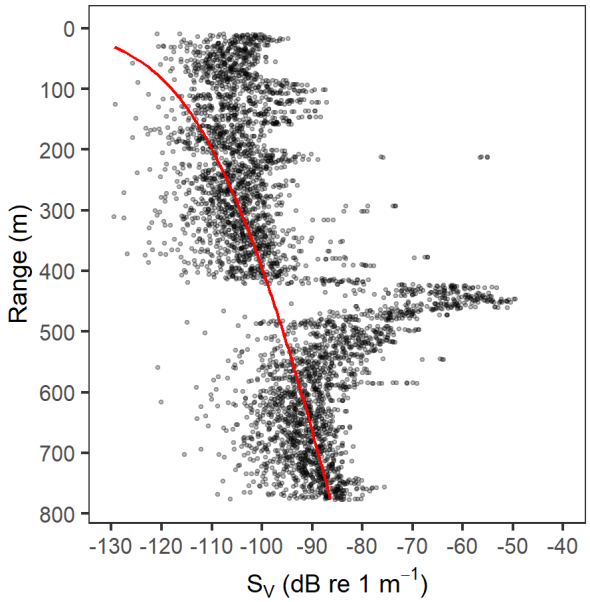

Figure S3-7. Example of raw S_V profile (black dots) of a single ping collected on June 06, 2017 at 06:07:27 UTC at 38 kHz from the hull-mounted EK60. The red curve shows the time varied gain function with a noise estimate of -160 dB at 1 m of the transducer. The peak in S_V between 600 and 500 m depth originates from the DSL.

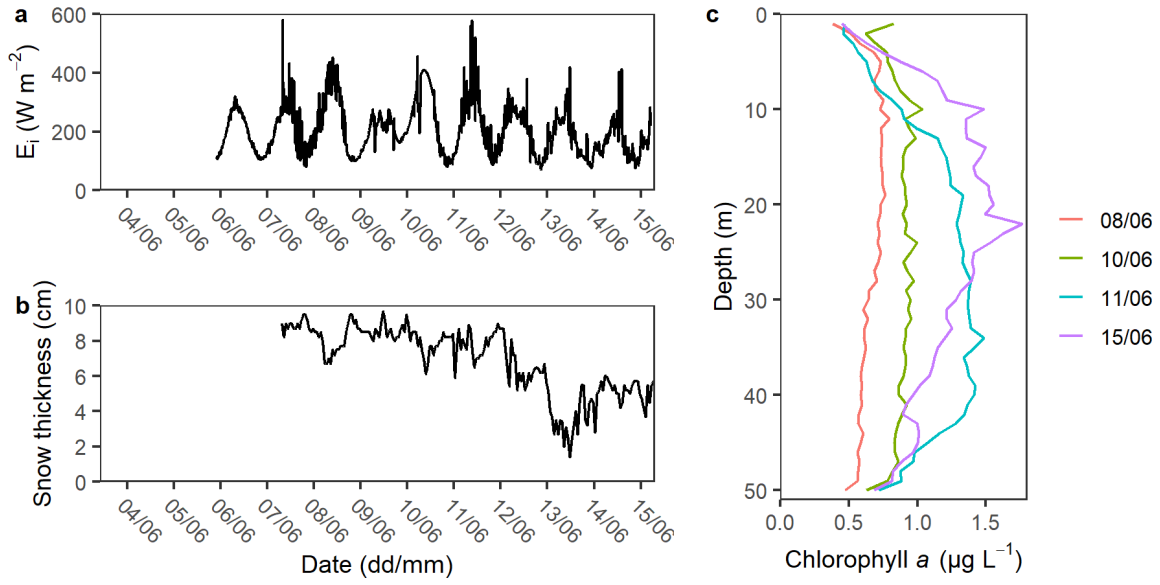

Figure S3-8. (a) Above-ice irradiance (Ei in W m-2), (b) snow thickness measured at the surface of the ice floe, and (c) chlorophyll *a* profiles from the top 50 m as measured by the handheld CTD deployed from the ice floe.

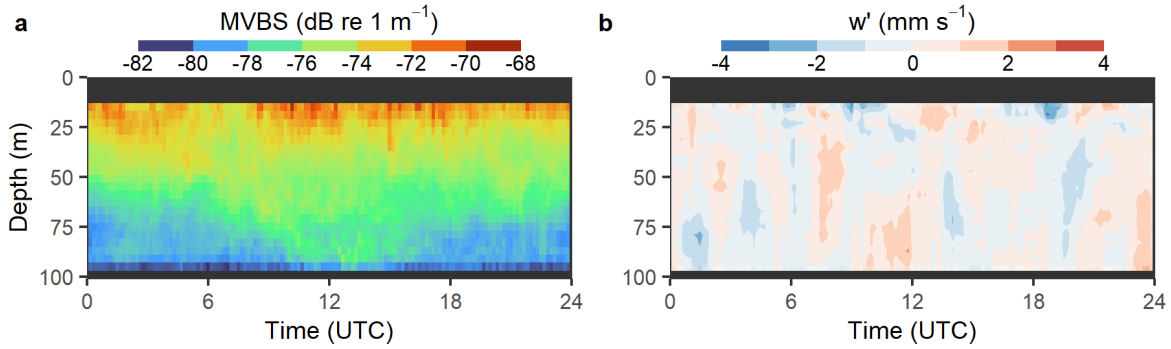

Figure S3-9. Mean 24 h composites of (a) mean volume backscattering strength (MVBS) and (b) vertical velocity anomalies (w') from the ice-tethered ADCP at 307.2 kHz between June 5-15. Net upward velocities (positive) are denoted by red contours and net downward velocities (negative) by blue contours. For vertical velocity anomalies, days when the tilt of the ADCP was changing too quickly were excluded (June 7, 10, and 11).

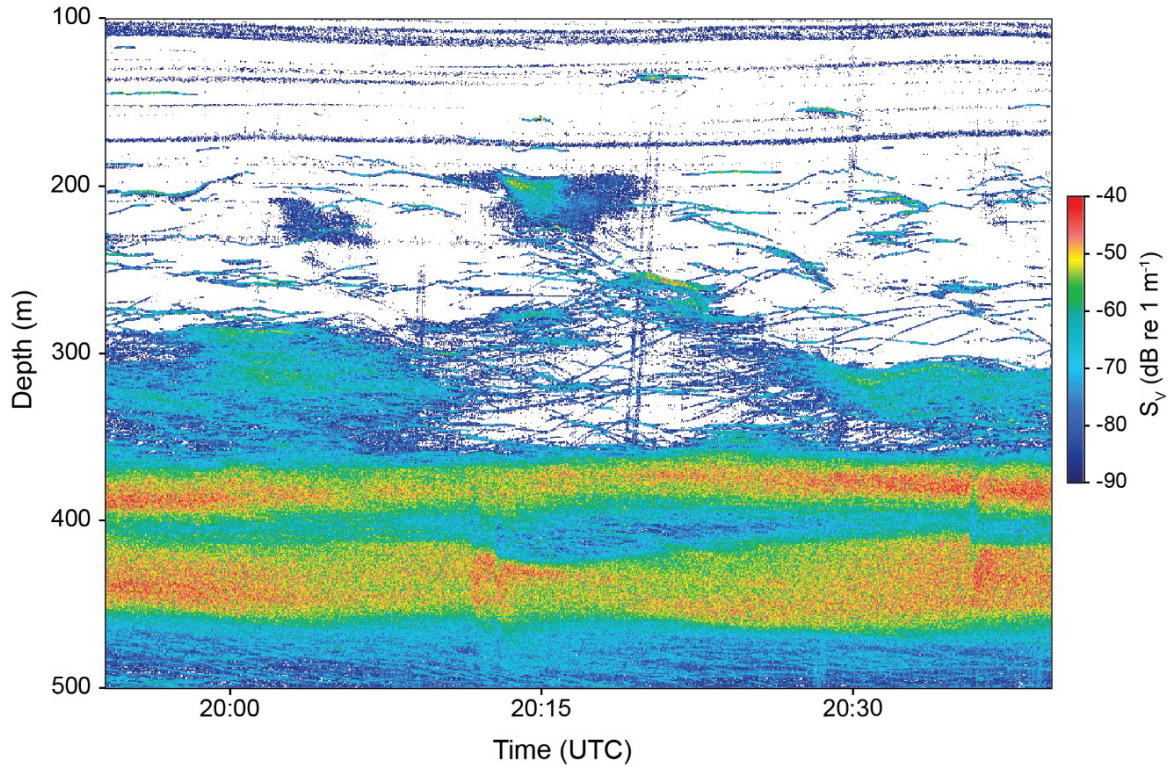

Figure S3-10. Example of an echogram of denoised S_V at 38 kHz from the hull-mounted EK60 on June 14, 2017, showing the inter-connection between scattered intermediate patches and the DSL. Single echoes can be seen migrating between the patches and the DSL.

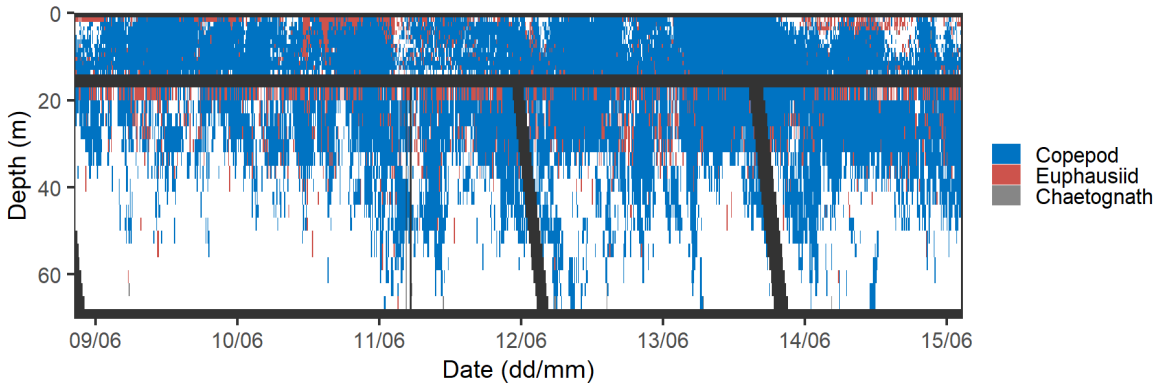

Figure S3-11. Echogram from the ice-tethered AZFP with echo-integration cell classified as copepod (blue), euphausiid (red), and chaetognath (grey) based on the multifrequency criterion of Darnis et al. (2017). Empty water is depicted in white and area with bad acoustic data (due to acoustic interference with other instruments, near-field, or dead zone near the sea ice) or with no data are black.

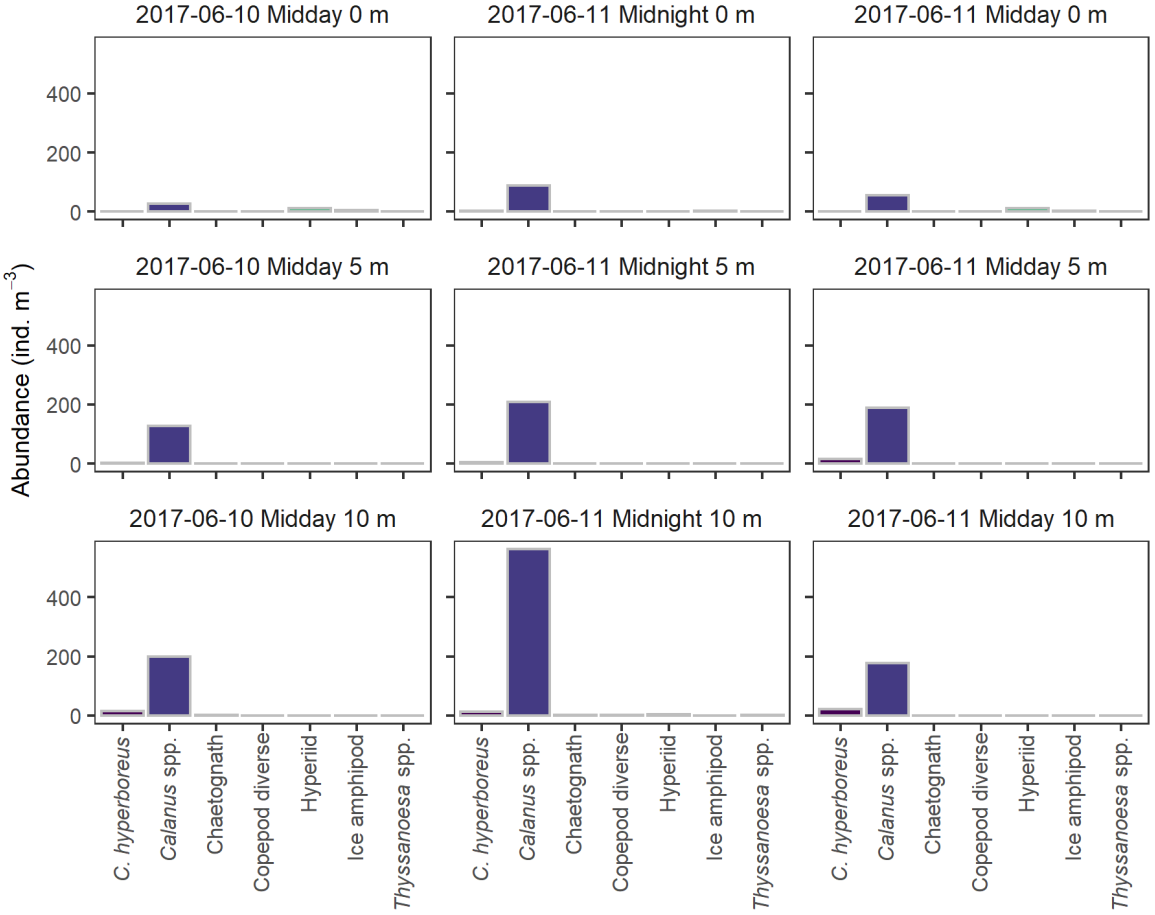

Figure S3-12. Mesozooplankton abundance at 0, 5, and 10 m under the ice collected by the ROVnet.

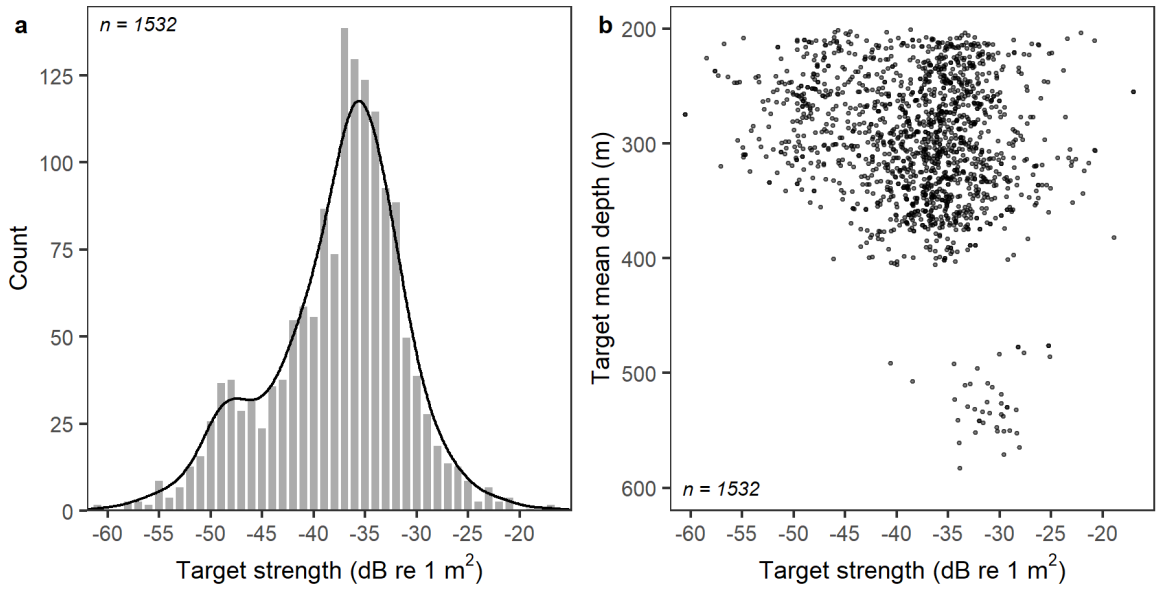

Figure S3-13. (a) Target strength histogram and kernel density curve (black line, bandwidth of 1.65) from single target tracks, i.e., single target tracked over at least 5 consecutive pings, between 200 and 600 m depth at 38 kHz. (b) Corresponding depth distribution of the single target tracks detected at 38 kHz between 200 and 600 m depth.

Table S3-1. Settings of the different echosounders used during the drift station. * The 18 kHz transducer was not calibrated; [a] the pulse length of the 70 kHz transducer was increased from 0.512 ms to 1.024 ms on June 9 at 12:30 UTC; [b] the pulse length of the 120 and 200 kHz was increased from 0.256 ms to 1.024 ms on June 9 at 12:30 UTC

Echosounder	Frequency (kHz)	Pulse length (ms)	Ping rate (Hz)	Beam width (°)	Gain (dB)	Nominal source level (dB re 1 µPa)	Transmitting power (W)
AZFP upward	38	0.500	0.5	12		208	23.9
AZFP upward	125	0.190	0.5	8		210	13.7
AZFP upward	200	0.170	0.5	8		210	14.3
AZFP upward	455	0.130	0.5	7		210	10.6
AZFP downward	38	1.000	0.25	12		208	23.9
AZFP downward	125	1.000	0.25	8		210	13.7
AZFP downward	200	1.000	0.25	8		210	14.3
AZFP downward	455	1.000	0.25	7		210	10.6
EK60	18*	1.024	~ 0.5	11			1000
EK60	38	1.024	~ 0.5	7	24.84		1000
EK60	70[a]	0.512/1.024	~ 0.5	7	25.78		750
EK60	120[b]	0.256/1.024	~ 0.5	7	24.54		250
EK60	200[b]	0.256/1.024	~ 0.5	7	24.58		150

Table S3-2. Parameters of Echoview single-echo detection algorithm for split beam echosounder (method 2) used to isolate single targets.

Parameters	**Values**
Compensated TS threshold (dB)	-100.0
Pulse length determination level (dB)	6.0
Minimum normalized pulse length	0.7
Maximum normalized pulse length	1.5
Beam compensation model	Simrad LOBE
Maximum beam compensation (dB)	3.0
Maximum standard deviation of minor-axis angles (°)	1.0
Maximum standard deviation of major-axis angles (°)	1.0

Table S3-3. Parameters of Echoview fish tracking algorithm used to detect single target tracks (named fish tracks in Echoview). Here, I tracked single targets over 5 consecutive pings with no missed detection between pings. Only single targets found to be within a maximum diameter of 2 m (athwartship and alongship) and 1 m range single targets from their position at the previous ping were retained.

Parameters	**Values**		
Data	4D (range, angles and time)		
Weights - Major axis	30		
Weights - Minor axis	40		
Weights - Range	40		
Weights - TS	0		
Weights - ping gap	3		
Track acceptance – Min. number of single targets in a track	5		
Track acceptance – Min. number of pings in track	5		
Track acceptance – Max. gap between single targets (pings)	0		
	Major axis (Athw.)	**Minor axis** (Along.)	**Range**
Track detection - Alpha	0.7	0.7	0.7
Track detection - Beta	0.5	0.5	0.5
Target gates - Exclusion distance (m)	2	2	1
Target gates - Missed ping expansion (%)	0	0	0

Table S3-4. Model fit statistics and parameter estimates for the generalized additive models (GAM) used to examine the relationship between the weighted mean depth (WMD in m) or backscatter intensity (s_A in m^2 nmi^{-2}) and environmental drivers for the SSL and DSL. Environmental drivers include bottom depth (Bot.), temperature of polar surface water (T_{PSW}), temperature of modified Atlantic water (T_{MAW}), and the tensor product of under-ice irradiance (E_d) and time of day. Significant drivers are highlighted in grey (*p*-value < 0.05).

		Model intercept			**Smooth terms**				**Model metrics**	
					s(Bot.)	**s(T_{PSW})**	**s(T_{MAW})**	**te(time, E_d)**		
SSL	WMD	Estimate	30.9	edf	3.687			7.669	r^2 adj.	0.63
		t-value	109.4	F	23.970			3.545	AR(1)	0.77
		p > |t|	< 0.001	*p*-value	*< 0.001*			*< 0.001*	Num. obs.	777
	log10(s_A)	Estimate	1.4	edf	2.460				r^2 adj.	0.43
		t-value	120.7	F	15.714				AR(1)	0.83
		p > |t|	< 0.001	*p*-value	*< 0.001*				Num. obs.	777
DSL	WMD	Estimate	416.9	edf	2.696		3.452		r^2 adj.	0.34
		t-value	512.6	F	6.736		3.350		AR(1)	0.68
		p > |t|	< 0.001	*p*-value	*< 0.001*		*0.006*		Num. obs.	1207
	log10(s_A)	Estimate	4.0	edf	3.678				r^2 adj.	0.70
		t-value	222.5	F	68.463				AR(1)	0.71
		p > |t|	< 0.001	*p*-value	*< 0.001*				Num. obs.	1207

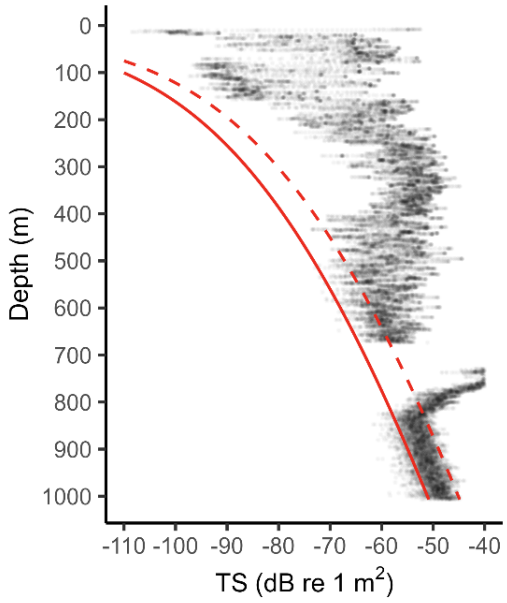

Figure S4-14. Noise levels of the hull-mounted echosounder at 38 kHz. The solid red line shows the estimated noise level, and the dashed red line the estimated noise plus 6 dB. Black dots represent a subset of TS from Smith Sound and bottom depth was 670 m.

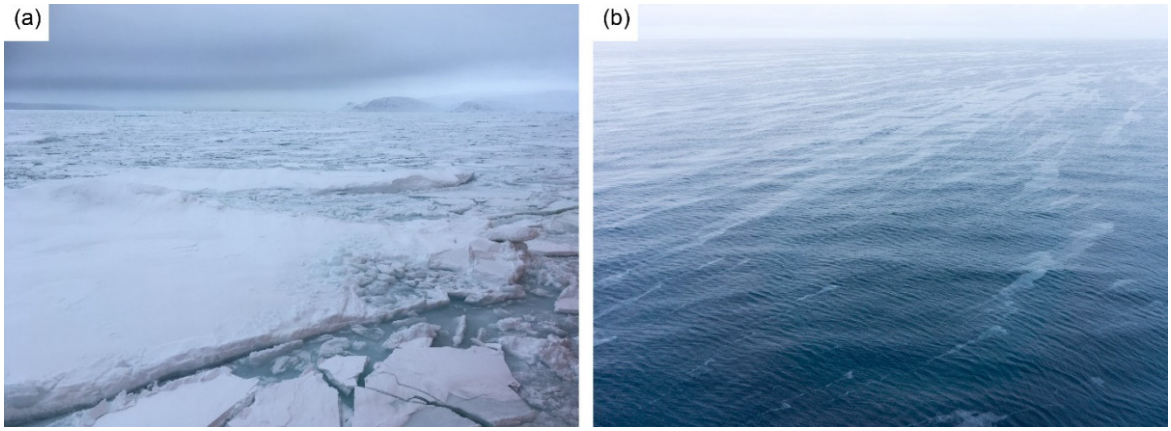

Figure S4-15. Sea ice cover in (a) Smith Sound on October 18th, 2021 and (b) Jones Sound on October 21st, 2021. Both photographs were taken around local noon (photo courtesy of Gaëlle Mével and Peter Sutherland).

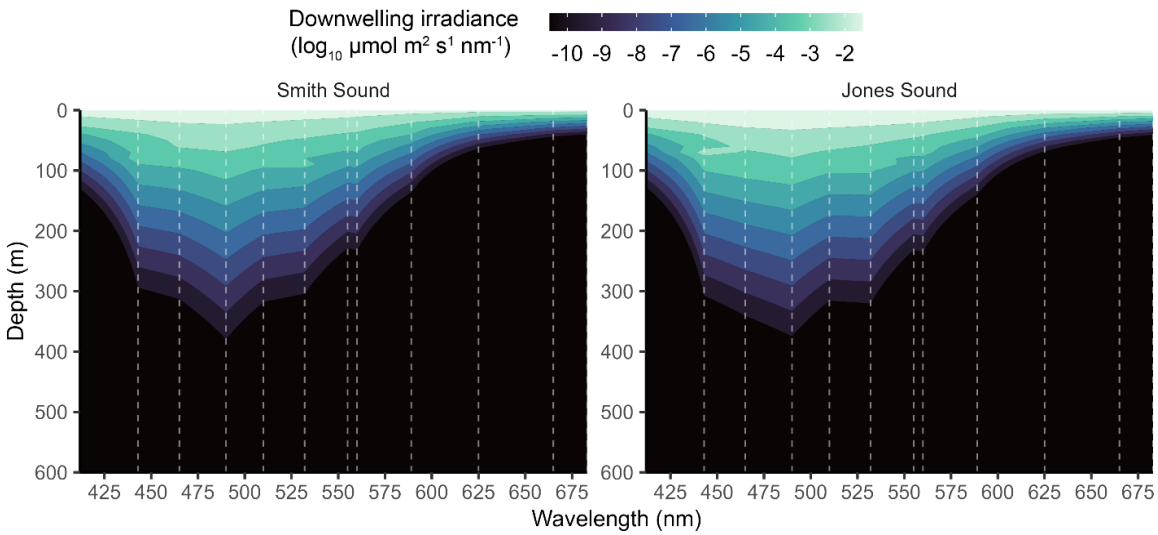

Figure S4-16. Average downwelling spectral irradiance in Smith Sound and Jones Sound at 14h local time (solar noon). The dotted vertical lines indicate wavelength at which coefficients of attenuations were evaluated.

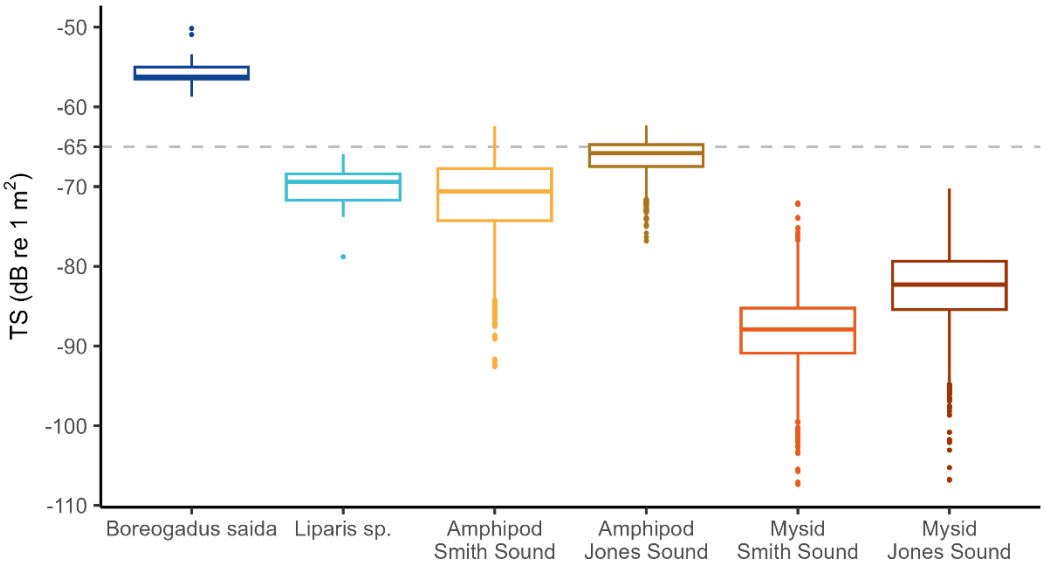

Figure S4-17. Boxplot of target strength (TS in dB re 1 m^2) of the four dominant taxa found in Smith Sound and Jones Sound. TS was estimated with TS-length relationships for the fish taxa (*Boreogadus saida* and *Liparis* sp.) and from PC-DWBA scattering models for macrozooplankton (amphipods and mysids), see the Methods section for more details. The dashed grey line indicate the TS threshold used in the single echo detection for discriminating between Arctic cod from other co-occurring species.

Table S4-5. Narrowband (CW: continuous wave) and broadband (FM: frequency modulated) echosounder settings used during the DarkEdge campaign.

Instrument	Transducer	Beam	Mode	Frequency (kHz)	Power (W)	Pulse length (ms)	Ramping	Ping rate (Hz)
EK80	ES38-7	Split	CW	38	2000	1024		~0.5-0.25
EK80	ES120-7C	Split	CW	120	250	1024		~0.5-0.25
WBAT	ES38-18DK	Split	FM	36-45	450	2048	Fast	0.5
WBAT	ES333-7CDK	Single	FM	283-333	50	2048	Fast	0.5

Table S4-6. Parameters of the "Single target detection - split beam method 2" algorithm used to detect single targets.

Parameter	Value
Compensated TS threshold (dB re 1 m^2)	-65
Pulse length determination level (dB re 1 W)	6
Min. normalized pulse length	0.50
Max. normalized pulse length	1.50
Beam compensation model	Simrad LOBE
Max. beam compensation (dB re 1 m^2)	3.00
Max. SD of minor-axis angle (°)	0.600
Max. SD of major-axis angle (°)	0.600